TECHNICAL REPORT STANDARD PAGE

1. Report No.	2. Government Accession No.	3. Recipient's Catalog No.
FHWA/LA.13/509		

4. Title and Subtitle	5. Report Date
Load Distribution and Fatigue Cost Estimates of Heavy Truck Loads on Louisiana State Bridges	November 2013
	6. Performing Organization Code LTRC Project Number: 10-1ST State Project Number: 736-99-1662

7. Author(s)	8. Performing Organization Report No.
Aziz Saber, Ph.D., P.E.	

9. Performing Organization Name and Address	10. Work Unit No.
Civil Engineering Program Louisiana Tech University 600 West Arizona Avenue Ruston, LA 71272	11. Contract or Grant No.

12. Sponsoring Agency Name and Address	13. Type of Report and Period Covered
Louisiana Department of Transportation and Development Louisiana Transportation Research Center 4101 Gourrier Avenue Baton Rouge, LA 70808	**Final report** **April 2009 - August 2012**
	14. Sponsoring Agency Code

15. Supplementary Notes

Conducted in Cooperation with the U.S. Department of Transportation, Federal Highway Administration

16. Abstract

The bridge in this study was evaluated and a monitoring system was installed to investigate the effects of heavy loads and the cost of fatigue for bridges on state highways in Louisiana. Also, this study is used to respond to Louisiana Senate Concurrent Resolution 35 (SCR-35). The superstructure of the bridge in this study was evaluated for safety and reliability under four different kinds of truck configuration and loads hauling sugarcane. The bridge model was verified by performing live load tests using 3S3 trucks with a gross vehicular weight (GVW) of 100,000 lb. on the structure. The bridge finite element model was analyzed under the different kinds of loading and the effects were listed and compared. The results of the analyses show that the pattern of response of the bridge under the different cases follows the same trend. Among the four different cases of loading configurations, case 4, which was GVW =148,000 lb. and a vehicle length of 92 ft., produced the largest tensile and compressive stresses in the members. The results from the bridge deck analyses confirm that the bridge deck is under a stable stress state, whether the stresses are in the tension zone or the compression zone. The heavy load as indicated in SCR-35 will cause damage to bridges.

The data from the monitoring system indicates that the average number of heavy loads during October, November, and December is 3.5 times higher than the rest of the year. The bridges are exposed to high cycles of repetition of heavy loads that will reduce the life span of the bridges by about 50%. The bridges that are built to last 75 years will be replaced after about 40 years in service. This seasonal impact is due to the sugarcane harvest and confirms the cost of fatigue, $0.9 per truck per trip per bridge, as determined in the previous study.

Based on the results of the studies presented in this report, increasing the gross vehicle weight of sugarcane trucks is not recommended. The heavy loads indicated in SCR-35 will cause premature fatigue damage to the main structural members and could cause their eventual structural failure. In addition, the majority of the Louisiana bridges currently in service were designed to accommodate lower loads than the bridge tested on this project. Therefore, based on the test results, one should expect that the proposed trucks to significantly shorten the remaining life span of Louisiana bridges. All these bridges should be rehabilitated prior to implementing SCR 35. The data from the monitoring system will provide a good source of information to review the current serviceability criteria used by the Louisiana Department of Transportation and Development (LADOTD) for the design of prestressed concrete bridge girders.

17. Key Words	18. Distribution Statement
Bridge, Cost, Fatigue, Girder, Heavy Load, Impact, Load Distribution, Instrumented Prestressed Girders, Slab, Sugarcane, Weigh-In-Motion, Live Load Testing.	**Unrestricted. This document is available through the National Technical Information Service, Springfield, VA 21161.**

19. Security Classif. (of this report)	20. Security Classif. (of this page)	21. No. of Pages	22. Price
N/A	N/A	209	

Project Review Committee

Each research project will have an advisory committee appointed by the LTRC Director. The Project Review Committee is responsible for assisting the LTRC Administrator or Manager in the development of acceptable research problem statements, requests for proposals, review of research proposals, oversight of approved research projects, and implementation of findings.

LTRC appreciates the dedication of the following Project Review Committee Members in guiding this research study to fruition.

LTRC Manager

Walid Alaywan, Ph.D., P.E.
Sr. Structural Research Engineer

Members

Arthur D'Andrea, P.E.
Gill Gautreau, P.E.
Michael Boudreaux, P.E.
Arturo Aguirre, P.E.

Directorate, Implementation Sponsor

Richard Savoie, P.E.
DOTD Chief Engineer

Load Distribution and Fatigue Cost Estimates of Heavy Truck Loads on Louisiana State Bridges

by

Aziz Saber, Ph.D., P.E.

Civil Engineering Program
Louisiana Tech University
600 West Arizona Avenue
Ruston, LA 71272

LTRC Project No. 10-1ST
State Project No. 736-99-1662

conducted for

Louisiana Department of Transportation and Development
Louisiana Transportation Research Center

November 2013

ABSTRACT

The bridge in this study was evaluated and a monitoring system was installed to investigate the effects of heavy loads and the cost of fatigue for bridges on state highways in Louisiana. Also, this study is used to respond to Louisiana Senate Concurrent Resolution 35 (SCR-35). The superstructure of the bridge in this study was evaluated for safety and reliability under four different kinds of truck configuration and loads hauling sugarcane. The bridge model was verified by performing live load tests using 3S3 trucks with a gross vehicular weight (GVW) of 100,000 lb. on the structure. The bridge finite element model was analyzed under the different kinds of loading and the effects were listed and compared. The results of the analyses show that the pattern of response of the bridge under the different cases follows the same trend. Among the four different cases of loading configurations, case 4, which was GVW =148,000 lb. and a vehicle length of 92 ft., produced the largest tensile and compressive stresses in the members. The results from the bridge deck analyses confirm that the bridge deck is under a stable stress state, whether the stresses are in the tension zone or the compression zone. The heavy load as indicated in SCR-35 will cause damage to bridges.

The monitoring system recorded strains and strain cycles that occurred within the range during the hour period. The data provided the relative magnitude of strain ranges for the various gauge locations. It also provided the strain reversals in the girders, which was an important factor for the fatigue analysis. The recorded data indicate that the bridge girders are subject to low cycles of high strain values and high cycles of low strain values. The girder performance under such conditions can be explained as follows: the high strain values exceed the serviceability criteria and can lead to cracks in the girders then the high cycles of low strain will lead to fatigue in the prestressed strands. Consequently, the girders will deteriorate and the life span of the bridge will be reduced. The data from the monitoring system indicates that the average number of heavy loads during October, November, and December is 3.5 times higher than the rest of the year. The bridges are exposed to high cycles of repetition of heavy loads that will reduce the life span of the bridges by about 50%. The bridges that are built to last 75 years will be replaced after about 40 years in service. This seasonal impact is due to the sugarcane harvest and confirms the cost of fatigue, $0.9 per truck per trip per bridge, as determined in the previous study.

Based on the results of the studies presented in this report, increasing the gross vehicle weight of sugarcane trucks is not recommended. The heavy loads indicated in SCR-35 will cause premature fatigue damage to the main structural members and could cause their eventual structural failure. In addition, the majority of the Louisiana bridges currently in service were designed to accommodate lower loads than the bridge tested on this project.

Therefore, based on the test results, one should expect that the proposed trucks to significantly shorten the remaining life span of Louisiana bridges. All these bridges should be rehabilitated prior to implementing SCR 35. The data from the monitoring system will provide a good source of information to review the current serviceability criteria used by the Louisiana Department of Transportation and Development (LADOTD) for the design of prestressed concrete bridge girders.

ACKNOWLEDGMENTS

This research project was sponsored by the Louisiana Transportation Research Center (LTRC) of the Louisiana Department of Transportation and Development (LADOTD) under research project number 10-1ST and state project number 736-99-1662.

The researchers want to express their gratitude to the Project Review Committee, many of whom provided direct assistance to the project team as they developed information needed to complete the study. During the course of this research project, the research team received valuable and much appreciated support and guidance from LTRC staff and engineers, especially Harold "Skip" Paul, Walid Alaywan, Ph.D., Mark Morvant, Zhongje "Doc" Zhang, Ph.D., and Christopher Abadie.

This study could not have been completed without the assistance of personnel from District 03. Personnel from district administration, construction engineering, maintenance, materials, and traffic all contributed to the successful completion of the project.

The assistance and support from the employees and members of the American Sugarcane League is much appreciated including Jim Simon, Ronnie Gonsoulin, and Dan Duplantis.

The assistance and support from the staff and employees at Bridge Diagnostic, Inc. is also much appreciated.

IMPLEMENTATION STATEMENT

This research delivered a field-verified model for analyzing and determining the effects due to applied loads. The monitoring system recorded strains and strain cycles that occurred within the range during the hour period. The data provided the relative magnitude of strain ranges for the various gauge locations. It also provided the strain reversals in the girders which is important factor for analysis.

The LADOTD should implement the data from the monitoring system to review the current serviceability criteria used by LADOTD for design of prestressed concrete bridge girders.

The LADOTD should not increase the gross vehicle weight of sugarcane trucks from the current vehicle FHWA Type 10 (3S3) GVW 100,000lb. The heavy loads indicated in Louisiana Senate Concurrent Resolution 35 (SCR35) will cause premature fatigue damage to the main structural members and could cause their eventual structural failure. In addition, the majority of Louisiana in service bridges were designed to accommodate lower loads than the bridge tested on this project. Therefore, based on the test results, one should expect the proposed trucks to significantly shorten the remaining life span of Louisiana bridges. All these bridges should be rehabilitated prior to implementing SCR 35.

The LADOTD should implement this bridge for their live load testing needs.

TABLE OF CONTENTS

ABSTRACT iii
ACKNOWLEDGMENTS v
IMPLEMENTATION STATEMENT vii
TABLE OF CONTENTS ix
LIST OF FIGURES xiii
LIST OF TABLES xix
INTRODUCTION 1
OBJECTIVE 3
SCOPE 5
METHODOLOGY 7
Description and Location of the Bridge 7
Instrumentation of the Bridge 8
Field Test 14
Analysis Overview 18
Method of Approach 20
TRIDIMENTIONAL Girder Element Type IPSL 21
PLATE Deck Element Type SBCR 21
Prismatic Space Truss Members 22
Modeling Assumptions 22
Bridge Geometry 22
Aspect Ratio 24
Boundary Conditions 24
Moving Load Analysis 25
Regression Analysis for the Truck Weights 26
Truck Parameters 29
Data Collection and Preprocessing 29
Regression Analysis 30
Evaluation of Fatigue 32
Fatigue in Louisiana State Bridges 32
Identification of Critical Bridges for Study 32
Analysis of Bridge Girders 33
Long-term Effects and Cost 34

DISCUSSION OF RESULTS....37
General Discussion....37
Model Verification....38
Live Load Test on the Bridge....38
Truck in Left Lane....38
Truck in Right Lane....38
System Behavior and Load Distribution....38
Results of Finite Element Analysis for Truck Loading....39
Comparison of Maximum Stresses in Girders, Left Lane....40
Comparison of Maximum Stresses in Girders, Right Lane....48
Comparison of Maximum Deflections in Girders....57
Comparison of Deck Stresses....59
Results and Discussion for Regression Analysis....60
Outside Lane....60
Inside Lane....62
Cost of Fatigue on Louisiana Bridges....66
CONCLUSIONS....71
RECOMMENDATIONS....73
ACRONYMS, ABBREVIATIONS, AND SYMBOLS....75
REFERENCES....77
APPENDIX A (ON ACCOMPANYING CD)
Comparison of Top and Bottom Elements of Instrumented Girders....81
APPENDIX B (ON ACCOMPANYING CD)
Effects of Truck Configuration on Flexural Stresses....115
APPENDIX C (ON ACCOMPANYING CD)
Effects of Truck Configurations on Deck Stresses....143
APPENDIX D (ON ACCOMPANYING CD)
Bridge Instrumentation Drawings....148
APPENDIX E (ON ACCOMPANYING CD)
Plot of Strains of The Auto Triggered Test....155
APPENDIX F (ON ACCOMPANYING CD)
Truck Types....163
APPENDIX G (ON ACCOMPANYING CD)
November Live Load Test Data....169

APPENDIX H (ON ACCOMPANYING CD)
Live Load Test Data for Different Truck Types.....173

LIST OF FIGURES

Figure 1 FHWA Type 10 vehicle (3S3) with GVW = 100,000 lb. 2
Figure 2 FHWA Type 10 vehicle (3S3) and two-axle dolly with GVW = 148,000 lb. 2
Figure 3 Plan view of the bridge 8
Figure 4 Data logger for the strain transducers 9
Figure 5 Installation of solar panel and the camera 9
Figure 6 Instrumentation plan of the bridge-top view 10
Figure 7 Instrumentation plan of the bridge- section view 11
Figure 8 Photo of strain gauge installed in the field 13
Figure 9 Schematic layout of the wheel path of the test truck on the bridge 14
Figure 10 Schematic layout of the 3S3 – 100 kip test truck 15
Figure 11 Strains at the bottom of girders in middle of Span 14E during Test 2 16
Figure 12 Strains at the bottom of girders in middle of Span 14E during Test 4 17
Figure 13 Photo of the test truck on left lane taken by the implanted camera 17
Figure 14 Photo of the test truck on right lane taken by the implanted camera 18
Figure 15 AASHTO standard HS20-44 truck 19
Figure 16 Louisiana sugarcane truck 3S3 with GVW=100,000 lb. 19
Figure 17 Louisiana sugarcane truck GVW-148 Opt-1 20
Figure 18 Louisiana sugarcane truck GVW-148 Opt-2 20
Figure 19 Schematic view of different elements used for finite element modeling of the bridge. 21
Figure 20 Typical cross section of the finite element model of the bridge 23
Figure 21 Plan view of the finite element model of the bridge 24
Figure 22 Moving load analysis for HS20-44 truck in longitudinal and transverse direction 26
Figure 23 Placement of wheel loads on left lane of span 14E of HS20-44 truck 26
Figure 24 3S3 Truck photograph with time stamp in right hand lane 28
Figure 25 3S3 Truck photograph with time stamp in left hand lane 28
Figure 26 Time/month heavy load count 34
Figure 27 Monthly heavy load count 35
Figure 28 Comparison of FEM strains with field test strains – truck on left lane 39
Figure 29 Comparison of FEM strains with field test strains – truck on right lane 39
Figure 30 Comparison of bending stress distribution of bottom elements - Girder B of Case I 40
Figure 31 Comparison of bending stress distribution of bottom elements - Girder B of Case I, Span 14E 41

Figure 32 Blow-out showing the tensile stress at midspan of Figure 31 41
Figure 33 Comparison of bending stress distribution of top elements - Girder B of Case I 42
Figure 34 Comparison of bending stress distribution of top elements - Girder B of Case I, Span 14E 43
Figure 35 Blow-out showing the tensile stress at right support of Span 14E, Figure 34..... 43
Figure 36 Comparison of bending stress distribution of bottom elements - Girder C of Case I 46
Figure 37 Comparison of bending stress distribution of top elements - Girder C of Case I 47
Figure 38 Comparison of bending stress distribution of bottom elements - Girder D of Case III..... 49
Figure 39 Comparison of bending stress distribution of bottom elements - Girder D of Case III, Span 14E 50
Figure 40 Blow-out showing the tensile stress at midspan of Figure 39 50
Figure 41 Comparison of bending stress distribution of top elements - Girder D of Case III..... 51
Figure 42 Comparison of bending stress distribution of top elements - Girder D of Case III, Span 14E 52
Figure 43 Blowout showing the compressive stress at midspan of Figure 42..... 52
Figure 44 Comparison of flexural stress distribution of top elements - Girder E of Case III 55
Figure 45 Comparison of flexural stress distribution of bottom elements - Girder E of Case III 55
Figure 46 Comparison of deflections of Girder D for Case III..... 57
Figure 47 Strain cycle at Gauge 14 at bottom of Girder E - outside lane..... 67
Figure 48 Strain cycle at Gauge 17 at bottom of Girder E - inside lane..... 67
Figure 49 Comparison of flexural stress distribution of top elements - Girder A of Case I 83
Figure 50 Comparison of flexural stress distribution of bottom elements - Girder A of Case I 83
Figure 51 Comparison of bending stress distribution of bottom elements - Girder D of Case I 84
Figure 52 Comparison of bending stress distribution of top elements - Girder C of Case I 84
Figure 53 Comparison of flexural stress distribution of top elements - Girder E of Case I..... 85

Figure 54 Comparison of flexural stress distribution of bottom elements - Girder E of Case I 85
Figure 55 Comparison of flexural stress distribution of top elements - Girder F of Case I 86
Figure 56 Comparison of flexural stress distribution of bottom elements - Girder F of Case I 86
Figure 57 Comparison of flexural stress distribution of top elements - Girder A of Case II 87
Figure 58 Comparison of flexural stress distribution of bottom elements - Girder A of Case II 87
Figure 59 Comparison of bending stress distribution of bottom elements - Girder B of Case II 88
Figure 60 Comparison of bending stress distribution of top elements - Girder B of Case II 88
Figure 61 Comparison of bending stress distribution of bottom elements - Girder C of Case II 89
Figure 62 Comparison of bending stress distribution of top elements - Girder C of Case II 89
Figure 63 Comparison of bending stress distribution of bottom elements - Girder D of Case II 90
Figure 64 Comparison of bending stress distribution of top elements - Girder D of Case II 90
Figure 65 Comparison of flexural stress distribution of top elements - Girder E of Case II 91
Figure 66 Comparison of flexural stress distribution of bottom elements - Girder E of Case II 91
Figure 67 Comparison of flexural stress distribution of top elements - Girder F of Case II 92
Figure 68 Comparison of flexural stress distribution of bottom elements - Girder F of Case II 92
Figure 69 Comparison of flexural stress distribution of top elements - Girder A of Case III 93
Figure 70 Comparison of flexural stress distribution of bottom elements - Girder A of Case III 93
Figure 71 Comparison of bending stress distribution of bottom elements - Girder B of Case III 94
Figure 72 Comparison of bending stress distribution of top elements -

Girder B of Case III 94
Figure 73 Comparison of bending stress distribution of bottom elements - Girder C of Case III 95
Figure 74 Comparison of bending stress distribution of top elements - Girder C of Case III 95
Figure 75 Comparison of flexural stress distribution of top elements - Girder F of Case III 96
Figure 76 Comparison of flexural stress distribution of bottom elements - Girder F of Case III 96
Figure 77 Comparison of flexural stress distribution of top elements - Girder A of Case IV 97
Figure 78 Comparison of flexural stress distribution of bottom elements - Girder A of Case IV 97
Figure 79 Comparison of bending stress distribution of bottom elements - Girder B of Case IV 98
Figure 80 Comparison of bending stress distribution of top elements - Girder B of Case IV 98
Figure 81 Comparison of bending stress distribution of bottom elements - Girder C of Case IV 99
Figure 82 Comparison of bending stress distribution of top elements - Girder C of Case IV 99
Figure 83 Comparison of bending stress distribution of bottom elements - Girder D of Case IV 100
Figure 84 Comparison of bending stress distribution of top elements - Girder D of Case IV 100
Figure 85 Comparison of flexural stress distribution of top elements - Girder E of Case IV 101
Figure 86 Comparison of flexural stress distribution of bottom elements - Girder E of Case IV 101
Figure 87 Comparison of flexural stress distribution of top elements - Girder F of Case IV 102
Figure 88 Comparison of flexural stress distribution of bottom elements - Girder F of Case IV 102
Figure 89 Comparison of deflections of Girder A for Case I 103
Figure 90 Comparison of deflections of Girder B for Case I 103
Figure 91 Comparison of deflections of Girder C for Case I 104
Figure 92 Comparison of deflections of Girder D for Case I 104

Figure 93 Comparison of deflections of Girder E for Case I 105
Figure 94 Comparison of deflections of Girder F for Case I 105
Figure 95 Comparison of deflections of Girder A for Case II 106
Figure 96 Comparison of deflections of Girder B for Case II 106
Figure 97 Comparison of deflections of Girder C for Case II 107
Figure 98 Comparison of deflections of Girder D for Case II 107
Figure 99 Comparison of deflections of Girder E for Case II 108
Figure 100 Comparison of deflections of Girder F for Case II 108
Figure 101 Comparison of deflections of Girder A for Case III 109
Figure 102 Comparison of deflections of Girder B for Case III 109
Figure 103 Comparison of deflections of Girder C for Case III 110
Figure 104 Comparison of deflections of Girder E for Case III 110
Figure 105 Comparison of deflections of Girder F for Case III 111
Figure 106 Comparison of deflections of Girder A for Case IV 111
Figure 107 Comparison of deflections of Girder B for Case IV 112
Figure 108 Comparison of deflections of Girder C for Case IV 112
Figure 109 Comparison of deflections of Girder D for Case IV 113
Figure 110 Comparison of deflections of Girder E for Case IV 113
Figure 111 Comparison of deflections of Girder E for Case IV 114
Figure 112 Plan view of bridge instrumentation- Span 12E 149
Figure 113 Plan view of bridge instrumentation- Span 13E. [Saber, A., 2010] 149
Figure 114 Plan view of bridge instrumentation- Span 14E. [Saber, A., 2010] 150
Figure 115 Plan view of bridge instrumentation- Span 15 E. [Saber, A., 2010] 150
Figure 116 Strain gauges in section G-G and section H-H. [Saber, A., 2010] 151
Figure 117 Strain gauges in section D-D. [Saber, A., 2010] 151
Figure 118 Strain gauges in section A-A and section B-B. [Saber, A., 2010] 152
Figure 119 Strain gauges in section C-C. [Saber, A., 2010] 152
Figure 120 Strain gauges in section F-F. [Saber, A., 2010] 153
Figure 121 Strain gauges in sections E1-E1, E2-E2 and E3. [Saber, A., 2010] 153
Figure 122 Plot of strains of the auto triggered test (truck on right lane) 157
Figure 123 Plot of strains of the auto triggered test (truck on left lane) 158
Figure 124 Plot of strains of the controlled test (out lane slow) 159
Figure 125 Plot of strains of the controlled test (out lane fast) 160
Figure 126 Plot of strains of the controlled test (in lane fast) 161
Figure 127 Truck type 3S2 165
Figure 128 Truck type 3S2 sugarcane 165
Figure 129 Truck type 3S3 166

Figure 130 Truck type 3S3 sugarcane 166
Figure 131 Truck type FHWA Class 6 167
Figure 132 Truck type FHWA Class 7 167
Figure 133 Live field data strain values vs. legal truck weight (inside lane) 186
Figure 134 Live field data strain values vs. legal truck weight (outside lane) 186
Figure 135 New Iberia Parish location 187
Figure 136 Bridge location, LA675 187

LIST OF TABLES

Table 1 Description of the bridge geometry 7
Table 2 Position and location of the strain transducers in different part of the bridge 12
Table 3 Summary of the live load test information 15
Table 4 Different load cases of trucks on the bridge 18
Table 5 Strain gauge location and description 27
Table 6 Truck types and legal weights 29
Table 7 Interpretation of correlation coefficient 31
Table 8 Case I - effects of truck configurations on flexural stresses - Girder B 44
Table 9 Case I - effects of truck configurations on flexural stresses - Girder C 48
Table 10 Case III - effects of truck configurations on flexural stresses - Girder D 53
Table 11 Case III - effects of truck configurations on flexural stresses - Girder E 56
Table 12 Effects of truck configurations on deflections - Girder D 58
Table 13 Case I - effects of truck configurations on deck stresses 59
Table 14 Correlation values for the live field data set (outside lane) 60
Table 15 Model summary R and R square values for the live field data (outside lane) 61
Table 16 ANOVA table for the live field data (outside lane) 61
Table 17 Coefficients table for the live field data (outside lane) 61
Table 18 Corresponding SPSS data sets with equation variables (outside lane) 62
Table 19 Actual truck weight vs. predicted truck weight 62
Table 20 Descriptive statistics for strain gauges (inside lane) 63
Table 21 Correlation values for the live field data set (inside lane) 63
Table 22 R and R square values for the live field data (inside lane) 64
Table 23 ANOVA table for the live field data (inside lane) 64
Table 24 Coefficients table for the live field data (inside lane) 64
Table 25 Corresponding SPSS data sets with equation variables (inside lane) 65
Table 26 Actual truck weight vs. predicted truck weight (inside lane) 65
Table 27 Preliminary list of critical bridges that will fail due to SCR-35 66
Table 28 Case I - Effects of truck configurations on flexural stresses - Girder A 117
Table 29 Case I - Effects of truck configurations on flexural stresses - Girder D 118
Table 30 Case I - Effects of truck configurations on flexural stresses - Girder E 119
Table 31 Case I - Effects of truck configurations on flexural stresses - Girder F 120
Table 32 Case II - Effects of truck configurations on flexural stresses - Girder A 121
Table 33 Case II - Effects of truck configurations on flexural stresses - Girder B 122
Table 34 Case II - Effects of truck configurations on flexural stresses - Girder C 123
Table 35 Case II - Effects of truck configurations on flexural stresses - Girder D 124

Table 36 Case II - Effects of truck configurations on flexural stresses - Girder E 125
Table 37 Case II - Effects of truck configurations on flexural stresses - Girder F 126
Table 38 Case III - Effects of truck configurations on flexural stresses - Girder A 127
Table 39 Case III - Effects of truck configurations on flexural stresses - Girder B 128
Table 40 Case III - Effects of truck configurations on flexural stresses - Girder C 129
Table 41 Case III - Effects of truck configurations on flexural stresses - Girder F 130
Table 42 Case IV - Effects of truck configurations on flexural stresses - Girder A 131
Table 43 Case IV - Effects of truck configurations on flexural stresses - Girder B 132
Table 44 Case IV - Effects of truck configurations on flexural stresses - Girder C 133
Table 45 Case IV - Effects of truck configurations on flexural stresses - Girder D 134
Table 46 Case IV - Effects of truck configurations on flexural stresses - Girder E 135
Table 47 Case IV - Effects of truck configurations on flexural stresses - Girder F 136
Table 48 Effects of truck configurations on deflections - Girder A 137
Table 49 Effects of truck configurations on deflections - Girder B 138
Table 50 Effects of truck configurations on deflections - Girder C 139
Table 51 Effects of truck configurations on deflections - Girder E 140
Table 52 Effects of truck configurations on deflections - Girder F 141
Table 53 Case II- Effects of truck configurations on deck stresses 145
Table 54 Case III- Effects of truck configurations on deck stresses 146
Table 55 Case IV- Effects of truck configurations on deck stresses 147
Table 56 November live load test data 171
Table 57 Live load data for 3S3 truck type 175
Table 58 Live load test data for 3S3 sugarcane truck type 176
Table 59 Live load test data for 3S2 truck type 177
Table 60 Live load test data for 3S2 sugarcane truck type 178
Table 61 Live load data for FHWA Class 6 truck type 179
Table 62 Live load data for FHWA Class 7 truck type 180
Table 63 Live load test data for Type 2 truck 181
Table 64 Live load test data for Type 18 truck 182
Table 65 Live load test data for 3S2 truck type 183
Table 66 Live load test data for 3S3 truck type 184
Table 67 Live load test data for 3S2 sugarcane truck type 185
Table 68 Live load test data for 3S3 sugarcane truck type 185

INTRODUCTION

The Transportation Equity Act 21 (TEA 21) of 1998 allows for heavier sugarcane truck loads on Louisiana interstate highways. These heavier loads are currently being applied to state and parish roads through trucks travelling from and to the processing plants. Generally, commercial vehicle weight and dimension laws are enforced by highway agencies to ensure that excessive damage (and subsequent losses of pavement life) is not imposed on highway infrastructures like bridges. The axle loads and total loads of heavy trucks, which are considered primarily responsible for decreasing the service life of bridges, are significant parameters of highway traffic. TEA 21 is allowing sugarcane trucks to haul loads up to 100,000 lb. Because highways and bridges have traditionally been designed for the legal load of 80,000 lb., permitted trucks of 100,000 lb. or more decrease the expected service life of the infrastructure. LTRC report 418 shows that there is fatigue damage from heavy truck loads (GVW 100,000-lb.) on Louisiana bridges and recommends a field investigation to verify the theoretical studies [*1*].

During the 2009 regular session, the Louisiana senate passed a concurrent resolution (SCR-35), sponsored by Senator McPherson, which urged the LADOTD to conduct a pilot study on alternative truck-trailer configurations to support the bio-fuels industry [*2*]. The senate concurrent resolution SCR-35 specifically requested that the study include vehicles hauling sugarcane biomass for alternative fuel and electricity generation. The alternative truck-trailer configuration will use extra axles under the load to reduce the impact on Louisiana roads. The alternative truck-trailer, when compared to the traditional trailer designs, will decrease the number of trucks and increase the total number of tons of sugarcane that travel on Louisiana roads.

On June 4, 2009, the Project Review Committee (PRC), including Jim Simon of the American Sugarcane League, met to discuss the details of this study and the SCR-35. The PRC approved that the roads and the bridges in and around Raceland, LA, where Raceland Raw Sugar Corporation (RRSC) is located, will be used to address SCR-35 in this study. In June, July, and August of 2009, the principal investigator, Dr. Aziz Saber, reviewed the bridge conditions in the Raceland area and performed multiple site visits accompanied by the project manager Dr. Walid Alaywan. The findings from these preliminary studies were shared with the Sugarcane League representatives, Dan Duplantis and Jim Simon. In August 2009, LTRC received information from the American Sugarcane League indicating that their members, located in New Iberia, were better prepared to provide the support for the study than those in Raceland. Also, they requested that the bridge monitoring system to be installed around the New Iberia area.

On November 11, 2009, a meeting was held in New Iberia regarding the SCR-35 and was attended by the principal investigator Dr. Saber; the American Sugarcane (ASC) League, Jim Simon and Ronnie Gonsoulin; and LTRC representatives, Chris Abadie and Dr. Alaywan. At that meeting, the ASC League representatives indicated their interest in considering two truck configurations to transport sugarcane harvest. The first option is shown in Figure 1, and based on the recommendation in LTRC Report Numbers 418 and 425 (3S3 Type truck at 100,000 lb.GVW) [*1, 3*]. The second option is shown in Figure 2, and similar to option one with a two-axle dolly attached to it. The truck weight was to be limited to 100,000 lb. and the dolly weight limited to 48,000 lb. for a total GVW of 148,000 lb. During the course of this work in 2010, Simon of the ASC indicated to LTRC that his league would like the response to SCR-35 to be limited to theoretical evaluations. The truck configuration in Figure 2 is not an FHWA vehicle type truck-trailer; therefore, the results of the previous studies, LTRC reports 418, 425, 321, and 398, have to be re-evaluated using the proposed configuration [*1, 3, 4, 5*].

Figure 1
FHWA Type 10 vehicle (3S3) with GVW = 100,000 lb.

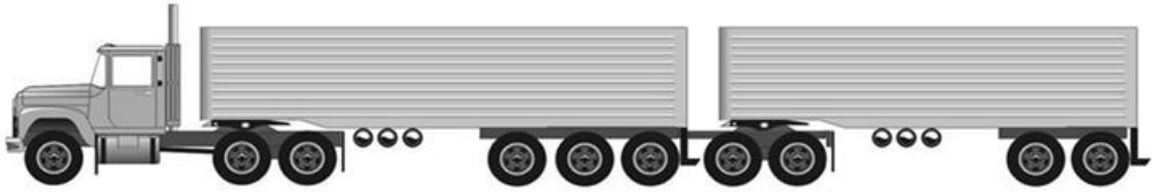

Figure 2
FHWA Type 10 vehicle (3S3) and two-axle dolly with GVW = 148,000 lb.

OBJECTIVE

The objective of this research was to develop an integrated system for monitoring live loads and verify the carrying capacity of highway bridges in Louisiana where heavy truck loads may have caused significant damage to state bridges. This study developed a monitoring system for synchronous measurements of live loads and structural responses of bridge components. The monitoring system integrated a distributed network of advanced strain and displacement sensors (continuous and peak). The anticipated major contributions include accumulated fatigue load spectra, strain measurements to determine in-service conditions, and adverse loading conditions on the bridge superstructure assessments.

SCOPE

The scope of the investigation on the impact of heavy truck loads on non-interstate bridges can be stated as follows:

- To study the effects of heavy truck loads (100,000 lb. and 148,000 lb.) on distribution of forces and moments on slab-girder bridges.
- To develop a long-term monitoring system that can assess the impact of heavy truck loads on safety, serviceability, and durability of non-interstate bridges.
- To determine the cost of the fatigue damage per heavy truck load (100,000 lb. and 148,000 lb.) per year.
- To investigate the use of strain measurements from the monitoring system to predict the gross vehicle weight of a truck.

METHODOLOGY

The bridge under investigation in this project is one of the bridges that is used repeatedly by heavy sugarcane trucks. Under these heavy truck loads, the variation of forces, moments, and deflections was studied. To implement it, a finite element model of the bridge was developed and analyzed under the heavy sugarcane loads. To verify the model, a field test was also performed. The results of the analysis and the field test were compared and recommendations for the effects of sugarcane truckloads on bridges were made based on the results of this investigation.

Description and Location of the Bridge

The bridge is located in south Louisiana in Iberia Parish along US 90 at LA 675. The state project number of this bridge is 424-04-0034 [*6*]. It consists of identical east and west bounds. The east bound has 25 spans with a length of 1,822 ft.; 21 out of 25 of those spans are 70 ft. long and are AASHTO Type III girders. The remaining four spans are more than 70 ft. long, and researchers are considering this part in the investigation. This part consists of six AASHTO Type IV modified girders with span lengths of 75.5 ft., 115.5 ft., 15.5 ft., and 75.8 ft., respectively. All four spans are continuous. The spacing of the girders is 7 ft. 2 in., and with the cantilever the bridge has a 40 ft. clear roadway. It has two lanes on it. The slab thickness is 7.5 in. between the girders. There is an end diaphragm at the ends and full depth continuous diaphragm at the intermediate bents. There are some half depth intermediate diaphragms also. The detail of the bridge is presented in Table 1 and Figure 3.

Table 1
Description of the bridge geometry

State Project Number	424-04-0034
Location	On US 90 in New Iberia at LA 675
Structure Type	Precast prestressed Bridge Girders
Span Length	Varying
Number of Spans	25
Skew	45° 25′ 52.5″
Girders	6, AASHTO Type IV Modified
Deck	7.5 in. cast in place.
Curbs and Parapet	Cast in place R/C parapets of 2.5 feet high.
Span Included in Study	12E to 15E

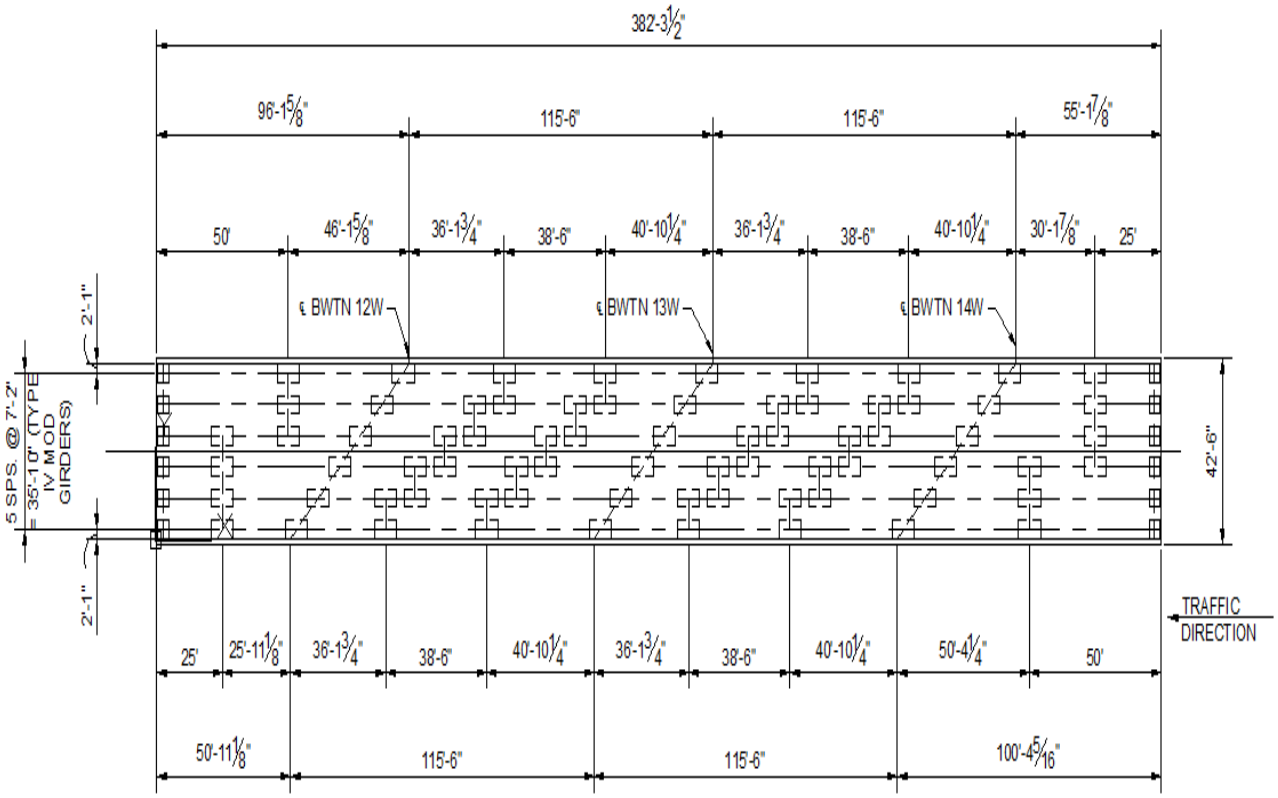

Figure 3
Plan view of the bridge

Instrumentation of the Bridge

Bridge Diagnostics, Inc. (BDI) was contracted by Louisiana Tech University to furnish and install a high-speed bridge monitoring system on the US 90 over the LA 675 Interchange in New Iberia, LA. This project involved two phases of installation. During the first phase, BDI installed 26 strain transducers and two data loggers along with a solar panel and battery backup system. The second phase consisted of installing an additional 16 strain transducers, a third data logger, and a high-speed digital camera to capture images of overloaded vehicles as they cross the bridge. In Figure 4, one of the data logger systems is shown in the picture as well as the battery at the lower part of the data logger box. In Figure 5, the solar panel for the energy supply to the monitoring system and the camera for taking photographs of the heavy trucks are also shown.

Figure 4
Data logger for the strain transducers

Figure 5
Installation of solar panel and the camera

A plan view of the strain transducers installed in the various components of the bridge is shown in Figure 6. In Figure 7, the cross sectional view of the instrumentation is shown. The strain gauges were installed under the bottom flange, the side of the top flange of the girder, in the diaphragms, in the decks, in the web, and in the bents. The transducers that were installed under the bottom flange of the girder at the midspan measure the maximum strain in

the girder. The transducers that were installed at the side of the top flange helped determine the location of the neutral axis of the composite section of the beam and the deck. If the readings of these transducers are close to zero then the neutral axis likely exists close to the line of these transducers. Similarly the transducer in the deck measured the deck strains. In Table 2, the details about the strain transducers are listed. All the strain transducers, according to their numerical identification number and their location and exact position in the bridge, are listed in this table. Figure 8 shows strain transducers installed in the field.

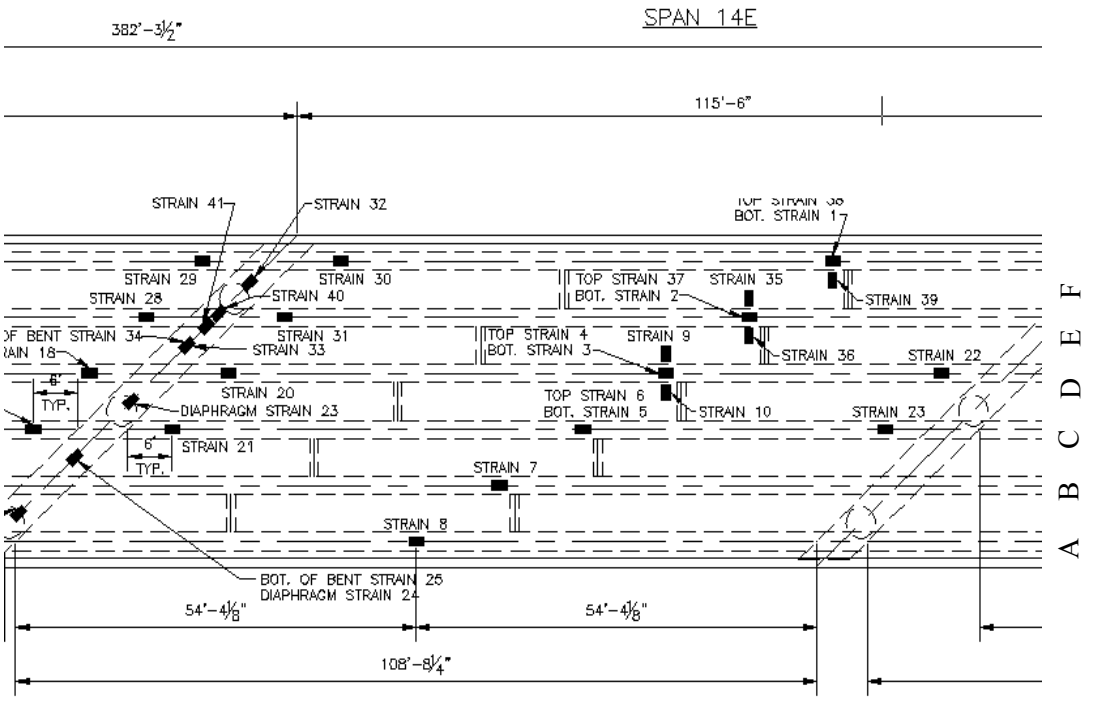

Figure 6
Instrumentation plan of the bridge-top view

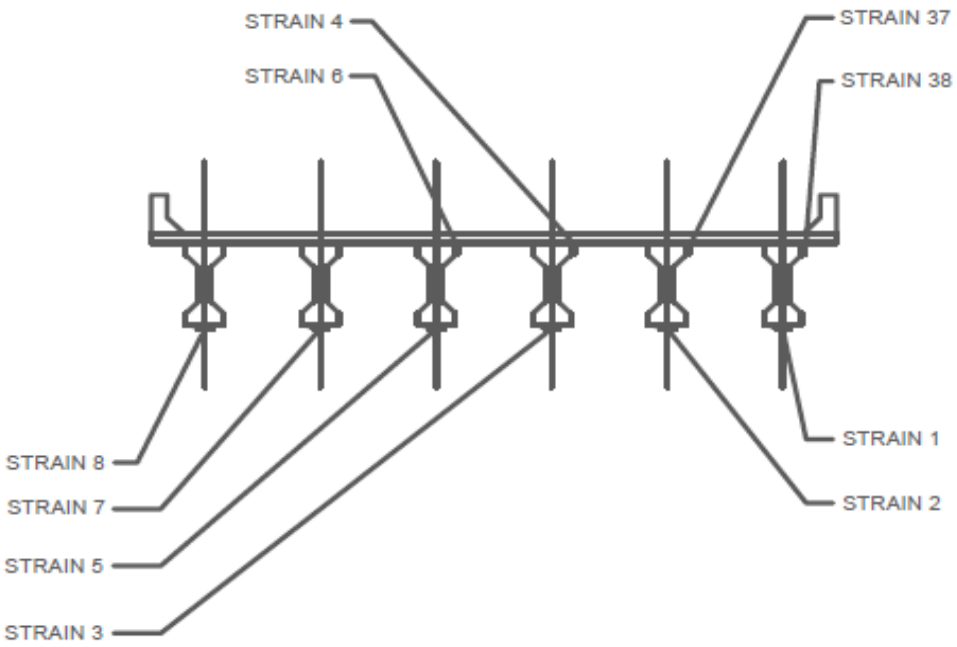

Figure 7
Instrumentation plan of the bridge- section view

Table 2
Position and location of the strain transducers in different part of the bridge

Girder	Strain	Location (ft.)	Description
A	8	54'- 4" from both supports (middle of span 14E)	Bottom of Girder
B	17	53'- 3" from both supports (middle span 13E ***Trigger 18μs)***	Bottom of Girder
	7	Middle of Span 14E	Bottom of Girder
C	16	Middle of Span 13E	Bottom of Girder
	19	6' left to the support between span 13E and 14E	Bottom of Girder
	21	6' right to the support between span 13E and 14E	Bottom of Girder
	5	Middle of Span 14E	Bottom of Girder
	6	Middle of Span 14E	Top Flange outside of girder
	23	6' left to the support between span 14E and 15E	Bottom of Girder
	12	37'-5 1/2" from both supports (middle of span 15E)	Bottom of Girder
D	15	Middle of Span 13E ***(Trigger 18μs)***	Bottom of Girder
	18	6' left to the support between span 13E & 14E	Bottom of Girder
	20	6' right to the support between span 13E & 14E	Bottom of Girder
	4	Middle of span 14E	Top Flange Outside of Girder
	3	Middle of span 14E	Bottom of Girder
	22	6' left to the support between span 14E & 15E	Bottom of Girder
	11	Middle of span 15E	Bottom of Girder
E	14	Middle of span 13E	Bottom of Girder
	28	Left to the support between span 13E & 14E	Bottom of Girder
	31	Right to the support between span 13E & 14E	Bottom of Girder
	2	Middle of span 14E	Bottom of Girder
	37	Middle of span 14E	Top Flange Outside of Girder
	41	At support between span 13E & 14E	Web Inside of Girder
	40	At support between span 13E and 14E	Web Inside of Girder
F	27	Middle of span 13E	Bottom of Girder
	29	Left to the support between span 13E & 14E	Bottom of Girder
	30	Right to the support between span 13E & 14E	Bottom of Girder
	1	Middle of span 14E	Bottom of Girder
	38	Middle of span 14E	Top Flange Outside of Girder
	42	At support between span 13E & 14E	Web Inside of Girder
Deck	10	17" from top flange inside of girder D (between girder C & D)	Bottom of Deck
	9	17" from top flange outside of girder D (between girder D & E)	Bottom of Deck
	36	20.25" from top flange inside of girder E (between girder D &E)	Bottom of Deck
	35	19.5" from top flange outside of girder E (between girder E & F)	Bottom of Deck
	39	21.5" from top flange inside of girder F (between girder E &F)	Bottom of Deck
Diaphragm	26	At support between span 13E & 14E (Between girder A & B)	Bottom Middle of Diaphragm
	24	At support between span 13E & 14E (Between girder B & C)	Bottom Middle of Diaphragm
	23	At support between span 13E & 14E (Between girder C & D)	Bottom Middle of Diaphragm
	33	At support between span 13E & 14E (Between girder D & E)	Bottom Middle of Diaphragm
	32	At support between span 13E & 14E (Between girder E & F)	Bottom Middle of Diaphragm
Bent	25	Between girder B & C (Bottom of bent)	Bottom Middle of Pile Cap
	34	Between girder D & E (bottom of bent)	Bottom Middle of Pile Cap

Figure 8
Photo of strain gauge installed in the field

The overall system was designed to capture "events" based on a trigger limit (strain magnitude) on two mid-span bottom strain transducers. These two are transducer #15 and #17. Transducer #15 is on Girder D and Transducer #17 is on Girder B. These two sensors are in Span 13E (one under the left lane and one under the right lane). A trigger limit of 18μs (microstrain) was defined for those sensors based on live load tests, practical experience, and theoretical analyses. Whenever the trigger limit exceeded the value of 18μs, the monitoring system recorded a block of data. This block included a predefined amount of data before and after a trigger occurred. Along with saving the block of data, the camera mounted on the bridge also takes a photo of the passing truck with a time stamp on it. This photo is automatically saved with the strain data and gives researchers some idea about the axle orientation of the vehicle passing over the bridge. The user can configure the trigger limit and the size of the data block at any time.

In order to support the data handling process, a live data monitoring website that manages the structural monitoring project was developed and can be accessed from anywhere in the world. It provides access to up-to-date data and automatically alerts the appropriate personnel if data exceeds any predefined limits. This entails everything from alerting a field technician that a data logger battery voltage is low to informing an analysis engineer if a sensor is outside the predefined limits. The website's time-based graphing utility facilitates easy data analysis and comparison along with allowing the user to view anywhere from five minutes to one year's worth of data in a given plot. The website also allows the user to view desired data in a table form as well as save the data to a text file for their own records and use.

Since the structural monitoring system was outfitted with a wireless communication link, its operation can be handled through the BDI Monitoring website. The initial layout of the data organization and reviewing options was configured for the bridge. Usernames and passwords were provided so the researchers could begin the data handling procedures from their offices.

Field Test

A field test was done to verify the finite element model simulated in GTSTRUDL. A test truck fully loaded with sugarcane was weighed in a weighing station and the 100-kip gross vehicular weight was confirmed and matched with the theoretical load distribution for the 3S3 truck. The distance between the axles and the wheel spacing was also measured. According to theoretical analysis, the driving path of the truck on each lane for the test was determined beforehand. A schematic layout of the wheel path of the test truck on each lane is shown in Figure 9. The schematic layout of the test truck is show in Figure 10.

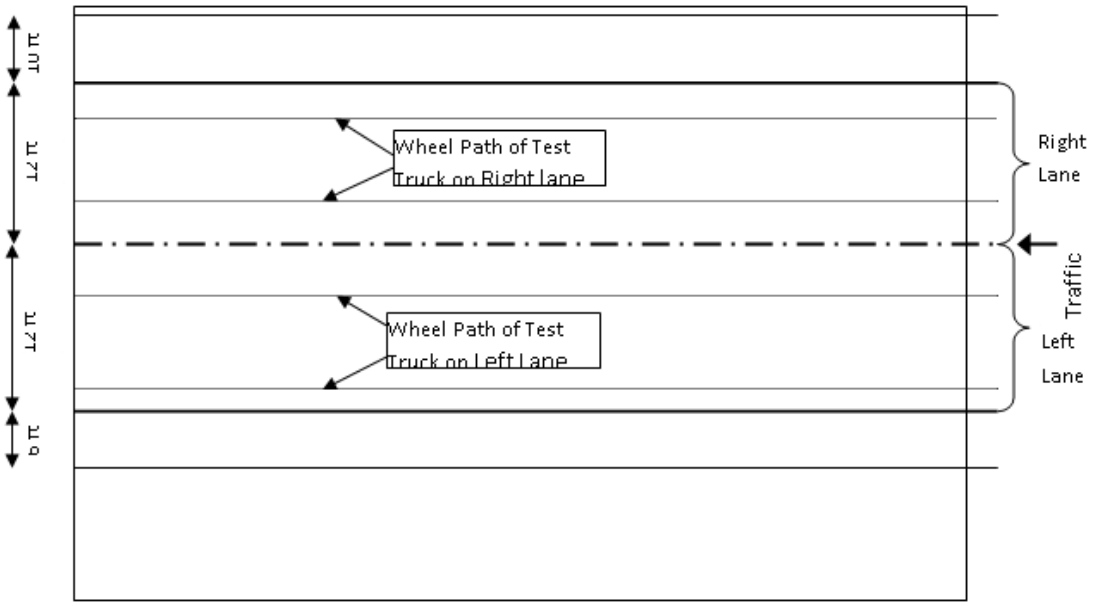

Figure 9
Schematic layout of the wheel path of the test truck on the bridge

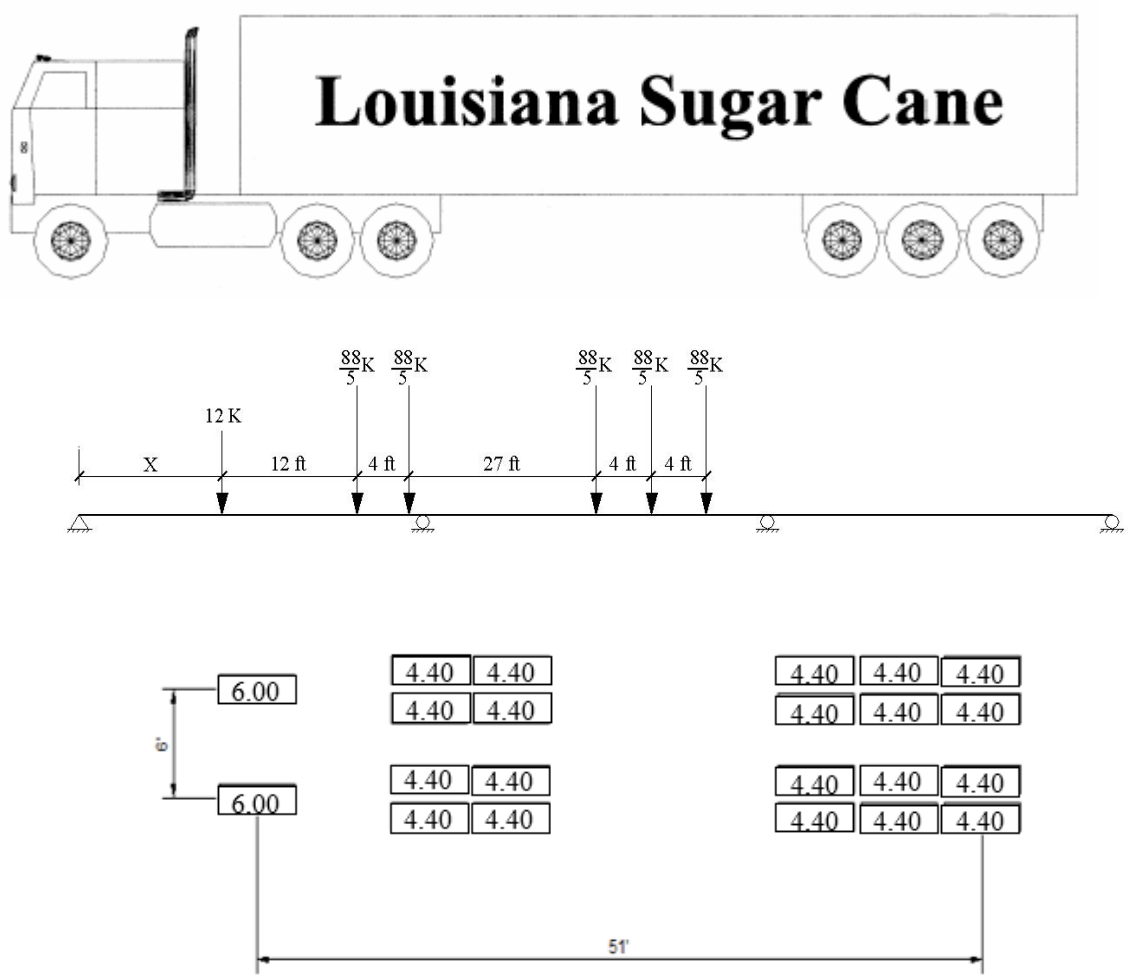

Figure 10
Schematic layout of the 3S3 – 100 kip test truck

The truck was driven over the bridge on different lanes and at different speeds. The bridge was closed to normal traffic for the duration of the test. The test information is presented in Table 3.

Table 3
Summary of the live load test information

Test	Type	Lane	Speed
2	Controlled	Inside	55mph
3	Controlled	Outside	5 mph
4	Controlled	Outside	55mph
5	Controlled	Inside	5mph
7	Auto Triggered	Outside	55mph
8	Auto Triggered	Inside	55mph

The live load test was mainly divided into two parts: controlled tests and auto triggered tests. A controlled test means that there was no triggering limit for the triggering gauge. The auto triggered test was performed in order to make sure that the triggering gauge worked and the system collected data correctly. Two different values of vehicle speed were selected, about 5 miles per hour and about 55 miles per hour. This was done in order to understand the effect of the impact of truck speed on the strain transducers. From Table 3, Tests 2 through 5 were the manual controlled tests and Tests 7 and 8 were the auto triggered tests. After the necessary calibration, four tests were made (Tests 2 through 5) on the bridge, two on the left lane and two on the right lane with slow (5 mph) and high (55 mph) speeds. Data was recorded for these four tests through the monitoring system. Then another two tests were performed by setting the triggering limit of transducer #15 and #17. The test on the left lane verifies for the triggering transducer #17, and the test on the right lane verifies for the triggering transducer #15.

During the live load tests, the strain readings were reviewed to determine the contribution of each girder to the behavior of the bridge as a system. The strains at the bottom of the girders in the middle of span 14 are presented in Figures 11 and 12. The results indicate that all the girders are in the same state of strain, tension or compression, and the magnitude of the strain in each girder is proportionate to its distance from the axle of the truck. This confirms that the load applied to the bridge is distributed between the girders based on their location and spacing.

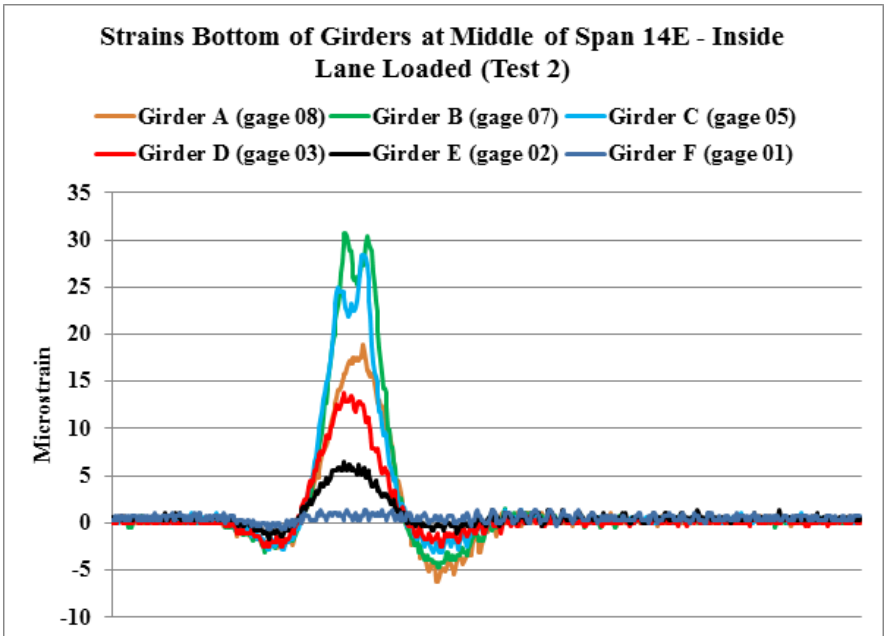

Figure 11
Strains at the bottom of girders in middle of Span 14E during Test 2

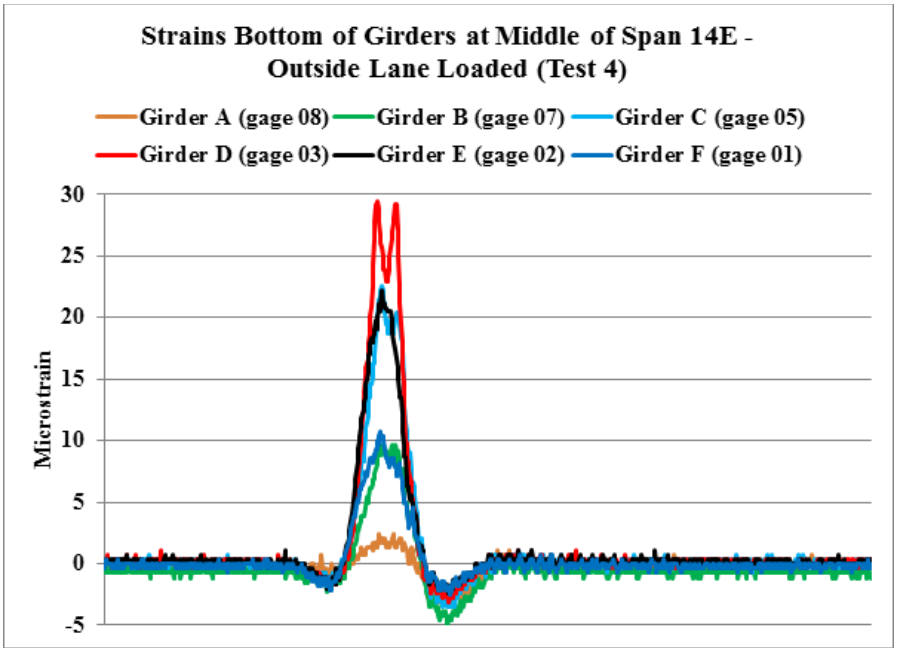

Figure 12
Strains at the bottom of girders in middle of Span 14E during Test 4

During the test, the camera implanted on the bridge took a photograph of the test trucks. Figure 13 shows the test truck travelling on the inside lane (left lane) on its predefined wheel path. Figure 14 shows the same test truck on its defined wheel path on the outside lane (right lane). The time stamp is shown on each of the two photos indicating the date and time of the test.

Figure 13
Photo of the test truck on left lane taken by the implanted camera

Figure 14
Photo of the test truck on right lane taken by the implanted camera

Analysis Overview

The finite element analysis was used to generate a model and analyze the responses of the bridge under different loadings. The finite element model of the bridge was used to determine the effects of HS20-44, 3S3, GVW-148 Option-1, and GVW-148 Option-2 trucks on the bridge. Four different cases were considered for each type of truck. For Case-I and Case-II, the truck loading was on the left lane of the eastbound roadway of the bridge. For Case-III and Case-IV, the truck loading was on the right lane of the bridge. In Case-I and Case-III, the truck loading produced the maximum positive moments in the girders, and in Case-II and Case-I, the truck loading produced the maximum negative moments in the girders. In Table 4, the different load cases are shown. The locations of the truck loading on the bridge deck to produce maximum and minimum stresses in the girders were determined using the theory of influence lines with the use of the GTSTRUDL moving load analysis tool.

Table 4
Different load cases of trucks on the bridge

Truck Location	Criteria	Case
Inside Lane (Left Lane)	Max Positive Moment	Case I
	Max Negative Moment	Case II
Outside Lane (Right Lane)	Max Positive Moment	Case III
	Max Negative Moment	Case IV

For each of the four different kinds of trucks, finite element analysis was made for each case. A total of 16 models were run and the responses of the truck loads were observed from the output of the GTSTRUDL finite element analysis. The effect of heavy truck loads on the bridge were then determined based on the stresses and deflection in the girder and in the deck. The study considered the following four different truck load configurations:

- HS20-44: GVW= 72 kips as shown in Figure 15.
- 3S3: GVW = 100 kips as shown in Figure 16.
- GVW-148 Opt-1: GVW =148 kip (100 ft.) as shown in Figure 17.
- GVW-148 Opt-2: GVW =148 kip (92 ft.) as shown in Figure 18.

The truck GVW-148 Opt-1 and GVW-148 Opt-2 have the same gross vehicular weight of 148 kips but the only difference between them is GVW-148 Opt-2 truck is shorter in length than GVW-148 Opt-1 truck.

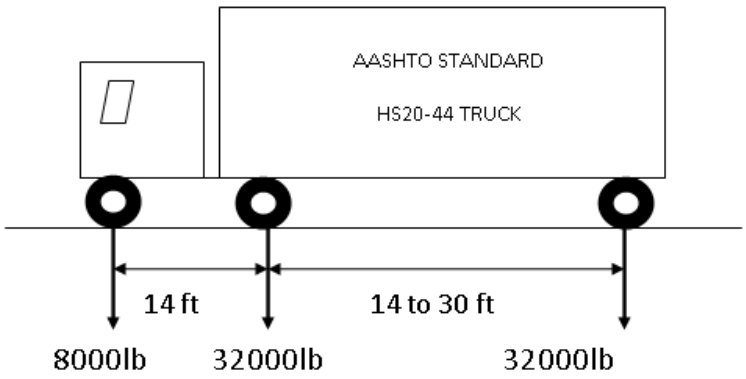

Figure 15
AASHTO standard HS20-44 truck

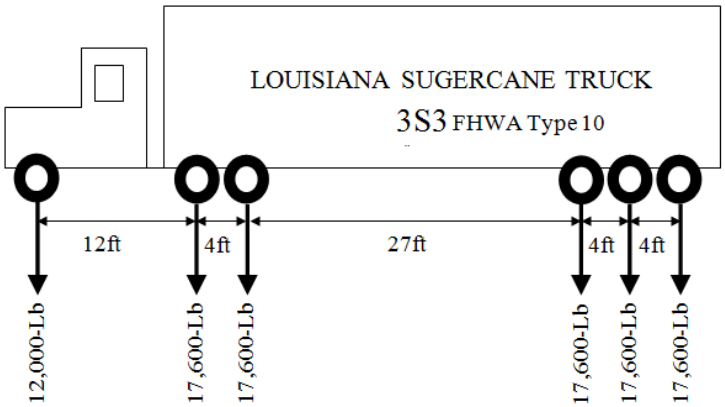

Figure 16
Louisiana sugarcane truck 3S3 with GVW=100,000 lb.

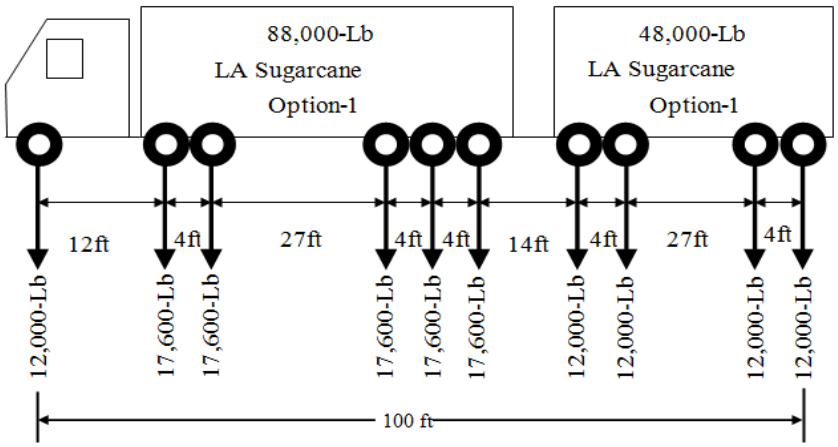

Figure 17
Louisiana sugarcane truck GVW-148 Opt-1

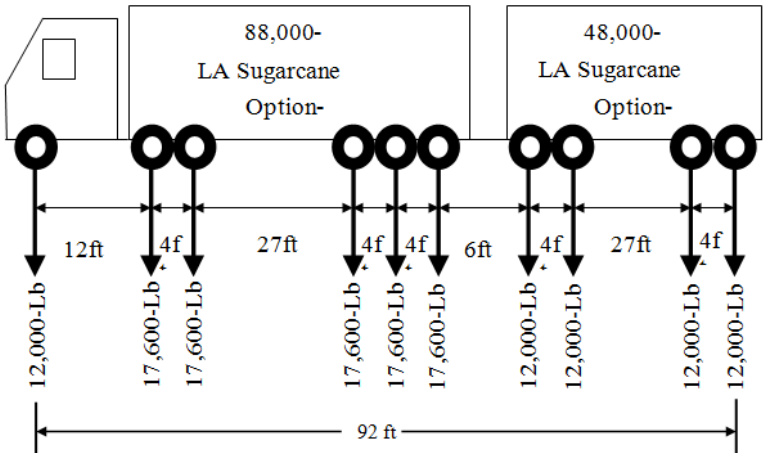

Figure 18
Louisiana sugarcane truck GVW-148 Opt-2

Method of Approach

The finite element method is one of the most popular and widely used methods to analyze complex structures where different elements of the structure act in correlation and manual calculation is very cumbersome and sometimes almost impossible. In this project, GTSTRUDL was used to simulate and analyze the models of the bridge. Three elements were chosen from the GTSTRUDL element library to build the model. Element type IPSL (Iso Parametric Solid Linear) is a kind of tridimensional element that was used to model the girder part of the bridges. The element type SBCR is a (stretch and bending couple response) capable element and the deck of the bridge was modeled using this element. The prismatic space truss element was used to model the diaphragms of the bridges and also used to model the connections between the deck and the girder. Arrangement of a typical plate girder is shown in Figure 19.

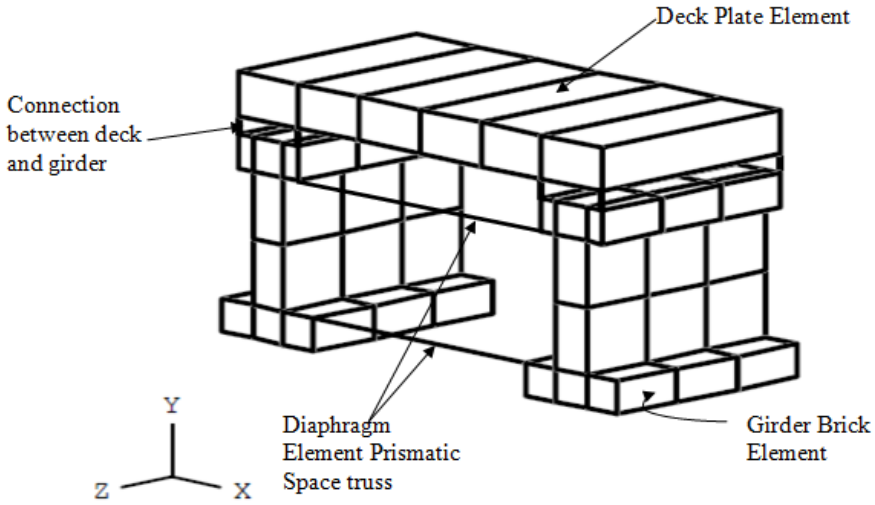

Figure 19
Schematic view of different elements used for finite element modeling of the bridge

TRIDIMENTIONAL Girder Element Type IPSL

IPSL is a tridimensional eight node brick element that specifies problems where a three-dimensional state of stress exists in the structure. The elements are solid with three degrees of freedom per nodal point. The degrees of freedoms are u_1, u_2, and u_3, which are in X, Y, and Z directions, respectively. Only loadings, which are concentrated loads and temperature changes, can be applied on the nodes. Moment type loads are not possible to apply on the nodes. The element itself can take body loads, surface loads, and edge loads.

GTSTRUDL can list the outputs from the IPSL element in different ways. It can list three dimensional displacements and reactions (if defined as supports) of the nodes. It also gives the average value of strains and stresses of each node (at the middle surface of the element). Principal stresses, strains, and von Mises stresses at the nodes can also be generated as outputs.

PLATE Deck Element Type SBCR

The SBCR plate elements is a two-dimensional element that is a combination of plane stresses and plate bending elements. This element is very useful to model and analyze curved and flat shells. This element has four nodes and it has five (u_1, u_2, u_3, u_4, u_5) or six (u_1, u_2, u_3, u_4, u_5, u_6) degrees of freedom on each node, where u_1, u_2, u_3 are displacements and u_4, u_5, u_6 are rotations about X, Y, and Z axes, respectively.

The SBCR plate element can take in plane and/or bending types of loading. Joint loads that this element can take are concentrated loads, temperature loads, and temperature gradient loads. The element loads it can take are edge loads, surface loads, and body loads. The SBCR element is restricted to a rectangular shape. GTSTRUDL can list the in-plane stresses at the middle surface of the element. It can also list moment resultants, shear resultants, and element forces at each nodal point of the element.

Prismatic Space Truss Members

Prismatic space truss members are used in those cases where the component of the structure is expected to take axial force only. It cannot take moment loads and it can take force loads only at the ends, but in the output it can only give an axial force. Self-weight can also be generated in prismatic space truss members.

Prismatic properties can be assigned directly for this element. The section properties are constant through the length of the member. The material properties can be assigned or GTSTRUDL can generate the default properties.

Modeling Assumptions

In order to facilitate the modeling and simulate the actual condition without hampering the results, the following assumptions are made:

- The slab has a uniform thickness over the width and length of the bridge
- All the girders are at the same level (no camber), identical, and parallel to each other
- The girders are continuous over the support bents
- The diaphragms are subjected to axial force only
- The parapet cross section is rectangular
- The trapezoidal portion of the girder section is assumed as rectangular
- A full composite action is assumed between the girder and the deck

Bridge Geometry

Four spans of the eastbound part of the bridge are evaluated. These four spans are continuous over the intermediate supports and at the two ends it has expansion joints. The four spans of the bridge are supported by five bents, which are the subject of our investigation. The total length of this part of the bridge is 382 ft. and 2 ½ in. and the maximum length of the spans are 115 ft. and 6 in. It has six girders equally spaced and all are modified AASHTO Type IV girders. The thickness of the deck is 7 ½ in. and has a cantilever portion with a parapet at the end. The spacing of the girders is 7 ft. and 2 in. Among the five bents of the bridge, the intermediate bents are skewed in an angle of $41^0 25' 52.5''$ perpendicular to the centerline of

the roadway. The continuous diaphragms and the slabs were casted at the same time in order to ensure continuity over the supports. The girder is connected with the slab through shear connector so that continuous action between slab and the girders is confirmed.

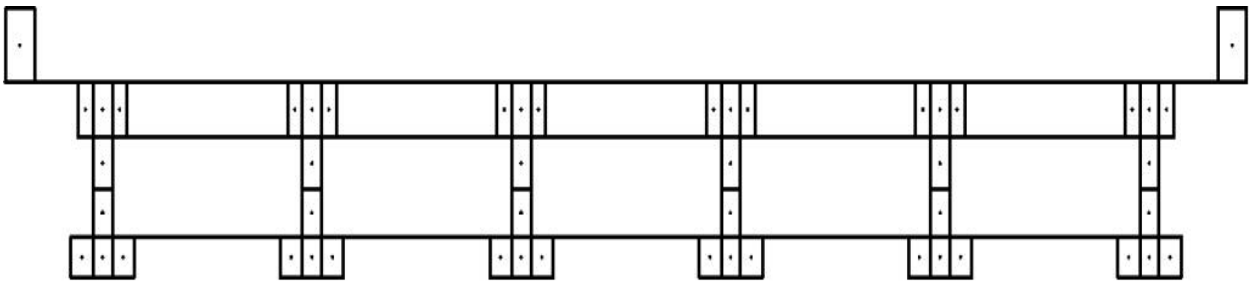

Figure 20
Typical cross section of the finite element model of the bridge

Material properties of the bridge were used in the finite element model of the bridge. The girders are made of high strength concrete with a compressive strength of 7500-psi based on project documents *[6]*. The other components of the bridge, like diaphragm, deck, and parapet, were modeled with a concrete compressive strength of 4500 psi. The elastic modulus was set in the GTSTRUDL input file according to the compressive strength of the components.

As mentioned earlier, the diaphragms were modeled as a prismatic element. The end diaphragms and the continuous diaphragms were modeled with two prismatic space truss members: one in the bottom connecting the top corner of the two adjacent bottom flanges and another at the top connecting the bottom corner of the top flange of two adjacent girders. The cross sections of the prismatic members were taken equal to the cross sectional areas of the diaphragm, but the continuous diaphragms were modeled with four prismatic members unlike two members in end diaphragms and intermediate diaphragms. Here, two prismatic space truss members connected the bottom flanges and two space truss members connected the top flanges. The total cross sectional area of the four members is equal to the cross sectional area of the continuous diaphragm and all four are of equal length.

The diaphragms are modeled in this manner because the axial forces in these members will convey information that is useful to determine whether the section is acting as a composite section. If tension forces are produced in bottom/top and compression in the other member then the neutral axis is somewhere between the two prismatic members. If both of them are either in tension or in compression, then it can be concluded that the neutral axis is not located between the two members and the composite action may not be taken place.

Prismatic members are also used to connect the deck plate elements and the girder brick element. This prismatic space truss member is modeled with a very small length (3/64 in.) and a relatively high cross sectional area. The small length of this member will ensure the deck and girder to stay very close to each other, which is very important to ensure the composite action, and it works as a shear connector.

The parapet was also modeled by using girder brick elements, and it was also connected with the deck using prismatic space truss members.

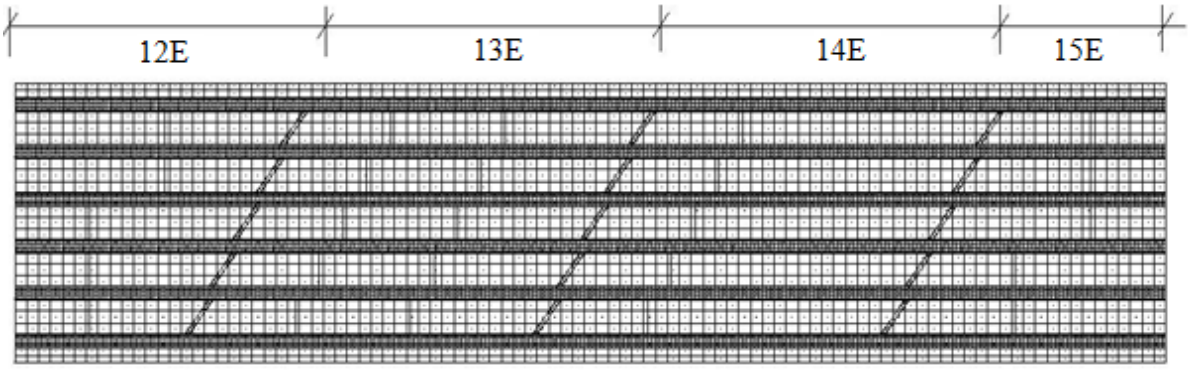

Figure 21
Plan view of the finite element model of the bridge

Aspect Ratio

The ratio between the maximum and the minimum dimension of a finite element is called the aspect ratio of the elements. This ratio must be less than or equal to four. If the ratio is more than four, the results are not reliable. An aspect ratio of one is desirable as it gives the most accurate result. However, a ratio up to four is quite acceptable.

$$\text{Aspect Ratio} = \frac{\text{Largest dimension of the element}}{\text{Smallest dimension of the element}}$$

In the finite element model, the maximum aspect ratio was 3.93 in the parapets and the minimum aspect ratio was 1.74 in the girders.

Boundary Conditions

The length of each IPSL element that compiles the girder is 15.75 in. The bottom flange of the girder has three elements. Thus the girder bottom has four nodes every 15.75 in. along its length. The five supports in the bridge were already described. The end supports of each girder are modeled with two lines of nodes, which means eights nodes. The intermediate supports are modeled with four lines of nodes, which results in 16 nodes. This was done in order to simulate the bearing pad under the girder over the bents. All degrees of freedom (u_1,

u_2, u_3) of these joints are restrained in order to make the girder continuous over the supports. These nodes act like pin supports, which means rotations are allowed. Another boundary condition that was used was at the ends of the bridge between the connection of the deck and girder. Researchers used a prismatic member to connect the girder and the deck and at the end of the bridge. Researchers released the Force Y, Moment Y and Moment Z at the joint that connected the prismatic member and the deck member at the two ends of the bridge.

Moving Load Analysis

In order to determine the critical location for all different types of trucks on the bridge deck, an influence line analysis was performed. These critical locations of the trucks gave researchers the maximum moment, maximum shear, and maximum deflection that could be generated in the bridge girders and deck.

To perform this analysis, a GTSTRUDL moving load generator is used. This tool is very useful to determine the critical locations of truck on a single continuous beam. In this investigation, there were six girders and researhers performed a moving load analysis on the second (Girder B) and the fourth girder (Girder D) to determine the location of the truck in the left lane and in the right lane. A simply supported continuous beam was taken and the span length was determined from the drawings of the second and fourth girders.

In the GTSTRUDL moving load generator, the trucks loads are defined in the beginning. The axle loads are assumed as concentrated loads. GTSTRUDL can move the truck over the continuous span in such a way that the truck starts travelling from one end of the bridge and stops at one foot intervals. For every stopped position of the truck, a shear force and moment diagram was drawn. GTSTRUDL also generates a load number for each position of the truck. Thus for every load number researchers had a moment and shear diagram. Inversely, for every moment and shear diagram they had a load number, which indicates the position of the truck on the bridge. Moment and shear envelopes can be produced in GTSTRUDL for all the loadings generated by the truck. From that envelope, researchers can find the maximum moment and shear and thereby find out the load by which this maximum value of moment and shear is generated. Ultimately, the location of the truck can be found as each load number represents a position of the truck on the bridge.

The location of the truck across the width of the bridge is also determined by using the GTSTRUDL moving load generator. Here there are six girders. Researchers considered a continuous beam with five spans over six pin supports. Thus the location of the truck across the bridge was determined. By superimposing the longitudinal and the transverse location of the truck, researchers can finally determine the location of the truck on the deck that will produce maximum moment and shear force. Figure 22 shows the travelling of the truck

along the length and across the width of the bridge. Figure 23 shows the placement of the wheels on the deck.

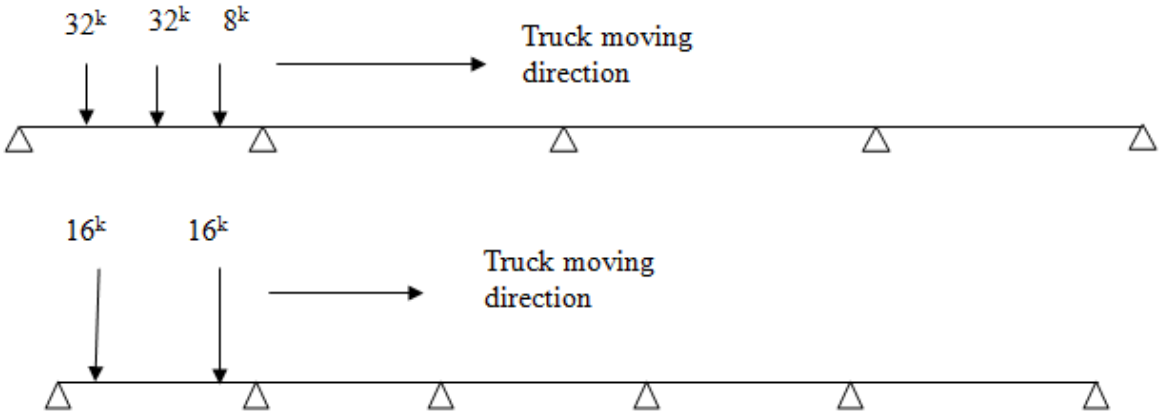

Figure 22
Moving load analysis for HS20-44 truck in longitudinal and transverse direction

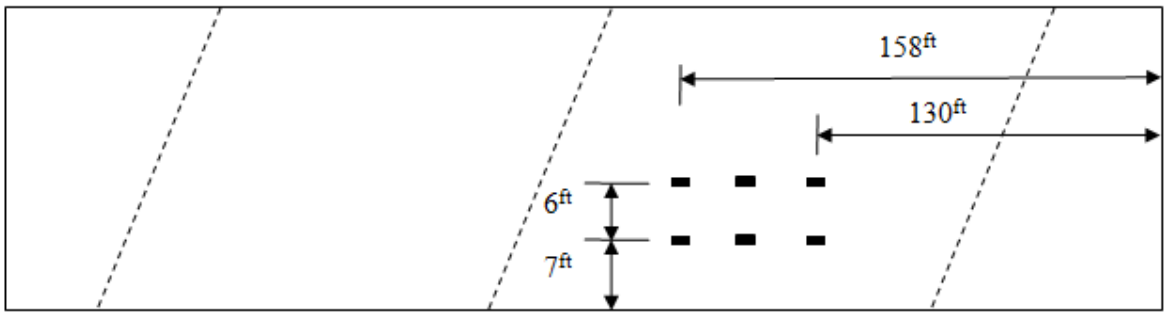

Figure 23
Placement of wheel loads on left lane of span 14E of HS20-44 truck

Regression Analysis for the Truck Weights

The installed monitoring system provided the opportunity to explore the use of a strain gauge measurement system to determine truck weights and possibly be used as a means to help replace the expensive weight measuring systems. For this experiment to be proven plausible, a regression analysis was performed on several data sets including: a controlled test and live field data.

One of the current methods of measuring truck weights in the state of Louisiana is the weigh-in-motion system. This system weighs a semi-truck while it is traveling along the interstate system. The system is only implemented in certain areas of the state, mainly on interstate sections on level ground. The areas that do not have weigh-in-motion still use the weigh stations along the interstate. Unfortunately, this type of system has limited applications and

cannot be used on overpasses and bridges. In order for the test to be successful, a regression analysis needed to be performed on live field test data and the controlled (November 2010) live load test. The live load test was designated the control test data since the truck's weight and speed were predetermined. These values were then compared to the live field data.

In this part of the study, data from Gauges 14, 17, 40, 41, and 42 were of primary interest. The gauge location and description can be seen below in Table 5 below.

Table 5
Strain gauge location and description

Girder No.	Strain Gauge No.	Location	Description
D	40	At support between Span 13 & 14	Web inside of girder
E	41	At support between Span 13 & 14	Web inside of girder
F	42	At support between Span 13 & 14	Web inside of girder
E	14	Middle of Span 13	Bottom of girder (Outside Lane)
B	17	Middle of Span 13	Bottom of girder (Inside Lane)

The system is activated when one of the two triggering gauges is triggered by a passing truck. Once these two strain gauges are activated, an electronic signal is sent to the other 40 strain gauges installed on the bridge. At the same time, another signal is sent to the camera positioned on the side of the bridge producing an image similar to Figure 24 (see Appendix F for other truck types.) Along with the picture of the truck, a corresponding time stamp is taken of the truck which was then used to find the correct strain values.

Figure 24
3S3 Truck photograph with time stamp in right hand lane

Figure 25
3S3 Truck photograph with time stamp in left hand lane

Truck Parameters

In order for the regression analysis to properly function, it is necessary to have different truck types. After reviewing all of the photographs, the four truck types were determined: 3S3 (Type 8), 3S2 (Type 6), FHWA Class 6 (Type 2), and FHWA Class 7 (Type 18). The truck types listed are based on the Federal Highway Administration (FHWA) and the Louisiana Department of Transportation and Development (LADOTD) labeling system *[7, 8]*. An addition was made to these truck types by including 3S3 and 3S2 sugarcane trucks, bringing the total to six. Because Louisiana has a law (RS 32:71) against driving trucks in the left-lane, fewer observances of trucks in the left lane were made. Other truck parameters that were considered were the legal loads of these truck types as specified by LADOTD *[8]*. This information can be seen below in Table 6.

Table 6
Truck types and legal weights

Truck Type	Legal Weight (lb.)
3S3 (Type 8)	88,000
3S3 Sugarcane (Type 8)	100,000
3S2 (Type 6)	80,000
3S2 Sugarcane (Type 6)	100,000
FHWA Class 6 (Type 2)	53,000
FHWA Class 7 (Type 18)	61,000

In the November 2010 live load test, a 3S3-sugarcane truck with a weight of 100,000 lb. was used. The two factors that were changed were the truck's speed and position on the bridge. The specific descriptions of each test were discussed previously in the report. Tests 2, 3, 4, 5, 7, and 8 were taken for the regression analysis since the data was for the outside and inside lanes.

Data Collection and Preprocessing

With the pictures and time stamps of the trucks, the data could then be collected from the spreadsheets provided by the monitoring system. In order to prevent any unnecessary data points from disrupting the experimental data, the system was designed to only collect and store an event (i.e., a particular truck type) when a minimum strain was reached. The system was set to activate and record when a strain of 18μs was exerted onto the bridge. This was then taken further by not including any heavy machinery vehicles such as cranes, flatbed trucks, and any truck carrying a wide load. Other cases that were removed included: two

trucks side-by-side and if another vehicle was next to the truck in the photo. The reasoning for this was the two trucks would cause much higher strain values and the resulting data would disrupt the regression model. When obtaining the strain values from the November 2010 live load test, the maximum values for strain gauges 14 and 17 were taken along with the corresponding values for strain gauges 40, 41, and 42. This process was repeated for the field data by finding the maximum strain value of an event. As seen in Appendices G and H each truck had its own event number or stamp number. It was important to connect all of the different strain values with their respective truck type. The complete spreadsheets for the live field data and the November live load test can be found in Appendix G and Appendix H.

Regression Analysis

For this experiment to work, a regression analysis needed to be performed to determine if the truck weights could be found from the strain values. As stated by Johnson and Wichern (1982) "[r]egression analysis is the statistical methodology for predicting values of one or more response (dependent) variables from a collection of predictor (independent) variable values" *[12]*. The main purposes of performing a regression analysis as specified by Kachigan (1982) are: (1) to determine whether or not a relationship exists between two variables; (2) to describe the nature of the relationship, should one exist, in the form of a mathematical equation; (3) to assess the degree of accuracy of description or prediction achieved by the regression equation; and (4) in the case of multiple regression, to assess the relative importance of the various predictor variables in their contribution to variation in the criterion variable" *[13]*. While collecting the data for this experiment, it became apparent that the regression analysis would have to be a multivariate or multiple regression. The difference between a multiple regression and a simple regression is that instead of one predictor variable several predictor variables are used. With a multiple regression, the errors of prediction is reduced and a better accountability for the variance of the criterion variable. Listed below are the equations that were used in this part of the study.

$$y' = a + b_1x_1 + b_2x_2 + b_3x_3 + b_4x_4, \quad (1)$$

where,
a = y-intercept
b_i = slope coefficient (i = 1, 2, 3, 4)
y' = predicted value
x_i = Independent Variable (i = 1, 2, 3, 4)

The standard formula for multiple regression is shown above and used to determine predicted value, y′. Before this equation can be solved, the four slope coefficients, b_i, and the y-intercept, a, have to be calculated. When working with a regression analysis, there is a possibility of errors in predicting y′ which include: the error in estimating the overall elevation or y-axis intercept of the true regression line, a, and the error in estimating the slope, b_i, true regression line. This is why a confidence band is to be implemented into solving for the predicted value. This method is also used when establishing a correlation between the variables. Listed in Table 7 is an explanation of correlation sizes and their interpretations.

Table 7
Interpretation of correlation coefficient

Size of the Correlation	Coefficient General Interpretation
0.8 to 1.0	Very strong relationship
0.6 to 0.8	Strong relationship
0.4 to 0.6	Moderate relationship
0.2 to 0.4	Weak relationship
0 to 0.2	Weak or no relationship

The need for a high correlation will give a more accurate predicted truck weight value. In order to complete the multiple regression analysis the program PASW Statistical Version 18 or (SPSS) was used. For the procedure, the four stains were designated the independent variables (x_1, x_2, x_3, and x_4); whereas, the truck weight was the dependent variable, Y. The reasoning for this setup was that the weight of the trucks was determinant on the four strain readings.

The point of view of the researcher is that it is of practical importance to determine the relationship between truck weights and the stresses recorded by the strain gauges. If a mathematical (equation) relationship can be established, one may then predict truck weight from the stress recorded by the sensor. It is important to note that available data did not have truck weight. What was observed was the stress recorded by the strain gauge at a given location on the bridge, the time when the strain was recorded, and the photographs of the different types of the trucks that were considered. In order to gain information on the weight of the truck, photographs of the truck were used to determine the truck type from which the legal weight of the truck was determined when fully loaded. Six truck types could be determined and therefore six weights. For each weight researchers observed the stresses, positive and negative, for each of the strain gauges listed in Table 5.

Evaluation of Fatigue

Fatigue evaluation of existing bridges has become increasingly important in the field of civil engineering. Within the last half century, several large bridges have collapsed due to fatigue damage. Fatigue is defined as the progressive localized permanent structural change that occurs in material subjected to repeated or fluctuating strains at stresses having a maximum value exceeding the strength of the material. Many mechanical systems incur failure, and fatigue is responsible for approximately 70% of these failures. The fracture of a structural member due to the repeated cycles of load or fluctuating loads is referred to as fatigue failure, while the corresponding number of load cycles or the time in which the member is subjected to these loads before fracture is considered the fatigue life *[14]*.

Fatigue in bridges is a concern when bridge components are subjected to localized cyclic loading. If loads on prestressed girders meet the serviceability criteria then fatigue is not an issue. However, fatigue damage occurs over long periods of time at specific locations, and the fact that bridge components may be susceptible to fatigue does not mean the bridge is inherently unsafe. Signs of fatigue can be identified before problems occur.

Fatigue in Louisiana State Bridges

In response to the SCR 35, the alternative truck-trailer configuration will use extra axles under the load to reduce the impact on Louisiana roads. Ideally, the alternative truck-trailer design, when compared to the traditional truck-trailer will simultaneously decrease the number of trucks and increase the total number of tons of sugarcane that travel on Louisiana roads.

The two new truck configurations recommended are GVW-148 Opt-1 (Figure 17) and GVW-148 Opt-2 (Figure 18), previously shown. Both truck weights will be limited to 100,000 lbs. with a dolly weight to be limited to 48,000 lb. for a total gross vehicle weight (GVW) of 148,000 lb.

The truck configurations proposed are not a FHWA Vehicle Type truck-trailer, and therefore the results of the previous studies, LTRC Reports 418, 425, and 398, need to be re-evaluated using the proposed truck trailer configuration [*1, 3, 5]*.

Identification of Critical Bridges for Study

The critical bridge list was obtained from Technical Report No. FHWA/LA.06/418 [*1*]. The critical bridges in that study were considered to be those located on the roads most traveled by sugarcane trucks. The roads considered were Louisiana state highways, U.S. numbered roads, and interstate highways. The review and selection process was based on two factors:

(1) the amount of sugarcane produced in each parish and (2) the parish's geographic location. The bridges located on these highways were grouped into two different categories based on their structural type for this study. The categories were (1) simple beam and (2) continuous beam.

The methodology used in the analysis phase evaluated the effect of the heavy loads imposed on the bridges from two new trucks designed to carry sugarcane, Louisiana Sugarcane Truck GVW-148 Option 1 with 100 ft. total length and GVW-148 Option 2 with 92 ft. total length (see Figures 17 and 18, respectively). The demand on the bridge girders due to the increased truck loads were calculated based on the inventory information on span type and geometry, i.e., simple span, continuous span, total length, length of main span, and number of approach spans.

From the list of critical sugarcane bridges, only the bridges with a span of 90 ft. (the minimum truck length) or greater were considered for the purpose of this study. They were evaluated using the same procedure discussed in the previous report LTRC 418 [*1*]. The new truck trailer configuration does not impact the previous study for bridges with a span shorter than 90 ft.

Analysis of Bridge Girders

The effects of the increased load on Louisiana bridges were determined by comparing the flexural and serviceability conditions of the bridges under their design load to the conditions under the GVW-148 Options 1 and 2 truck configurations. The effects of the increased loads were determined based on the ratio of the maximum moments for each bridge studied. The design load for the bridge, as listed in the bridge inventory, was used for comparison. The new truck loads were based on the GVW-148 Options 1 and 2 truck configuration as shown in Figures 17 and 18.

Simple Span Bridges. The standard truck configurations HS20-44, as provided in AASHTO, were used for comparison to the two new truck configurations *[10,11]*. The effects of the GVW-148 Opt-1 and Opt-2 truck configurations on the identified bridges were investigated by comparing the flexural, shear, and serviceability conditions. Each of the truck loads were placed on the bridge girder with simple supports and spans greater than 90 ft. Absolute maximum moment of the bridge girder was calculated under the load configuration.

Continuous Span Bridges. The effects of the GVW-148 Options 1 and 2 truckloads on continuous span bridges designed for HS20-44 truckloads were also determined.

Long-term Effects and Cost

The need for a new truck configuration stems from the demand on the truck industry, faced with increasing the gross vehicle weight to get more carrying capacity. Conversely, bridge owners in the United States must control the loading on the bridges to limit the deterioration of the existing bridge infrastructure to keep the structure in safe operating conditions. The long-term effects of heavy trucks hauling sugarcane on bridges and bridge decks play an important role in the bridge life evaluation. Overloaded trucks traveling across these bridges will increase the cost of maintenance and rehabilitation. An accurate estimation for the cost of the damage is hard to obtain since fatigue damage may lead to many actions including repair, testing, rehabilitation, and replacement.

The data from the monitoring system was reviewed and evaluated to determine the effects of heavy truck loads on state bridges. The data between August 2010 and July 2011 was reviewed and strain gauge readings and the associated trucks crossing over the bridge and causing the strain readings, in Gauges 15 and 17, were of 18 micro-strain or larger. The number of trucks causing these events during the day and night is shown in Figure 26. The number of these events occurred during the one year span is presented in Figure 27.

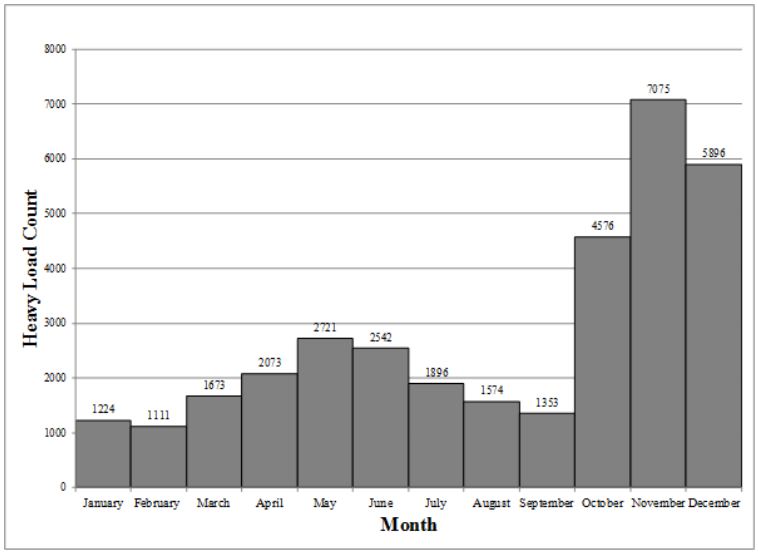

Figure 26
Time/month heavy load count

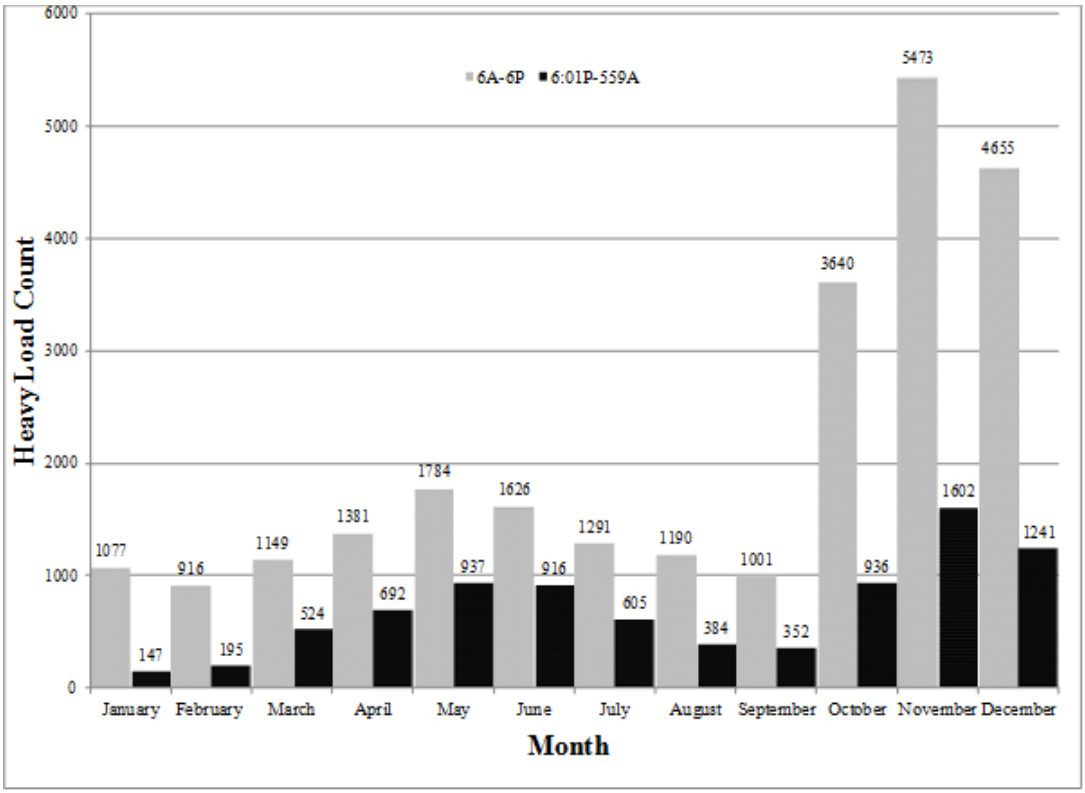

Figure 27
Monthly heavy load count

DISCUSSION OF RESULTS

General Discussion

In order to implement the objectives of this study, a finite element modeling of the bridge, listed in Table 1, was done and tested under different kinds of heavy truck loadings. In this study, the bridge geometry is constant and the truck loadings and its locations were the parameters that are changing. The researchers used four truck types, and each truck was run on four locations of the bridge. The trucks considered in this study were AASHTO HS20-44 Standard truck, 3S3 (FHWA Type 10), GVW148 Opt-1 and GVW148 Opt-2 [*7, 10, 11*]. These truck configurations were already described in previous sections of this report.

The monitoring system installed on the bridge for a long-term effect for heavy truck loads crossing the bridge was used for the live load test. A theoretical analysis was made for the different trucks to determine the location producing maximum positive and negative moment on each lane of the bridge. The wheel paths of the truck on the deck of the bridge in the time of live load test were determined so that the field test conditions matched the conditions of theoretical analysis. The drawings of the instrumentation plan of the bridge are given in Appendix D. Before performing the final analysis of the bridge for heavy trucks, the researchers verified the model by comparing it with the field test made on the bridge using the 3S3 truck. The stains recorded from the live load test and the strains obtained from the FE model were close enough to make it a reliable model.

In this study, four different load cases were considered for the truck loading according to their location on the bridge deck. When the truck is in the left lane (inside lane) of the span 14E producing maximum positive moment in the girders, then it was Case I. Case II deals with trucks located on the left lane but producing maximum negative moments in the girders. Similarly for Case III, the truck was on the right lane (outside lane), creating maximum positive moment in the girders and for Case IV, the truck was on the right lane, creating maximum negative moment in the girders. Finite element analysis of the bridge was done under four different load cases and four different truck loadings. Under each load case the effects (girder stress, girder deflections, and deck stresses) of the four different heavy trucks were listed and compared. The results are presented in Appendix A.

The theoretical results provided an understanding of how the heavy trucks loading affected the stresses and deflection of the bridge components. Based on the theoretical results, a comparison among the different heavy trucks was seen.

Model Verification

Live Load Test on the Bridge

In order to verify the finite element model of the bridge, a live load test was performed. The 3S3 truck that was used for the live load test was driven both in the left and right lane. The wheel path of the test truck was determined previously from finite element analysis. The strain responses of the transducers were recorded and these strain values were matched with the values obtained from finite element analysis. The model was verified for the truck location at the left lane (Cases I and II) as well as for the truck location at the right lane (Cases III and IV).

Truck in Left Lane

Three strain transducers were located at the midspan and at the bottom of the girder B, C, and D. These three girders were directly under the wheel loads of the test trucks. The numbers of the strain transducers located at the bottom of midspan of these three girders were #7, #5, and #3. The maximum positive strains that occurred in these three girders at the time of the test truck passing over the left lane were recorded. These strains were then compared with the theoretical results obtained from the finite element analysis of the model. The results are presented in Figure 28, which shows the theoretical values of the strains are close enough, within 2 micro-strain, to the field test value, so the model can be interpreted as a reliable model.

Truck in Right Lane

As researchers already did for the left lane, the maximum positive strains that occurred in these three girders at the time of the test truck passing over the right lane were recorded. These strains were then compared with the theoretical results obtained from the finite element analysis of the model. The results are presented in Figure 29, which shows the theoretical values of the strains are close enough, within 2 micro-strain, to the field test value and the model can be interpreted as a reliable model.

System Behavior and Load Distribution

The FE model for the bridge was reviewed to ensure that all the components behave as a system and simulate the field responses. The results indicated that all the girders are in the same state of strain, tension and/or compression, and the magnitude of the strain in each girder is proportionate to its distance from the axle of the truck. This confirms that the load applied to the bridge is distributed between the girders based on their location and spacing. Similar behavior was confirmed and presented previously in Figures 28 and 29 of this report.

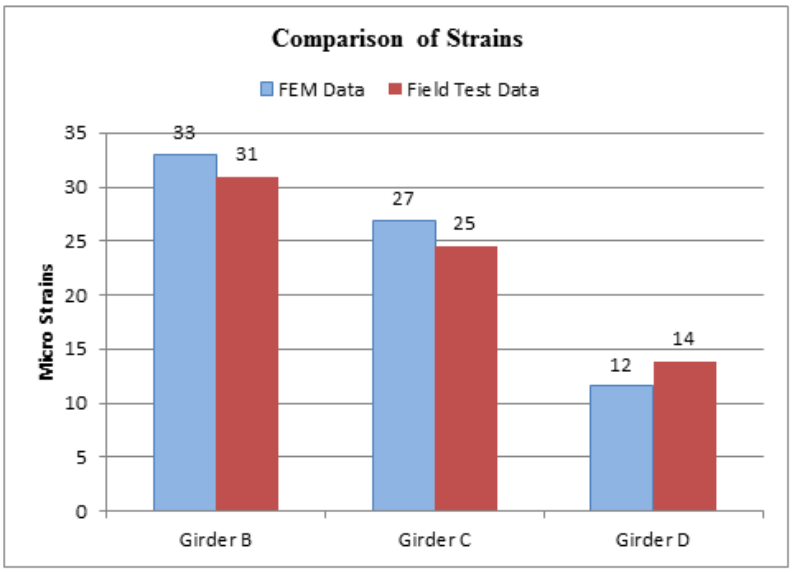

Figure 28
Comparison of FEM strains with field test strains – truck on left lane

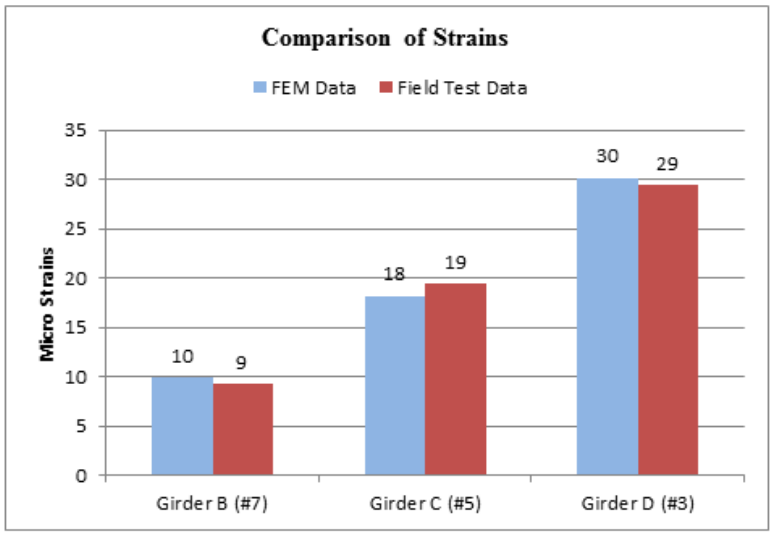

Figure 29
Comparison of FEM strains with field test strains – truck on right lane

Results of Finite Element Analysis for Truck Loading

The bridge in this study has six girders. Researchers selected Girder-B and Girder-C as the critical ones when the truck is in the left lane (Case I & Case II) and Girder-D and Girder-E as the critical ones when the truck is in the right lane. This is because of the change in stresses and deflections due to the different truck loadings, which are significant in these girders. All the stresses presented in the following tables and figures are stresses due to truck live loads only. The results of the other girders are in Appendix A and Appendix B.

Researchers will compare the top girder stresses, the bottom girder stresses and the girder deflections for these girders in this section — as well as the deck stresses for the different kinds of truck loadings.

Comparison of Maximum Stresses in Girders, Left Lane

Figure 30 shows the stress distribution of the bending stress of the bottom fiber of Girder B as a function of distance along the girder. The primary vertical axis shows the stresses in psi and the primary horizontal axis shows the distance of the girder in feet. All the trucks show the same pattern of stress distribution as expected.

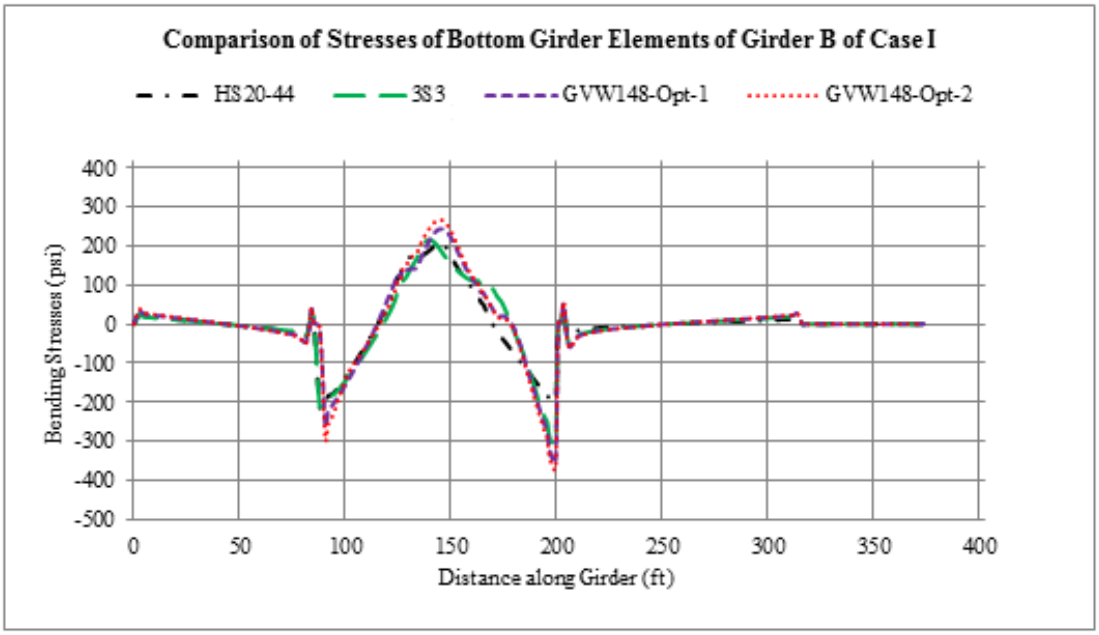

Figure 30
Comparison of bending stress distribution of bottom elements - Girder B of Case I

The length of the girder consists of four spans. Starting from the left, they are: Span 15E, 14E, 13E, and 12E. In the finite element model, all the trucks are located on Span 14E, which is from 85 ft. to 200 ft. and the truck moves from left to right. In Figure 30, the majority of the stress variations occurred in Span 14E due to the presence of the truck loadings on it.

In Figure 31, researchers plotted Span 14E only and can see that for the bottom elements of the girder, the maximum tensile stress occurred at the middle of the Span 14E, and maximum negative stress occurred at the interior part of this girder adjacent to the supports. For further clarification, researchers plotted a blow out of the maximum tensile zone of Span 14E in Figure 32. This blow up is provided to show the stress distribution due to different truck loadings. As the truck loadings increase from HS20-44 to GVW-148 Opt-2, the maximum tensile stress also increases.

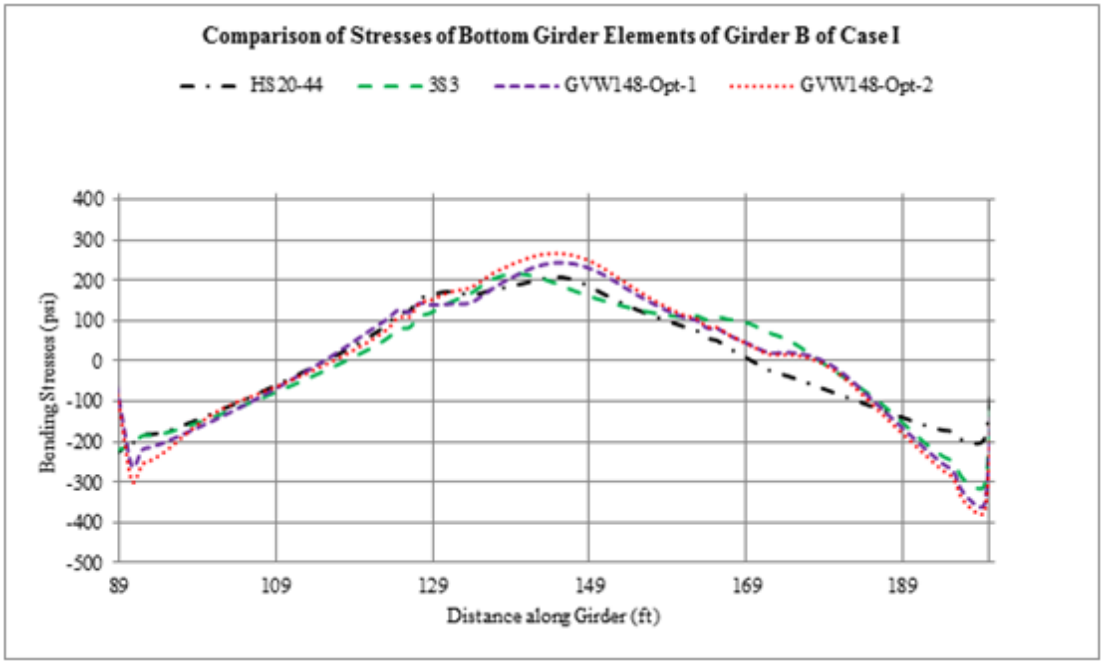

Figure 31
Comparison of bending stress distribution of bottom elements - Girder B of Case I, Span 14E

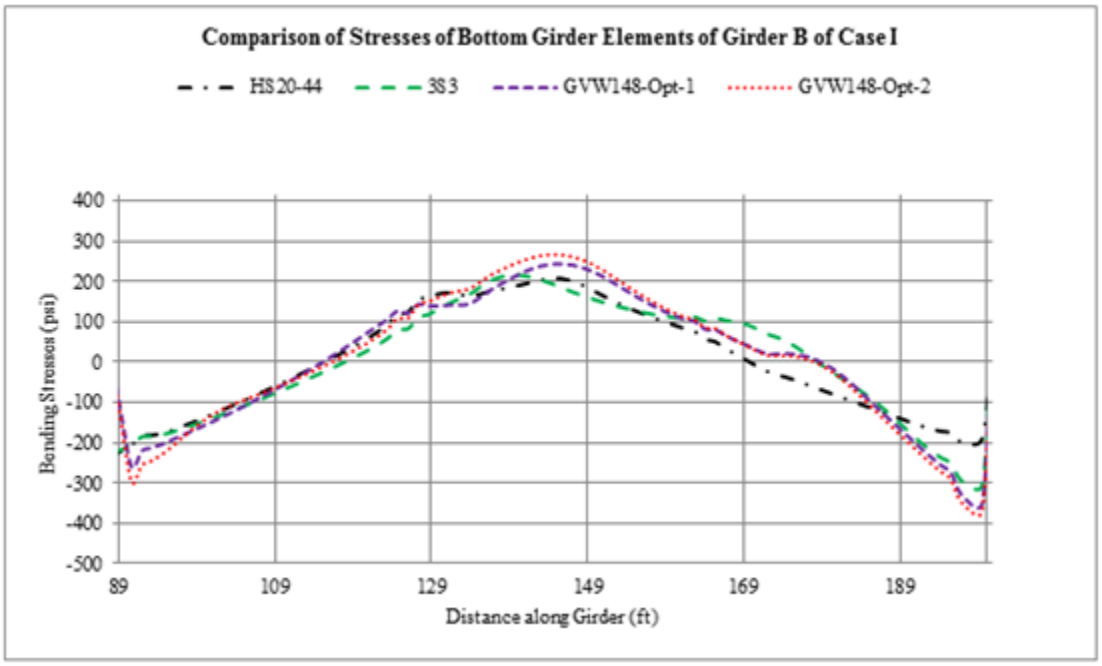

Figure 32
Blow-out showing the tensile stress at midspan of Figure 31

Figure 33 shows the stress distribution of the bending stress of the top fiber of Girder B in Case-I as a function of distance along the girder. Figure 30 and 33 represent the same girder and the same load case but Figure 33 shows the stress comparison of the top girder elements, and Figure 30 shows the stress comparison of bottom girder elements.

In Figure 33, the stress distribution pattern due to different truck loadings is following the same trend as expected. Here the maximum tensile and compressive stresses are occurring at Span 14 E due to the presence of the truck loads in this span.

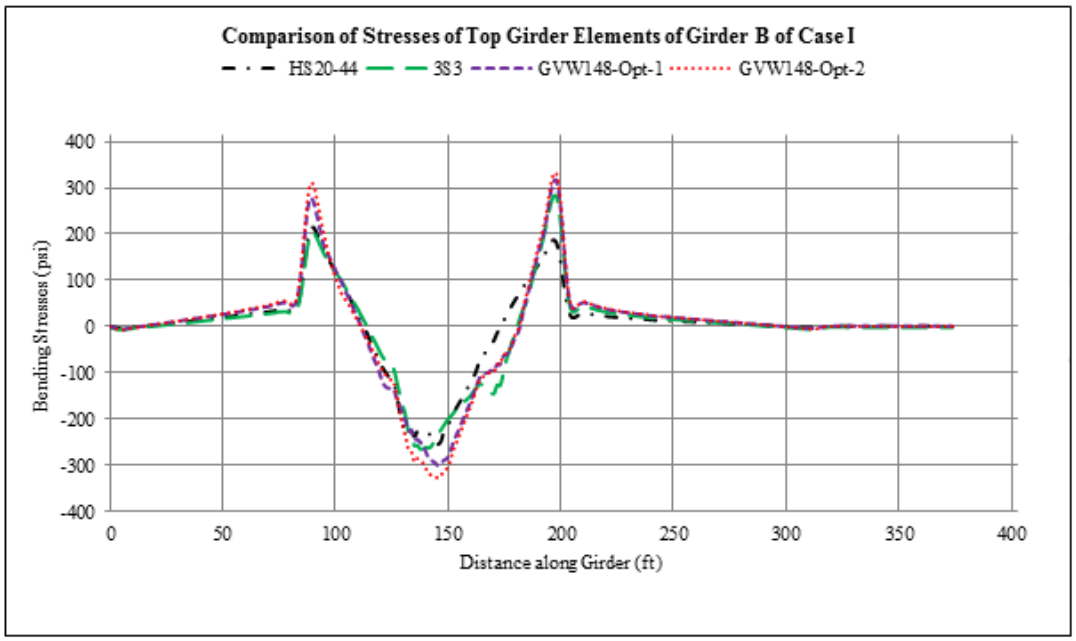

Figure 33
Comparison of bending stress distribution of top elements - Girder B of Case I

In Figure 34, the stress distribution is a function of distance along the girder and is plotted for Span 14E of Case-I. The top elements of the girder were subjected to compression at the midspan and to tension at and over the support. This behavior is completely opposite of what was seen in Figure 31, but this is the expected output. For further clarification, researchers plotted a blow out of the maximum tensile zone of Span 14E in Figure 35. This blow up is provided to show the stress distribution due to different truck loadings. As the truck loadings increase from HS20-44 to GVW-148 Opt-2, the maximum tensile stress also increases.

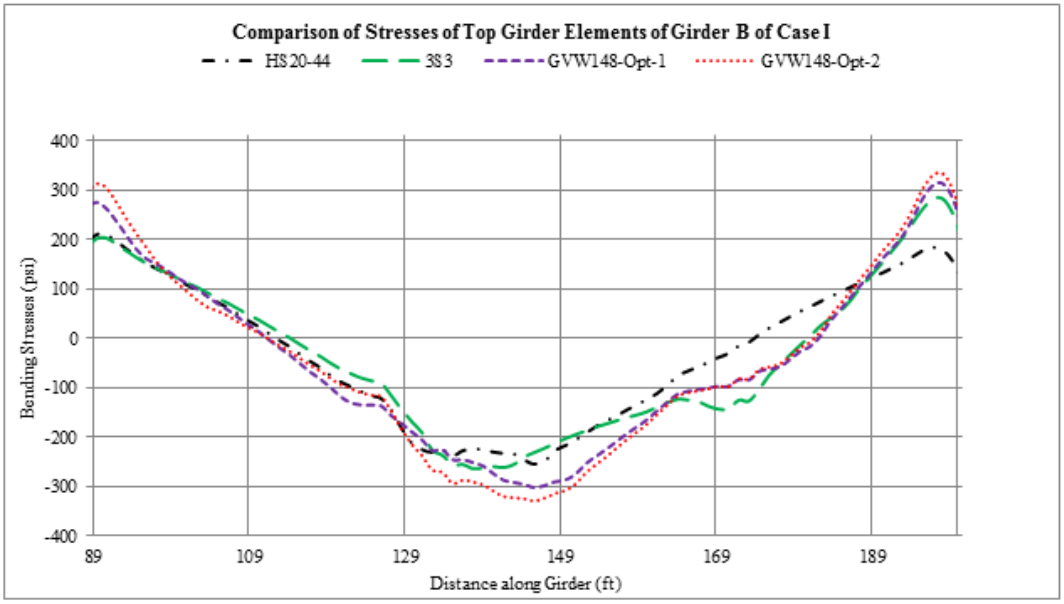

Figure 34
Comparison of bending stress distribution of top elements - Girder B of Case I, Span 14E

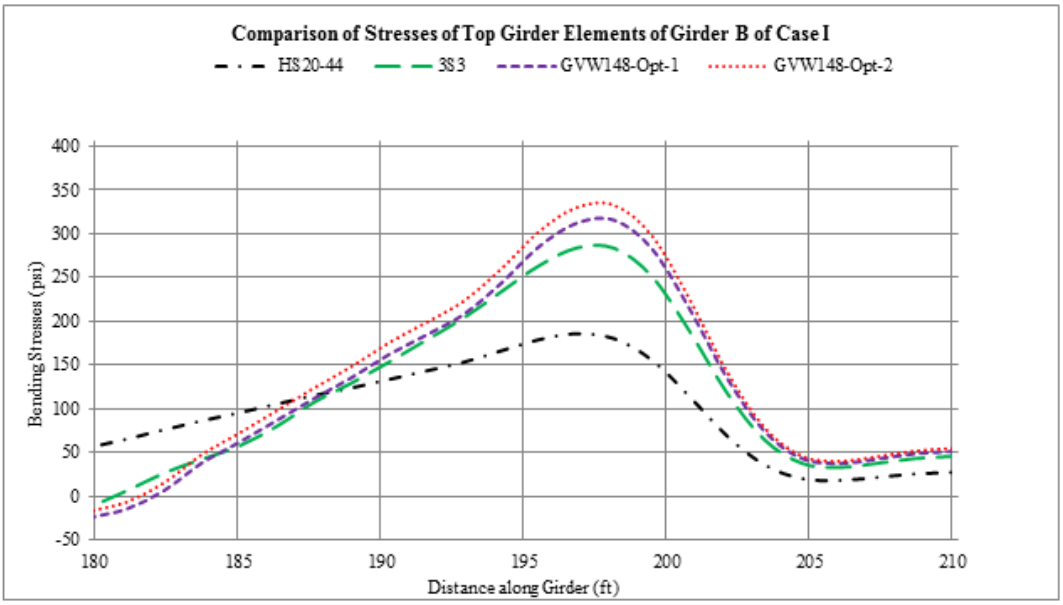

Figure 35
Blow-out showing the tensile stress at right support of Span 14E, Figure 34

In Table 8, the results that were presented from Figures 30 and 31 are accumulated in a single table and the numerical values of the critical stresses are listed.

Table 8
Case I - effects of truck configurations on flexural stresses - Girder B

Span	Location	Stress	HS20-44 (psi)	3S3 (psi)	GVW148 Opt-1 (psi)	GVW148 Opt-2 (psi)	Change in Stresses		
							3S3 vs HS20	Opt-1 vs HS20	Opt-2 vs HS20
15E	Top Elements	Max +ve	92.37	87.23	131.33	141.65	-5	39	49
							N*	42%	53%
		Max -ve	-4.94	-4.81	-6.67	-7.19	0.1	-2	-2
							N*	N*	N*
	Bottom Elements	Max +ve	29.88	29.74	38.88	42.17	-0.1	9	12
							N*	N*	N*
		Max -ve	-32.72	-30.38	-46.24	-50.37	2	-14	-18
							N*	N*	N*
14E	Top Elements	Max +ve	212.37	283.07	314.93	331.81	71	103	119
							33%	48%	56%
		Max -ve	-254.6	-262.86	-300.86	-328.07	-8	-46	-73
							N*	18%	29%
	Bottom Elements	Max +ve	207.69	215.46	243.98	267	8	36	59
							N*	17%	29%
		Max -ve	-216.7	-306.93	-353.67	-371.67	-90	-137	-155
							42%	63%	72%
13E	Top Elements	Max +ve	69.23	118.11	135.37	141.76	49	66	73
							71%	96%	105%
		Max -ve	-3.24	-4.47	-5.01	-5.32	-1	-2	-2
							N*	N*	N*
	Bottom Elements	Max +ve	31.26	47.63	53.66	56.61	16	22	25
							N*	N*	81%
		Max -ve	-30.73	-51.24	-57.92	-60.76	-21	-27	-30
							N*	88%	98%
12E	Top Elements	Max +ve	0.286	0.575	0.653	0.679	0.3	0.4	0.4
							N*	N*	N*
		Max -ve	-0.327	-0.201	-0.207	-0.241	0.1	0.1	0.1
							N*	N*	N*
	Bottom Elements	Max +ve	0.056	0.133	0.148	0.153	0.1	0.1	0.1
							N*	N*	N*
		Max -ve	-0.196	-0.424	-0.484	-0.50	-0.2	-0.3	-0.3
							N*	N*	N*

N*(Negligible): The difference is less than 25 psi.

In Table 8, the results from Figures 30 and 33 are summed up. The table is divided into four main parts. Each part represents one of the four spans of the girder, from 15E to 12E. Under each of these spans, researchers listed both the top element results and the bottom element results. The results for the top and bottom elements are further divided into two parts as maximum negative and maximum positive values, which represents maximum compression and maximum tension respectively.

The magnitude of maximum tensile stress and maximum compressive stress under each span are listed for four different kinds of truck loadings.

Taking HS20-44 as a benchmark, researchers tried to understand the stress behavior of 3S3, GVW-148 Opt-1, and GVW-148 Opt-2 trucks. The GVW of these trucks are 1100 kips, 148 kips, and 148 kips, respectively. The GVW-148 Opt-1 and GVW-148 Opt-2 trucks have the same GVW and same axle loading. However, GVW-148 Opt-1 has a total length of 100 ft. while the the GVW-148 Opt-2 has a total length of 92 ft. All these trucks are heavier than a standard HS20-44 truck (72 kip). The stresses generated in the girders due to these three trucks are supposed to be greater than the stress due to HS20-44. The last three columns of the table show the change in stresses of the three heavy trucks with respect to HS20-44 trucks. Both numerical and percentage changes of the stresses are listed. Any stress differentials less than 25 psi were ignored and not shown in percentage changes.

The effects of heavy trucks loads provide maximum stresses in Span 14E and minimum stresses in Span 12E. Spans 13E and 15E show a kind of similar response, as both of these spans are located adjacent to the loaded span (14E).

The maximum tensile stress is caused by GVW-148 Opt-2, and the magnitude of the stress is 331.81 psi. This is 119 psi greater in magnitude and 56% higher in percentage than the HS20-44 truck loading. The location of this stress is at the top elements of the girder at the support. Since this stress occurred at the top of the girder at the support, a majority of the effects of this stress will be taken by the deck because the deck is attached with the top elements of the girder. At the bottom of the midspan of Span 14E, the maximum tensile stress due to GVW-148 Opt-2 truck loading is 267 psi, which is 59 psi greater in magnitude and 29% greater in percentage than the standard HS20-44 truck loading under Case I.

The maximum compressive stress is also caused by GVW-148 Opt-2, and the magnitude of the stress is -371.67 psi. This is 155 psi greater in magnitude and 72% in percentage than the HS20-44 truck loading. The location of this stress is at the bottom elements of the girder at the support. The maximum compressive stress of the top elements at the midspan due to

GVW-148 Opt-2 truck is 328 psi, which is 73 psi greater in magnitude and 29% greater in percentage than standard HS20-44 truck loading.

The comparison of positive flexural stresses, negative flexural stresses, and change in stresses due 3S3 and GVW-148 Opt-1 with HS20-44 in terms of magnitude and percentage for Case I is shown in Table 8. The effects of GVW-148 Opt-1 in the stresses are less than GVW-148 Opt-2 truck loading despite having the same gross vehicular loads and the same number of axles and wheels. This is due to the shorter length of the GVW-148 Opt-2 truck.

In Figures 36 and 37 and in Table 9, the stress comparison of girder C for Case I is illustrated.

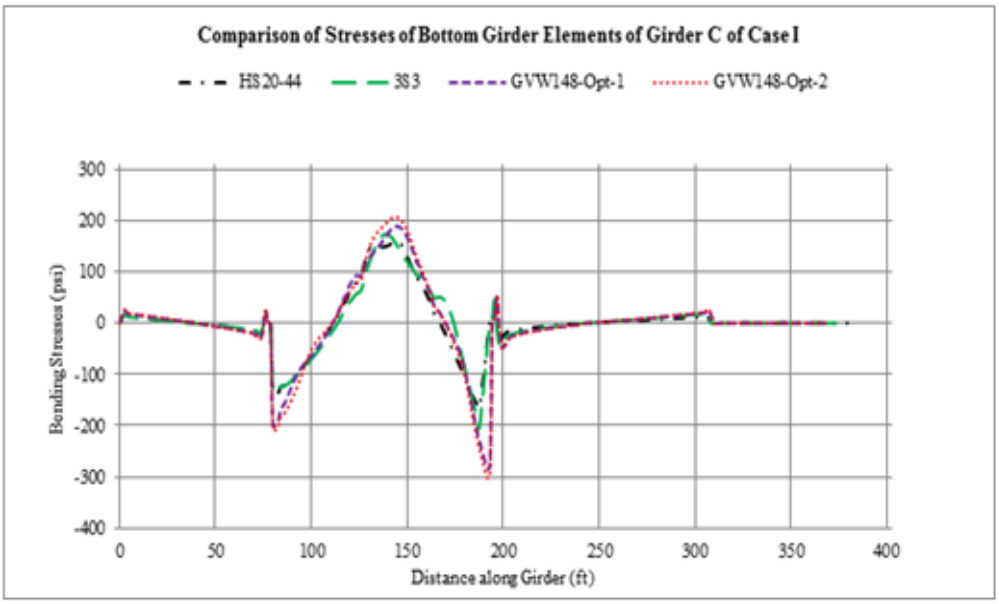

Figure 36
Comparison of bending stress distribution of bottom elements - Girder C of Case I

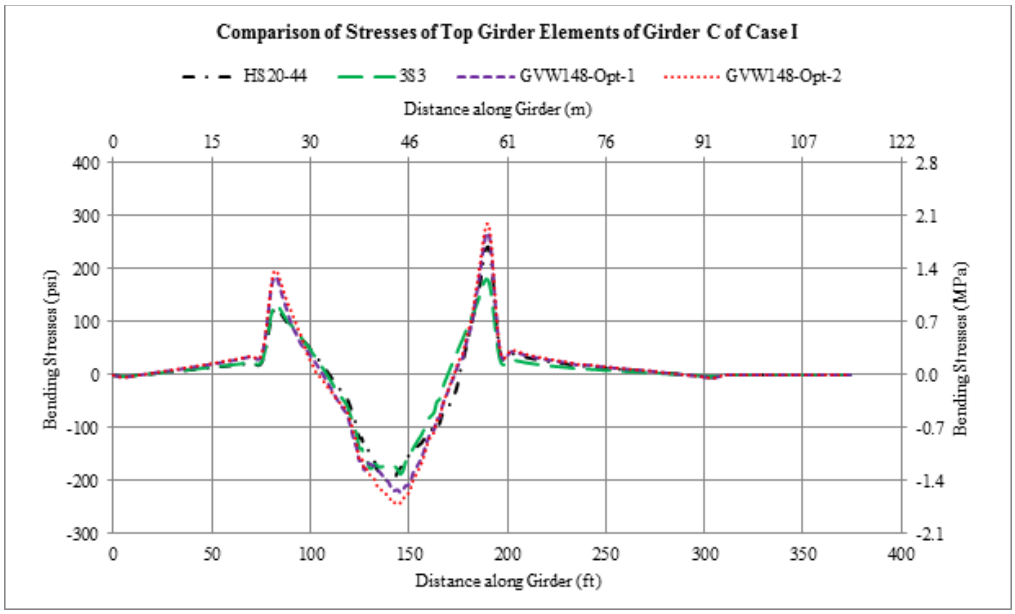

Figure 37
Comparison of bending stress distribution of top elements - Girder C of Case I

Table 9
Case I - effects of truck configurations on flexural stresses - Girder C

Span	Location	Stress	HS20-44 (psi)	3S3 (psi)	GVW148 Opt-1 (psi)	GVW148 Opt-2 (psi)	Change in Stresses		
							3S3 vs HS20	Opt-1 vs HS20	Opt-2 vs HS20
15E	Top Elements	Max +ve	52.86	56.44	82.07	85.29	4	29	32
							N*	55%	61%
		Max -ve	-3.02	-3.18	-4.38	-4.66	-0.2	-1	-2
							N*	N*	N*
	Bottom Elements	Max +ve	17.99	17.29	24.61	26.22	-1	7	8
							N*	N*	N*
		Max -ve	-20.42	-18.78	-30.68	-31.26	2	-10	-11
							N*	N*	N*
14E	Top Elements	Max +ve	240.95	180.67	267.96	285.04	-60	27	44
							-25%	11%	18%
		Max -ve	-198.21	-186.94	-221.80	-241.89	11	-24	-44
							N*	N*	22%
	Bottom Elements	Max +ve	159.87	173.38	189.07	207.04	14	29	47
							N*	18%	30%
		Max -ve	-165.61	-203.97	-279.00	-297.06	-38	-113	-131
							23%	68%	79%
13E	Top Elements	Max +ve	103.37	71.47	107.95	114.81	-32	5	11
							-31%	N*	N*
		Max -ve	-4.58	-3.07	-5.27	-5.56	2	-1	-1
							N*	N*	N*
	Bottom Elements	Max +ve	31.28	45.35	51.20	54.18	14	20	23
							N*	N*	N*
		Max -ve	-31.49	-45.16	-47.53	-50.57	-14	-16	-19
							N*	N*	N*
12E	Top Elements	Max +ve	0.459	0.325	0.441	0.474	-0.1	0.0	0.0
							N*	N*	N*
		Max -ve	-0.037	-0.008	-0.059	-0.057	0.0	0.0	0.0
							N*	N*	N*
	Bottom Elements	Max +ve	0.036	0.041	0.100	0.098	0.0	0.1	0.1
							N*	N*	N*
		Max -ve	-0.500	-0.689	-0.808	-0.852	-0.2	-0.3	-0.4
							N*	N*	N*

N*(Negligible): The difference is less than 25 psi.

Comparison of Maximum Stresses in Girders, Right Lane

In the theoretical analysis, all four cases have given similar patterns of stress distribution. Case III was chosen for the discussion of the theoretical results for trucks traveling in the right lane. Furthermore when the truck is in the right lane, Girder D and Girder E take the

most amounts of stress and strain will be illustrated. The results of the rest of the girders are given in Appendices A and B.

Figure 38 shows the stress distribution of the bending stress of the bottom fiber of Girder D as a function of distance along the girder. The primary vertical axis shows the stresses in psi and the primary horizontal axis shows the distance of the girder in feet.

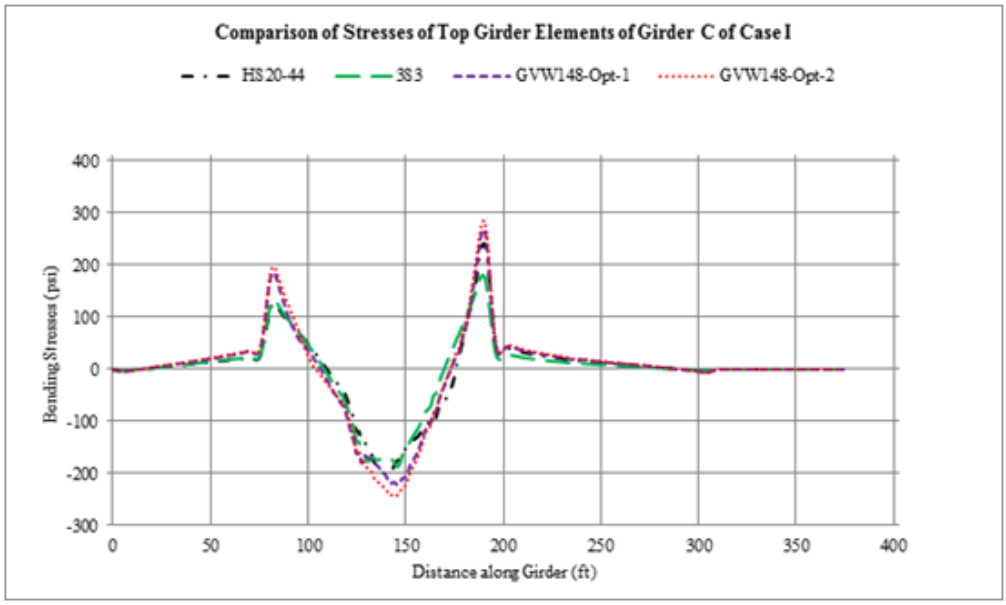

Figure 38
Comparison of bending stress distribution of bottom elements - Girder D of Case III

The length of the girder consists of four spans. Starting from the left, they are: Span 15E, 14E, 13E, and 12E. In the finite element model, all of the trucks are located on Span 14E, ranging from 70 ft. to 185 ft. and the truck moves from left to right.

In Figure 38, it can be seen that a majority of the stress variations occurred in Span 14E due to the presence of the truck loadings on it. Figure 39 only shows Span 14E. The maximum tensile stress occurred at the middle of Span 14E and maximum negative stresses occurred at the interior part of the girder adjacent to the supports. For further clarification, researchers plotted a blow up of the maximum tensile zone of Span 14E in Figure 40. This blow up is provided to show the stress distribution due to different truck loadings. It was observed that, as the truck loadings increase from HS20-44 to GVW-148 Opt-2, the maximum tensile stress also increases. It should also be noted that the location of maximum stresses for different truck loadings are very close to each other.

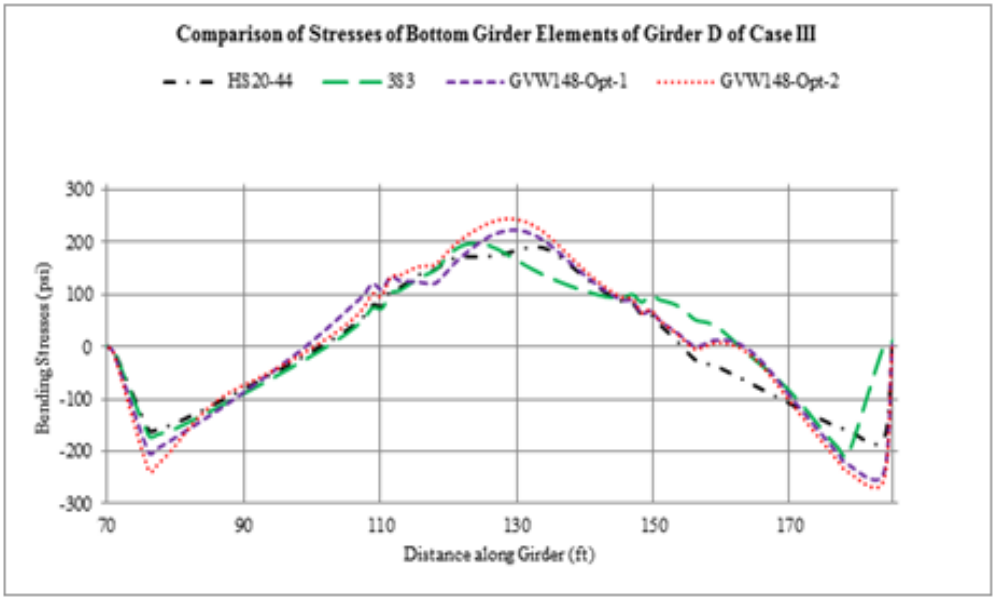

Figure 39
Comparison of bending stress distribution of bottom elements - Girder D of Case III, Span 14E

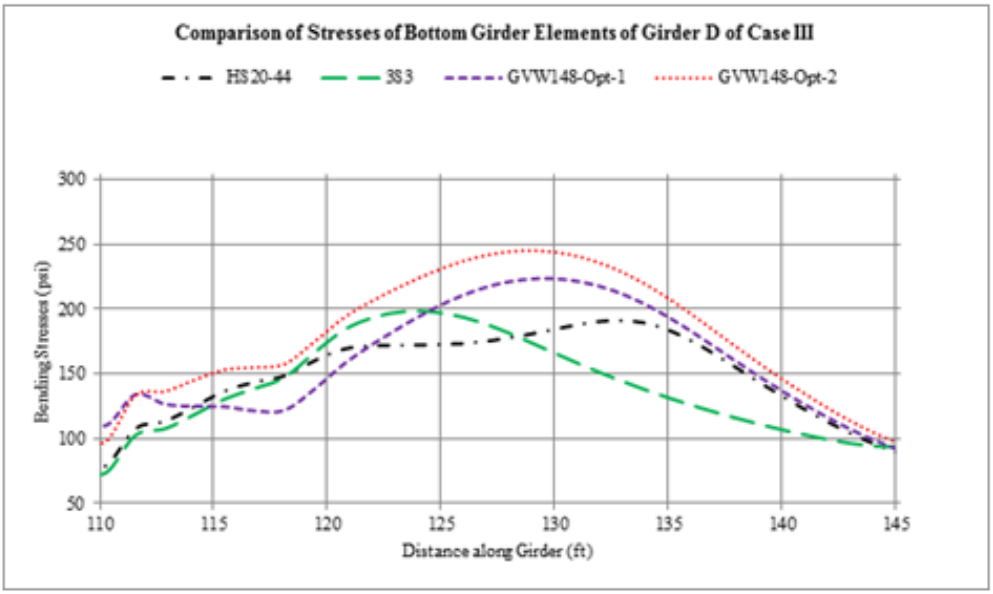

Figure 40
Blow-out showing the tensile stress at midspan of Figure 39

Figure 41 shows the stress distribution of the bending stress of the top fiber of Girder D in Case III as a function of distance along the girder. Figures 38 and 41 represent the same girder and the same load case but the first shows the stress comparison of the top girder elements and the second shows the stress comparison of the bottom girder elements.

In Figure 41, the stress distribution pattern due to the different truck loadings is following the same trend as expected. Here the maximum tensile and compressive stresses are occurring at Span 14 E due the presence of the truck loads in this span.

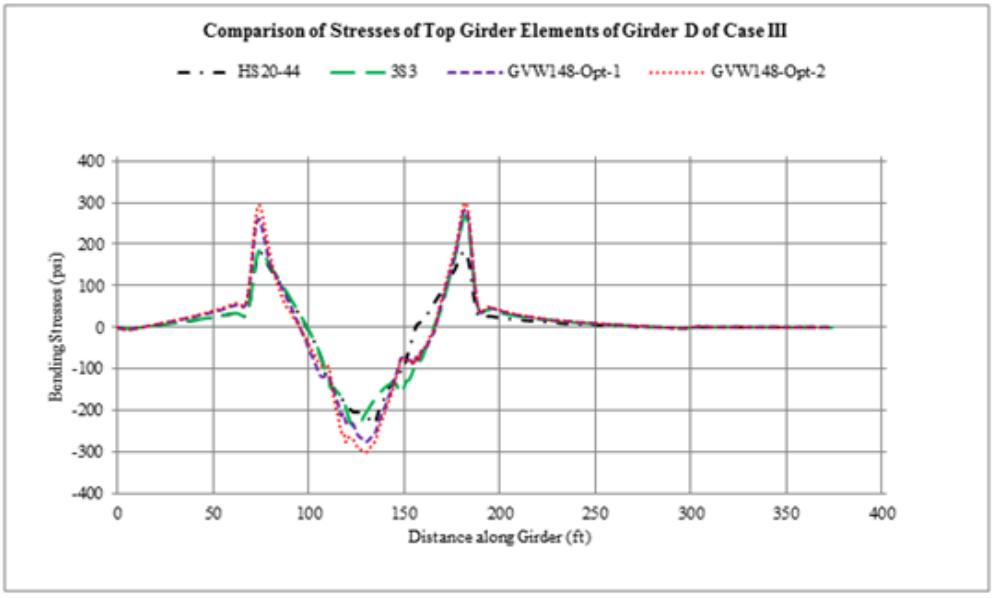

Figure 41
Comparison of bending stress distribution of top elements - Girder D of Case III

In Figure 42, the stress distribution is a function of distance along the girder and is plotted for Span 14E of Case III, Girder D. The top elements of the girder were subjected to compression at the midspan and to tension at and over the support. This behavior is completely opposite of what was shown in Figure 39, but this is the expected output. For further clarification, a blow up of the maximum compressive zone of span 14E was plotted in Figure 43. This blow up shows the stress distribution due to different truck loadings. As the truck loadings increase from HS20-44 to GVW-148 Opt-2, the maximum compressive stress also increases.

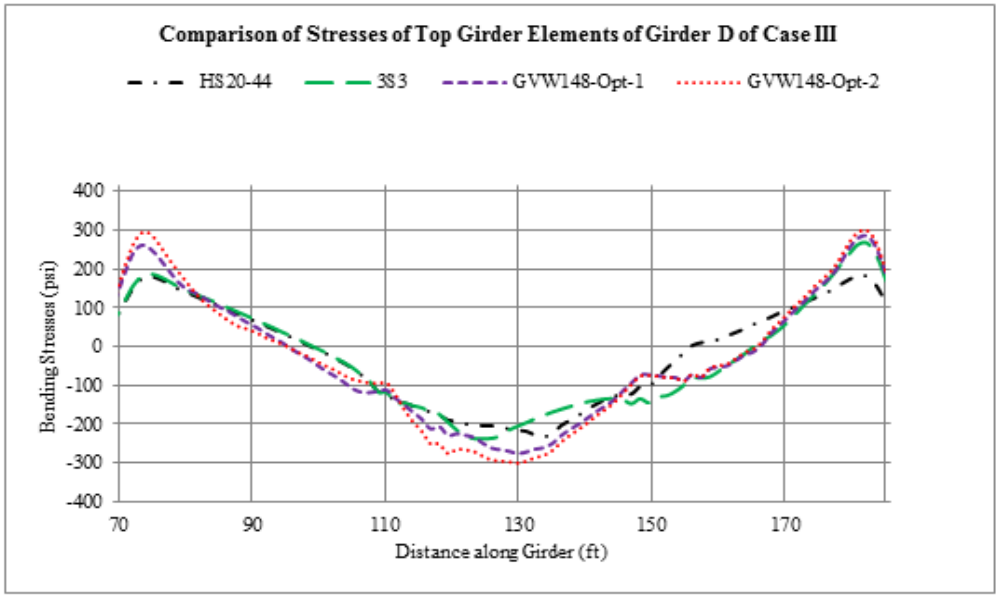

Figure 42
Comparison of bending stress distribution of top elements - Girder D of Case III, Span 14E

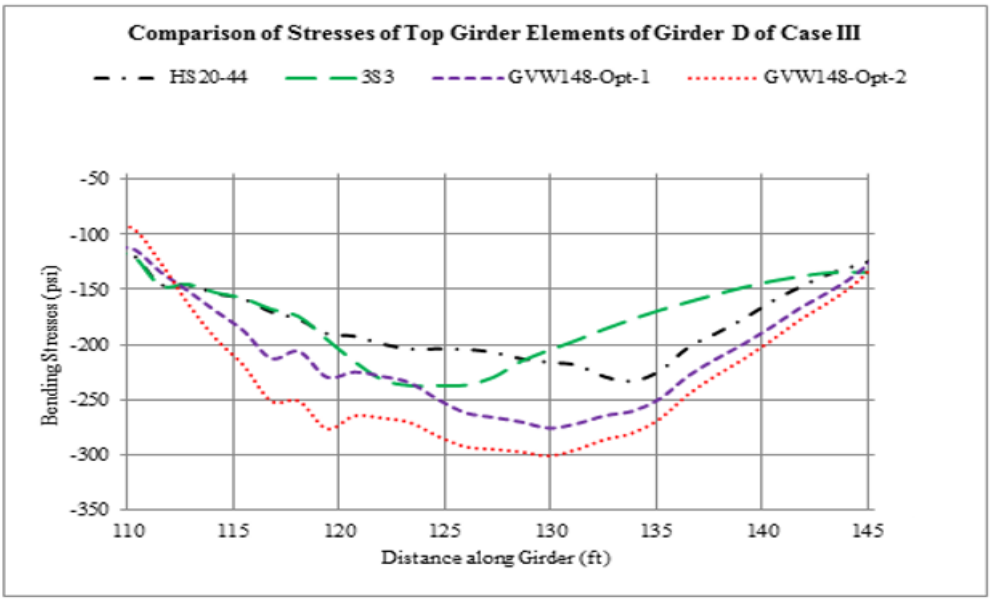

Figure 43
Blowout showing the compressive stress at midspan of Figure 42

In Table 10, the results from Figures 38 and Figure 42 are summed up. The table is divided into four main parts. Each part represents one of the four spans of the girder, from 15E to 12E. Under each of these spans both of the top elements results and the bottom elements results are listed. The results for the top and bottom elements are further divided into two parts as maximum negative and maximum positive values, which represents maximum compression and maximum tension respectively. The magnitude of maximum tensile stress

and maximum compressive stress under each span are listed for four different kinds of truck loadings.

Table 10
Case III - effects of truck configurations on flexural stresses - Girder D

Span	Location	Stress	HS20-44 (psi)	3S3 (psi)	GVW148 Opt-1 (psi)	GVW148 Opt-2 (psi)	Change in Stresses		
							3S3 vs. HS20-44	Opt-1 vs. HS20-44	Opt-2 vs. HS20-44
15E	Top Elements	Max +ve	74.43	76.37	128.30	138.60	2	54	64
							N*	72%	86%
		Max -ve	-4.10	-4.22	-6.22	-6.71	0	-2	-3
							N*	N*	N*
	Bottom Elements	Max +ve	24.51	25.20	36.95	39.98	1	12	15
							N*	N*	N*
		Max -ve	-30.30	-30.97	-47.07	-51.31	-1	-17	-21
							N*	N*	N*
14E	Top Elements	Max +ve	183.19	266.13	283.90	298.59	83	101	115
							45%	55%	63%
		Max -ve	-233.24	-237.28	-275.76	-300.96	-4	-43	-68
							N*	18%	29%
	Bottom Elements	Max +ve	191.30	198.11	223.60	245.17	7	32	54
							N*	17%	28%
		Max -ve	-177.42	-209.43	-242.07	-256.58	-32	-65	-79
							18%	36%	45%
13E	Top Elements	Max +ve	75.22	116.77	123.48	129.02	42	48	54
							55%	64%	72%
		Max -ve	-1.90	-2.34	-2.21	-2.36	-0.4	-0.3	-0.5
							N*	N*	N*
	Bottom Elements	Max +ve	27.65	40.09	45.37	47.76	12	18	20
							N*	N*	N*
		Max -ve	-30.38	-47.49	-53.73	-56.26	-17	-23	-26
							N*	N*	85%
12E	Top Elements	Max +ve	0.545	0.937	1.191	1.240	0.4	0.6	0.7
							N*	N*	N*
		Max -ve	-0.030	-0.049	-0.048	-0.050	0.0	0.0	0.0
							N*	N*	N*
	Bottom Elements	Max +ve	0.214	0.358	0.400	0.417	0.1	0.2	0.2
							N*	N*	N*
		Max -ve	-0.631	-1.022	-1.155	-1.207	-0.4	-0.5	-0.6
							N*	N*	N*

N*(Negligible): The difference is less than 25 psi

Taking HS20-44 as a standard, researchers tried to understand the stress behavior of 3S3, GVW-148 Opt-1 and GVW-148 Opt-2 trucks. The standard GVW for a 3S3 truck is 100 kips, GVW-148 Opt-1 is 148 kips, and GVW 148 Opt-2 is also 148 kips but has a different wheel orientation than GVW-148 Opt-1 truck. All three trucks are heavier than standard HS20-44 trucks (72 kips). So the stresses generated in the girders due to these three trucks are supposed to be greater than the stress due to HS20-44. The last three columns of Table 10 show a change in stresses of the three heavy trucks with respect to HS20-44 trucks. Both numerical and percentage changes of the stresses are listed. Any stress changes less than 25 psi were ignored and not shown in percentage changes.

The effects of heavy trucks loads present maximum stresses in Span 14E and minimum stresses in Span 12E. Span 13E and 15E showed a kind of similar response as both of these spans were located adjacent to the loaded span (14E).

The maximum tensile stress was caused by the truck GVW-148 Opt-2 and the magnitude of the stress was 298.59 psi. This is 115 psi greater in magnitude and 63% in percentage than the HS20-44 truck loading. The location of this stress was at the top element of the girder at the support. Since this stress occurred at the top of the girder at the support, a majority of the effects of this stress were taken by the deck because the deck was attached with the top elements of the girder. At the bottom of the midspan of Span 14E, the maximum tensile stress due to GVW-148 Opt-2 truck loading was 245.17 psi, which was 54 psi greater in magnitude and 28% greater in percentage than the standard HS20-44 truck loading under Case III.

The maximum compressive stress was also caused by the truck GVW-148 Opt-2 and the magnitude of the stress was -300.96 psi. This was -68 psi greater in magnitude and 29% in percentage than the HS20-44 truck loading. The location of this stress was at the top elements of the girder at the midspan. The maximum compressive stress of the bottom elements at the support due to GVW-148 Opt-2 truck was -256.58 psi, which is -79-psi greater in magnitude and 45% greater in percentage than the standard HS20-44 truck loading.

Similarly, the comparison of 3S3 and GVW-148 Opt-1 with HS20-44 in terms of magnitude and percentage for Case III is shown in Table 10. Here, the effects of GVW-148 Opt-1 in the stresses were less than GVW-148 Opt-2 truck loading in spite of having the same gross vehicular loads and the same number of axles and wheels. This is due to the shorter length of GVW-148 Opt-2 truck. In Figures 44 and 45, and Table 11, the stress comparison of Girder E for Case III is illustrated.

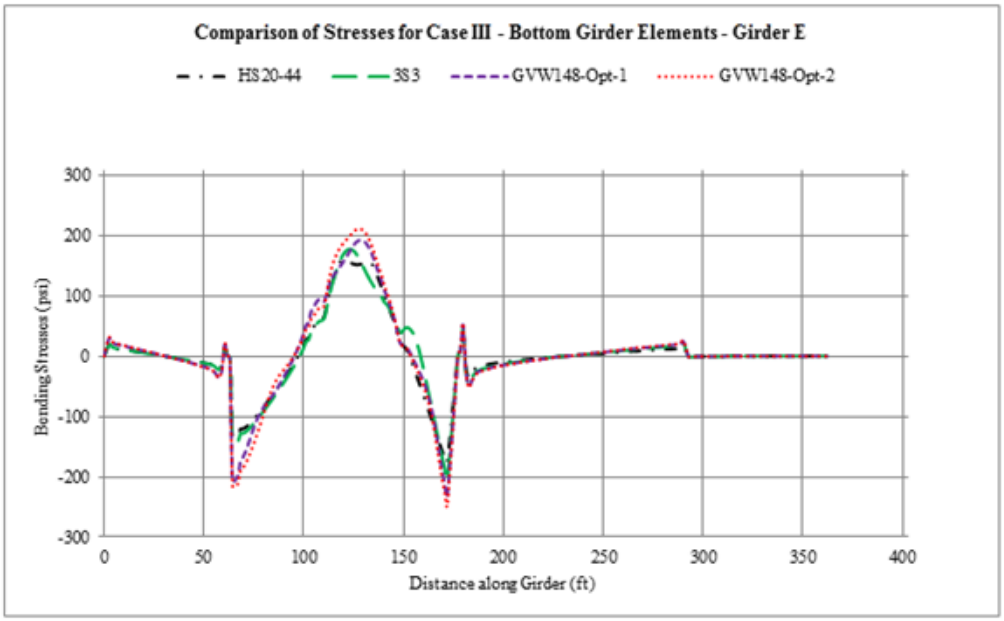

Figure 44
Comparison of flexural stress distribution of top elements - Girder E of Case III

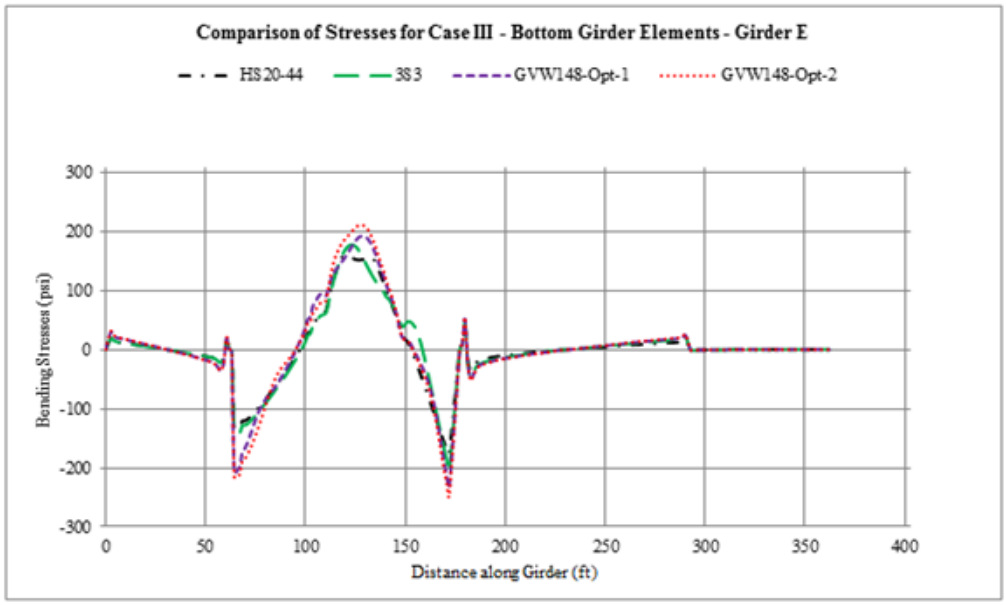

Figure 45
Comparison of flexural stress distribution of bottom elements - Girder E of Case III

Table 11
Case III - effects of truck configurations on flexural stresses - Girder E

Span	Location	Stress	HS20-44 (psi)	3S3 (psi)	GVW148 Opt-1 (psi)	GVW148 Opt-2 (psi)	Change in Stresses		
							3S3 vs. HS2-440	Opt-1 vs. HS20-44	Opt-2 vs. HS20-44
15E	Top Elements	Max +ve	52.23	58.98	90.30	94.24	7	38	42
							N*	73%	80%
		Max -ve	-3.12	-3.29	-4.86	-5.16	-0.2	-2	-2
							N*	N*	N*
	Bottom Elements	Max +ve	19.86	20.30	30.35	32.02	0.4	10	12
							N*	N*	N*
		Max -ve	-21.33	-21.68	-34.38	-35.39	-0.4	-13	-14
							N*	N*	N*
14E	Top Elements	Max +ve	208.84	247.10	274.67	292.29	38	66	83
							18%	32%	40%
		Max -ve	-194.63	-204.14	-227.93	-249.62	-10	-33	-55
							N*	17%	28%
	Bottom Elements	Max +ve	160.36	178.04	193.22	211.92	18	33	52
							N*	20%	32%
		Max -ve	-176.04	-205.52	-232.11	-248.13	-29	-56	-72
							17%	32%	41%
13E	Top Elements	Max +ve	90.30	106.11	110.99	118.05	16	21	28
							N*	N*	31%
		Max -ve	-3.31	-4.13	-4.79	-5.05	-0.8	-2	-2
							N*	N*	N*
	Bottom Elements	Max +ve	33.98	45.90	51.93	54.97	12	18	21
							N*	N*	N*
		Max -ve	-34.50	-45.86	-48.31	-51.41	-11	-14	-17
							N*	N*	N*
12E	Top Elements	Max +ve	0.307	0.703	0.712	0.762	0.4	0.4	0.5
							N*	N*	N*
		Max -ve	-0.067	-0.068	-0.082	-0.086	0.0	0.0	0.0
							N*	N*	N*
	Bottom Elements	Max +ve	0.103	0.138	0.146	0.155	0.0	0.0	0.1
							N*	N*	N*
		Max -ve	-0.583	-0.725	-0.753	-0.807	-0.1	-0.2	-0.2
							N*	N*	N*

N*(Negligible): The difference is less than 25 psi.

Comparison of Maximum Deflections in Girders

Bridge models for the four different cases were run in order to determine the maximum deflection among the different girders. The resultant deflections of each girder, due to the four different kinds of trucks, were plotted in figures and listed in tables. Girder D was selected as the critical girder and Case III as the critical cases for the stress distributions. The same girder and cases for the deflection were also selected.

The deflection of Girder D for the different kind of truck loading for Case III is plotted in Figure 46. The overall behavior of the girder due to the truck loads was as expected. All the maximum deflections due to each kind of truck loading were located in Span 14 E because of the presence of the truck on the span. The vertical axis shows the vertical deflection of the girder and the horizontal axis represents the distance along the length of the girder. Here downward deflection is assumed negative in Figure 46.

Figure 46 illustrates that as the gross vehicular load increases, the maximum deflection increases. The maximum deflections took place at the midspan of Span 14E, which was as expected and reasonable.

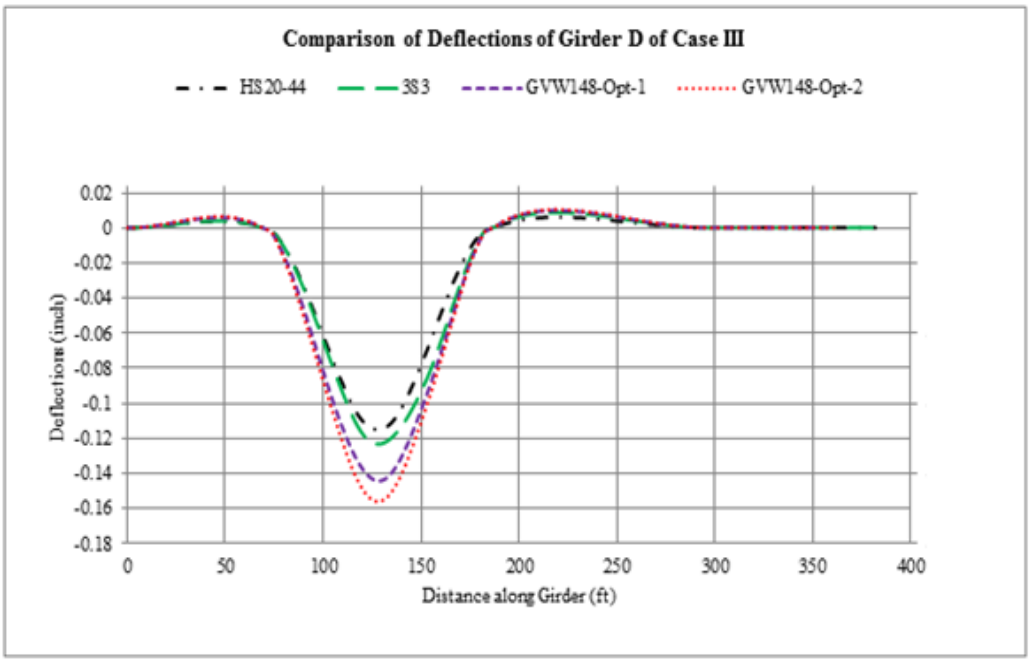

Figure 46
Comparison of deflections of Girder D for Case III

The maximum deflections for all four different cases and all four kinds of trucks for Girder D are listed in Table 12. Here the downward deflection is assumed to be positive for convenience. In Table 12, the maximum deflection in Girder D for Case III is due to GVW-148 Opt-2 trucks and the magnitude is 0.16 in. This value of maximum deflection is within

the serviceability limits of the structures. Also, the difference among the girders in maximum deflection is not significant and varies within the range of 0.12 in. for a standard HS20-44 truck to 0.16 in. for GVW-148 Opt-2. Because of the difference of deflections among the various trucks, the numerical difference and percentage increase of deflections were not shown in Table 12. So the short-term effect of heavy truck loads on the deflection of the bridge was negligible.

Table 12
Effects of truck configurations on deflections - Girder D

Span	Case	Maximum Deflections			
		HS20-44 (in.)	3S3 (in.)	GVW148 Opt-1 (in.)	GVW148 Opt-2 (in.)
15E	I	-1.6E-03	-1.5E-03	-2.1E-03	-2.2E-03
	II	-1.8E-03	-2.1E-03	-1.5E-03	-2.1E-03
	III	-4.0E-03	-4.1E-03	-6.0E-03	-6.5E-03
	IV	-5.0E-03	-6.5E-03	-1.6E-03	-2.3E-03
14E	I	0.05	0.05	0.06	0.07
	II	0.05	0.06	0.07	0.07
	III	0.12	0.12	0.14	0.16
	IV	0.11	0.12	0.13	0.14
13E	I	-5.7E-03	-7.7E-03	-8.8E-03	-9.3E-03
	II	-4.9E-03	-6.7E-03	-7.4E-03	-7.1E-03
	III	-6.2E-03	-8.8E-03	-9.9E-03	-10E-03
	IV	-4.7E-03	-6.2E-03	-7.5E-03	-7.1E-03
12E	I	49E-06	95E-06	110E-06	110E-06
	II	35E-06	58E-06	66E-06	59E-06
	III	-40E-06	-66E-06	-74E-06	-77E-06
	IV	-26E-06	-38E-06	-49E-06	-44E-06

Note: Downward deflections of the girder are assumed positive.

Comparison of Deck Stresses

In this section, the results on how the bridge deck was affected by the heavy truck loads are presented. In the finite element analysis of the bridge under different heavy truck loads, the stresses were measured at the top surface and at the bottom surface of the deck slab. Stresses on the longitudinal and transverse direction and the shear stress were measured. The maximum tensile and compressive stresses on the top and bottom surfaces are listed for different truck loadings, as shown in Table 13.

In Table 13, the flexural stresses increase with the gross vehicular loads of the trucks except for HS20-44 trucks. This is due to the higher GVW loads of the heavier trucks. These results from the bridge deck analyses indicate that the bridge deck was under a stable stress state, whether the stresses are in the tension or the compression zone.

Table 13
Case I - effects of truck configurations on deck stresses

Direction	Location	Stress	HS20-44 (psi)	3S3 (psi)	GVW148 Opt-1 (psi)	GVW148 Opt-2 (psi)
Longitudinal	Top	Max +ve	50	67	74	76
		Max -ve	-220	-105	-111	-118
	Bottom	Max +ve	221	103	110	113
		Max -ve	-55	-61	-73	-85
Transverse	Top	Max +ve	159	143	162	170
		Max -ve	-421	-271	-285	-295
	Bottom	Max +ve	421	271	285	295
		Max -ve	-159	-144	-162	-170
Shear	Top	Max +ve	32	37	42	44
		Max -ve	-43	-39	-42	-38
	Bottom	Max +ve	44	41	34	40
		Max -ve	-31	-36	-33	-44

Results and Discussion for Regression Analysis

Outside Lane

The SPSS software was used to perform multiple regression analyses on the field data set collected with trucks in the outside lane. The purpose of using this data set was to see if the regression analysis could predict the truck weights. The weight of the truck was the dependent variable and the four strain value sets were the independent variables. The first task for the regression analysis was to determine the correlation of the data sets; the results can be seen in Table 14. The Pearson Correlation values are also presented in this table. The value for a Pearson's can fall between 0.00 (no correlation) and 1.00 (perfect correlation).

Table 14
Correlation values for the live field data set (outside lane)

		Strain 14	Strain 40	Strain 41	Strain 42	Legal Truck Weight
Strain14	Pearson Correlation	1	.267	.378	.260	.220
	Sig. (2-tailed)		.003	.000	.004	.016
	N	120	120	120	120	120
Strain40	Pearson Correlation	.267	1	.079	.163	-.172
	Sig. (2-tailed)	.003		.391	.076	.060
	N	120	120	120	120	120
Strain41	Pearson Correlation	.378	.079	1	.420	.133
	Sig. (2-tailed)	.000	.391		.000	.147
	N	120	120	120	120	120
Strain42	Pearson Correlation	.260	.163	.420	1	.038
	Sig. (2-tailed)	.004	.076	.000		.684
	N	120	120	120	120	120
Legal Truck Weight	Pearson Correlation	.220	-.172	.133	.038	1
	Sig. (2-tailed)	.016	.060	.147	.684	
	N	120	120	120	120	120

Referring to Table 7, as seen in the above data, the correlation values are a moderate to weak relationship. These findings raise some concern for the results of the analysis since a higher correlation is needed to prove the accuracy of the relationship. Next the multiple regression analysis was performed and the results can be seen in Tables 15, 16, and 17.

Table 15
Model summary R and R square values for the live field data (outside lane)

Model	R	R Square	Adjusted R Square	Std. Error of the Estimate
1	.329[a]	.108	.077	17404.432

a. Predictors: (Constant), Strain 42, Strain 40, Strain 14, Strain 41

Table 16
ANOVA table for the live field data (outside lane)

Model		Sum of Squares	df	Mean Square	F	Sig.
1	Regression	4.232E9	4	1.058E9	3.492	.010[a]
	Residual	3.484E10	115	3.029E8		
	Total	3.907E10	119			

a. Predictors: (Constant), Strain 42, Strain 40, Strain 14, Strain 41

Note: Dependent Variable was the legal truck weight.

Table 17
Coefficients table for the live field data (outside lane)

Model		Unstandardized Coefficients		Standardized Coefficients	t	Sig.
		B	Std. Error	Beta		
1	(Constant)	60106.398	9134.851		6.580	.000
	Strain14	985.104	363.460	.268	2.710	.008
	Strain40	-6272.686	2351.138	-.246	-2.668	.009
	Strain41	139.612	245.083	.058	.570	.570
	Strain42	-161.816	970.158	-.016	-.167	.868

Note: Dependent Variable was the legal truck weight.

In Table 15, the R-squared value is shown as 0.108 (~11%), which means that there is a weak relationship between the variables. The data points were graphed in EXCEL and are presented in figure 133 in Appendix H. The ANOVA table, Table 16, shows that the residual value is greater than the regression value, which will result in the data having a lower significance. Lastly in Table 17, the variables are given to solve for the mathematical function discussed previously in this report ($y' = a + b_1x_1 + b_2x_2 + b_3x_3 + b_4x_4$,). These values are arranged as shown in Table 18.

Table 18
Corresponding SPSS data sets with equation variables (outside lane)

SPSS Variable	Equation Variable	
(Constant)	a	60,106.398
Strain14	b_1	985.104
Strain40	b_2	-6,272.686
Strain41	b_3	139.612
Strain42	b_4	-161.816

With all of the data compiled for use in SPSS, the relationship from the regression analysis was used to predict the weight of the test truck from the November 2010 test. If the predicted value was close to the known weight of 100,000 lb. then the relationship can be confirmed.

Table 19
Actual truck weight vs. predicted truck weight

Nov. 2010	Strain 14	Strain 40	Strain 41	Strain 42	Actual Truck Weight	Predicted Truck Weight (lb.)	Error
Test 3	22.31	1.71	17.82	3.25	100,000	73,300	27%
Test 4	20.55	2.05	16.79	3.97	100,000	69,185	31%
Test 7	21.25	1.37	19.88	0.36	100,000	75,144	25%

As previously seen, the predicted truck weight was around 30,000 lb. off of the actual truck weight of the November 2010 test truck. These results confirmed that, with a low R-squared value, the overall results will be less accurate.

Inside Lane

The SPSS software was again used to perform a multiple regression analysis on the field data collected for trucks in the inside lane. The first task for the regression analysis was to determine the correlation of the data sets. The mean and standard deviation for each strain gauge is presented in Table 20 while the Pearson Correlation values are presented in Table 21. The value for a Pearson's can fall between 0.00 (no correlation) and 1.00 (perfect correlation).

Table 20
Descriptive statistics for strain gauges (inside lane)

	Mean	Std. Deviation	N
Strain17	31.97960	5.125644	75
Strain41	3.66677	9.896255	75
Strain42	-.04569	2.507648	75
Strain40	.89181	.729597	75
Truck Weight	75466.67	15683.813	75

Table 21
Correlation values for the live field data set (inside lane)

		Strain17	Strain41	Strain42	Strain40	Truck Weight
Strain17	Pearson Correlation	1	-.113	-.104	.032	-.048
	Sig. (2-tailed)		.335	.374	.786	.682
	N	75	75	75	75	75
Strain41	Pearson Correlation	-.113	1	.658	.275	-.088
	Sig. (2-tailed)	.335		.000	.017	.454
	N	75	75	75	75	75
Strain42	Pearson Correlation	-.104	.658	1	.538	-.223
	Sig. (2-tailed)	.374	.000		.000	.054
	N	75	75	75	75	75
Strain40	Pearson Correlation	.032	.275	.538	1	-.287
	Sig. (2-tailed)	.786	.017	.000		.013
	N	75	75	75	75	75
Truck Weight	Pearson Correlation	-.048	-.088	-.223	-.287	1
	Sig. (2-tailed)	.682	.454	.054	.013	
	N	75	75	75	75	75

Table 21 presents values that have a moderate to weak relationship. These results predicted the relationship that the regression analysis provided. Next the multiple regression analysis was performed and the results can be seen in Tables 22, 23, and 24.

Table 22
R and R square values for the live field data (inside lane)

Model	R	R Square	Adjusted R Square	Std. Error of the Estimate
1	.307[a]	.094	.042	15347.639

a. Predictors: (Constant), Strain40, Strain17, Strain41, Strain42

Table 23
ANOVA table for the live field data (inside lane)

Model		Sum of Squares	df	Mean Square	F	Sig.
1	Regression	1.714E9	4	4.285E8	1.819	.135[a]
	Residual	1.649E10	70	2.356E8		
	Total	1.820E10	74			

a. Predictors: (Constant), Strain40, Strain17, Strain41, Strain42

Note: Dependent Variable was the legal truck weight.

Table 24
Coefficients table for the live field data (inside lane)

Model		Unstandardized Coefficients		Standardized Coefficients		
		B	Std. Error	Beta	t	Sig.
1	(Constant)	84088.540	11554.060		7.278	.000
	Strain17	-151.172	352.302	-.049	-.429	.669
	Strain41	109.474	241.501	.069	.453	.652
	Strain42	-968.336	1090.010	-.155	-.888	.377
	Strain40	-4746.644	2938.826	-.221	-1.615	.111

Note: Dependent Variable was the legal truck weight.

Table 22 presents the R-squared value as 0.094 (~ 9%), which means there is a very weak relationship between the variables. The data points were graphed in EXCEL and are presented in Figure 134 in Appendix H. The ANOVA table shows that the residual value approaches the total sum of squares itself, which represents weak results. Also, from the ANOVA table one can obtain the R-squared value by dividing the sum of squares for the regression, 1.714E9, by the total sum of squares, 1.820E10, resulting in 0.0942. This indicates that the independent variables (strain values) together explain about 9.4% of the variation in truck weight. Lastly in Table 24, the variables are given to solve for the mathematical function discussed previously in this report. These values are arranged as shown in Table 25.

Table 25
Corresponding SPSS data sets with equation variables (inside lane)

SPSS Variable	Equation Variable	
(Constant)	a	84,088.540
Strain17	b_1	-151.172
Strain40	b_2	-4,746.644
Strain41	b_3	109.474
Strain42	b_4	-968.336

With the data compiled and used in SPSS, the relationship from the regression analysis was used to predict the weight of the test truck from the November 2010 test. The results can be seen in Table 26.

Table 26
Actual truck weight vs. predicted truck weight (inside lane)

	Strain 17	Strain 40	Strain 41	Strain 42	Actual Truck Weight (lbs)	Predicted Truck Weight (lbs)	Error
Test 2	25.06	1.722	9.26	1.09	100,000	72,085	28%
Test 5	26.41	1.724	-2.411	-0.008	100,000	71,657	28%
Test 8	29.09	0.027	7.206	1.805	100,000	78,604	21%

As shown from the previous two sections, no significant statistical relationship can be determined between the truck weight and measured strain. The reasoning behind this conclusion could be because from the photograph of the truck, it was not possible to determine if the truck was fully loaded or not, which could have led to inaccuracies in the estimated truck weight. Truck speed combined with the magnitude of street roughness could also influence the effective weight on a sensor and hence the recorded strain, and the distance of the truck from the sensor would have an effect on the strain recorded.

Cost of Fatigue on Louisiana Bridges

Bridge cost combines new design, rehabilitation, and fatigue costs; however, the focus of this portion of the study only considers the cost of fatigue resulting from the increase in load permits from the new truck configurations.

The bridges impacted by this study are designed under the standard HS20 or H18 truck load *[10, 11]*. The new, heavier configuration will increase the cost of maintenance and rehabilitation. This study attempted to provide an approximate estimation of the cost of damage. An accurate estimate is difficult to obtain because fatigue damage can lead to repairs, rehabilitation, or maintenance. The methodology used to evaluate the cost can be referenced to prior publications (LTRC report numbers 418 and 425) *[1, 3]*.

The proposed truck configuration will affect bridges with span length of 90 ft. or longer. There are five bridges that will be impacted on US90 and LA1. These bridges are listed in Table 27. The impact on these bridges will be significant and will cause damage to some of the bridge elements, local failure, and may result in bridge failure. Therefore, it is recommended that these bridges are retrofitted before the new truck configuration is approved and authorized on these Louisiana highways.

Table 27
Preliminary list of critical bridges that could fail due to SCR-35

Support Type	Structure No.	Control Section	Structure Type	Total Length	Max Span Length	No. of Main Spans	Design Load	State Route
Simple	61240500614251	050-06	COPSGR	1458	94	20	20	LA1
Continuous	61610500708321	050-07	STCPLG	2469	200	44	20	LA1
Continuous	61610500708322	050-07	STCPLG	2469	200	44	20	LA1
Simple	03234240409661	424-04	COPSGR	1452	138	17	18	US90
Simple	03234240409662	424-04	COPSGR	1452	138	17	18	US90

The monitoring system also recorded strains every hour and strain cycles that occurred within the range during the hour period. The range for the strains was between 5 and 45 microstrains for the minimum and maximum, as shown on the horizontal axis in Figures 47 and 48. The data provide the relative magnitude of strain ranges for the various gauge locations. Since the data is recorded hourly, it also provides the strain reversals in the girders which is an important factor for fatigue analysis. The recorded data indicate that the bridge girders are subject to low cycles of high strain values, above 33 microstrains, and high cycles of low strain values. The girder performance under such conditions can be explained as

follows: the high strain values exceed the serviceability criteria and can lead to cracks in the girders, then the high cycles of low strain will lead to fatigue in the prestressed strands. Consequently, the girders will deteriorate and the span life of the bridge will be reduced.

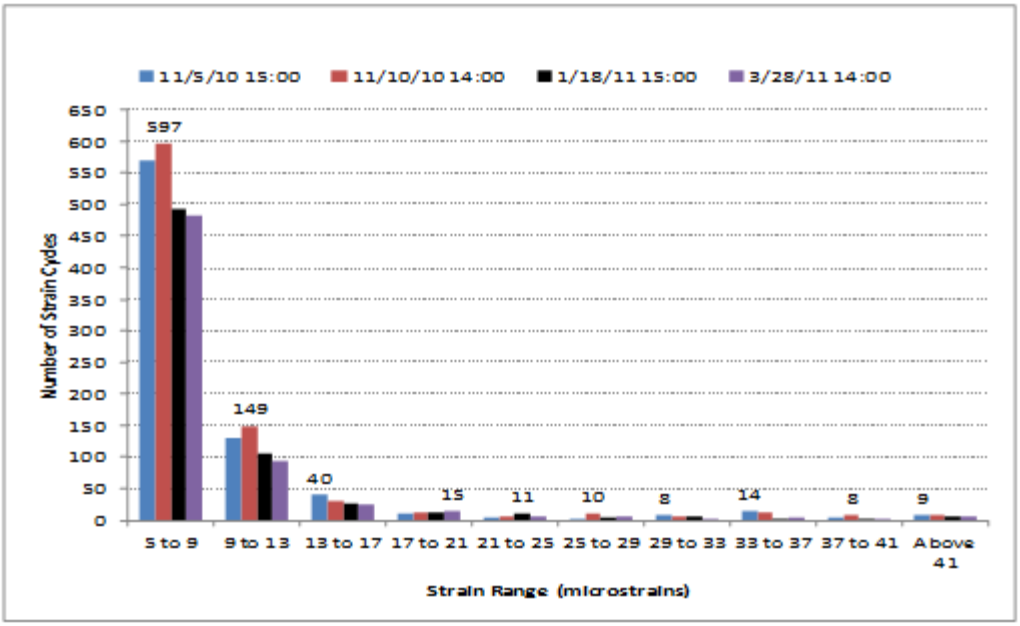

Figure 47
Strain cycle at Gauge 14 at bottom of Girder E - outside lane

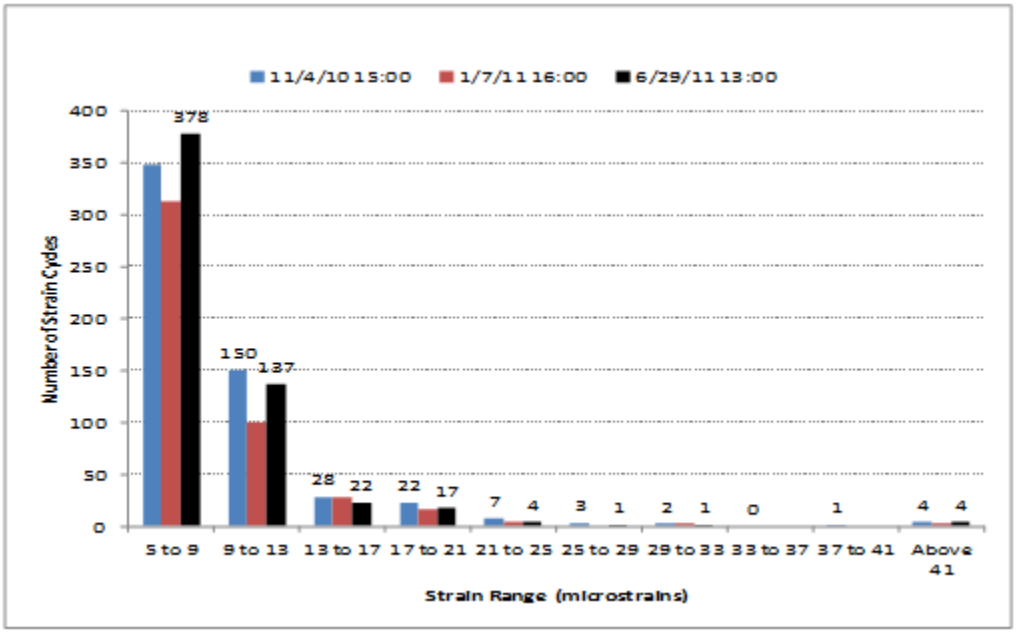

Figure 48
Strain cycle at Gauge 17 at bottom of Girder E- inside lane

The data from the monitoring system shown in Figure 26 and Figure 27 indicates that the average number of heavy load during October, November, and December is 3.5 times higher than the rest of the year. The bridges are exposed to a high cycle of repetition of heavy loads that will reduce the life span of the bridges by about 50%. The bridges that are built to last 75 years will require replacement after about 40 years in service. This seasonal impact is due to the sugarcane harvest, and these results confirm the cost of fatigue ($0.9 per truck per trip per bridge) as determined in the previous studies (LTRC report numbers 418 and 425) *[1, 3]*.

The economic impact of overweight permitted vehicles hauling sugarcane on Louisiana highways should address the fiscal impact on the state responsible for the maintenance and safety of the roads and bridges, and the impact to the sugarcane producers.

Sugarcane is grown in 24 parishes and is currently hauled to market by truck trailer combinations. Current state laws allow truck operators hauling certain agricultural commodities, including sugarcane, to purchase overweight permits and haul at GVW (gross vehicle weight) in excess of the legislated GVW limit of 80,000 lb.

The previous studies that were sponsored by LTRC indicated that the cost of pavement damage produced by trucks hauling sugarcane in excess of 80,000 lb. far exceeded the permit charged for the overweight. The GVW of a vehicle is not the only determinant of the impact of vehicles on pavement behavior and the bridge safety. The highway systems are stressed by the loads on individual axles and axle groups directly in contact with the pavement and the bridges. The GVW along with the number and types of axles and the spacing between the axles are used to determine the axle load. The accumulated stresses and strains affect the life span of roads and bridges. As the axle load increases, pavement deterioration increases quite rapidly, and life span of bridge is reduced. A fourth power relationship between the axle load and deterioration has been the rule of thumb for pavements and a third power relationship for the life span of bridges.

The sugarcane producers should consider other options to increase the GVW without increasing the damage to the highway systems. These options include:

(1) Change an axle type by adding one axle to make a tandem to produce a triple axle group or increase the spacing of the axles permits a higher GVW without increasing the damage to the highway systems.

(2) Use lighter trucks and different trailer types. By using lighter weight trailers, the investment costs are significantly reduced, and the light weight of the trailer allows hauling more sugarcane per truckload.

(3) Incorporate the mill delivery system or bin transport system. Mill delivery system or "Roll off" Bin Transport System improves harvest and transport efficiency. In this system, sugarcane would be loaded into standard bins in the field, and the bins would be loaded in trucks for transport to the sugar mills. Harvester operation is not dependent on truck availability, and loaded bins can be hauled to the mill day or night— whenever needed. Trailer and bin weight is approximately 22,000 – 26,000 lb. One bin or basket holds the same amount of sugarcane as one standard cane trailer. However, increased trailer weight may reduce maximum load by 1-2 tons of cane per truck load. One truck/trailer can handle approximately 15 bins. So there is a significant reduction in total number of trucks and trailers required. The trailer can be self-dumping at the mill or used with a rear dump system. Significant cost savings can be made in trailer tires and brakes as well as the number of trucks and trailers required. In addition, there are possible cost savings at the mill related to handling and moving cane. The number of bins required would need to be determined for specific mill situations (logistics related to quantity of cane and distance hauled).

All the three options are feasible, but an appropriate decision must be made by the legislature. Switching to any one of these options would prove very beneficial to the sugarcane industry in the long term.

CONCLUSIONS

The bridge in this study was evaluated and a monitoring system was installed to investigate the effects of heavy loads and cost of fatigue for bridges on state highways in Louisiana. Also, this study is used to respond to SCR-35. The superstructure of the bridge in this study was evaluated for safety and reliability under four different kinds of truck configuration and loads hauling sugarcane. The bridge model was verified by performing live load tests on the structure. The bridge finite element model was analyzed under the different kinds of loading and the effects were listed and compared. The results of the analyses show that the pattern of response of the bridge under the four different cases follows the same trend. Among the four different cases of loading configurations, Case IV which was GVW =148,000 lb. and vehicle length of 92 ft., produced the largest tensile and compressive stresses in the members. The results from the bridge deck analyses indicated that the ratio of tensile stresses at the top surface is of the same magnitude as the ratio of compressive stresses at the bottom surface. Also, the ratio of compressive stresses at the top surface is of the same magnitude as the ratio of tensile stresses at the bottom surface. These similarities confirm that the bridge deck is under a stable stress state, whether the stresses are in the tension zone or the compression zone. The heavy load as indicated in SCR-35 will cause damage to bridges, specifically with spans longer than 90 ft.

During the live load tests, the strain readings were reviewed to determine the contribution of each girder to the behavior of the bridge as a system. The strains in the girders indicated that all the girders are in the same state of strain, tension, or compression, and the magnitude of the strain in each girder is related to its distance from the axle of the truck. This confirms to the design specifications that the load applied to the bridge is distributed between the girders based on their location and spacing. The results of the linear regression analyses used to determine the truck gross vehicle weight from the strains recorded by the monitoring system were not conclusive.

The monitoring system also records strains every hour and strain cycles that occurred within the range during the hour period. The data provide the relative magnitude of strain ranges for the various gauge locations. It also provides the strain reversals in the girders, which is an important factor for fatigue analysis. The recorded data indicated that the bridge girders are subject to low cycles of high strain values, above 33-microstrains, and high cycles of low strain values. The girder performance under such conditions can be explained as follows: the high strain values exceed the serviceability criteria and can lead to cracks in the girders then the high cycles of low strain will lead to fatigue in the prestressed strands. Consequently, the girders will deteriorate and the life span of the bridge will be reduced. The data from the

monitoring system indicated that the average number of heavy loads during October, November, and December is 3.5 times higher than the rest of the year. The bridges are exposed to a high cycle of repetition of heavy loads that will reduce the life span of the bridges by about 50%. The bridges that are built to last 75 years will require replacement after about 40 years in service. This seasonal impact is due to the sugarcane harvest, and these results confirm the cost of fatigue ($0.9 per truck per trip per bridge), as determined in the previous studies (LTRC report numbers 418 and 425) *[1, 3]*.

RECOMMENDATIONS

Based on the results of the studies presented in this report, the following is recommended:

- Maintain current gross vehicle weight of sugarcane trucks on Louisiana interstate bridges.

- Maintain the current truck configuration 3S3 used to haul sugarcane with a GVW of 100,000 lb. uniformly distributed. This will result in the least amount of fatigue cost on the network.

The heavy loads indicated in SCR-35 will cause structural failure of bridge girders. The Off-system bridges are generally designed for lower loads than on-system bridges. As a result, the impact of sugarcane trucks can be very detrimental to the span life of these bridges, and requires further evaluations. All these bridges, on and off system, should be rehabilitated prior to considering implementing the SCR 35.

As a result, it is recommended to maintain the monitoring system installed on this project, and continue collecting field data that will assist in developing the trend in the bridge performance. The strain data and heavy load truck pictures will provide a good source of information to evaluate and revise the current serviceability criteria used by LADOTD for design of prestressed concrete bridge girders [*9*]. Also, the data should be further investigated to establish a mathematical relationship between strains and axle loads thus eliminating the use of weigh-in-motion equipment.

ACRONYMS, ABBREVIATIONS, AND SYMBOLS

AASHTO	American Association of State Highway and Transportation Officials
BDI	Bridge Diagnostic Inc.
FHWA	Federal Highway Administration
GVW	Gross Vehicle Weight
GTSTRUDL	Georgia Tech Structural Design Language
IPSL Element	Iso Parametric Solid Linear Element
LADOTD	Louisiana Department of Transportation and Development
LTRC	Louisiana Transportation Research Center
PRC	Project Review Committee
RRSC	Raceland Raw Sugar Corporation
SBCR Element	A Plate element with Stretching and Bending Coupled Response

REFERENCES

1. Saber, A., Roberts, F., and Zhou, X. "Monitoring System to Determine the Impact of Sugarcane Truckloads on Non-Interstate Bridges." Louisiana Transportation Research Center, Report No. 418, Baton Rouge, LA, December 2006.

2. Louisiana Senate Concurrent Resolution 35. June 2009

3. Saber, A., Roberts, F., and Ranadhur, A. "Evaluating the Effects of Heavy Sugarcane Truck Operations on Repair Coast of Low Volume Highways." Louisiana Transportation Research Center, Report No. 425, Baton Rouge, LA, 2008.

4. Roberts, F., Djakfar, L., "Preliminary Assessment of Pavement Damage Due to Heavier Loads on Louisiana Highways." Louisiana Transportation Research Center, Report No. 321, Baton Rouge, LA, 1999.

5. Roberts, F., Saber, A., Ranadhir, A., and Zhou, X. "Effects of Hauling Timber, Lignite Coal, and Coke Fuel on Louisiana Highways and Bridges." Submitted to LADOTD-LTRC Report No. 398, March 2005.

6. Project Documents for Louisiana State Project No. 424-04-0034.

7. Federal Highway Administration. "Section 19: FHWA Vehicle Classification Figures." http://onlinemanuals.txdot.gov/txdotmanuals/tda/fhwa_vehicle_classification_figures.htm #i1106433. Accessed March 17, 2011.

8. Louisiana Department of Transportation. "License Weight."

9. "Bridge Design Manual." Louisiana Department of Transportation and Development, Fourth Edition.

10. AASHTO LRFD Bridge Design Specifications. *Third Edition.* American Association of State Highway and Transportation Officials, Washington D.C.

11. AASHTO, Standard Specifications for Highway Bridges. *Sixteenth Edition.* American Association of State Highway and Transportation Officials, Washington D.C., 1996.

12. Johnson, R.A., and Wichern, D.W. "Multivariate Linear Regression Models." *Applied Multivariate Statistical Analysis. 2nd Edition,* Prentice-Hall, Inc., Englewood Cliffs, NJ., 1982, pp 273.

13. Kachigan, S.K. "Chapter 11: Regression Analysis." *Statistical Analysis: An Interdisciplinary Introduction to Univariate and Multivariate Methods.* Radius Press, New York, NY, 1982, pp. 283-260.

14. Minnesota Department of Transportation http://www.dot.state.mn.us/i35wbridge/bridgeinspectiondefs.pdf

15. Bruce, B., Russell, H., Roller, J. "Fatigue and Shear Behavior of HPC Bulb-Tee Girders." Louisiana Transportation Research Center, Report No. 382, Baton Rouge, LA, October 2003.

16. Saber, A., Zhou, X., and Alaywan, W. "Monitoring Louisiana Bridges for Heavy Truck Loads Hauling Sugarcane." Transportation Research Board, Washington D.C., January 2008.

17. Saber, A., Morvant, M., and Zhang, Z. "Effects of Heavy Truck Operations on Repair Costs of Low Volume Highways." Transportation Research Board, Washington D.C., January 2009.

18. Saber, A., and Roberts, F. "Cost of Higher Truck Loads on Remaining Safe Life of Louisiana Bridges." Transportation Research Board, Washington D.C., January 2006.

19. Saber, A., Roberts, F., Alaywan, W., and Zhou, X. "Impact of Higher Truck Loads on Remaining Safe Life of Louisiana Concrete Bridge Girders." Proceedings of the 2006 Concrete Bridge Conference, Reno, NV, May 2006.

20. Saber, A., Roberts, F., Alaywan, W., and Zhou, X. "Impact of Higher Truck Loads on Remaining Safe Life of Louisiana Bridge Decks." Proceedings of the 9th International Conference, Applications of Advanced Technology in Transportation, Chicago, IL, August 2006.

21. Saber, A., Roberts, F., and Toups, J. "Effects of Continuity Diaphragm for Skewed Continuous Span Precast Concrete Girder Bridges." *Precast/Prestressed Concrete Institute (PCI) Journal* March/April 2007, pp. 108-114.

22. Saber, A., and Kahn, L. "Stability of Long-Span Prestensioned High Performance Concrete Girders." Proceedings of the 7th International Conference on High Performance Concrete, Washington D.C., 2005.

23. Saber, A., Toups, J., Guice, L., and Tayebi, A. “Continuity Diaphragm for Skewed Continuous Span Precast Prestressed Concrete Girder Bridges.” Submitted to LADOTD-LTRC Report FHWA/LA-04-383, July 2003.

24. Sanders, W.W., and Elleby, H.A. “Distribution of Wheel Loads on Highway Bridges.” NCHRP Report No. 83. Highway Research Board, Washington D.C., 1970.

25. AASHTO Guide for Design of Pavement Structures. American Association of State Highway and Transportation Officials, Washington D.C.

26. Boresi, A., and Schmidt, R. *Advanced Mechanics of Materials.* John Wiley & Sons, New Jersey, 2003, pp. 567-569.

APPENDIX A

Comparison of Top and Bottom Elements of Instrumented Girders

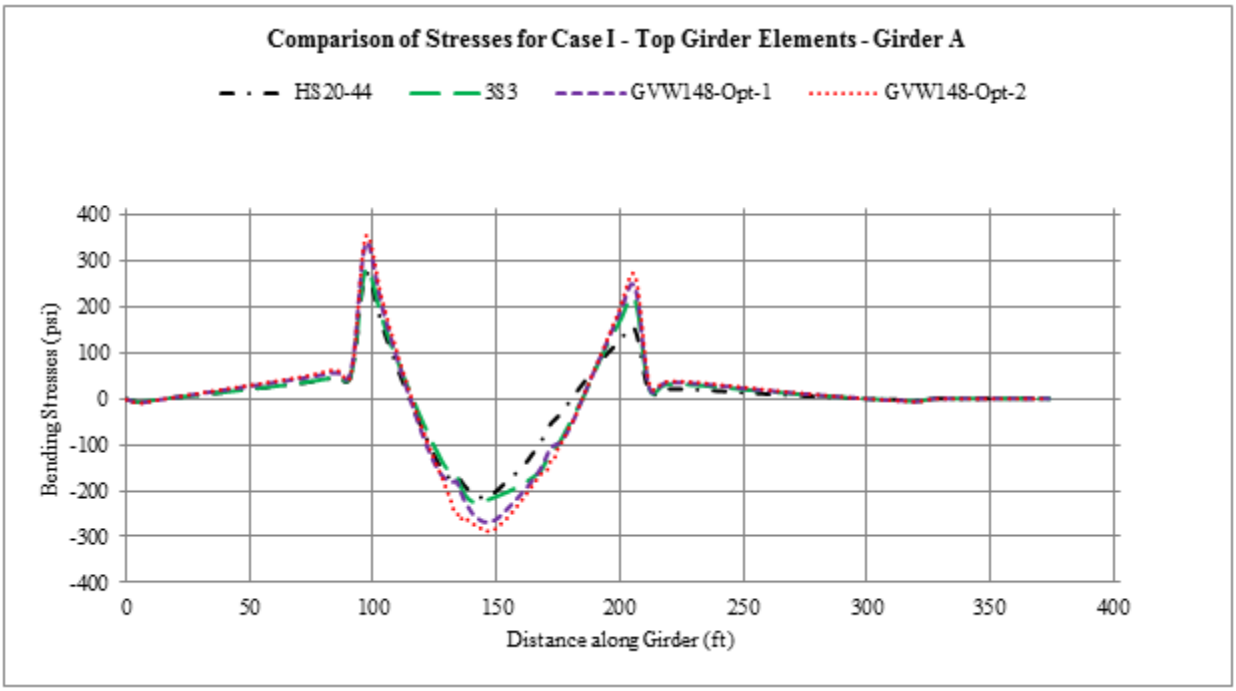

Figure 49
Comparison of flexural stress distribution of top elements - Girder A of Case I

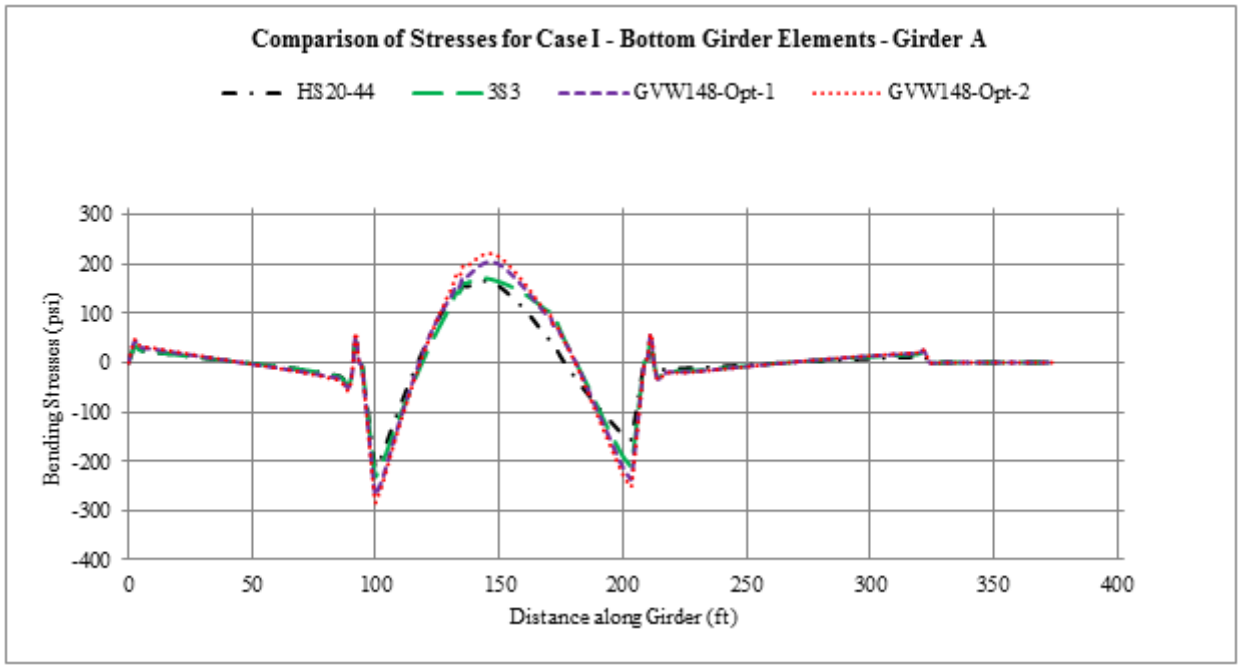

Figure 50
Comparison of flexural stress distribution of bottom elements - Girder A of Case I

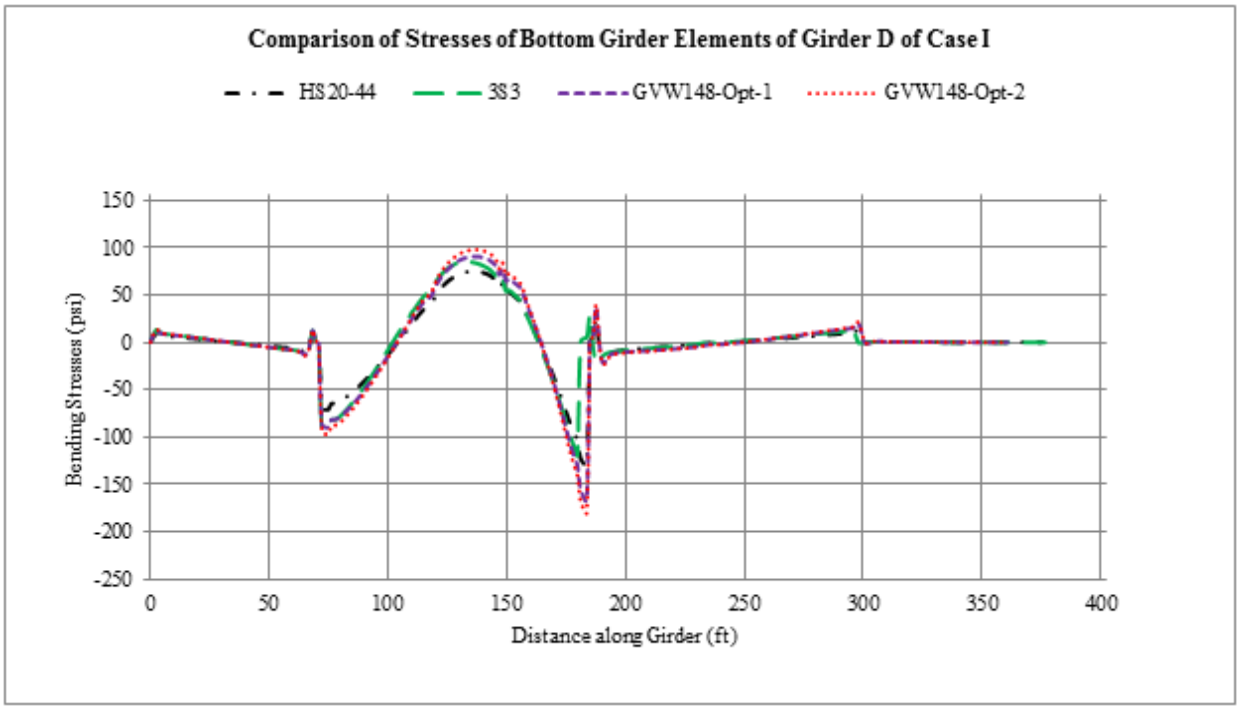

Figure 51
Comparison of bending stress distribution of bottom elements - Girder D of Case I

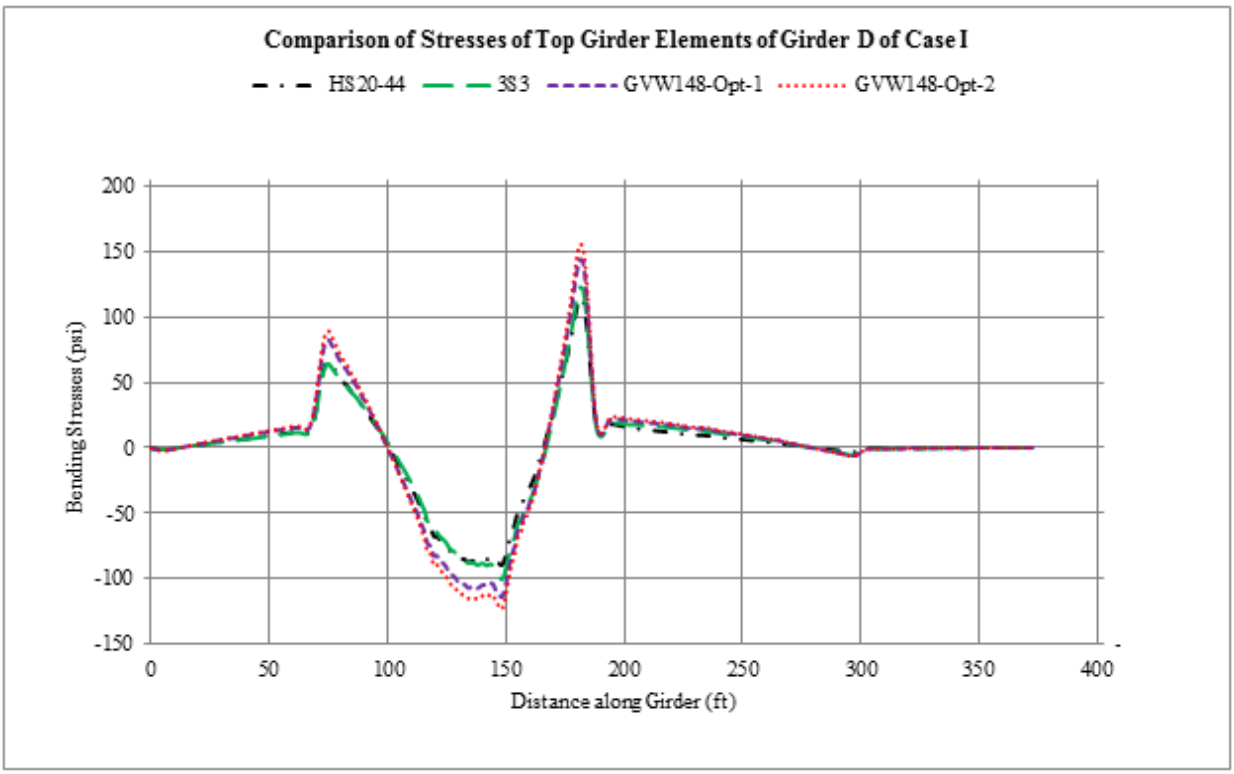

Figure 52
Comparison of bending stress distribution of top elements - Girder C of Case I

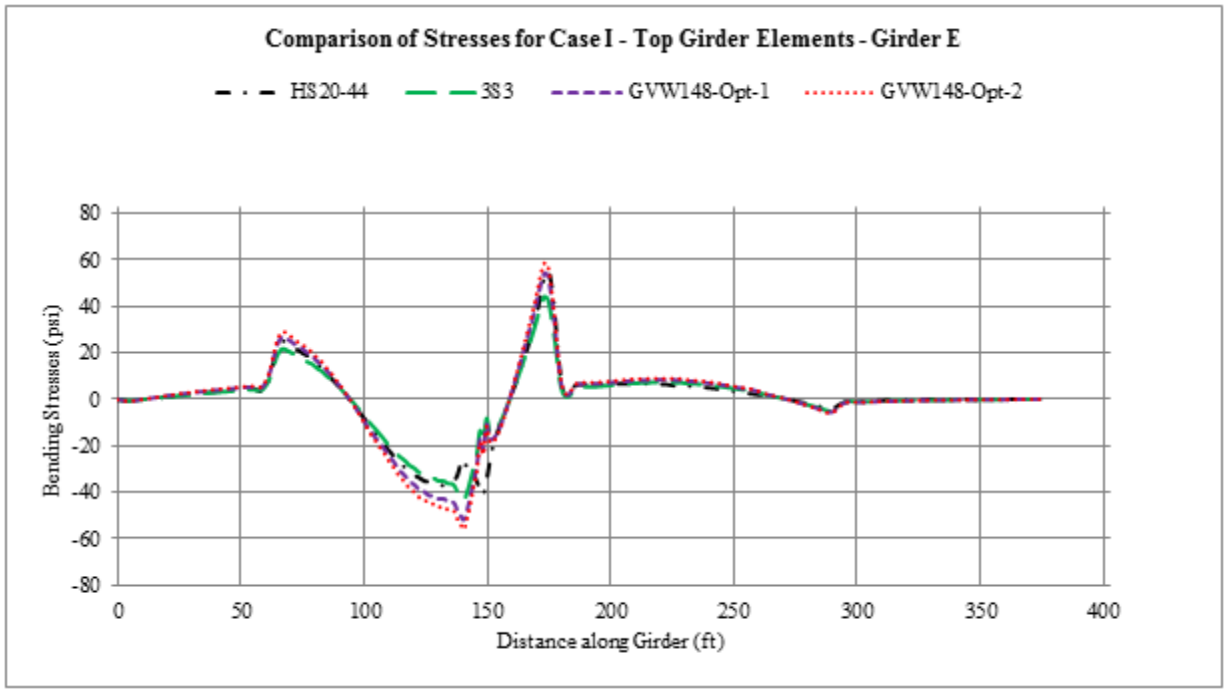

Figure 53
Comparison of flexural stress distribution of top elements - Girder E of Case I

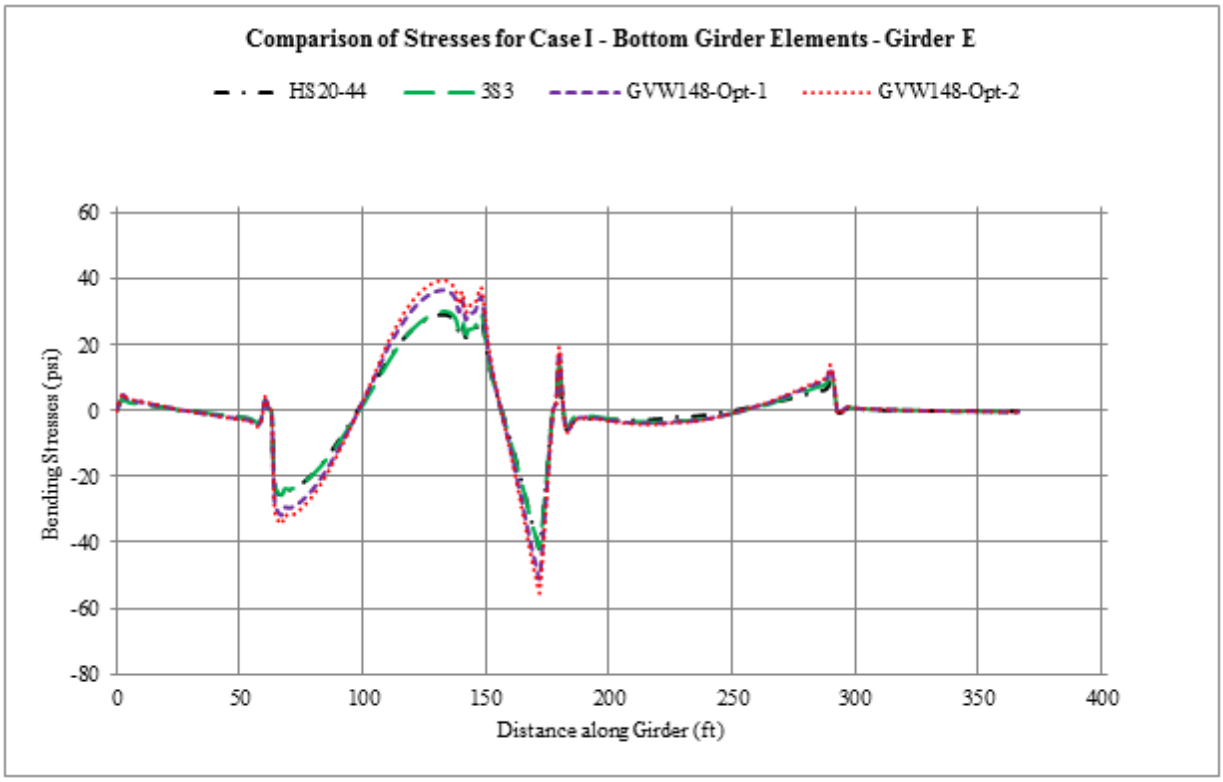

Figure 54
Comparison of flexural stress distribution of bottom elements - Girder E of Case I

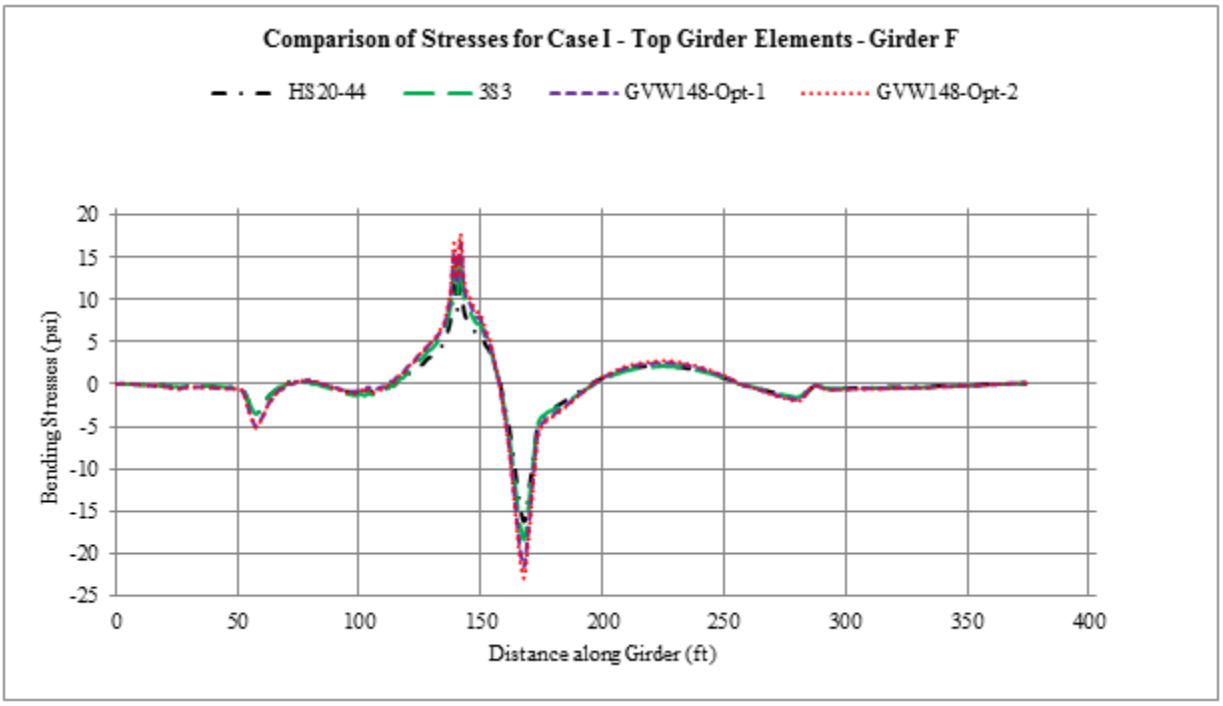

Figure 55
Comparison of flexural stress distribution of top elements - Girder F of Case I

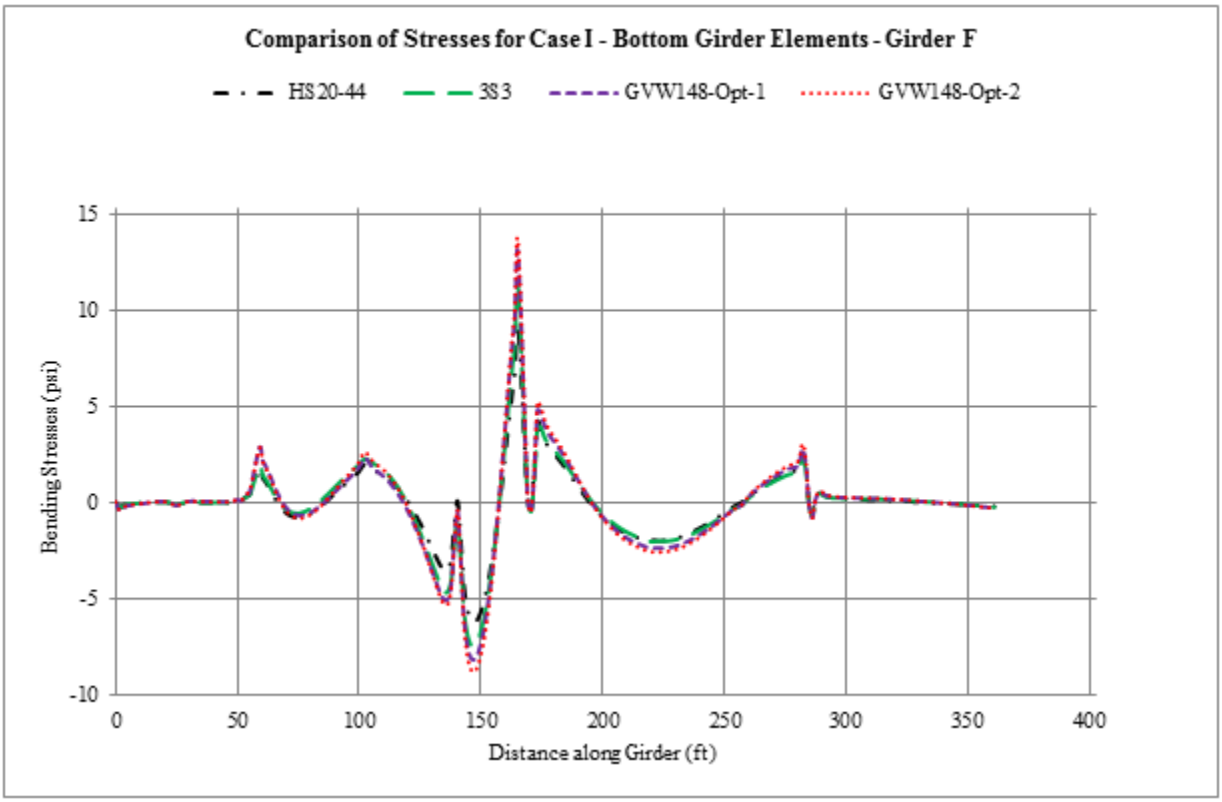

Figure 56
Comparison of flexural stress distribution of bottom elements - Girder F of Case I

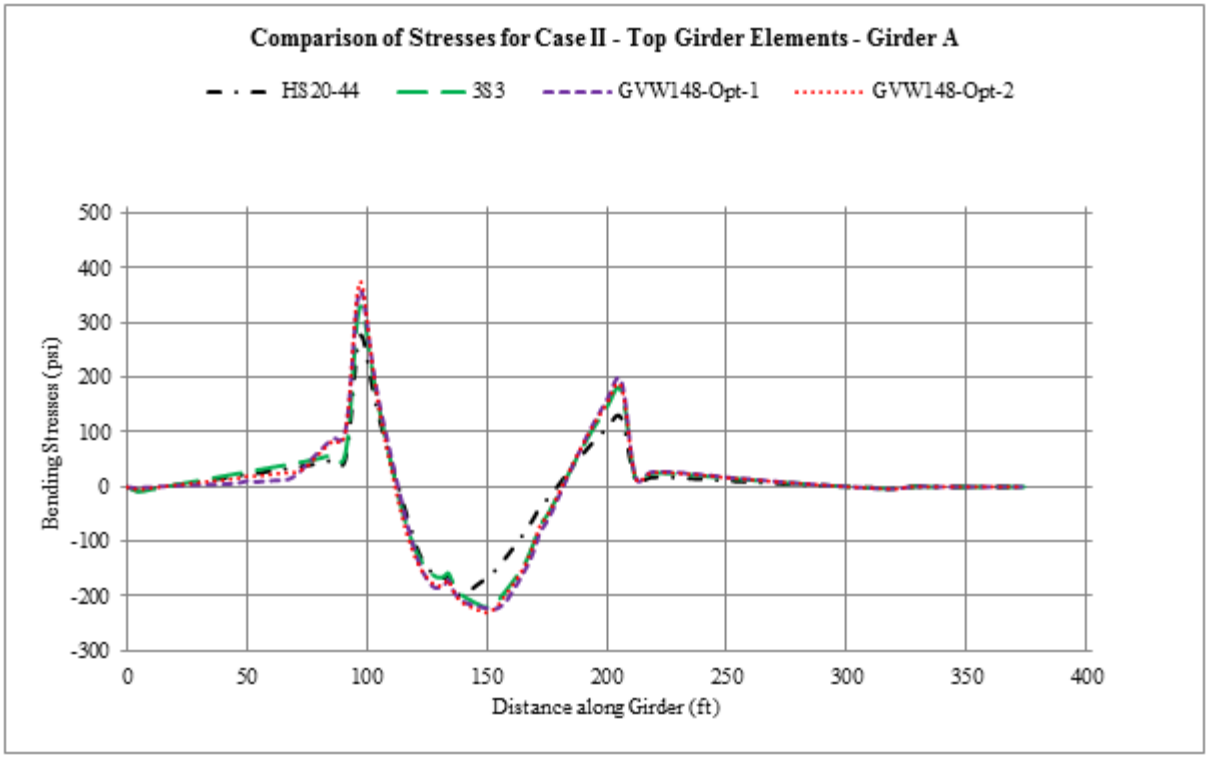

Figure 57
Comparison of flexural stress distribution of top elements - Girder A of Case II

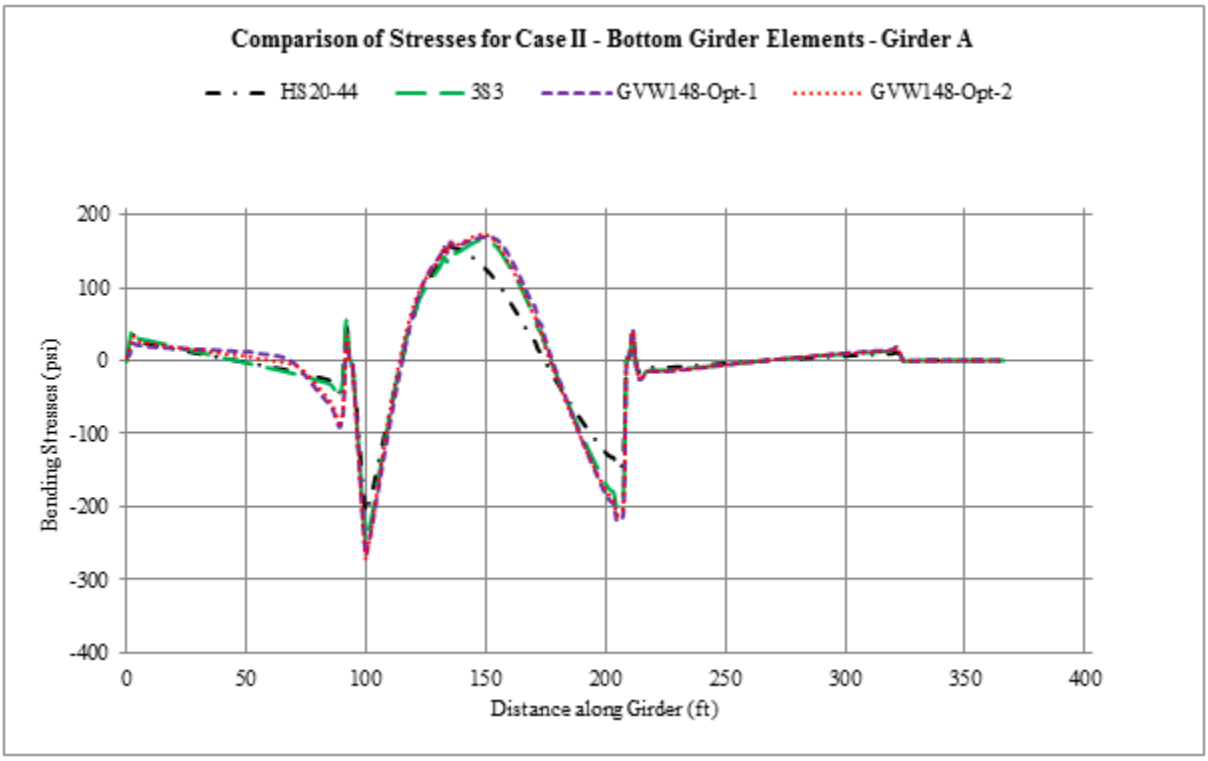

Figure 58
Comparison of flexural stress distribution of bottom elements - Girder A of Case II

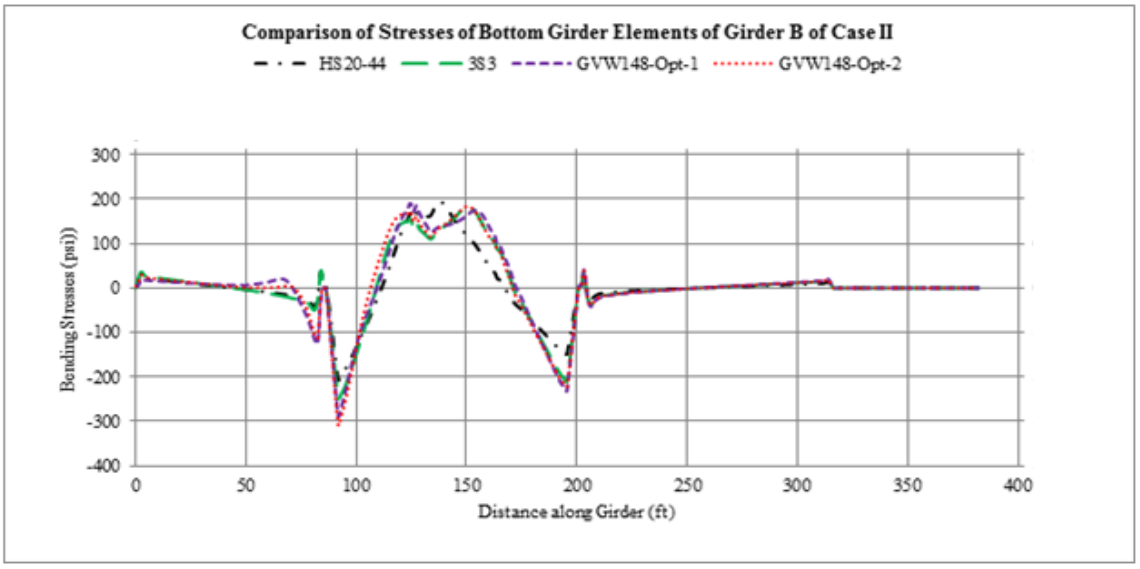

Figure 59
Comparison of bending stress distribution of bottom elements - Girder B of Case II

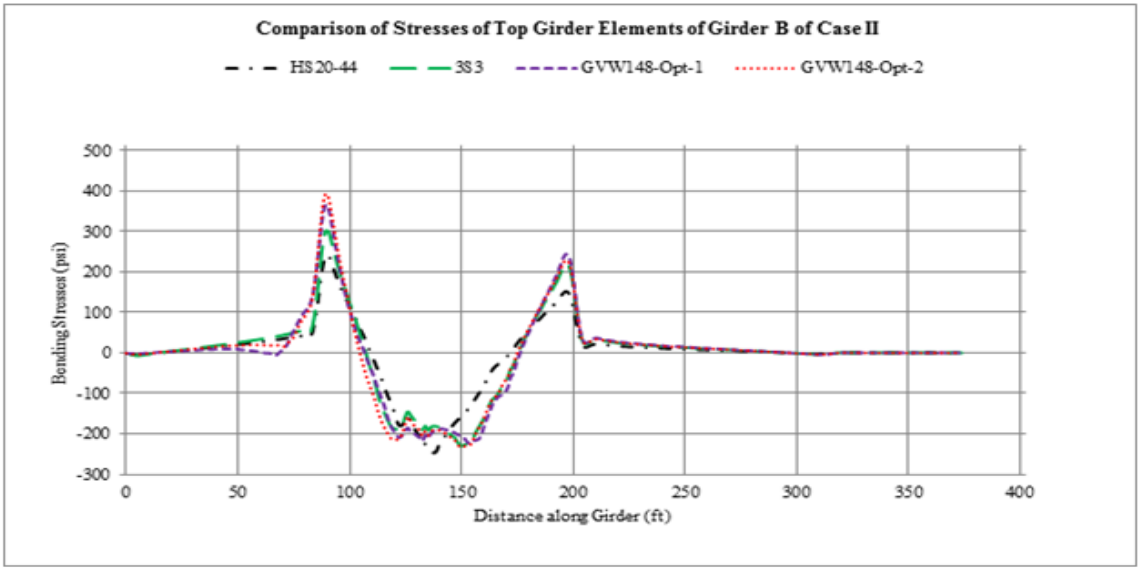

Figure 60
Comparison of bending stress distribution of top elements - Girder B of Case II

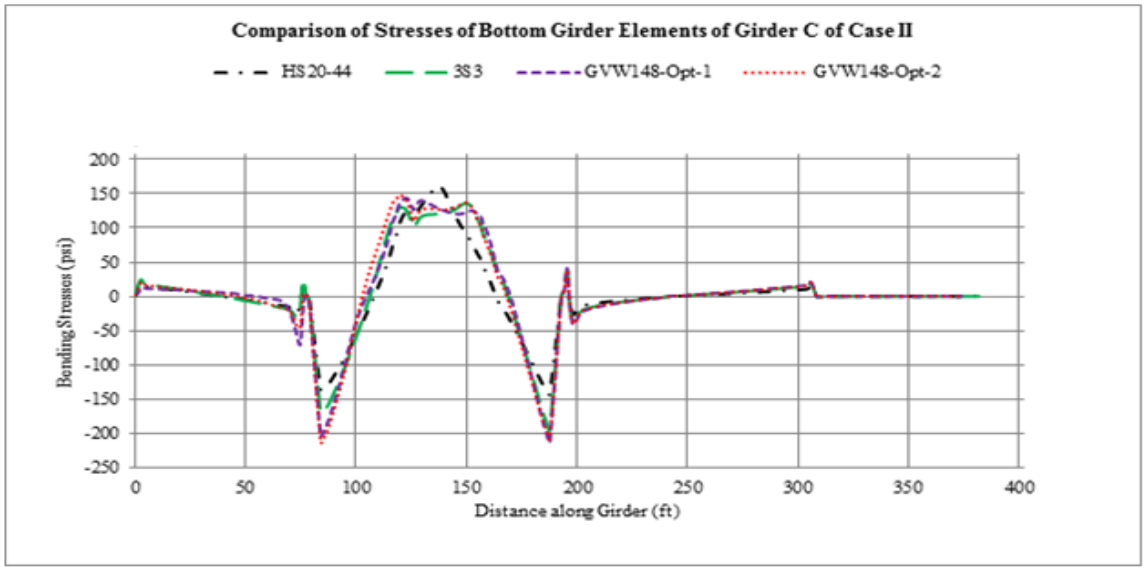

Figure 61
Comparison of bending stress distribution of bottom elements - Girder C of Case II

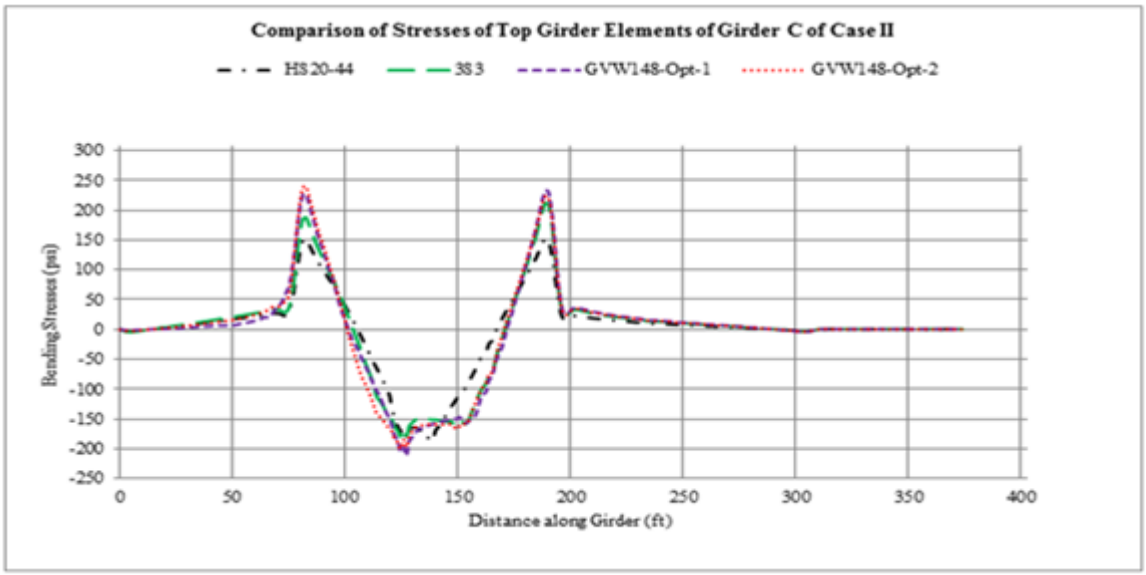

Figure 62
Comparison of bending stress distribution of top elements - Girder C of Case II

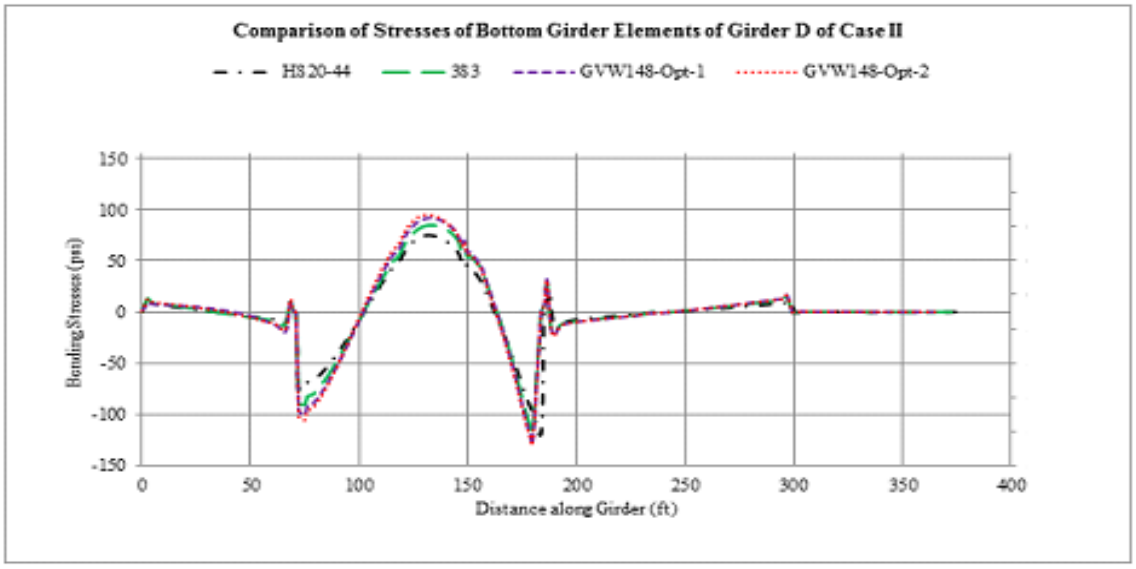

Figure 63
Comparison of bending stress distribution of bottom elements - Girder D of Case II

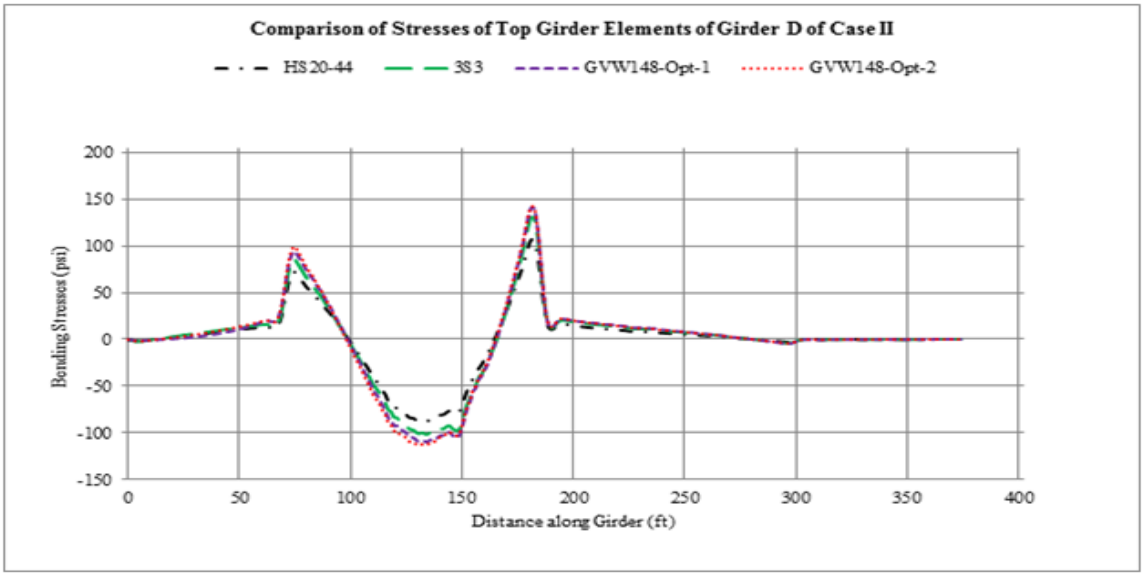

Figure 64
Comparison of bending stress distribution of top elements - Girder D of Case II

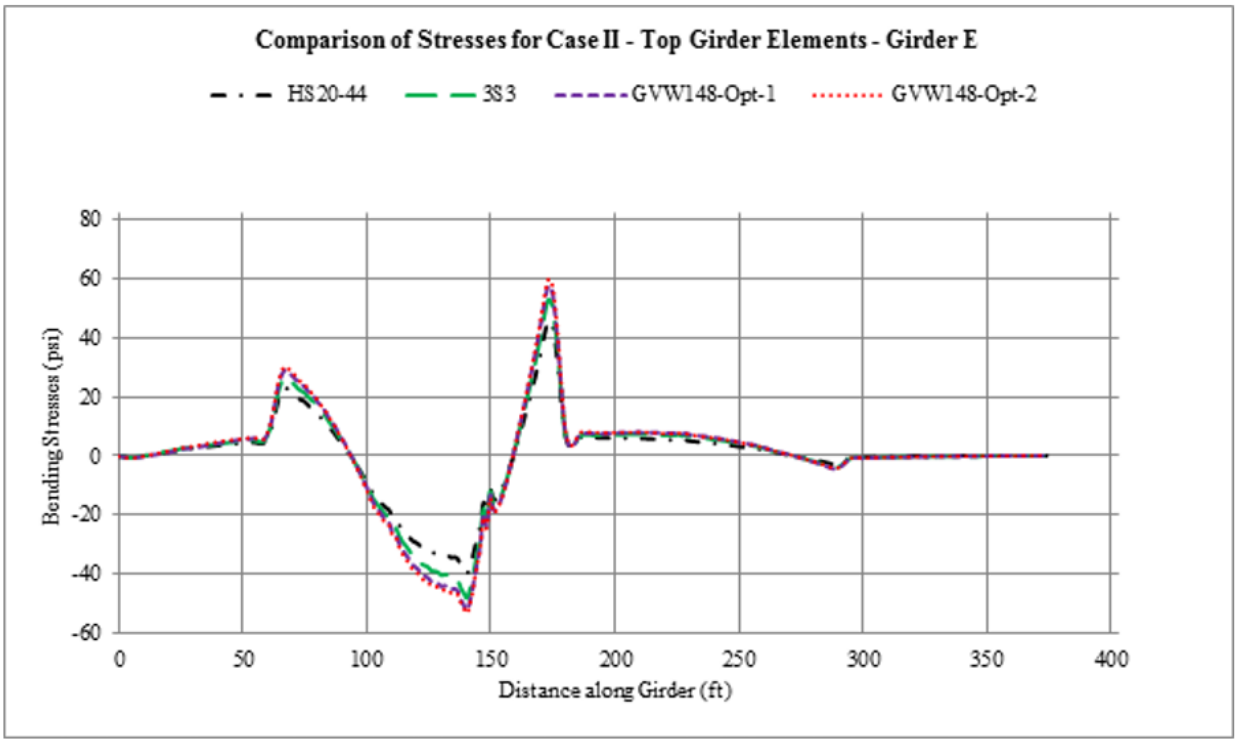

Figure 65
Comparison of flexural stress distribution of top elements - Girder E of Case II

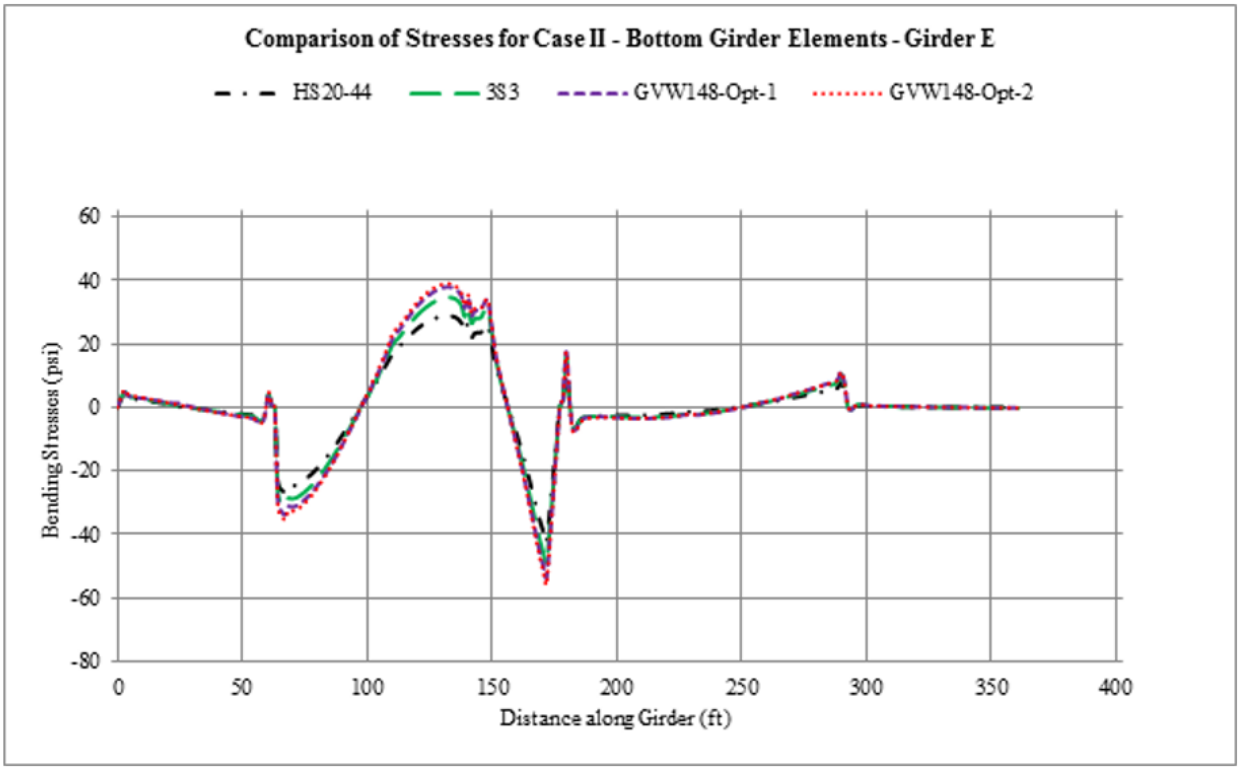

Figure 66
Comparison of flexural stress distribution of bottom elements - Girder E of Case II

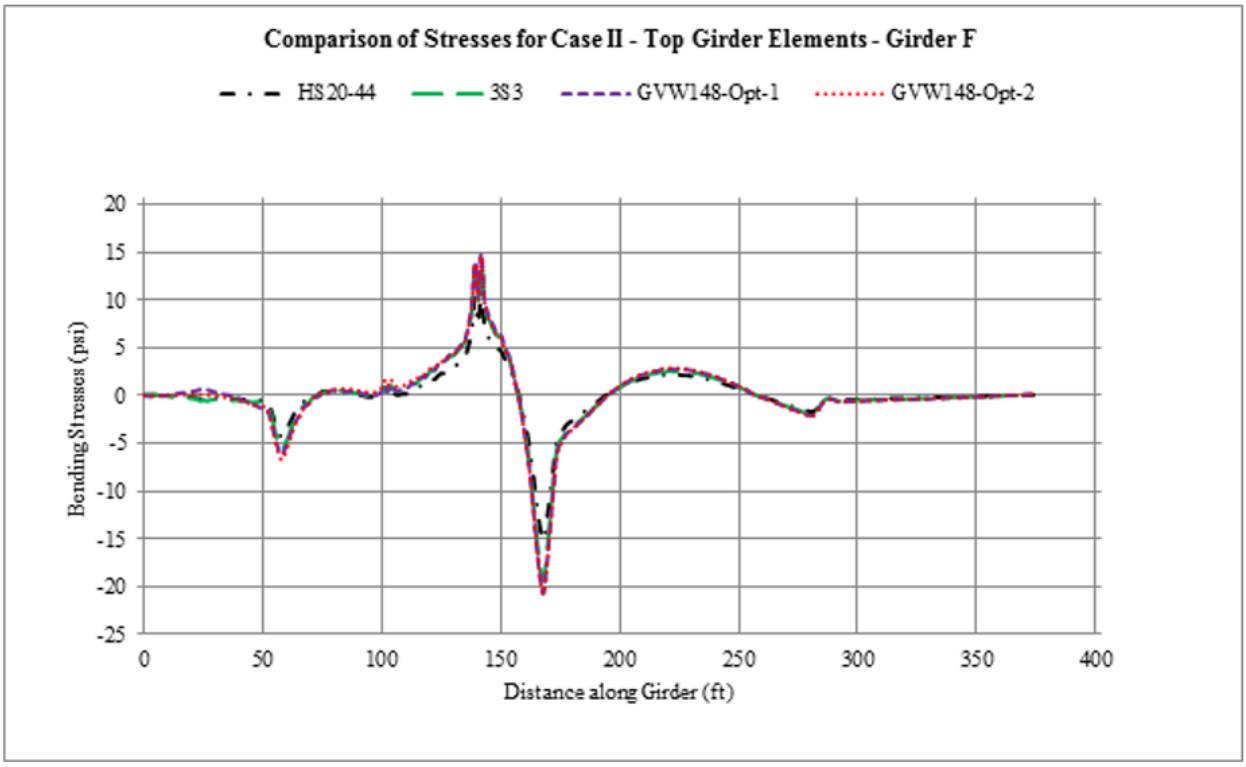

Figure 67
Comparison of flexural stress distribution of top elements - Girder F of Case II

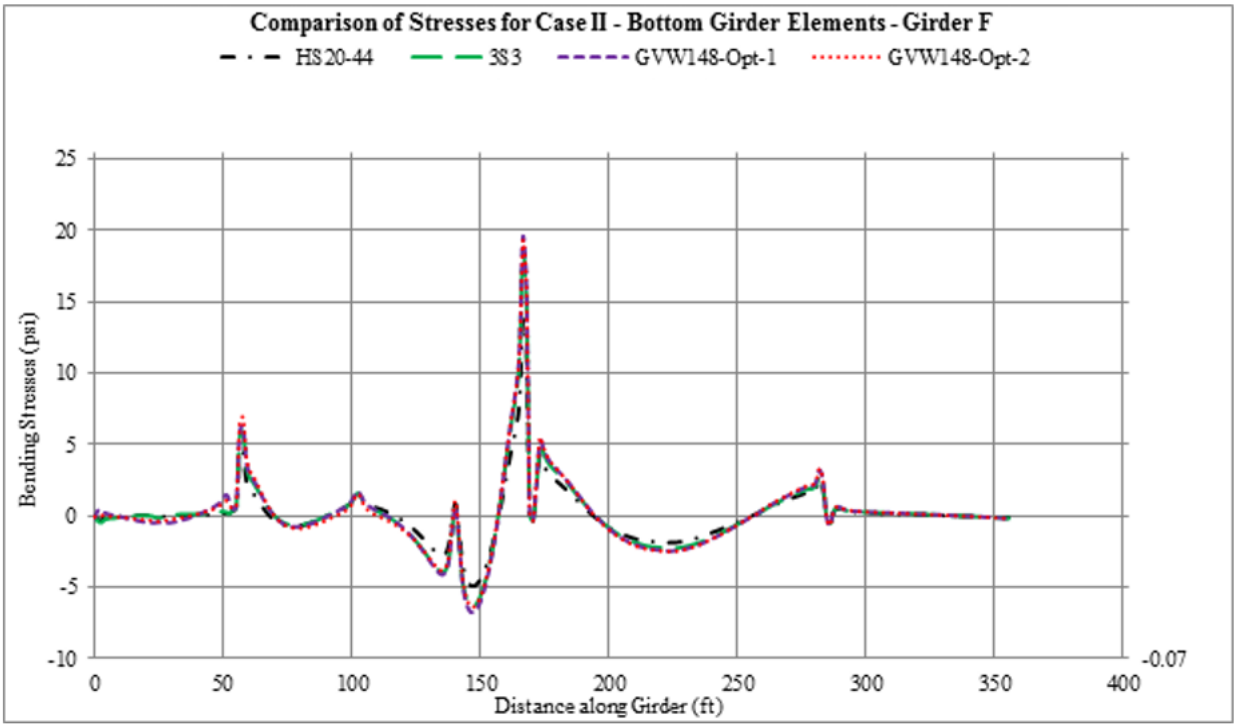

Figure 68
Comparison of flexural stress distribution of bottom elements - Girder F of Case II

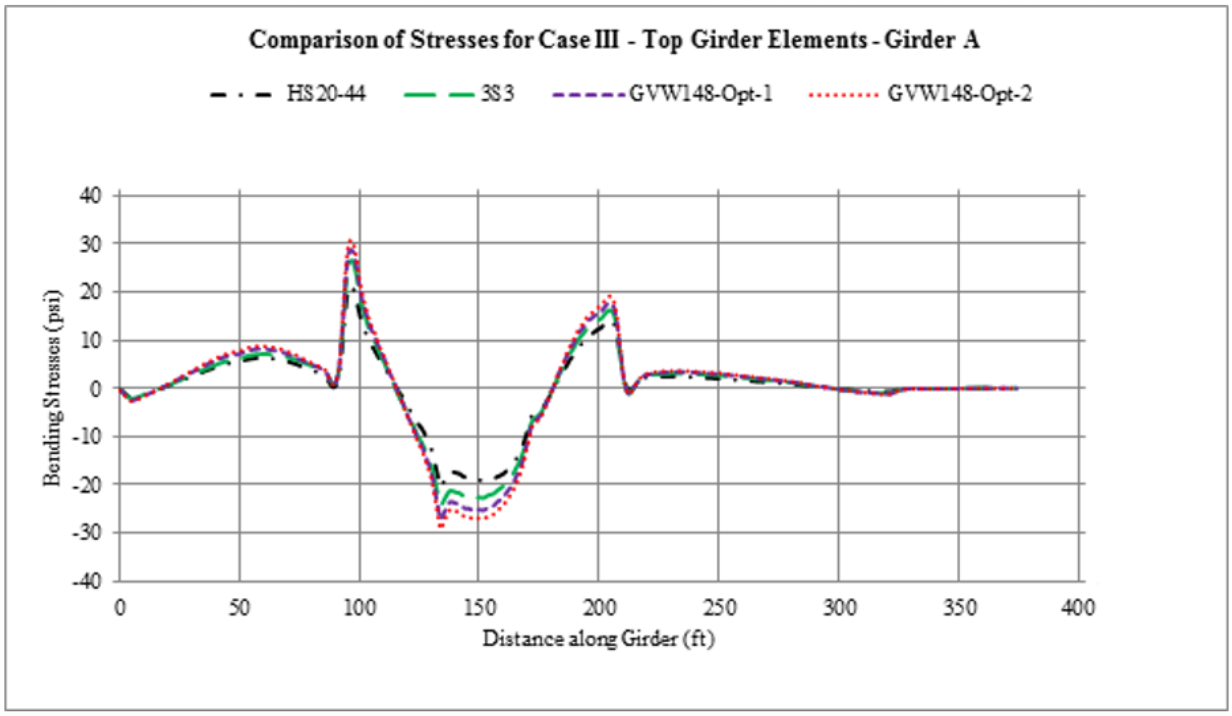

Figure 69
Comparison of flexural stress distribution of top elements - Girder A of Case III

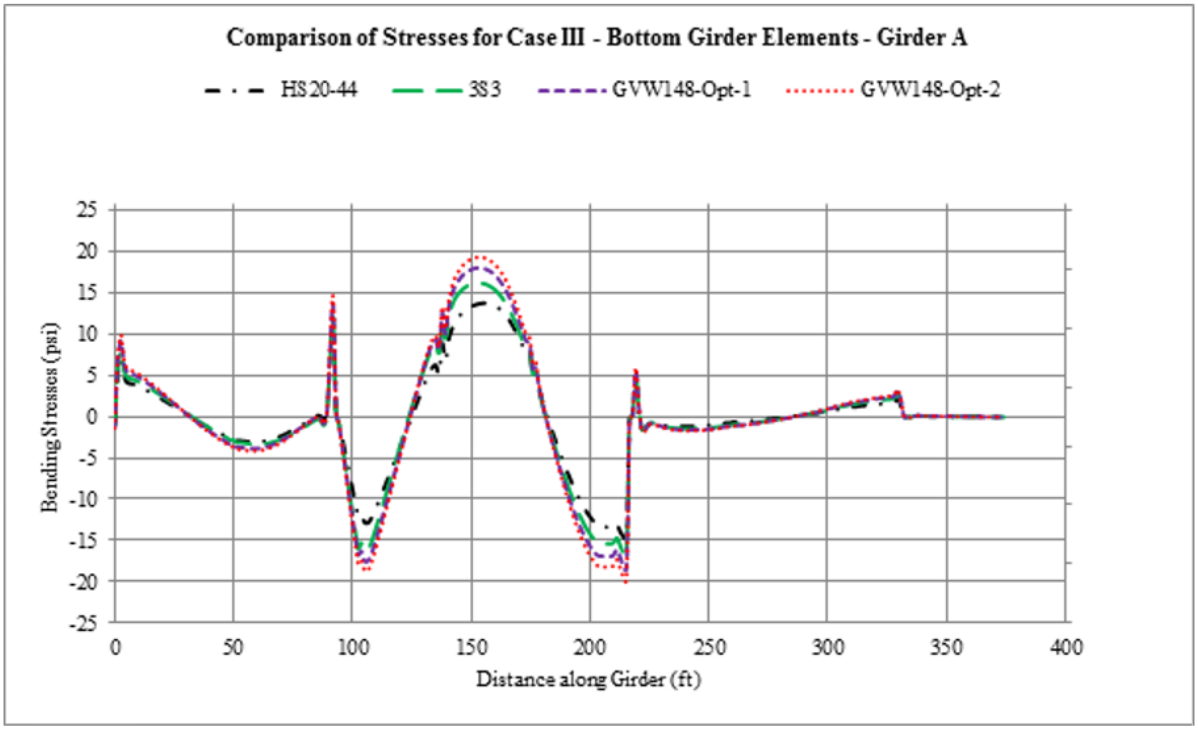

Figure 70
Comparison of flexural stress distribution of bottom elements - Girder A of Case III

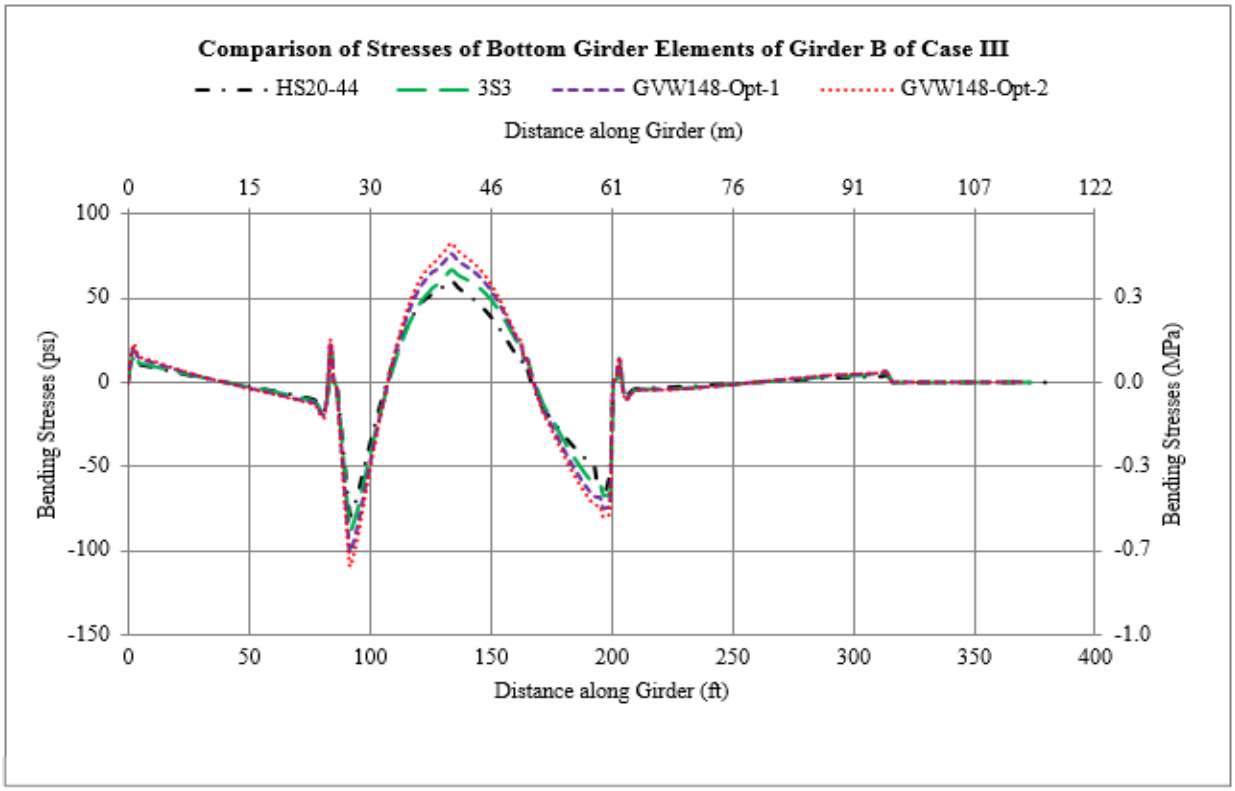

Figure 71
Comparison of bending stress distribution of bottom elements - Girder B of Case III

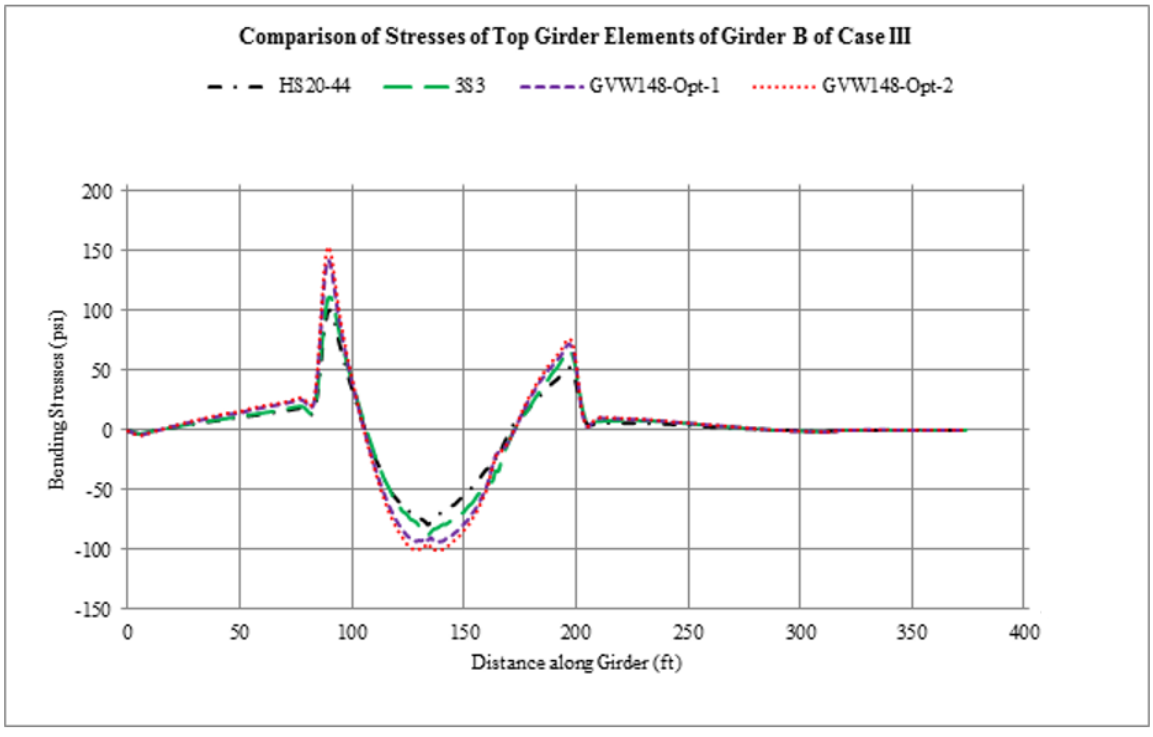

Figure 72
Comparison of bending stress distribution of top elements - Girder B of Case III

Figure 73
Comparison of bending stress distribution of bottom elements - Girder C of Case III

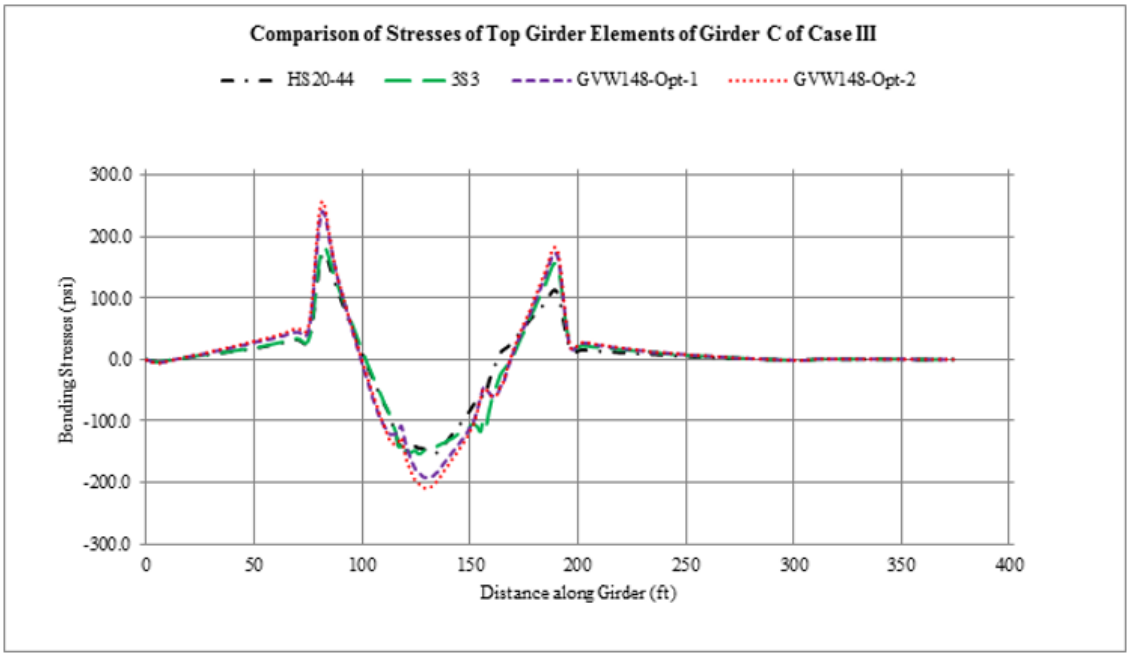

Figure 74
Comparison of bending stress distribution of top elements - Girder C of Case III

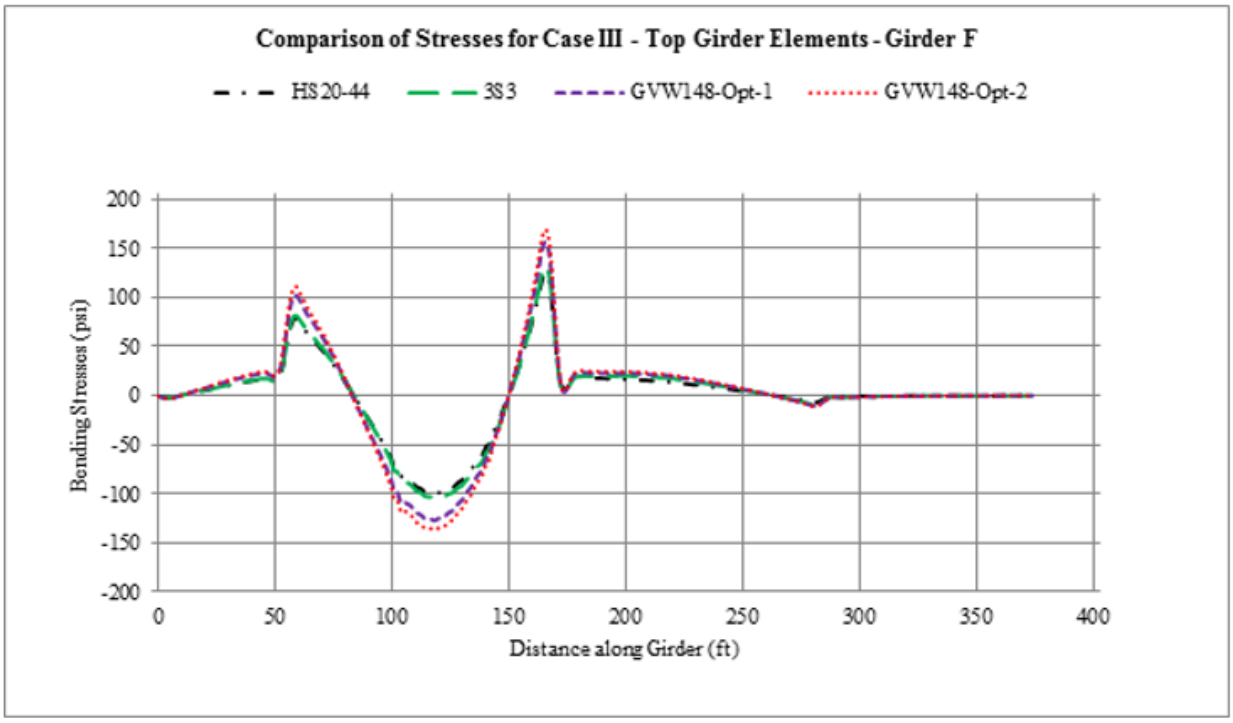

Figure 75
Comparison of flexural stress distribution of top elements - Girder F of Case III

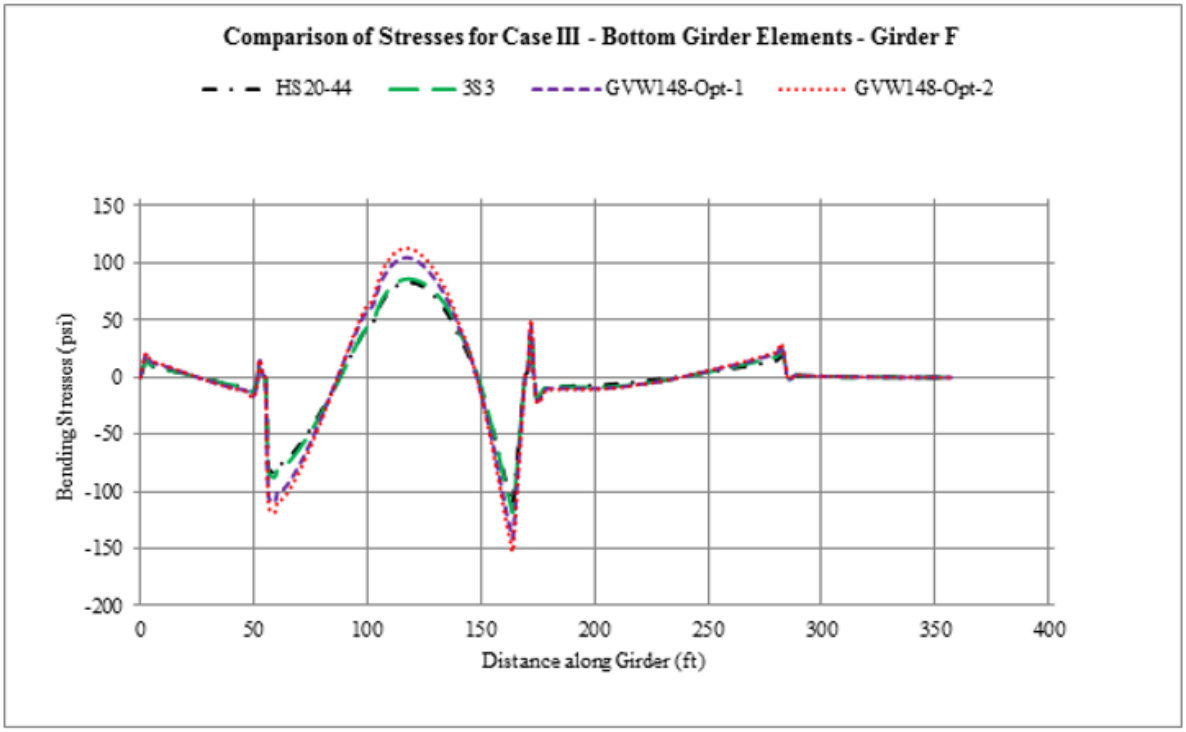

Figure 76
Comparison of flexural stress distribution of bottom elements - Girder F of Case III

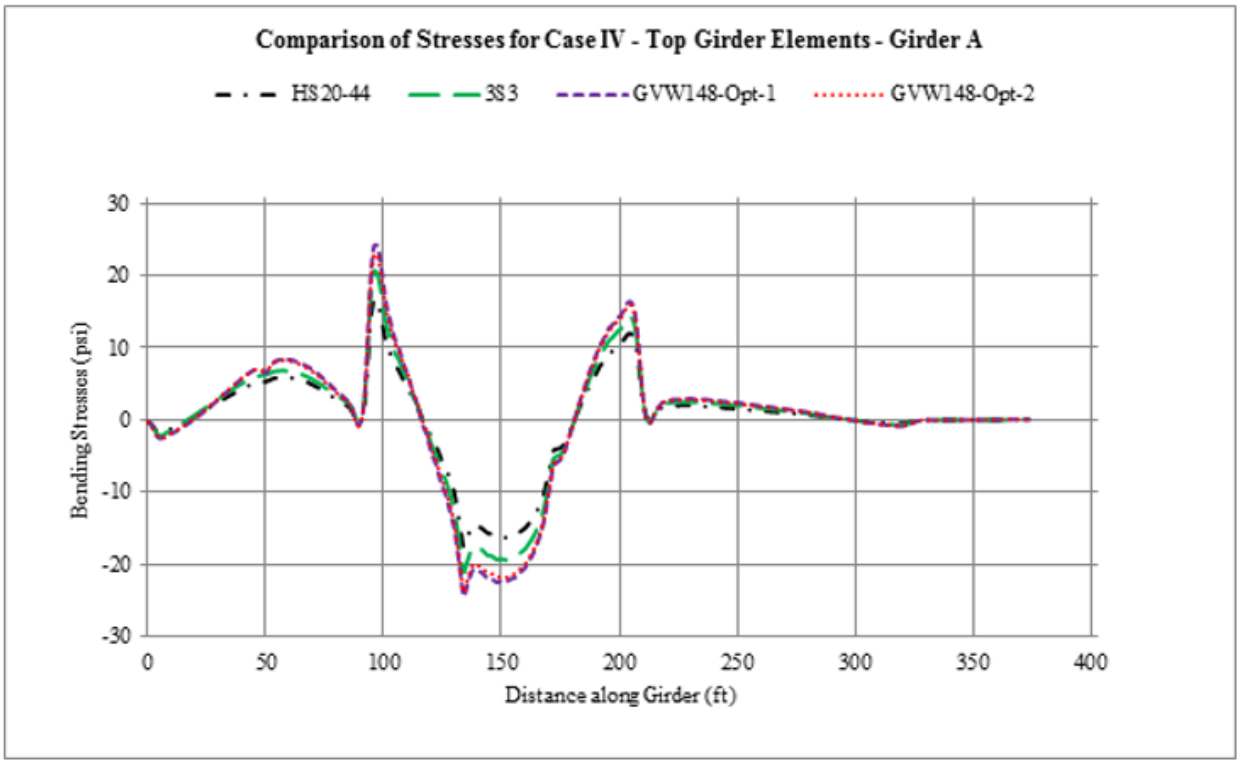

Figure 77
Comparison of flexural stress distribution of top elements - Girder A of Case IV

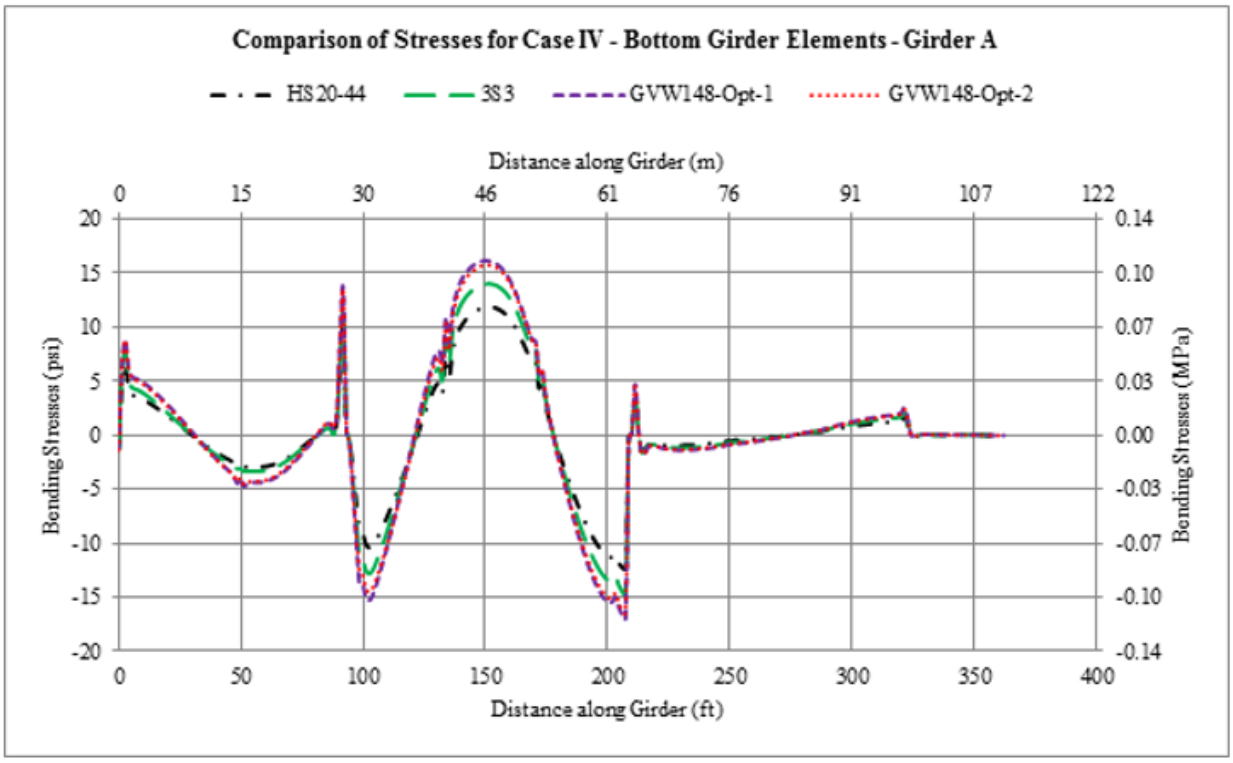

Figure 78
Comparison of flexural stress distribution of bottom elements - Girder A of Case IV

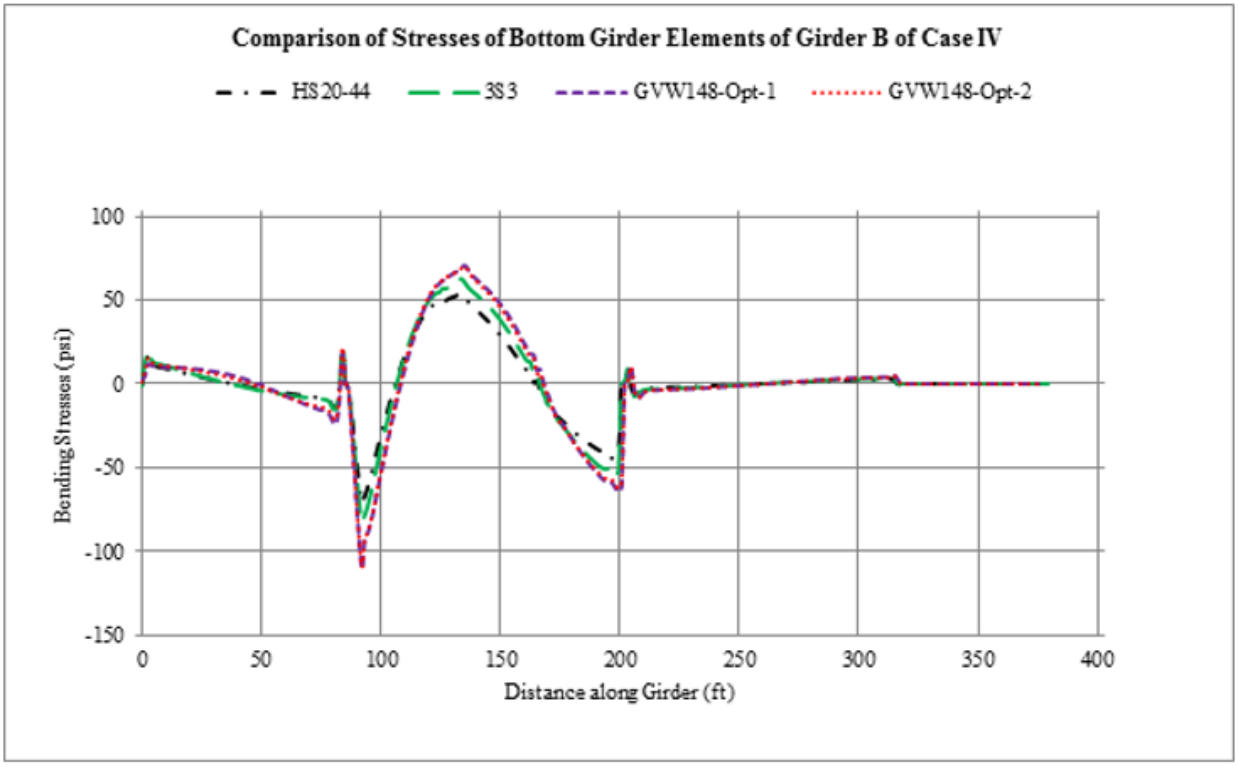

Figure 79
Comparison of bending stress distribution of bottom elements - Girder B of Case IV

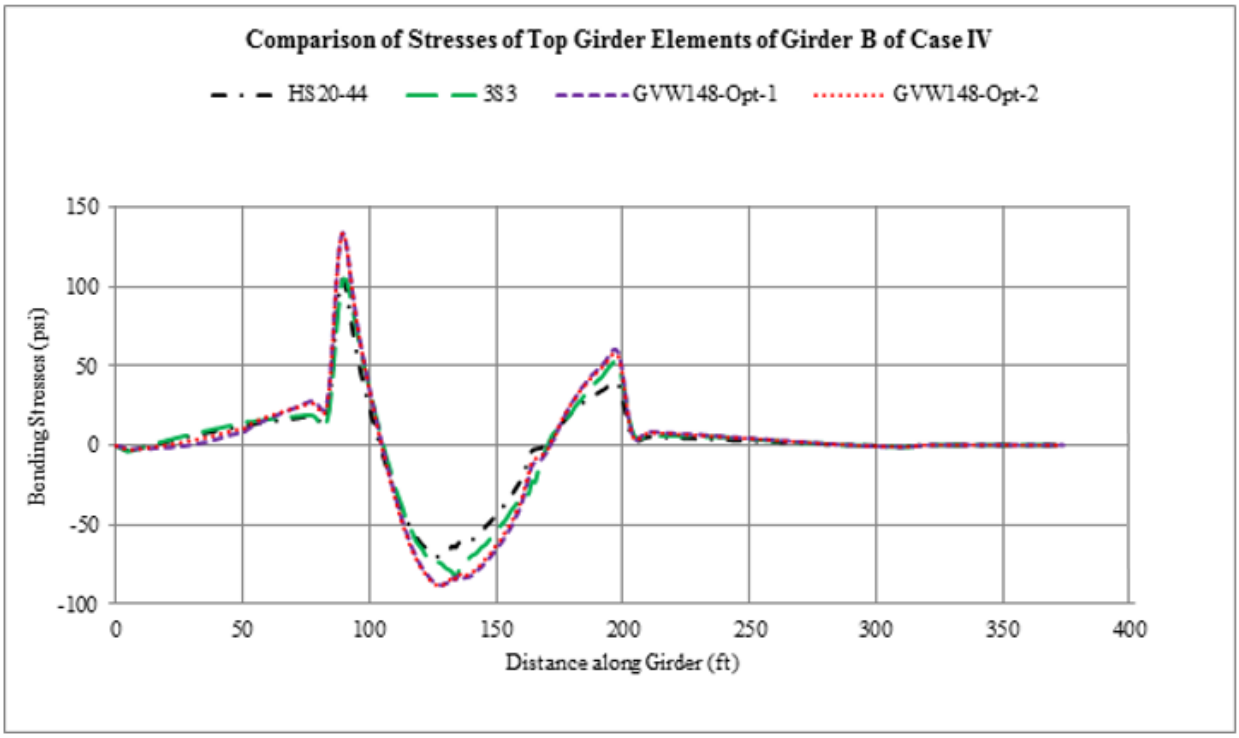

Figure 80
Comparison of bending stress distribution of top elements - Girder B of Case IV

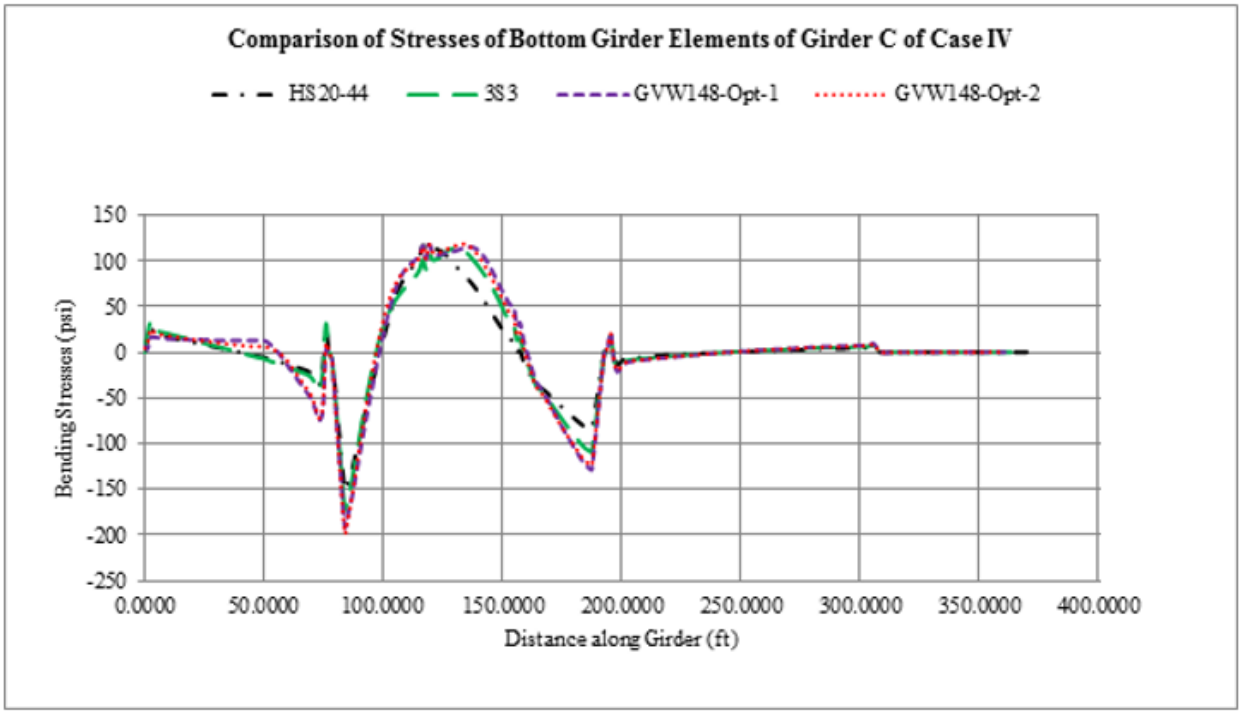

Figure 81
Comparison of bending stress distribution of bottom elements - Girder C of Case IV

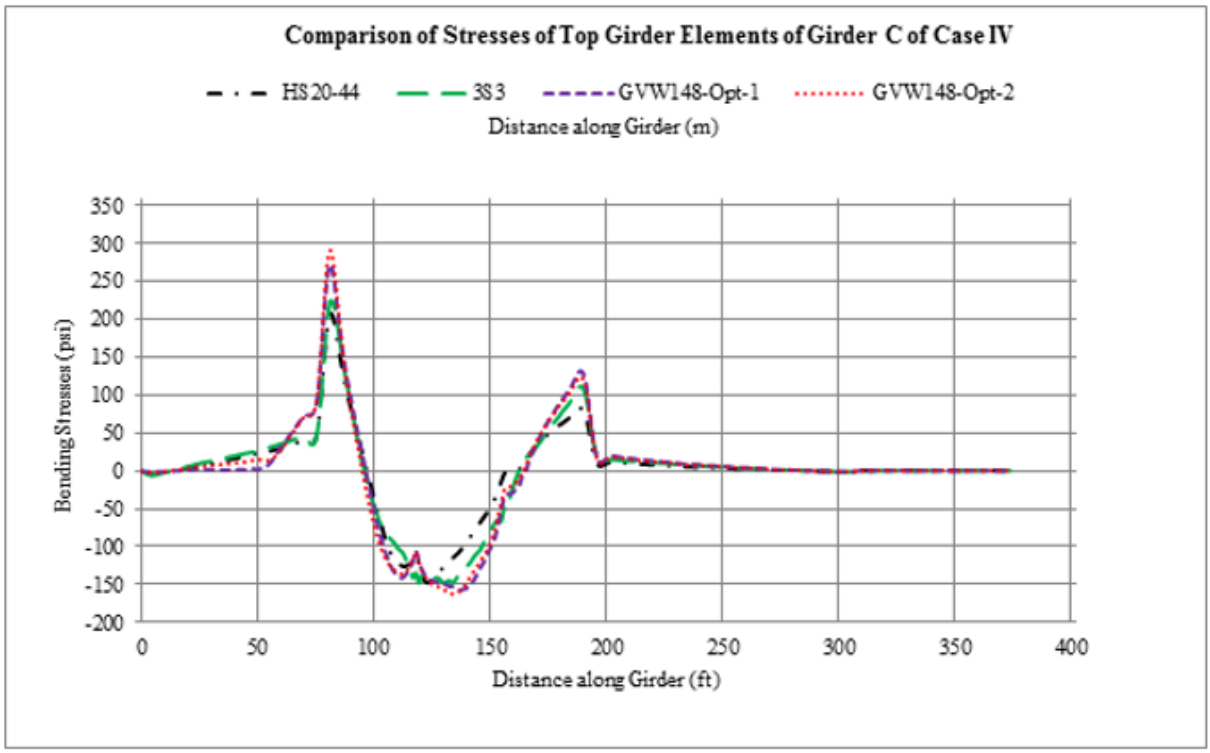

Figure 82
Comparison of bending stress distribution of top elements - Girder C of Case IV

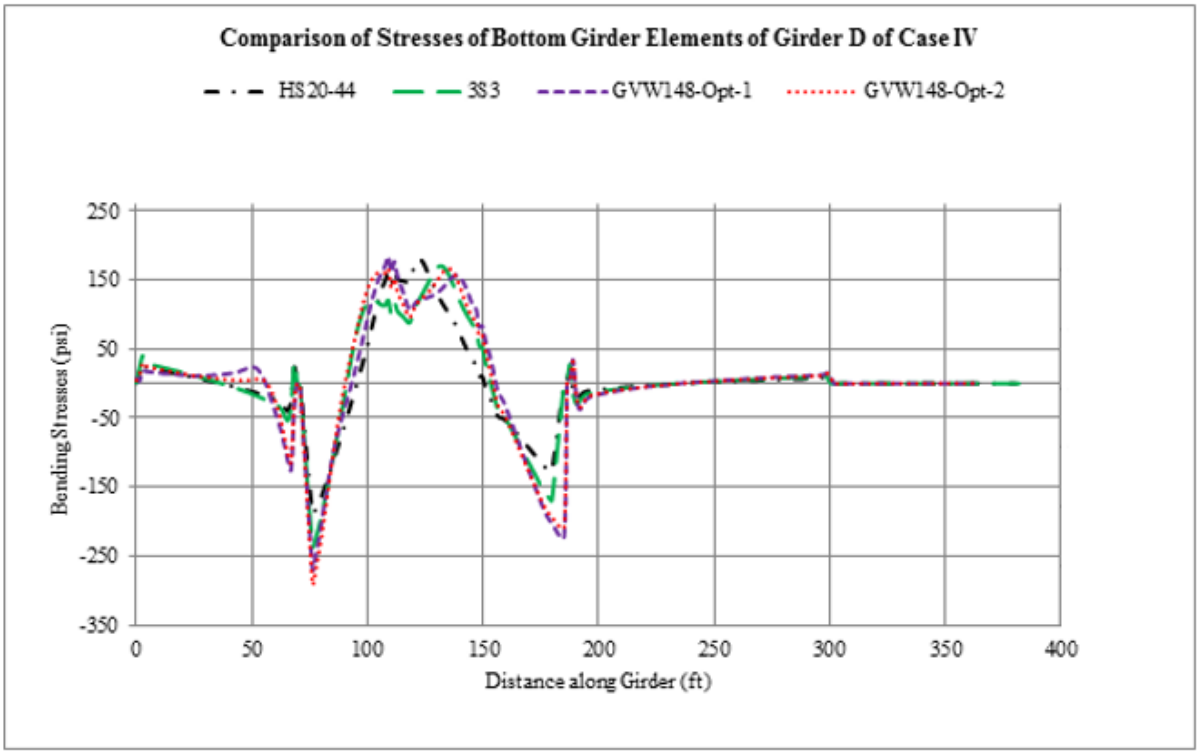

Figure 83
Comparison of bending stress distribution of bottom elements - Girder D of Case IV

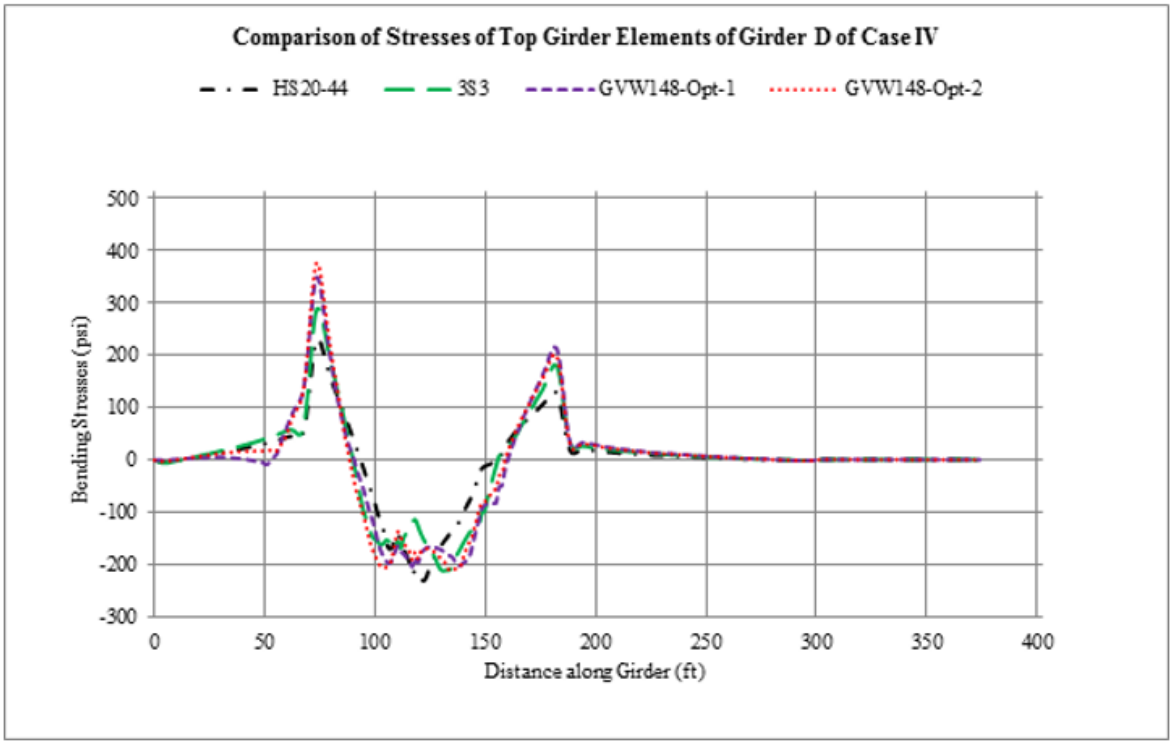

Figure 84
Comparison of bending stress distribution of top elements - Girder D of Case IV

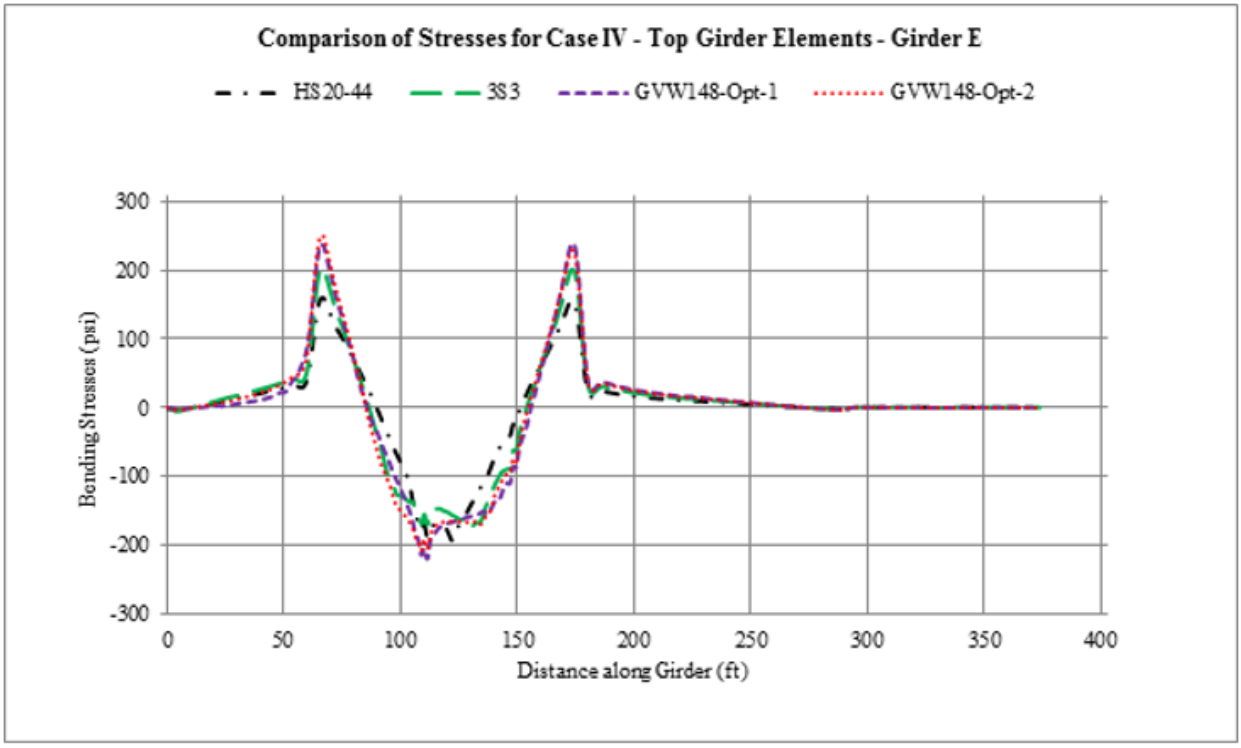

Figure 85
Comparison of flexural stress distribution of top elements - Girder E of Case IV

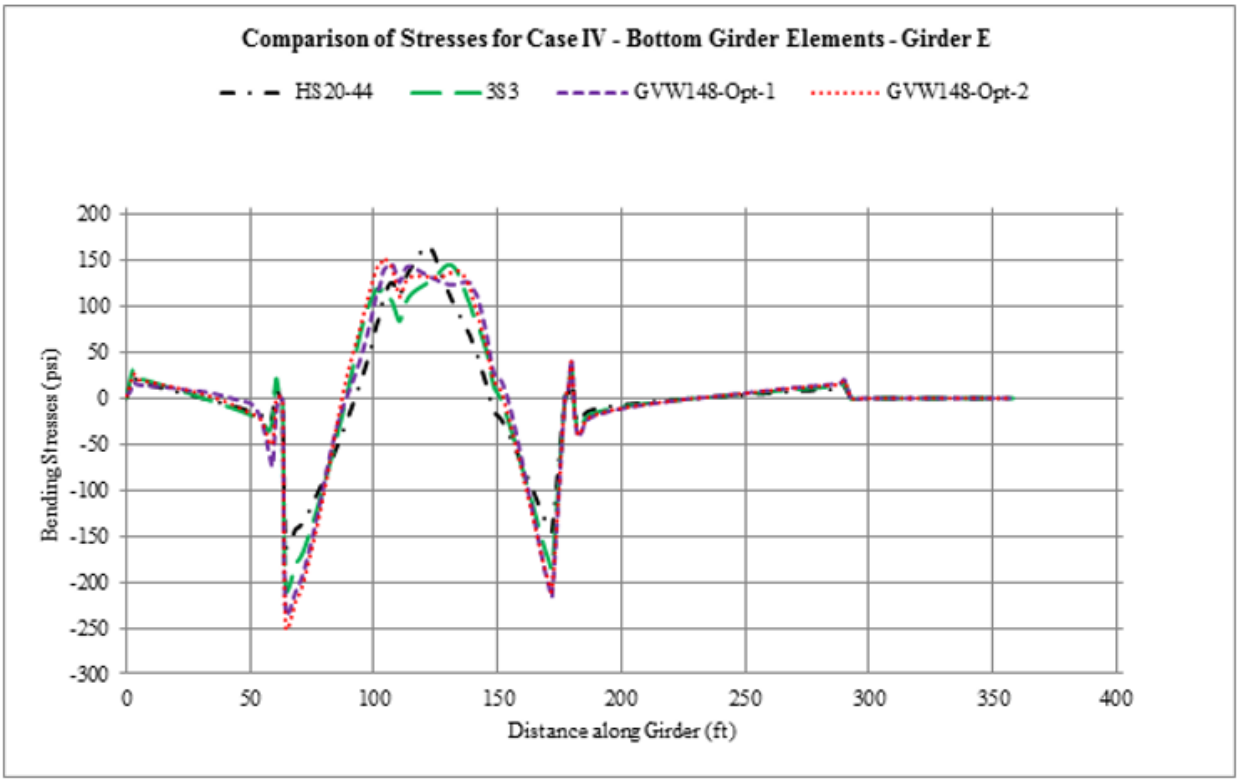

Figure 86
Comparison of flexural stress distribution of bottom elements - Girder E of Case IV

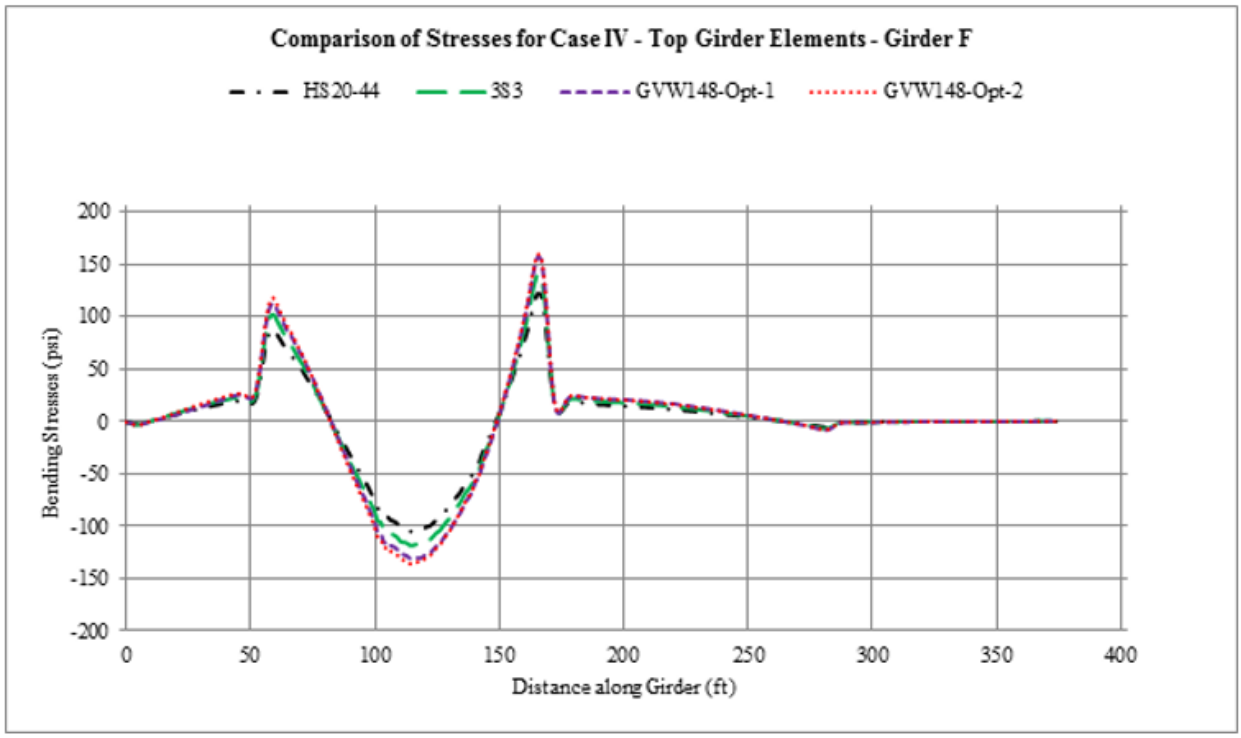

Figure 87
Comparison of flexural stress distribution of top elements - Girder F of Case IV

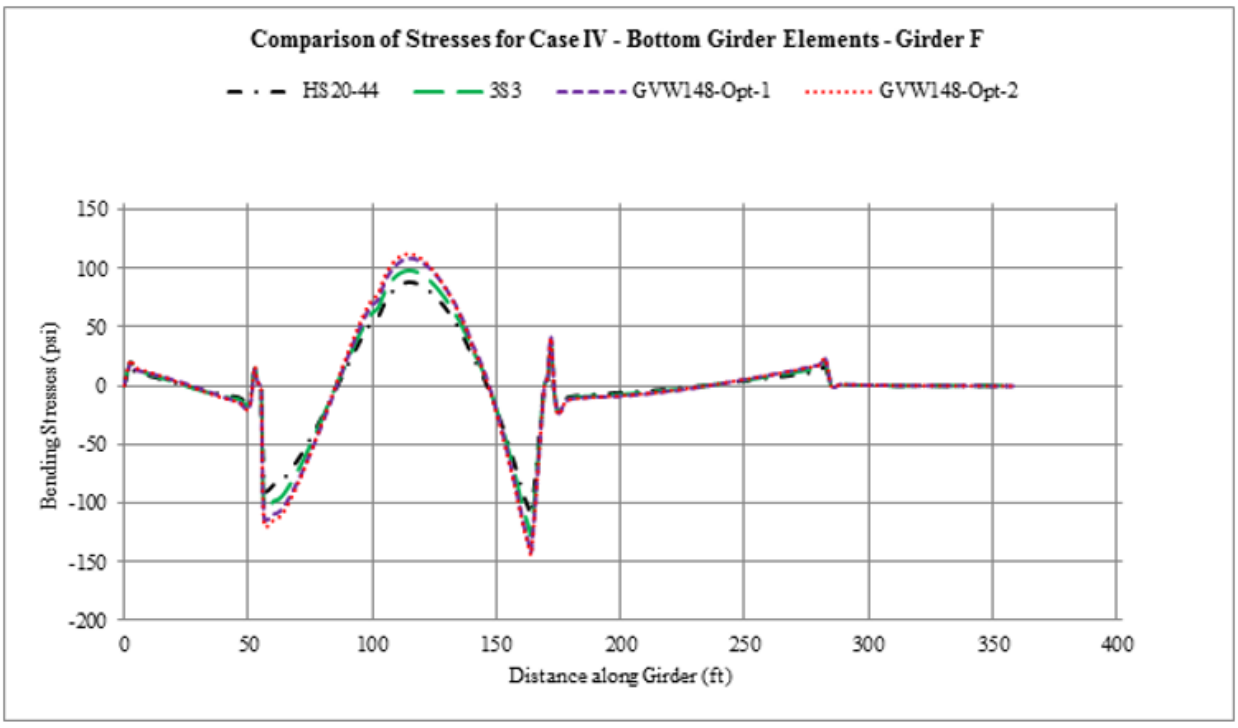

Figure 88
Comparison of flexural stress distribution of bottom elements - Girder F of Case IV

Figure 89
Comparison of deflections of Girder A for Case I

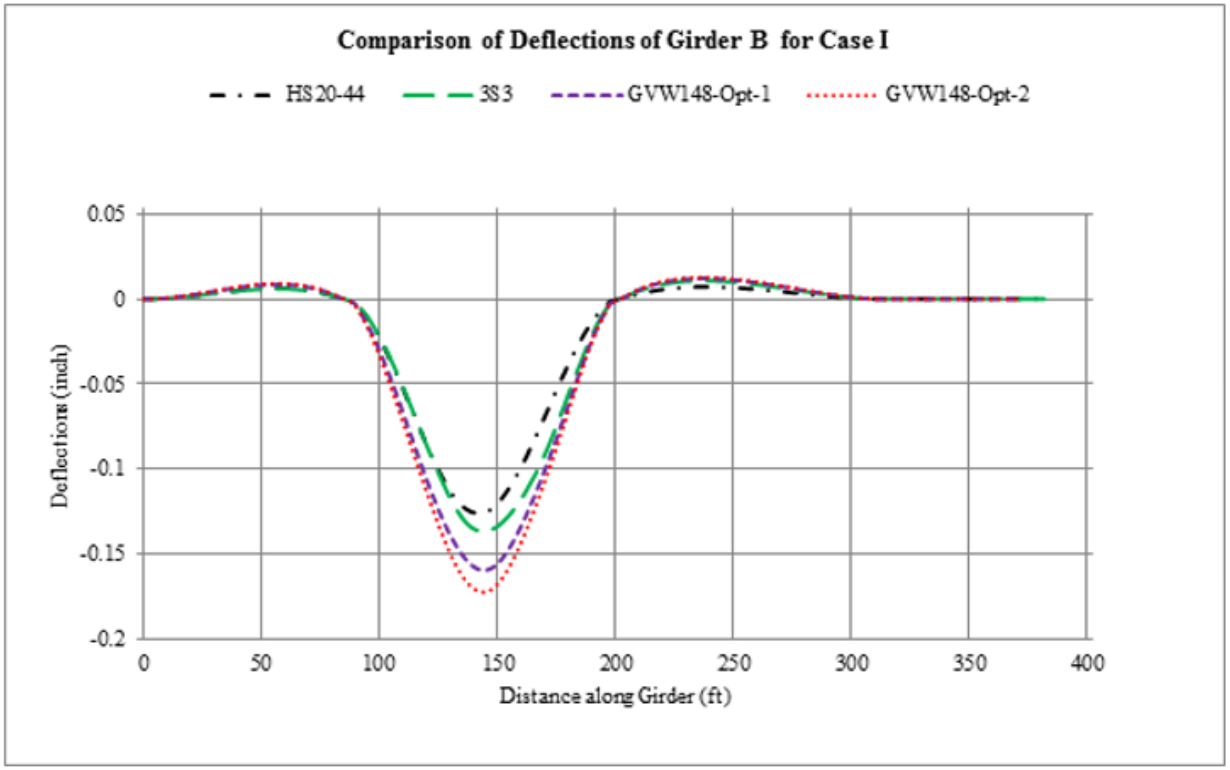

Figure 90
Comparison of deflections of Girder B for Case I

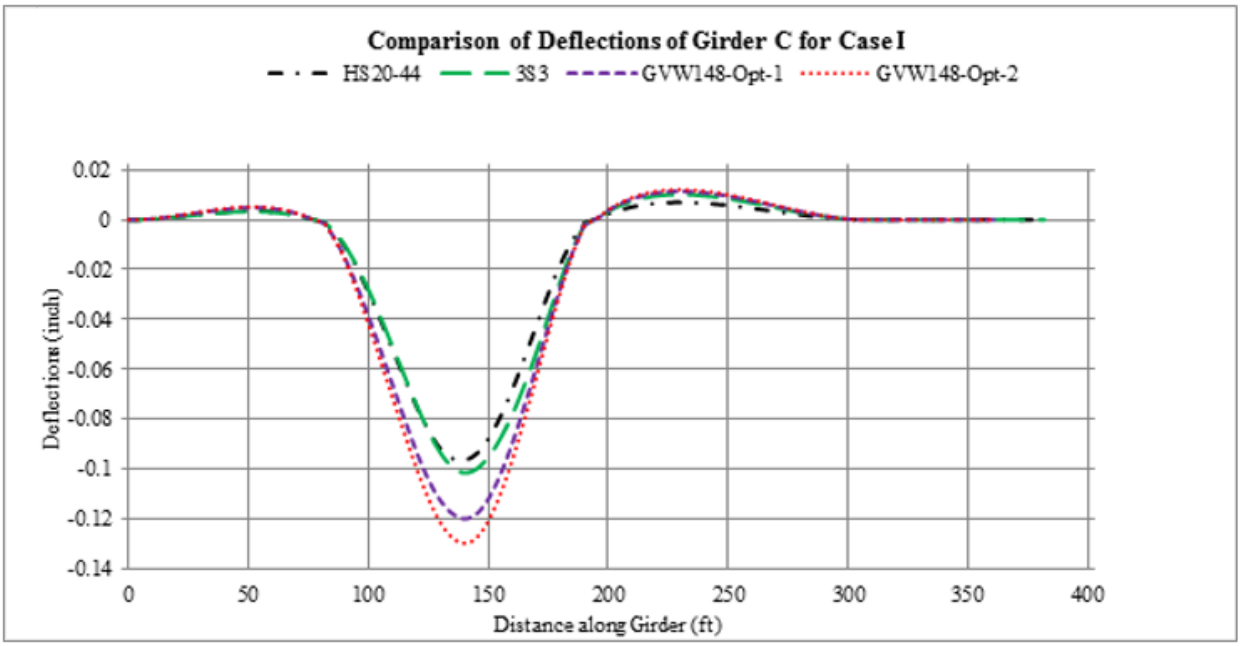

Figure 91
Comparison of deflections of Girder C for Case I

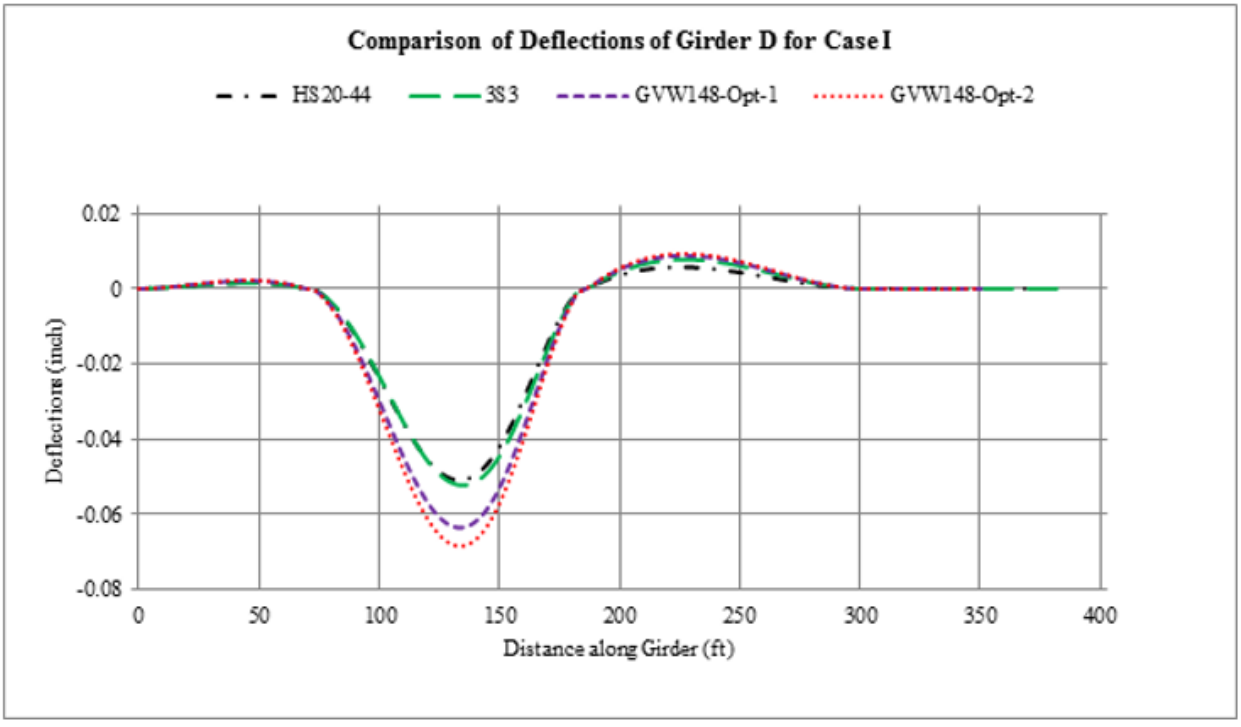

Figure 92
Comparison of deflections of Girder D for Case I

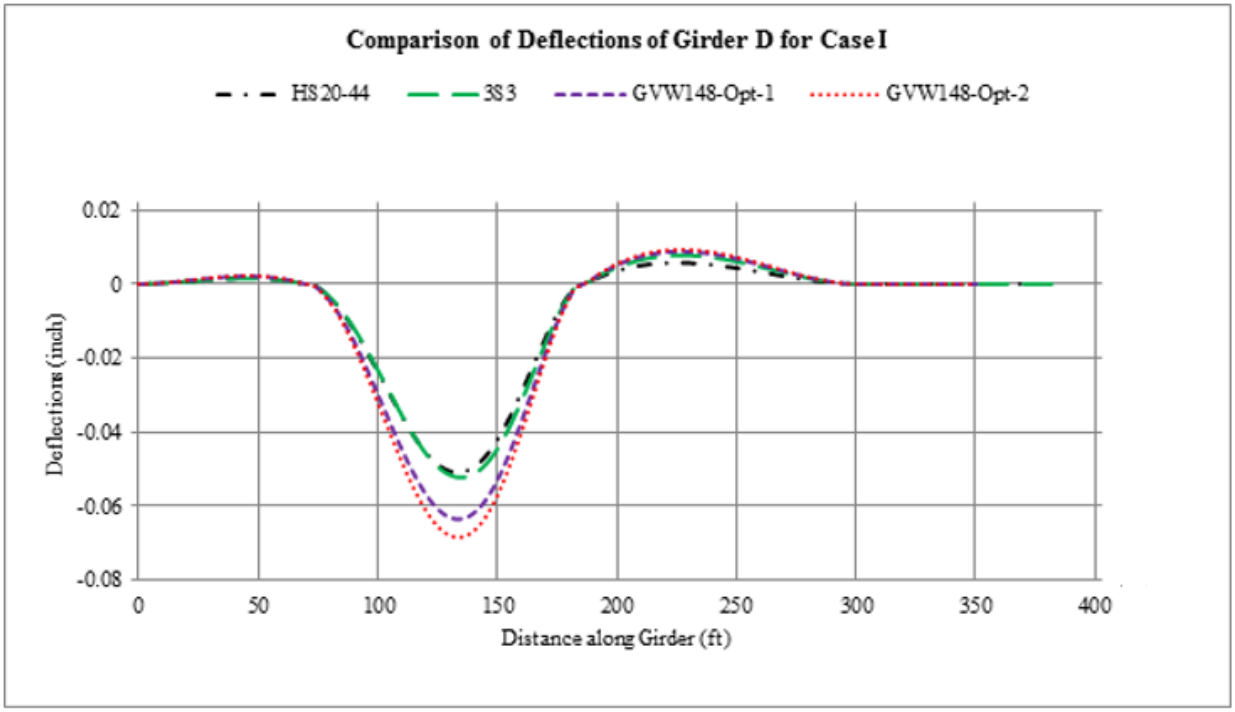

Figure 93
Comparison of deflections of Girder E for Case I

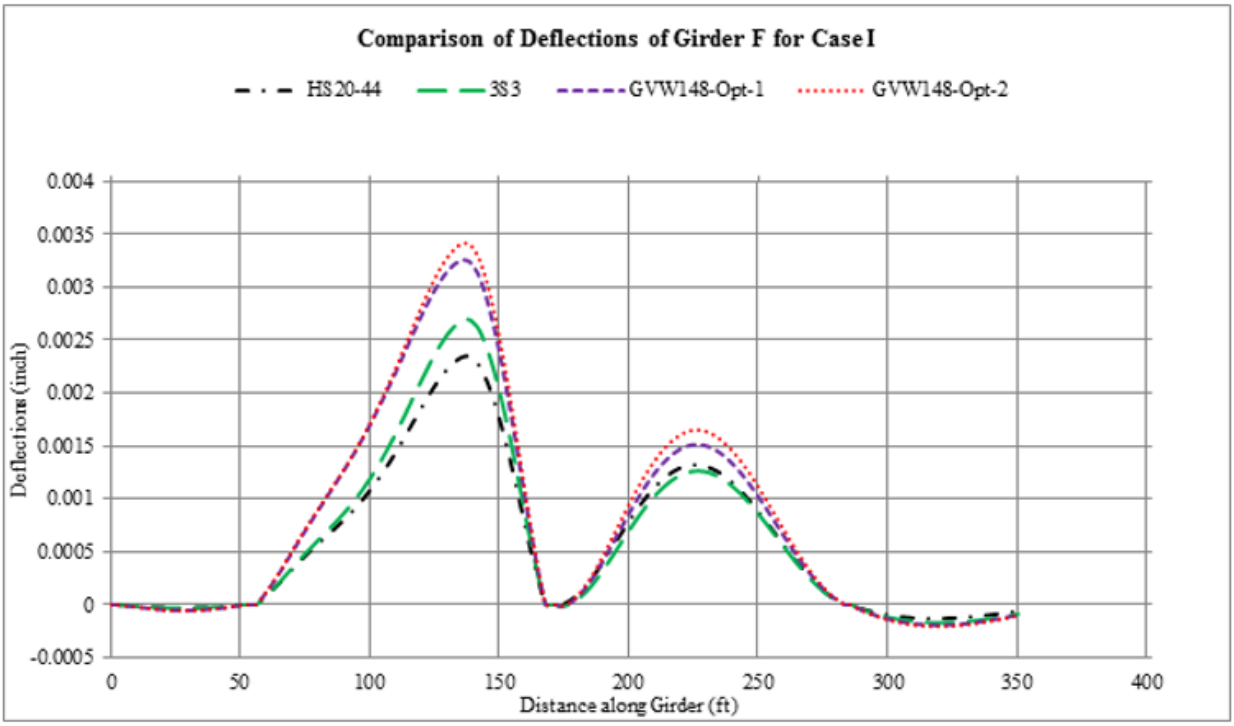

Figure 94
Comparison of deflections of Girder F for Case I

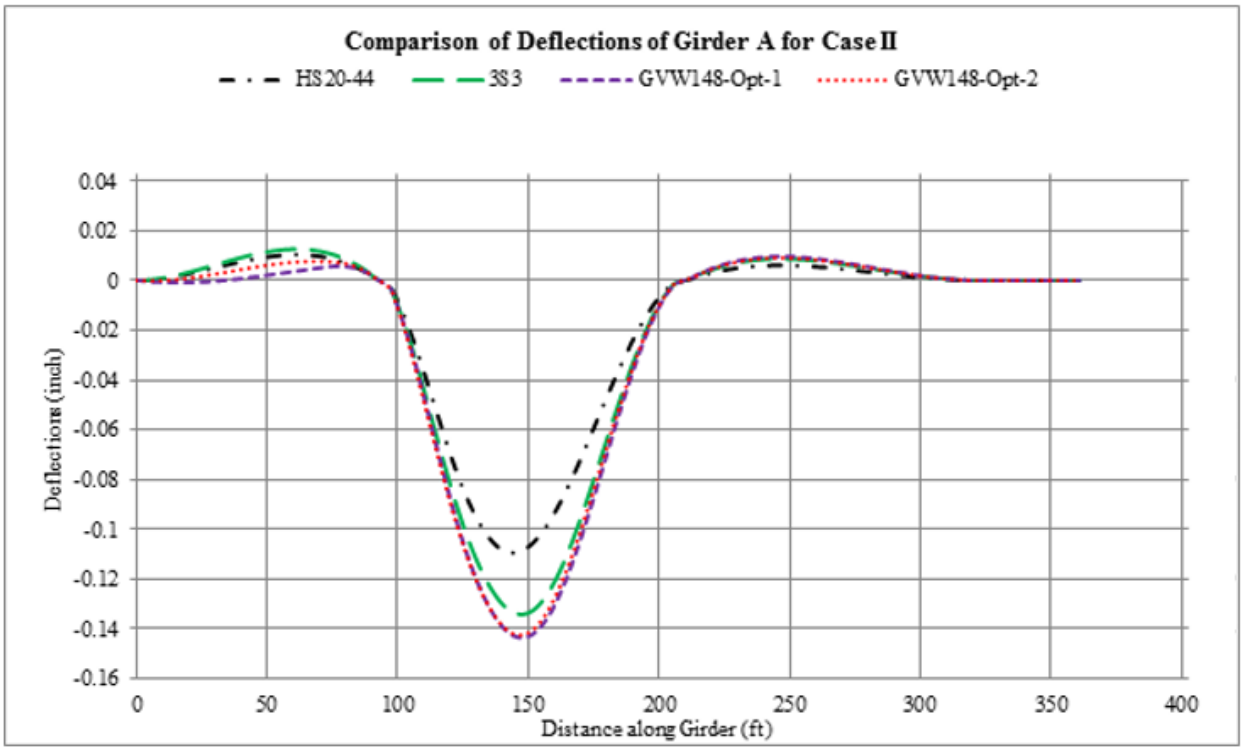

Figure 95
Comparison of deflections of Girder A for Case II

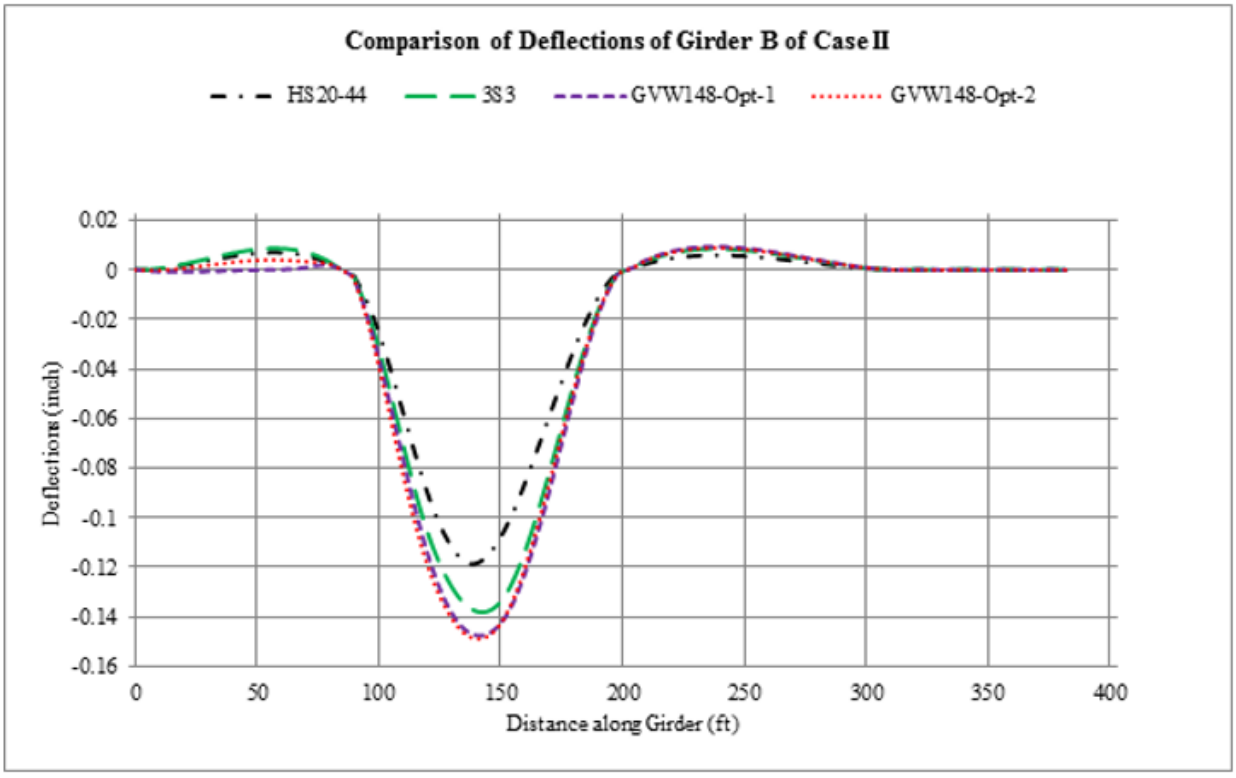

Figure 96
Comparison of deflections of Girder B for Case II

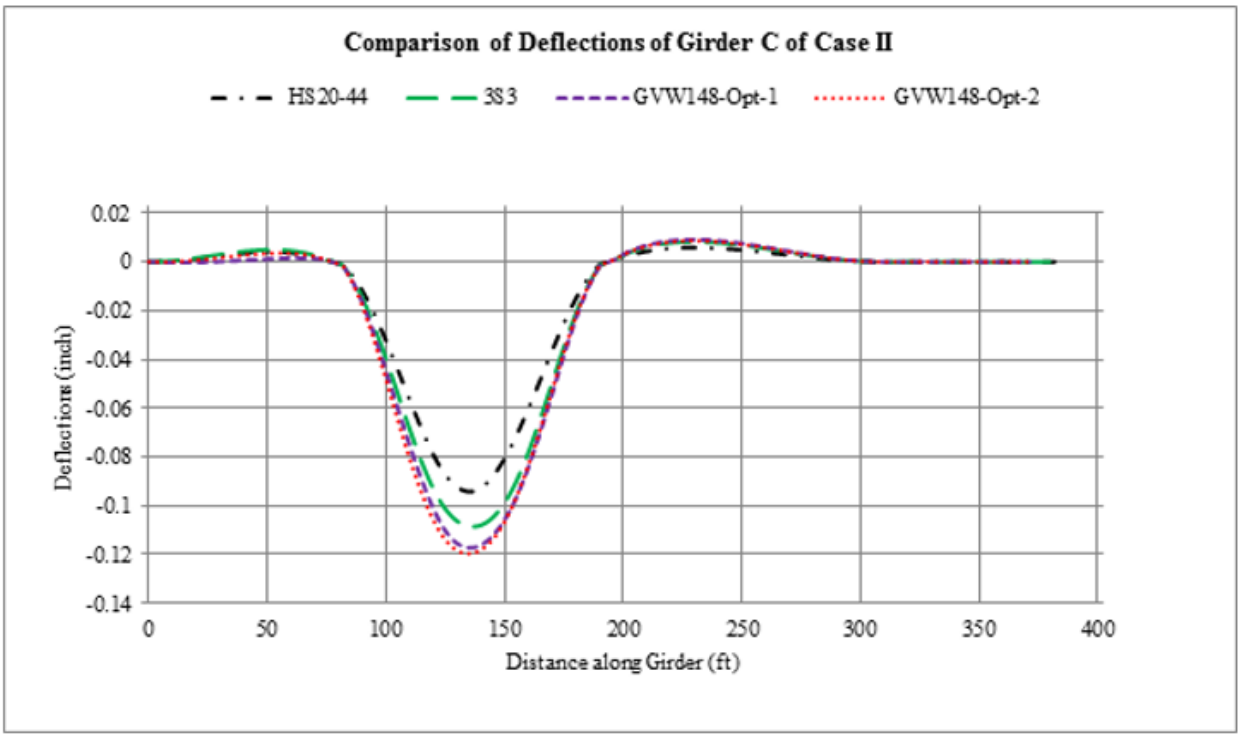

Figure 97
Comparison of deflections of Girder C for Case II

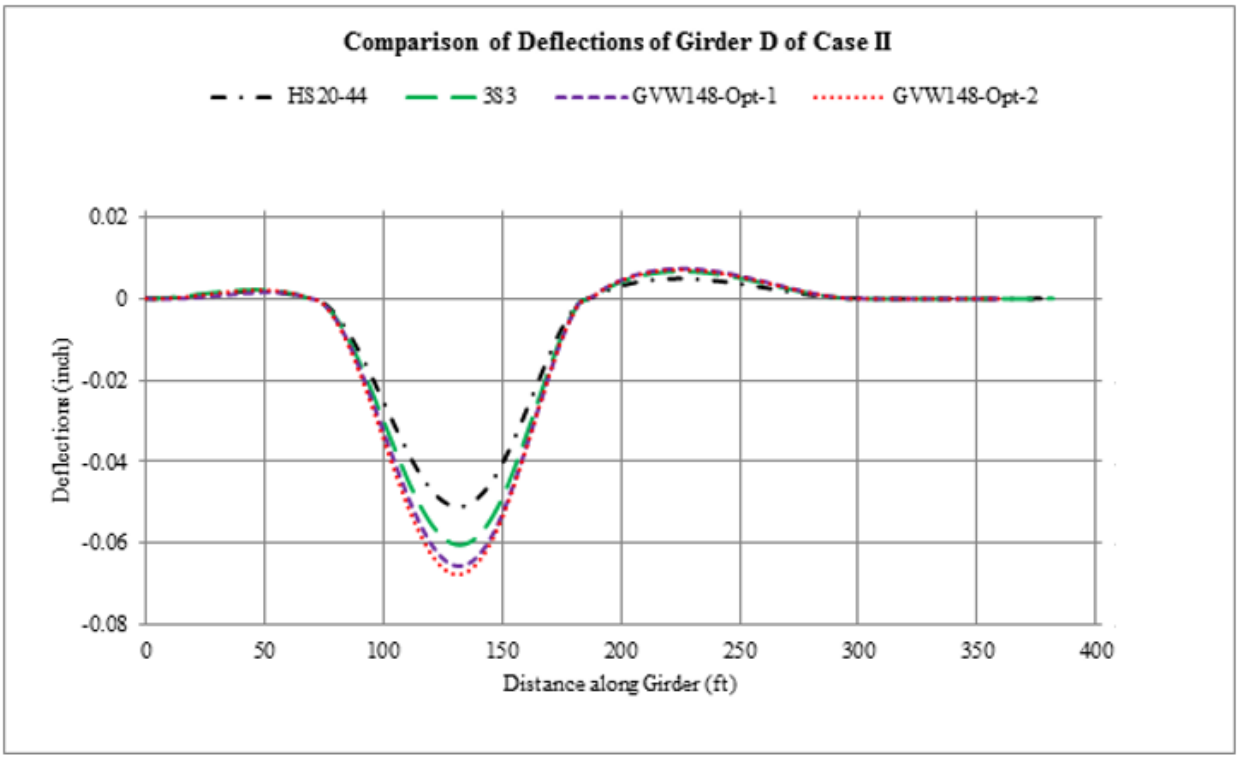

Figure 98
Comparison of deflections of Girder D for Case II

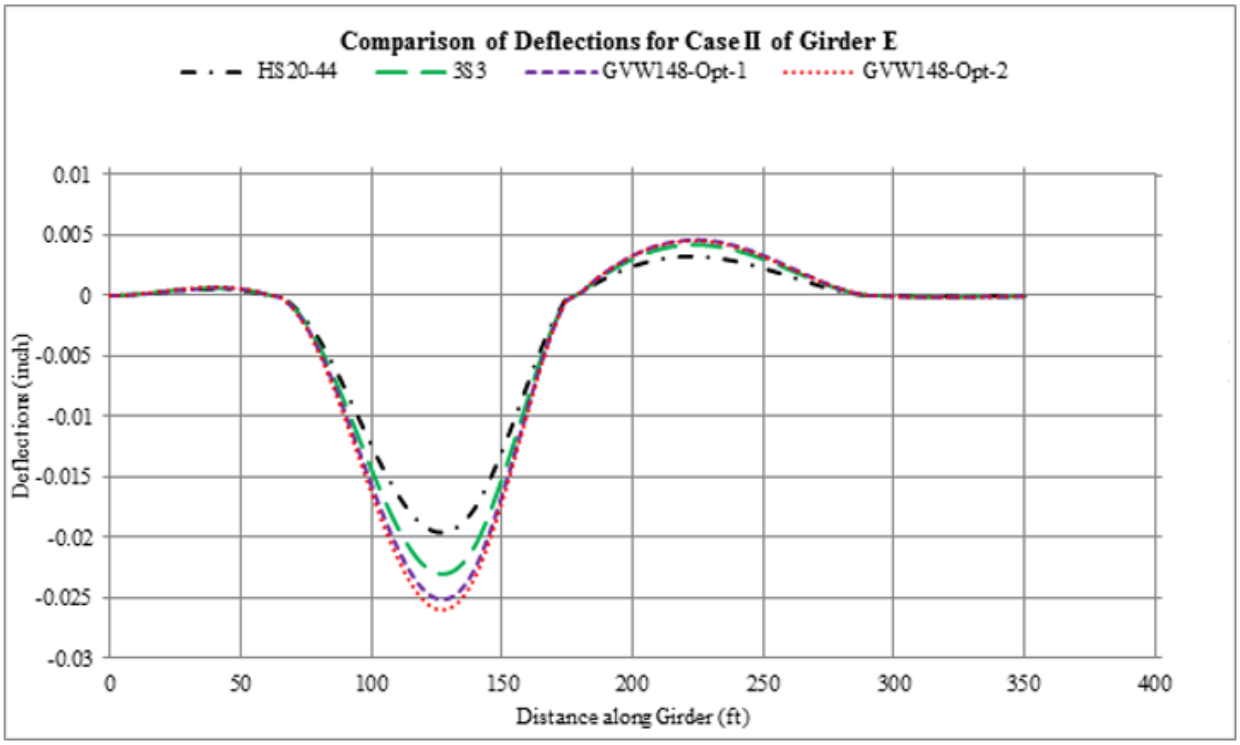

Figure 99
Comparison of deflections of Girder E for Case II

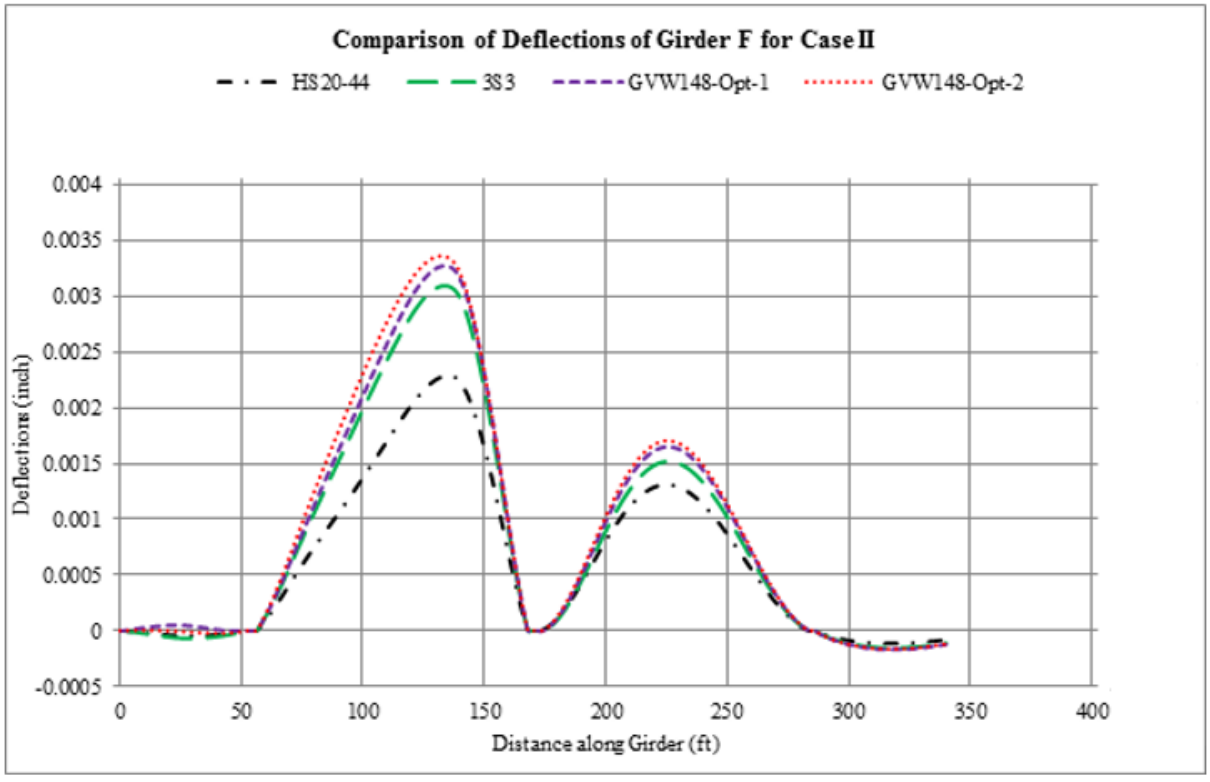

Figure 100
Comparison of deflections of Girder F for Case II

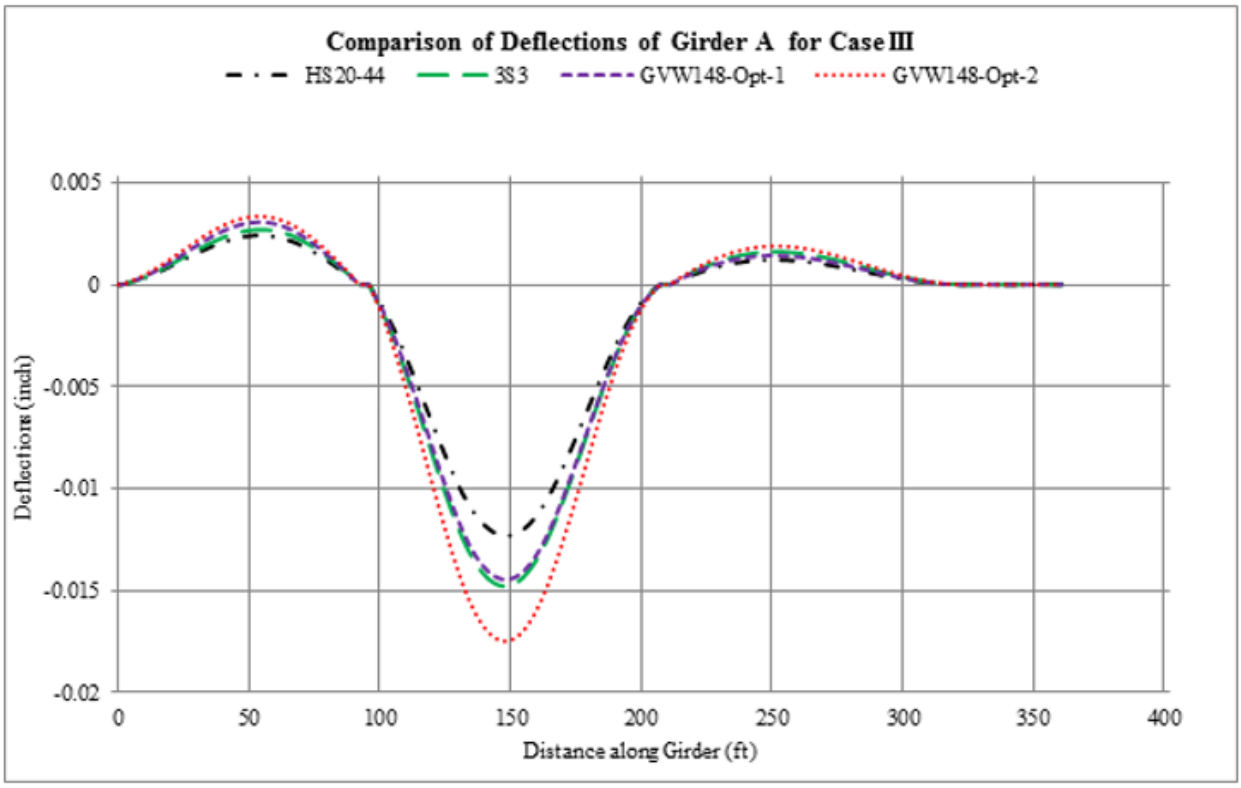

Figure 101
Comparison of deflections of Girder A for Case III

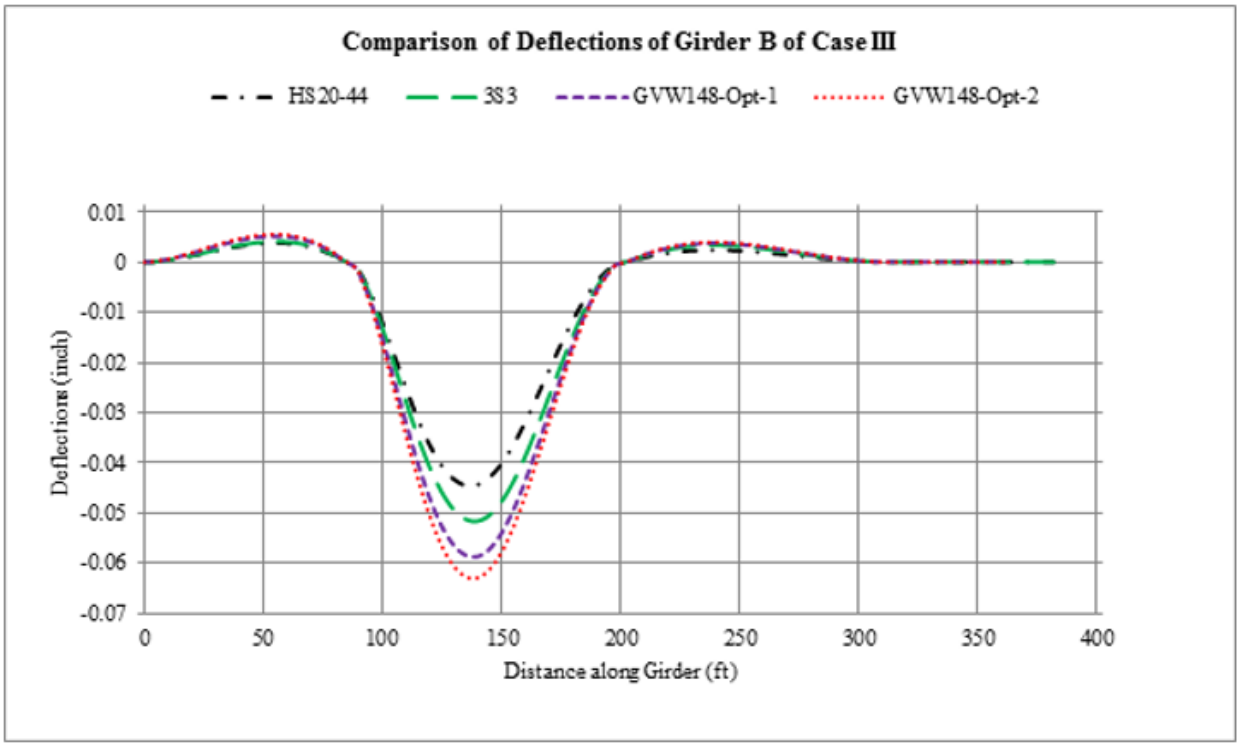

Figure 102
Comparison of deflections of Girder B for Case III

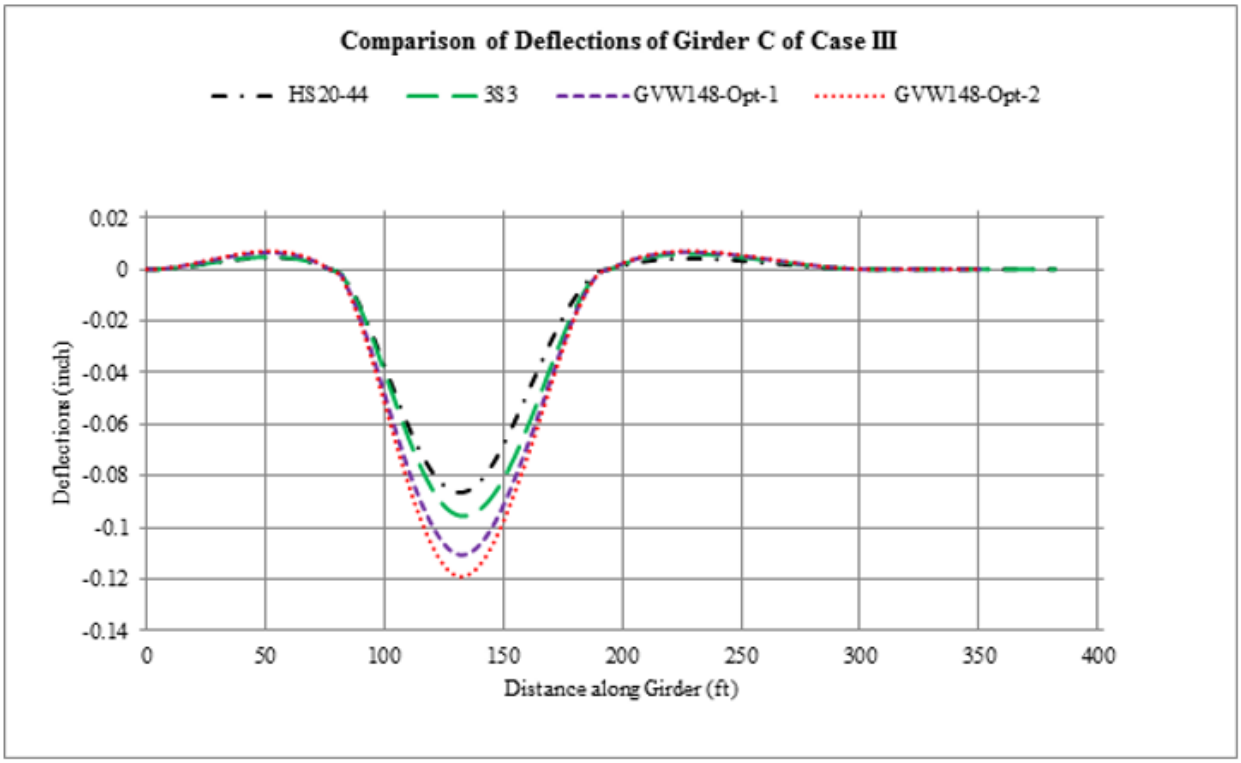

Figure 103
Comparison of deflections of Girder C for Case III

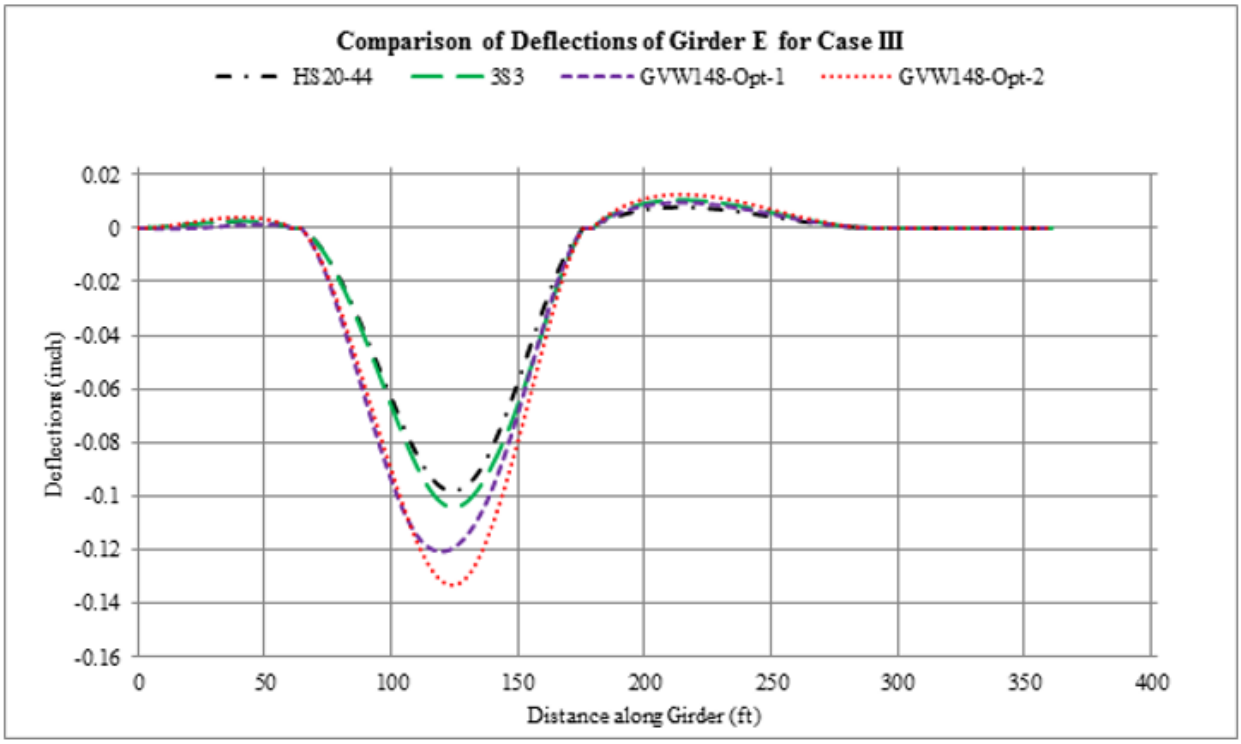

Figure 104
Comparison of deflections of Girder E for Case III

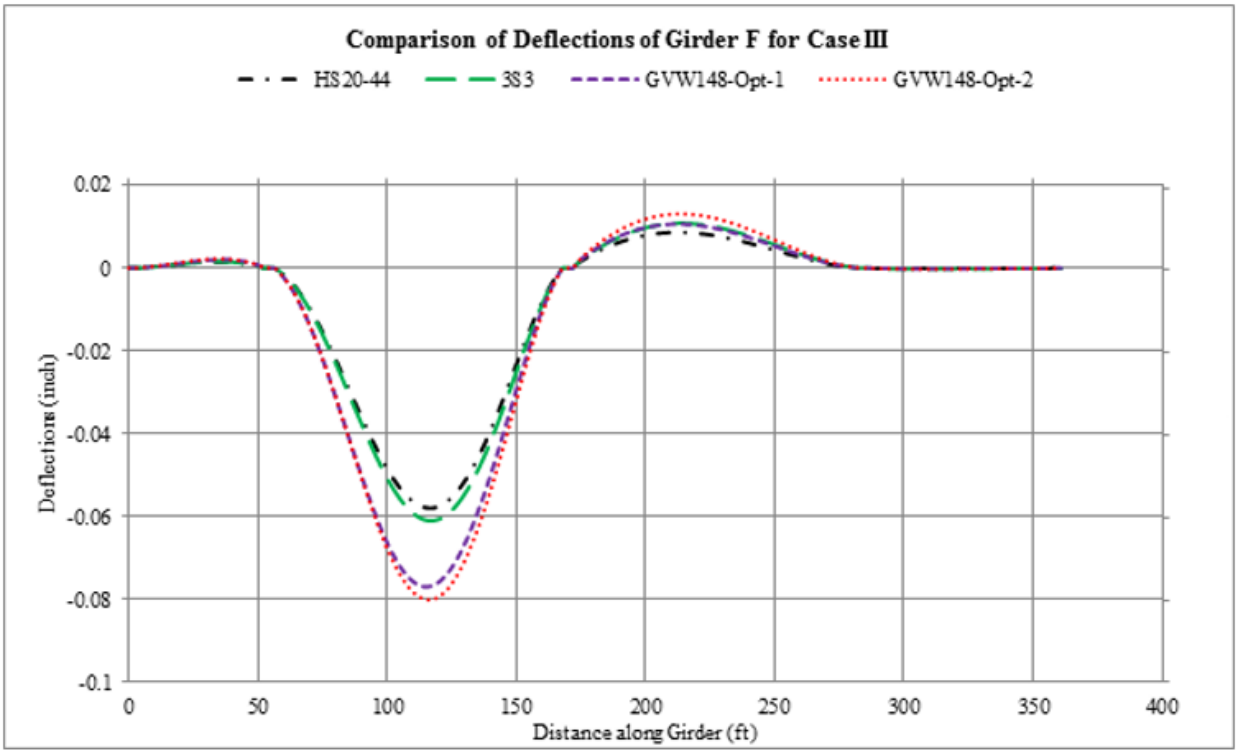

Figure 105
Comparison of deflections of Girder F for Case III

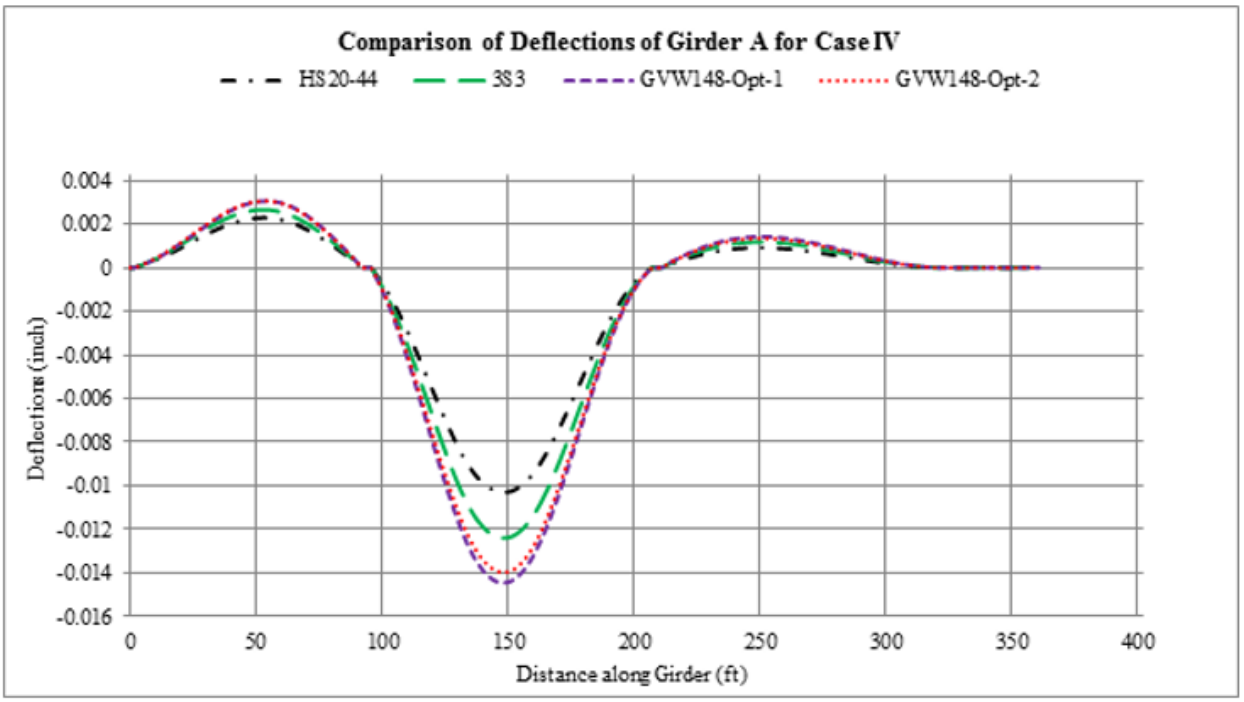

Figure 106
Comparison of deflections of Girder A for Case IV

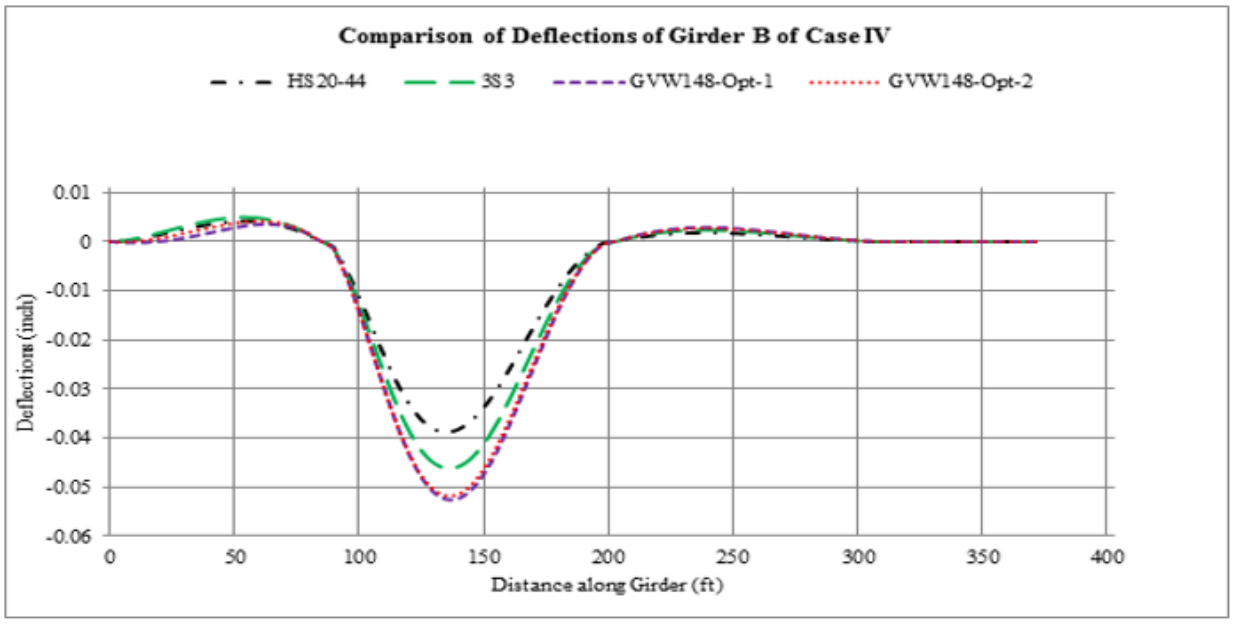

Figure 107
Comparison of deflections of Girder B for Case IV

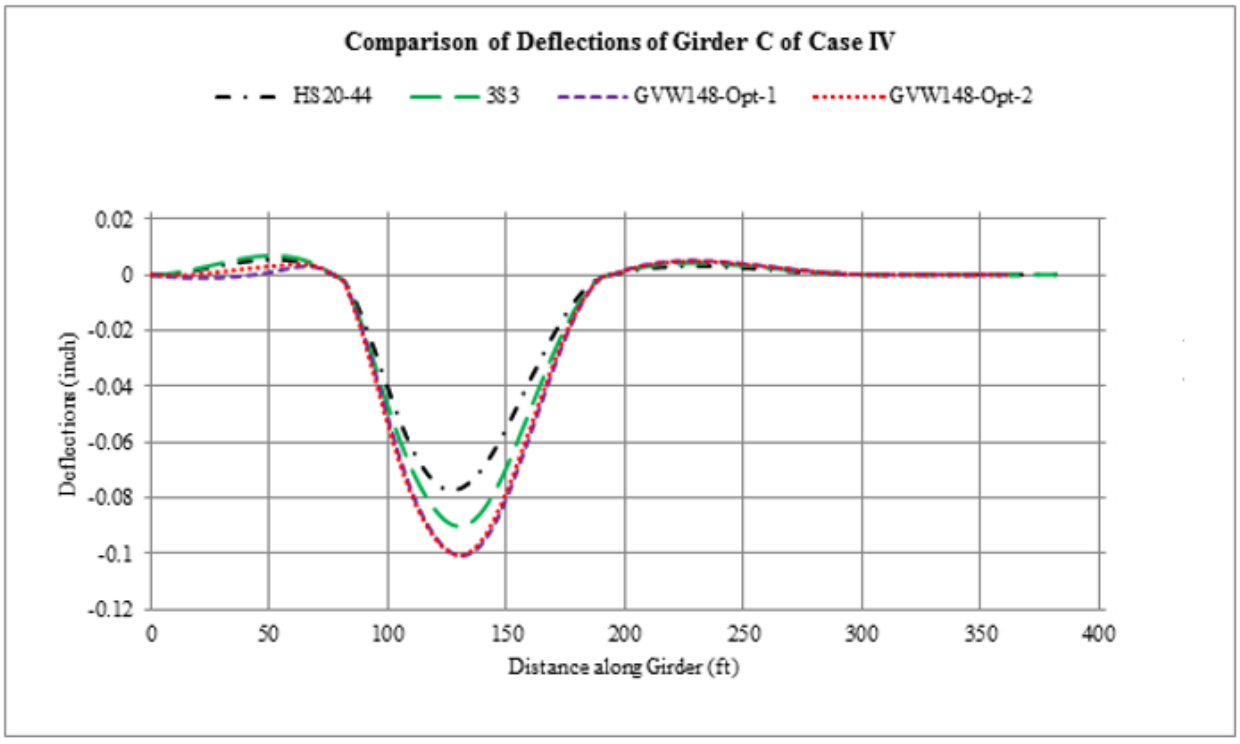

Figure 108
Comparison of deflections of Girder C for Case IV

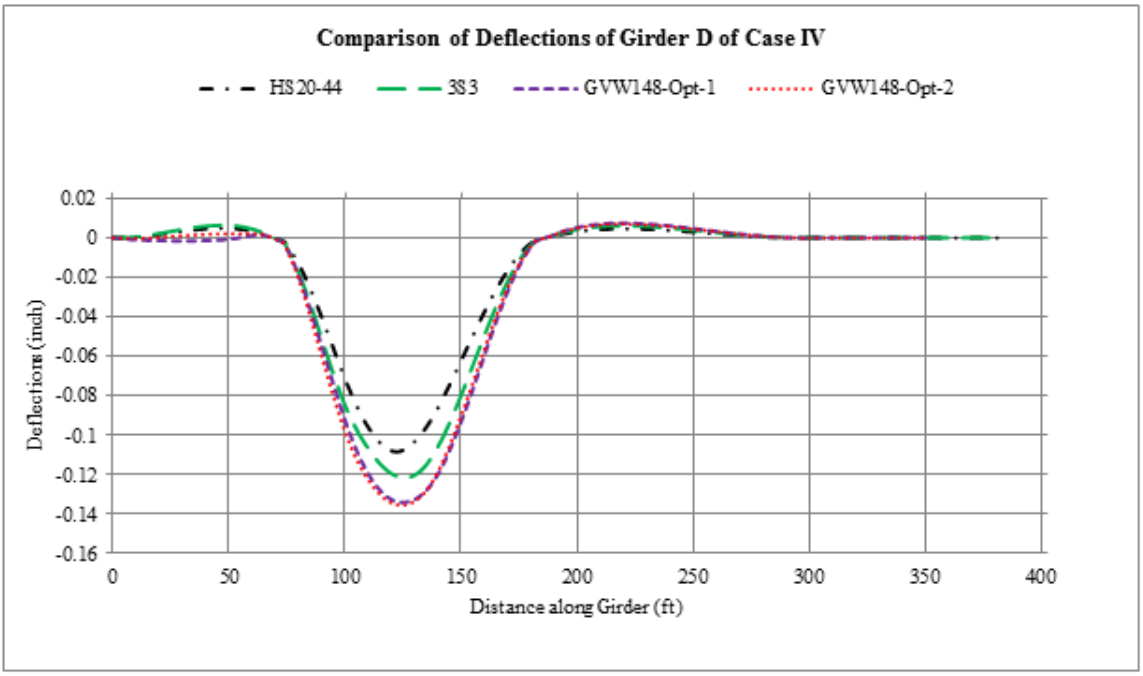

Figure 109
Comparison of deflections of Girder D for Case IV

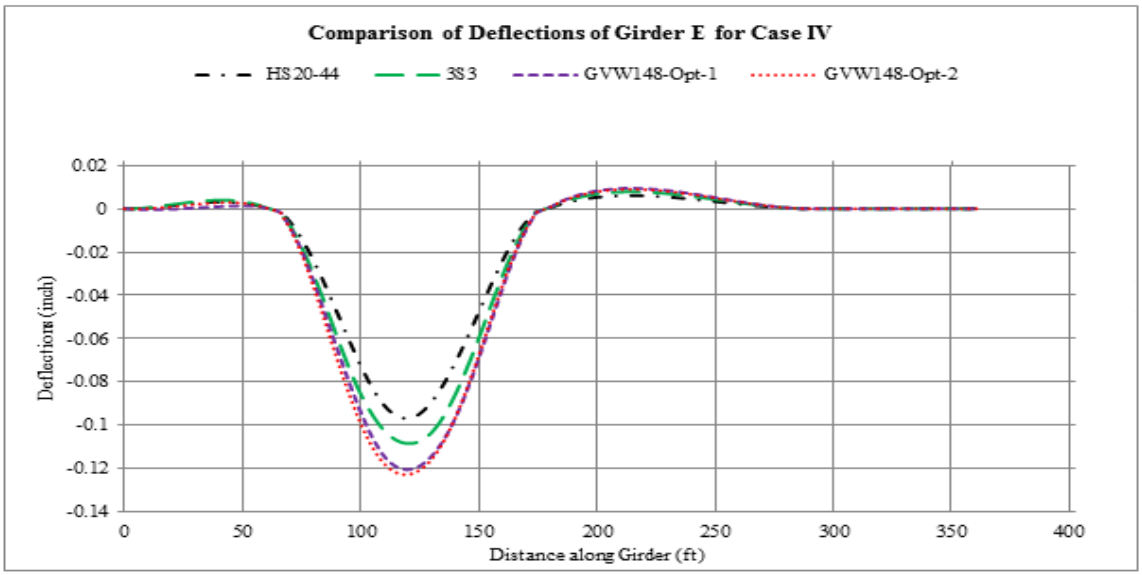

Figure 110
Comparison of deflections of Girder E for Case IV

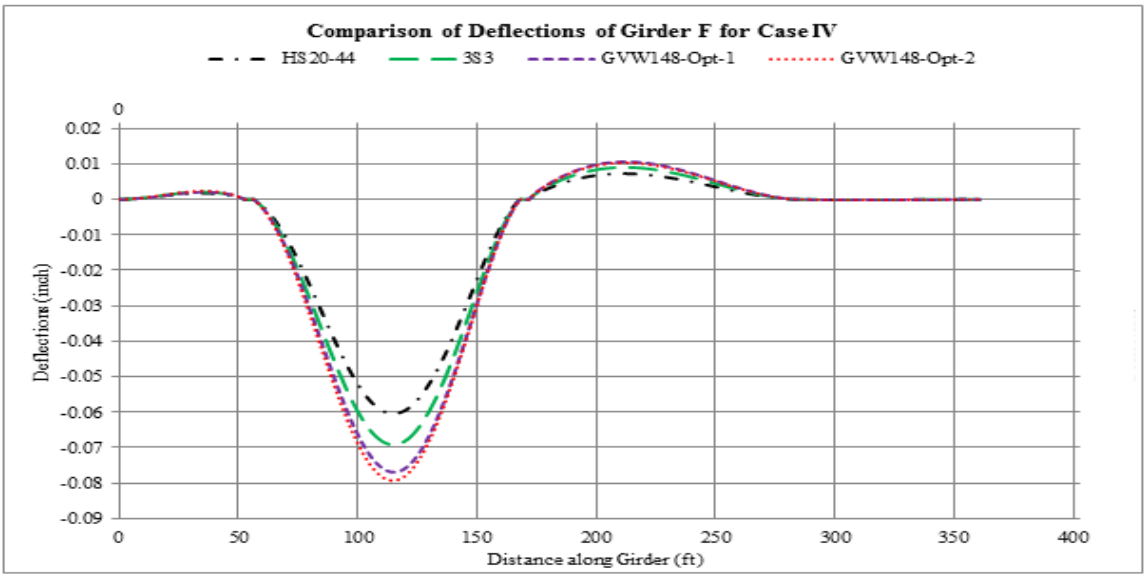

Figure 111
Comparison of deflections of Girder E for Case IV

APPENDIX B

Effects of Truck Configuration on Flexural Stresses

Table 28
Case I - Effects of truck configurations on flexural stresses - Girder A

Span	Location	Stress	HS20-44 (psi)	3S3 (psi)	GVW148 Opt-1 (psi)	GVW148 Opt-2 (psi)	Change in Stresses		
							3S3 vs. HS20-44	Opt-1 vs. HS20-44	Opt-2 vs. HS20-44
15E	Top Elements	Max +ve	121.40	124.54	150.06	144.52	3	29	23
							N*	24%	19%
		Max -ve	-6.71	-6.71	-8.85	-9.64	0.0	-2	-3
							N*	N*	N*
	Bottom Elements	Max +ve	43.30	43.57	53.79	61.32	0.3	10	18
							N*	N*	N*
		Max -ve	-42.20	-44.19	-49.16	-55.62	-2	-7	-13
							N*	N*	N*
14E	Top Elements	Max +ve	272.44	283.48	339.29	354.76	11	67	82
							N*	25%	30%
		Max -ve	-216.61	-225.36	-268.28	-288.09	-9	-52	-71
							N*	24%	33%
	Bottom Elements	Max +ve	166.12	171.55	204.27	221.53	5	38	55
							N*	23%	33%
		Max -ve	-213.03	-230.26	-267.82	-282.31	-17	-55	-69
							N*	26%	33%
13E	Top Elements	Max +ve	51.82	75.40	85.90	102.55	24	34	51
							N*	66%	98%
		Max -ve	-3.34	-5.01	-5.62	-6.19	-2	-2	-3
							N*	N*	N*
	Bottom Elements	Max +ve	33.85	50.29	56.66	59.86	16	23	26
							N*	N*	77%
		Max -ve	-19.76	-28.46	-32.02	-33.88	-9	-12	-14
							N*	N*	N*
12E	Top Elements	Max +ve	0.28	0.40	0.45	0.20	0.1	0.2	-0.1
							N*	N*	N*
		Max -ve	-0.42	-0.66	-0.74	-1.15	-0.2	-0.3	-0.7
							N*	N*	N*
	Bottom Elements	Max +ve	0.026	0.042	0.048	0.050	0.0	0.0	0.0
							N*	N*	N*
		Max -ve	-0.248	-0.360	-0.403	-0.426	-0.1	-0.2	-0.2
							N*	N*	N*

N*(Negligible): The difference is less than 25 psi.

Table 29
Case I - Effects of truck configurations on flexural stresses - Girder D

Span	Location	Stress	HS20-44 (psi)	3S3 (psi)	GVW148 Opt-1 (psi)	GVW148 Opt-2 (psi)	Change in Stresses		
							3S3 vs HS20	Opt-1 vs HS20	Opt-2 vs HS20
15E	Top Elements	Max +ve	28.04	26.94	35.15	37.97	-1	7	10
							N*	N*	N*
		Max -ve	-1.67	-1.57	-2.23	-2.38	0.1	-1	-1
							N*	N*	N*
	Bottom Elements	Max +ve	9.75	13.17	12.82	13.74	3	3	4
							N*	N*	N*
		Max -ve	-10.37	-13.29	-12.74	-13.79	-3	-2	-3
							N*	N*	N*
14E	Top Elements	Max +ve	114.48	122.50	144.08	155.49	8	30	41
							N*	26%	36%
		Max -ve	-89.73	-100.69	-114.25	-123.44	-11	-25	-34
							N*	N*	38%
	Bottom Elements	Max +ve	74.92	85.13	90.62	97.69	10	16	23
							N*	N*	N*
		Max -ve	-129.74	-119.02	-166.59	-179.48	11	-37	-50
							N*	28%	38%
13E	Top Elements	Max +ve	45.31	45.70	53.55	58.10	0.4	8	13
							N*	N*	N*
		Max -ve	-3.44	-5.52	-6.17	-6.49	-2	-3	-3
							N*	N*	N*
	Bottom Elements	Max +ve	24.63	15.32	37.47	39.86	-9	13	15
							N*	N*	N*
		Max -ve	-19.29	-21.68	-21.19	-23.13	-2	-2	-4
							N*	N*	N*
12E	Top Elements	Max +ve	0.033	0.064	0.073	0.076	0.0	0.0	0.0
							N*	N*	N*
		Max -ve	-0.613	-1.363	-1.491	-1.544	-0.8	-0.9	-0.9
							N*	N*	N*
	Bottom Elements	Max +ve	0.337	0.421	0.847	0.876	0.1	0.5	0.5
							N*	N*	N*
		Max -ve	-0.542	-0.205	-0.969	-1.019	0.3	-0.4	-0.5
							N*	N*	N*

N*(Negligible): The difference is less than 25 psi.

Table 30
Case I - Effects of truck configurations on flexural stresses - Girder E

Span	Location	Stress	HS20-44 (psi)	3S3 (psi)	GVW148 Opt-1 (psi)	GVW148 Opt-2 (psi)	Change in Stresses		
							3S3 vs. HS20-44	Opt-1 vs. HS20-44	Opt-2 vs. HS20-44
15E	Top Elements	Max +ve	8.87	9.06	11.32	12.26	0.2	2	3
							N*	N*	N*
		Max -ve	-0.66	-0.58	-0.78	-0.84	0.1	-0.1	-0.2
							N*	N*	N*
	Bottom Elements	Max +ve	3.84	3.65	4.86	5.25	-0.2	1	1
							N*	N*	N*
		Max -ve	-3.64	-3.58	-4.35	-4.71	0.1	-1	-1
							N*	N*	N*
14E	Top Elements	Max +ve	55.25	44.24	54.34	58.84	-11	-1	4
							N*	N*	N*
		Max -ve	-41.14	-43.37	-51.83	-55.86	-2	-11	-15
							N*	N*	N*
	Bottom Elements	Max +ve	29.22	30.13	36.66	39.62	1	7	10
							N*	N*	N*
		Max -ve	-41.69	-41.46	-50.85	-55.04	0.2	-9	-13
							N*	N*	N*
13E	Top Elements	Max +ve	22.22	15.01	19.05	20.67	-7	-3	-2
							N*	N*	N*
		Max -ve	-4.00	-4.97	-5.58	-5.91	-1	-2	-2
							N*	N*	N*
	Bottom Elements	Max +ve	13.84	15.53	17.99	19.37	2	4	6
							N*	N*	N*
		Max -ve	-5.47	-4.36	-5.74	-6.28	1	-0.3	-1
							N*	N*	N*
12E	Top Elements	Max +ve	0.070	0.094	0.106	0.111	0.0	0.0	0.0
							N*	N*	N*
		Max -ve	-0.943	-1.135	-1.240	-1.305	-0.2	-0.3	-0.4
							N*	N*	N*
	Bottom Elements	Max +ve	0.671	1.048	1.153	1.217	0.4	0.5	0.5
							N*	N*	N*
		Max -ve	-0.351	-0.568	-0.634	-0.667	-0.2	-0.3	-0.3
							N*	N*	N*

N*(Negligible): The difference is less than 25 psi.

Table 31
Case I - Effects of truck configurations on flexural stresses - Girder F

Span	Location	Stress	HS20-44 (psi)	3S3 (psi)	GVW148 Opt-1 (psi)	GVW148 Opt-2 (psi)	Change in Stresses		
							3S3 vs. HS20-44	Opt-1 vs. HS20-44	Opt-2 vs. HS20-44
15E	Top Elements	Max +ve	0.05	0.05	0.08	0.08	0.0	0.0	0.0
							N*	N*	N*
		Max -ve	-1.51	-1.52	-2.12	-2.19	0.0	-0.6	-0.7
							N*	N*	N*
	Bottom Elements	Max +ve	0.34	0.33	0.43	0.46	0.0	0.1	0.1
							N*	N*	N*
		Max -ve	-0.19	-0.22	-0.40	-0.36	0.0	0.0	0.0
							N*	N*	N*
14E	Top Elements	Max +ve	12.56	14.67	16.63	17.78	2	4	5
							N*	N*	N*
		Max -ve	-16.19	-18.28	-21.48	-22.84	-2	-5	-7
							N*	N*	N*
	Bottom Elements	Max +ve	9.07	11.13	12.83	13.43	2	4	4
							N*	N*	N*
		Max -ve	-6.21	-7.47	-8.18	-8.81	-1	-2	-3
							N*	N*	N*
13E	Top Elements	Max +ve	2.23	2.16	2.57	2.80	-0.1	0	1
							N*	N*	N*
		Max -ve	-11.08	-11.92	-14.17	-15.15	-0.8	-3	-4
							N*	N*	N*
	Bottom Elements	Max +ve	4.23	3.97	4.83	5.25	-0.3	1	1
							N*	N*	N*
		Max -ve	-1.98	-2.01	-2.37	-2.57	0.0	-0.4	-0.6
							N*	N*	N*
12E	Top Elements	Max +ve	0.101	0.145	0.169	0.178	0.0	0.1	0.1
							N*	N*	N*
		Max -ve	-0.515	-0.512	-0.603	-0.653	0.0	-0.1	-0.1
							N*	N*	N*
	Bottom Elements	Max +ve	0.499	0.458	0.551	0.601	0.0	0.1	0.1
							N*	N*	N*
		Max -ve	-0.361	-0.450	-0.501	-0.538	-0.1	-0.1	-0.2
							N*	N*	N*

N*(Negligible): The difference is less than 25 psi.

Table 32
Case II - Effects of truck configurations on flexural stresses - Girder A

Span	Location	Stress	HS20-44 (psi)	3S3 (psi)	GVW148 Opt-1 (psi)	GVW148 Opt-2 (psi)	Change in Stresses		
							3S3 vs HS20	Opt-1 vs HS20	Opt-2 vs HS20
15E	Top Elements	Max +ve	125.86	150.86	190.22	195.31	25	64	69
							20%	51%	55%
		Max -ve	-7.20	-8.77	-2.02	-5.07	-1.6	5	2
							N*	N*	N*
	Bottom Elements	Max +ve	46.17	56.21	23.16	33.69	10.0	-23	-12
							N*	N*	N*
		Max -ve	-42.34	-49.94	-90.61	-84.75	-8	-48	-42
							N*	114%	100%
14E	Top Elements	Max +ve	277.09	329.99	359.15	375.49	53	82	98
							19%	30%	36%
		Max -ve	-198.99	-220.07	-224.19	-229.92	-21	-25	-31
							N*	13%	16%
	Bottom Elements	Max +ve	158.28	166.13	169.77	173.23	8	11	15
							N*	N*	N*
		Max -ve	-207.90	-245.81	-265.03	-268.95	-38	-57	-61
							18%	27%	29%
13E	Top Elements	Max +ve	42.53	59.89	66.05	62.43	17	24	20
							N*	N*	N*
		Max -ve	-2.73	-3.91	-4.33	-4.08	-1	-2	-1
							N*	N*	N*
	Bottom Elements	Max +ve	27.71	39.41	43.59	41.07	12	16	13
							N*	N*	N*
		Max -ve	-16.17	-22.75	-25.11	-23.70	-7	-9	-8
							N*	N*	N*
12E	Top Elements	Max +ve	0.226	0.317	0.350	0.330	0.1	0.1	0.1
							N*	N*	N*
		Max -ve	-0.343	-0.503	-0.561	-0.526	-0.2	-0.2	-0.2
							N*	N*	N*
	Bottom Elements	Max +ve	0.022	0.031	0.033	0.032	0.0	0.0	0.0
							N*	N*	N*
		Max -ve	-0.205	-0.290	-0.321	-0.304	-0.1	-0.1	-0.1
							N*	N*	N*

N*(Negligible): The difference is less than 25 psi.

Table 33
Case II - Effects of truck configurations on flexural stresses - Girder B

Span	Location	Stress	HS20-44 (psi)	3S3 (psi)	GVW148 Opt-1 (psi)	GVW148 Opt-2 (psi)	Change in Stresses		
							3S3 vs. HS20-44	Opt-1 vs. HS20-44	Opt-2 vs. HS20-44
15E	Top Elements	Max +ve	107.37	136.10	211.40	218.10	29	104	111
							27%	97%	103%
		Max -ve	-5.47	-6.75	-6.31	-4.20	-1	-1	1
							N*	N*	N*
	Bottom Elements	Max +ve	36.88	39.23	20.94	29.31	2	-16	-8
							N*	N*	N*
		Max -ve	-41.75	-49.14	-124.91	-112.10	-7	-83	-70
							N*	199%	169%
14E	Top Elements	Max +ve	240.43	301.02	365.68	393.01	61	125	153
							25%	52%	63%
		Max -ve	-247.38	-229.27	-223.94	-233.59	18	23	14
							N*	N*	N*
	Bottom Elements	Max +ve	194.27	183.48	190.82	184.03	-11	-3	-10
							N*	N*	N*
		Max -ve	-206.44	-248.27	-287.27	-307.81	-42	-81	-101
							20%	39%	49%
13E	Top Elements	Max +ve	92.03	136.47	152.70	141.98	44	61	50
							48%	66%	54%
		Max -ve	-2.70	-3.74	-4.11	-3.92	-1	-1	-1
							N*	N*	N*
	Bottom Elements	Max +ve	25.59	36.81	40.87	38.44	11	15	13
							N*	N*	N*
		Max -ve	-24.52	-36.54	-40.96	-37.91	-12	-16	-13
							N*	N*	N*
12E	Top Elements	Max +ve	0.215	0.352	0.403	0.360	0.1	0.2	0.1
							N*	N*	N*
		Max -ve	-0.305	-0.349	-0.362	-0.378	0.0	-0.1	-0.1
							N*	N*	N*
	Bottom Elements	Max +ve	0.041	0.075	0.088	0.077	0.0	0.0	0.0
							N*	N*	N*
		Max -ve	-0.161	-0.241	-0.279	-0.245	-0.1	-0.1	-0.1
							N*	N*	N*

N*(Negligible): The difference is less than 25 psi.

Table 34
Case II - Effects of truck configurations on flexural stresses - Girder C

Span	Location	Stress	HS20-44 (psi)	3S3 (psi)	GVW148 Opt-1 (psi)	GVW148 Opt-2 (psi)	Change in Stresses		
							3S3 vs. HS20-44	Opt-1 vs. HS20-44	Opt-2 vs. HS20-44
15E	Top Elements	Max +ve	65.00	80.78	121.50	118.66	16	57	54
							N*	87%	83%
		Max -ve	-3.59	-4.42	-1.31	-3.15	-1	2	0.4
							N*	N*	N*
	Bottom Elements	Max +ve	20.19	24.90	12.57	20.68	5	-8	0.5
							N*	N*	N*
		Max -ve	-23.86	-29.73	-69.74	-45.44	-6	-46	-22
							N*	192%	N*
14E	Top Elements	Max +ve	152.44	212.18	232.99	240.13	60	81	88
							39%	53%	58%
		Max -ve	-187.67	-179.19	-211.29	-200.18	8	-24	-13
							N*	N*	N*
	Bottom Elements	Max +ve	160.96	136.03	143.31	148.27	-25	-18	-13
							N*	N*	N*
		Max -ve	-143.08	-195.47	-212.90	-213.96	-52	-70	-71
							37%	49%	50%
13E	Top Elements	Max +ve	58.69	85.01	94.27	89.14	26	36	30
							45%	61%	52%
		Max -ve	-2.53	-3.57	-3.95	-3.73	-1	-1	-1
							N*	N*	N*
	Bottom Elements	Max +ve	26.05	36.84	40.77	38.72	11	15	13
							N*	N*	N*
		Max -ve	-26.02	-37.33	-41.34	-39.19	-11	-15	-13
							N*	N*	N*
12E	Top Elements	Max +ve	0.267	0.401	0.447	0.424	0.1	0.2	0.2
							N*	N*	N*
		Max -ve	-0.001	-0.007	-0.009	-0.005	0.0	0.0	0.0
							N*	N*	N*
	Bottom Elements	Max +ve	0.033	0.046	0.050	0.049	0.0	0.0	0.0
							N*	N*	N*
		Max -ve	-0.416	-0.598	-0.661	-0.630	-0.2	-0.2	-0.2
							N*	N*	N*

N*(Negligible): The difference is less than 25 psi.

Table 35
Case II - Effects of truck configurations on flexural stresses - Girder D

Span	Location	Stress	HS20-44 (psi)	3S3 (psi)	GVW148 Opt-1 (psi)	GVW148 Opt-2 (psi)	Change in Stresses		
							3S3 vs. HS20-44	Opt-1 vs. HS20-44	Opt-2 vs. HS20-44
15E	Top Elements	Max +ve	30.72	36.39	42.12	43.41	6	11	13
							N*	N*	N*
		Max -ve	-1.88	-2.28	-1.47	-2.18	-0.4	0.4	-0.3
							N*	N*	N*
	Bottom Elements	Max +ve	10.93	13.17	9.32	12.88	2	-2	2
							N*	N*	N*
		Max -ve	-11.32	-13.29	-20.15	-18.34	-2	-9	-7
							N*	N*	N*
14E	Top Elements	Max +ve	106.62	130.68	140.95	142.15	24	34	36
							N*	32%	33%
		Max -ve	-87.81	-101.61	-109.67	-113.14	-14	-22	-25
							N*	N*	29%
	Bottom Elements	Max +ve	75.12	85.13	92.08	95.24	10	17	20
							N*	N*	N*
		Max -ve	-118.41	-119.02	-128.15	-129.95	-0.6	-10	-12
							N*	N*	N*
13E	Top Elements	Max +ve	42.20	51.13	54.80	55.58	9	13	13
							N*	N*	N*
		Max -ve	-2.76	-4.08	-4.57	-4.25	-1	-2	-1
							N*	N*	N*
	Bottom Elements	Max +ve	21.41	28.80	31.64	30.69	7	10	9
							N*	N*	N*
		Max -ve	-18.20	-21.68	-23.11	-23.67	-3	-5	-5
							N*	N*	N*
12E	Top Elements	Max +ve	0.024	0.040	0.045	0.040	0.0	0.0	0.0
							N*	N*	N*
		Max -ve	-0.415	-0.763	-0.887	-0.762	-0.3	-0.5	-0.3
							N*	N*	N*
	Bottom Elements	Max +ve	0.219	0.421	0.492	0.417	0.2	0.3	0.2
							N*	N*	N*
		Max -ve	-0.436	-0.205	-0.236	-0.202	0.2	0.2	0.2
							N*	N*	N*

N*(Negligible): The difference is less than 25 psi.

Table 36
Case II - Effects of truck configurations on flexural stresses - Girder E

Span	Location	Stress	HS20-44 (psi)	3S3 (psi)	GVW148 Opt-1 (psi)	GVW148 Opt-2 (psi)	Change in Stresses		
							3S3 vs. HS20-44	Opt-1 vs. HS20-44	Opt-2 vs. HS20-44
15E	Top Elements	Max +ve	9.71	11.14	12.00	12.61	1	2	3
							N*	N*	N*
		Max -ve	-0.67	-0.79	-0.82	-0.93	-0.1	-0.2	-0.3
							N*	N*	N*
	Bottom Elements	Max +ve	4.18	4.91	4.78	5.56	0.7	1	1
							N*	N*	N*
		Max -ve	-3.73	-4.23	-4.97	-4.86	-0.5	-1	-1
							N*	N*	N*
14E	Top Elements	Max +ve	45.70	52.85	57.60	59.81	7	12	14
							N*	N*	N*
		Max -ve	-39.90	-48.21	-52.35	-53.36	-8	-12	-13
							N*	N*	N*
	Bottom Elements	Max +ve	28.82	34.65	37.90	38.93	6	9	10
							N*	N*	N*
		Max -ve	-42.33	-49.25	-53.64	-55.65	-7	-11	-13
							N*	N*	N*
13E	Top Elements	Max +ve	17.43	19.34	21.08	22.28	2	4	5
							N*	N*	N*
		Max -ve	-2.90	-4.08	-4.52	-4.30	-1	-2	-1
							N*	N*	N*
	Bottom Elements	Max +ve	12.81	16.04	17.46	17.48	3	5	5
							N*	N*	N*
		Max -ve	-6.28	-6.51	-7.05	-7.69	-0.2	-0.8	-1
							N*	N*	N*
12E	Top Elements	Max +ve	0.046	0.069	0.077	0.071	0.0	0.0	0.0
							N*	N*	N*
		Max -ve	-0.509	-0.806	-0.899	-0.819	-0.3	-0.4	-0.3
							N*	N*	N*
	Bottom Elements	Max +ve	0.521	0.788	0.876	0.811	0.3	0.4	0.3
							N*	N*	N*
		Max -ve	-0.275	-0.415	-0.463	-0.428	-0.1	-0.2	-0.2
							N*	N*	N*

N*(Negligible): The difference is less than 25 psi.

Table 37
Case II - Effects of truck configurations on flexural stresses - Girder F

Span	Location	Stress	HS20-44 (psi)	3S3 (psi)	GVW148 Opt-1 (psi)	GVW148 Opt-2 (psi)	Change in Stresses		
							3S3 vs. HS20-44	Opt-1 vs. HS20-44	Opt-2 vs. HS20-44
15E	Top Elements	Max +ve	0.06	0.09	0.66	0.12	0.0	1	0
							N*	N*	N*
		Max -ve	-1.87	-2.44	-3.17	-3.19	-1	-1	-1
							N*	N*	N*
	Bottom Elements	Max +ve	0.37	0.43	1.47	1.06	0.1	1	1
							N*	N*	N*
		Max -ve	-0.29	-0.47	-0.51	-0.41	-0.2	0	0
							N*	N*	N*
14E	Top Elements	Max +ve	10.88	14.00	14.88	14.55	3	4	4
							N*	N*	N*
		Max -ve	-15.11	-19.33	-20.65	-20.74	-4	-6	-6
							N*	N*	N*
	Bottom Elements	Max +ve	13.75	18.54	19.55	19.28	5	6	6
							N*	N*	N*
		Max -ve	-4.94	-6.39	-6.78	-6.40	-2	-2	-1
							N*	N*	N*
13E	Top Elements	Max +ve	2.24	2.56	2.78	2.89	0.3	1	1
							N*	N*	N*
		Max -ve	-10.61	-13.13	-14.07	-14.28	-3	-4	-4
							N*	N*	N*
	Bottom Elements	Max +ve	4.22	4.89	5.24	5.44	1	1	1
							N*	N*	N*
		Max -ve	-1.89	-2.29	-2.47	-2.51	-0.4	-0.6	-0.6
							N*	N*	N*
12E	Top Elements	Max +ve	0.087	0.121	0.137	0.132	0.0	0.1	0.0
							N*	N*	N*
		Max -ve	-0.496	-0.595	-0.642	-0.657	-0.1	-0.1	-0.2
							N*	N*	N*
	Bottom Elements	Max +ve	0.492	0.577	0.621	0.643	0.1	0.1	0.2
							N*	N*	N*
		Max -ve	-0.317	-0.418	-0.450	-0.439	-0.1	-0.1	-0.1
							N*	N*	N*

N*(Negligible): The difference is less than 25 psi.

Table 38
Case III - Effects of truck configurations on flexural stresses - Girder A

Span	Location	Stress	HS20-44 (psi)	3S3 (psi)	GVW148 Opt-1 (psi)	GVW148 Opt-2 (psi)	Change in Stresses		
							3S3 vs. HS20-44	Opt-1 vs. HS20-44	Opt-2 vs. HS20-44
15E	Top Elements	Max +ve	10.09	12.68	13.83	14.89	3	4	5
							N*	N*	N*
		Max -ve	-1.94	-2.16	-2.51	-2.72	-0.2	-1	-1
							N*	N*	N*
	Bottom Elements	Max +ve	10.69	11.99	13.57	14.54	1	3	4
							N*	N*	N*
		Max -ve	-3.06	-3.36	-3.87	-4.16	0	-1	-1
							N*	N*	N*
14E	Top Elements	Max +ve	21.10	26.47	28.63	30.61	5	8	10
							N*	N*	N*
		Max -ve	-20.50	-24.25	-27.18	-29.13	-4	-7	-9
							N*	N*	N*
	Bottom Elements	Max +ve	13.75	16.20	18.04	19.34	2	4	6
							N*	N*	N*
		Max -ve	-13.43	-16.22	-17.56	-18.72	-3	-4	-5
							N*	N*	N*
13E	Top Elements	Max +ve	2.88	3.09	3.40	3.63	0	1	1
							N*	N*	N*
		Max -ve	-0.76	-1.09	-1.24	-1.27	0	0	-1
							N*	N*	N*
	Bottom Elements	Max +ve	4.06	5.09	5.60	5.96	1	2	2
							N*	N*	N*
		Max -ve	-14.71	-16.85	-18.46	-19.85	-2	-4	-5
							N*	N*	N*
12E	Top Elements	Max +ve	0.015	0.025	0.031	0.032	0.0	0.0	0.0
							N*	N*	N*
		Max -ve	-0.231	-0.349	-0.392	-0.411	-0.1	-0.2	-0.2
							N*	N*	N*
	Bottom Elements	Max +ve	2.168	2.832	3.135	3.327	0.7	1.0	1.2
							N*	N*	N*
		Max -ve	-0.055	-0.080	-0.088	-0.092	0.0	0.0	0.0
							N*	N*	N*

N*(Negligible): The difference is less than 25 psi.

Table 39
Case III - Effects of truck configurations on flexural stresses - Girder B

Span	Location	Stress	HS20-44 (psi)	3S3 (psi)	GVW148 Opt-1 (psi)	GVW148 Opt-2 (psi)	Change in Stresses		
							3S3 vs. HS20-44	Opt-1 vs. HS20-44	Opt-2 vs. HS20-44
15E	Top Elements	Max +ve	42.77	47.27	64.30	69.92	5	22	27
							N*	N*	63%
		Max -ve	-2.88	-3.09	-4.27	-4.65	-0.2	-1	-2
							N*	N*	N*
	Bottom Elements	Max +ve	16.92	18.09	23.85	25.30	1	7	8
							N*	N*	N*
		Max -ve	-16.55	-18.34	-19.46	-21.37	-2	-3	-5
							N*	N*	N*
14E	Top Elements	Max +ve	100.10	111.00	142.28	153.59	11	42	53
							N*	42%	53%
		Max -ve	-79.25	-87.76	-93.40	-100.59	-9	-14	-21
							N*	N*	N*
	Bottom Elements	Max +ve	60.74	67.07	76.57	82.67	6	16	22
							N*	N*	N*
		Max -ve	-78.87	-88.28	-101.14	-109.00	-9	-22	-30
							N*	N*	38%
13E	Top Elements	Max +ve	19.29	24.47	21.24	22.70	5	2	3
							N*	N*	N*
		Max -ve	-1.09	-1.55	-1.50	-1.58	-0.5	-0.4	-0.5
							N*	N*	N*
	Bottom Elements	Max +ve	9.16	12.54	14.03	14.83	3	5	6
							N*	N*	N*
		Max -ve	-7.30	-9.03	-9.92	-10.59	-2	-3	-3
							N*	N*	N*
12E	Top Elements	Max +ve	0.060	0.084	0.101	0.106	0.0	0.0	0.0
							N*	N*	N*
		Max -ve	-0.180	-0.277	-0.284	-0.296	-0.1	-0.1	-0.1
							N*	N*	N*
	Bottom Elements	Max +ve	0.061	0.083	0.092	0.098	0.0	0.0	0.0
							N*	N*	N*
		Max -ve	-0.036	-0.035	-0.040	-0.042	0.0	0.0	0.0
							N*	N*	N*

N*(Negligible): The difference is less than 25 psi.

Table 40
Case III - Effects of truck configurations on flexural stresses - Girder C

Span	Location	Stress	HS20-44 (psi)	3S3 (psi)	GVW148 Opt-1 (psi)	GVW148 Opt-2 (psi)	Change in Stresses		
							3S3 vs. HS20-44	Opt-1 vs. HS20-44	Opt-2 vs. HS20-44
15E	Top Elements	Max +ve	65.00	80.78	121.50	118.66	16	57	54
							N*	87%	83%
		Max -ve	-3.59	-4.42	-1.31	-3.15	-1	2	0.4
							N*	N*	N*
	Bottom Elements	Max +ve	20.19	24.90	12.57	20.68	5	-8	0.5
							N*	N*	N*
		Max -ve	-23.86	-29.73	-69.74	-45.44	-6	-46	-22
							N*	192%	N*
14E	Top Elements	Max +ve	152.44	212.18	232.99	240.13	60	81	88
							39%	53%	58%
		Max -ve	-187.67	-179.19	-211.29	-200.18	8	-24	-13
							N*	N*	N*
	Bottom Elements	Max +ve	160.96	136.03	143.31	148.27	-25	-18	-13
							N*	N*	N*
		Max -ve	-143.08	-195.47	-212.90	-213.96	-52	-70	-71
							37%	49%	50%
13E	Top Elements	Max +ve	58.69	85.01	94.27	89.14	26	36	30
							45%	61%	52%
		Max -ve	-2.53	-3.57	-3.95	-3.73	-1	-1	-1
							N*	N*	N*
	Bottom Elements	Max +ve	26.05	36.84	40.77	38.72	11	15	13
							N*	N*	N*
		Max -ve	-26.02	-37.33	-41.34	-39.19	-11	-15	-13
							N*	N*	N*
12E	Top Elements	Max +ve	0.267	0.401	0.447	0.424	0.1	0.2	0.2
							N*	N*	N*
		Max -ve	-0.001	-0.007	-0.009	-0.005	0.0	0.0	0.0
							N*	N*	N*
	Bottom Elements	Max +ve	0.033	0.046	0.050	0.049	0.0	0.0	0.0
							N*	N*	N*
		Max -ve	-0.416	-0.598	-0.661	-0.630	-0.2	-0.2	-0.2
							N*	N*	N*

N*(Negligible): The difference is less than 25 psi.

Table 41
Case III - Effects of truck configurations on flexural stresses - Girder F

Span	Location	Stress	HS20-44 (psi)	3S3 (psi)	GVW148 Opt-1 (psi)	GVW148 Opt-2 (psi)	Change in Stresses		
							3S3 vs. HS20-44	Opt-1 vs. HS20-44	Opt-2 vs. HS20-44
15E	Top Elements	Max +ve	34.30	35.49	45.15	48.92	1	11	15
							N*	N*	N*
		Max -ve	-2.29	-2.35	-3.15	-3.39	0.0	-1	-1
							N*	N*	N*
	Bottom Elements	Max +ve	14.49	14.92	19.87	21.37	0.4	5	7
							N*	N*	N*
		Max -ve	-12.49	-12.91	-16.44	-17.81	0.4	-4	-5
							N*	N*	N*
14E	Top Elements	Max +ve	124.57	131.39	156.08	168.83	7	32	44
							N*	25%	36%
		Max -ve	-100.21	-104.67	-127.21	-137.17	-4	-27	-37
							N*	27%	37%
	Bottom Elements	Max +ve	82.96	85.86	104.50	112.76	3	22	30
							N*	N*	36%
		Max -ve	-111.72	-117.62	-140.43	-151.87	-6	-29	-40
							N*	26%	36%
13E	Top Elements	Max +ve	41.03	39.68	47.83	52.19	-1	7	11
							N*	N*	N*
		Max -ve	-6.84	-9.37	-10.55	-11.16	-3	-4	-4
							N*	N*	N*
	Bottom Elements	Max +ve	33.76	41.04	47.25	50.47	7	13	17
							N*	N*	N*
		Max -ve	-18.82	-17.28	-20.57	-22.55	2	-2	-4
							N*	N*	N*
12E	Top Elements	Max +ve	0.070	0.108	0.125	0.130	0.0	0.1	0.1
							N*	N*	N*
		Max -ve	-1.185	-1.818	-2.008	-2.107	-0.6	-0.8	-0.9
							N*	N*	N*
	Bottom Elements	Max +ve	1.083	1.669	1.843	1.931	0.6	0.8	0.8
							N*	N*	N*
		Max -ve	-0.439	-0.677	-0.761	-0.797	-0.2	-0.3	-0.4
							N*	N*	N*

N*(Negligible): The difference is less than 25 psi.

Table 42
Case IV - Effects of truck configurations on flexural stresses - Girder A

Span	Location	Stress	HS20-44 (psi)	3S3 (psi)	GVW148 Opt-1 (psi)	GVW148 Opt-2 (psi)	Change in Stresses		
							3S3 vs. HS20-44	Opt-1 vs. HS20-44	Opt-2 vs. HS20-44
15E	Top Elements	Max +ve	7.66	9.79	10.96	10.47	2	3	3
							N*	N*	N*
		Max -ve	-1.89	-2.20	-2.58	-2.56	-0.3	-1	-1
							N*	N*	N*
	Bottom Elements	Max +ve	9.89	11.25	13.58	13.30	1.4	4	3
							N*	N*	N*
		Max -ve	-2.95	-3.35	-4.76	-4.58	-0.4	-2	-2
							N*	N*	N*
14E	Top Elements	Max +ve	16.63	20.60	24.21	22.93	4	8	6
							N*	N*	N*
		Max -ve	-17.62	-21.09	-24.44	-23.84	-3	-7	-6
							N*	N*	N*
	Bottom Elements	Max +ve	11.88	14.02	16.15	15.76	2	4	4
							N*	N*	N*
		Max -ve	-12.33	-14.69	-16.95	-16.47	-2	-5	-4
							N*	N*	N*
13E	Top Elements	Max +ve	2.72	2.97	3.22	3.26	0.3	1	1
							N*	N*	N*
		Max -ve	-0.55	-0.73	-0.90	-0.84	-0.2	-0.4	-0.3
							N*	N*	N*
	Bottom Elements	Max +ve	3.17	3.98	4.71	4.49	1	2	1
							N*	N*	N*
		Max -ve	-1.37	-1.57	-1.74	-1.74	-0.2	-0.4	-0.4
							N*	N*	N*
12E	Top Elements	Max +ve	0.012	0.016	0.021	0.020	0.0	0.0	0.0
							N*	N*	N*
		Max -ve	-0.158	-0.219	-0.276	-0.253	-0.1	-0.1	-0.1
							N*	N*	N*
	Bottom Elements	Max +ve	0.040	0.058	0.076	0.069	0.0	0.0	0.0
							N*	N*	N*
		Max -ve	-0.038	-0.051	-0.063	-0.058	0.0	0.0	0.0
							N*	N*	N*

N*(Negligible): The difference is less than 25 psi.

Table 43
Case IV - Effects of truck configurations on flexural stresses - Girder B

Span	Location	Stress	HS20 (psi)	3S3 (psi)	GVW148 Opt-1 (psi)	GVW148 Opt-2 (psi)	Change in Stresses		
							3S3 vs. HS20-44	Opt-1 vs. HS20-44	Opt-2 vs. HS20-44
15E	Top Elements	Max +ve	48.44	42.23	63.41	62.14	-6	15	14
							N*	N*	N*
		Max -ve	-3.45	-3.76	-2.32	-3.08	-0.3	1	0.4
							N*	N*	N*
	Bottom Elements	Max +ve	18.68	22.82	18.81	21.78	4	0.1	3.1
							N*	N*	N*
		Max -ve	18.68	22.82	18.81	21.78	4	0.1	3.1
							N*	N*	N*
14E	Top Elements	Max +ve	104.64	104.63	133.85	133.75	0.0	29	29
							N*	28%	28%
		Max -ve	-70.24	-82.51	-88.23	-88.70	-12	-18	-18
							N*	N*	N*
	Bottom Elements	Max +ve	54.15	62.83	70.84	70.31	9	17	16
							N*	N*	N*
		Max -ve	-70.82	-82.42	-109.08	-108.23	-12	-38	-37
							N*	54%	53%
13E	Top Elements	Max +ve	12.49	19.24	18.75	18.04	7	6	6
							N*	N*	N*
		Max -ve	-0.69	-1.07	-1.12	-1.04	-0.4	-0.4	-0.4
							N*	N*	N*
	Bottom Elements	Max +ve	6.86	8.97	10.89	10.25	2	4	3
							N*	N*	N*
		Max -ve	-5.70	-7.31	-8.64	-8.29	-2	-3	-3
							N*	N*	N*
12E	Top Elements	Max +ve	0.049	0.059	0.076	0.073	0.0	0.0	0.0
							N*	N*	N*
		Max -ve	-0.101	-0.173	-0.179	-0.161	-0.1	-0.1	-0.1
							N*	N*	N*
	Bottom Elements	Max +ve	0.044	0.059	0.072	0.067	0.0	0.0	0.0
							N*	N*	N*
		Max -ve	-0.030	-0.038	-0.041	-0.042	0.0	0.0	0.0
							N*	N*	N*

N*(Negligible): The difference is less than 25 psi.

Table 44
Case IV - Effects of truck configurations on flexural stresses - Girder C

Span	Location	Stress	HS20-44 (psi)	3S3 (psi)	GVW148 Opt-1 (psi)	GVW148 Opt-2 (psi)	Change in Stresses		
							3S3 vs. HS20-44	Opt-1 vs. HS20-44	Opt-2 vs. HS20-44
15E	Top Elements	Max +ve	99.55	100.76	153.45	161.37	1	54	62
							N*	54%	62%
		Max -ve	-4.88	-5.99	-1.23	-3.29	-1	4	2
							N*	N*	N*
	Bottom Elements	Max +ve	27.33	33.90	16.49	24.92	7	-11	-2
							N*	N*	N*
		Max -ve	-34.84	-41.39	-74.55	-72.36	-7	-40	-38
							N*	114%	108%
14E	Top Elements	Max +ve	207.67	224.03	271.96	291.10	16	64	83
							N*	31%	40%
		Max -ve	-147.77	-148.09	-157.49	-162.35	-0.3	-10	-15
							N*	N*	N*
	Bottom Elements	Max +ve	122.43	114.42	117.88	118.53	-8	-5	-4
							N*	N*	N*
		Max -ve	-150.91	-171.39	-191.00	-197.65	-20	-40	-47
							N*	27%	31%
13E	Top Elements	Max +ve	28.00	43.05	45.85	42.82	15	18	15
							N*	N*	N*
		Max -ve	-0.92	-1.43	-1.43	-1.36	-0.5	-0.5	-0.4
							N*	N*	N*
	Bottom Elements	Max +ve	13.21	17.57	21.56	20.17	4	8	7
							N*	N*	N*
		Max -ve	-12.78	-17.02	-20.96	-19.52	-4	-8	-7
							N*	N*	N*
12E	Top Elements	Max +ve	0.233	0.285	0.406	0.371	0.1	0.2	0.1
							N*	N*	N*
		Max -ve	-0.021	-0.028	-0.038	-0.034	0.0	0.0	0.0
							N*	N*	N*
	Bottom Elements	Max +ve	0.127	0.177	0.225	0.205	0.1	0.1	0.1
							N*	N*	N*
		Max -ve	-0.264	-0.359	-0.448	-0.413	-0.1	-0.2	-0.1
							N*	N*	N*

N*(Negligible): The difference is less than 25 psi.

Table 45
Case IV - Effects of truck configurations on flexural stresses - Girder D

Span	Location	Stress	HS20-44 (psi)	3S3 (psi)	GVW148 Opt-1 (psi)	GVW148 Opt-2 (psi)	Change in Stresses		
							3S3 vs. HS20-44	Opt-1 vs. HS20-44	Opt-2 vs. HS20-44
15E	Top Elements	Max +ve	105.85	131.55	205.45	213.75	26	100	108
							24%	94%	102%
		Max -ve	-5.18	-6.61	-8.68	-3.62	-1	-4	2
							N*	N*	N*
	Bottom Elements	Max +ve	30.82	40.22	24.06	29.50	9	-7	-1
							N*	N*	N*
		Max -ve	-39.54	-53.12	-124.82	-114.40	-14	-85	-75
							N*	216%	189%
14E	Top Elements	Max +ve	229.42	288.32	349.32	376.65	59	120	147
							26%	52%	64%
		Max -ve	-231.46	-211.87	-204.57	-212.46	20	27	19
							N*	-12%	N*
	Bottom Elements	Max +ve	180.33	170.51	184.11	166.44	-10	4	-14
							N*	N*	N*
		Max -ve	-188.43	-235.92	-269.16	-290.20	-47	-81	-102
							25%	43%	54%
13E	Top Elements	Max +ve	47.28	73.68	82.59	75.78	26	35	29
							56%	75%	60%
		Max -ve	-1.32	-1.94	-1.94	-1.88	-0.6	-0.6	-0.6
							N*	N*	N*
	Bottom Elements	Max +ve	9.37	12.45	33.71	31.56	3	24	22
							N*	N*	N*
		Max -ve	-21.52	-29.43	-37.13	-34.14	-8	-16	-13
							N*	N*	N*
12E	Top Elements	Max +ve	0.408	0.515	0.758	0.681	0.1	0.4	0.3
							N*	N*	N*
		Max -ve	-0.144	-0.460	-0.069	-0.115	-0.3	0.1	0.0
							N*	N*	N*
	Bottom Elements	Max +ve	0.141	0.202	0.262	0.236	0.1	0.1	0.1
							N*	N*	N*
		Max -ve	-0.437	-0.607	-0.775	-0.707	-0.2	-0.3	-0.3
							N*	N*	N*

N*(Negligible): The difference is less than 25 psi.

Table 46
Case IV - Effects of truck configurations on flexural stresses - Girder E

Span	Location	Stress	HS20-44 (psi)	3S3 (psi)	GVW148 Opt-1 (psi)	GVW148 Opt-2 (psi)	Change in Stresses		
							3S3 vs. HS20-44	Opt-1 vs. HS20-44	Opt-2 vs. HS20-44
15E	Top Elements	Max +ve	72.23	92.93	128.72	127.52	21	56	55
							N*	78%	77%
		Max -ve	-4.00	-5.10	-1.99	-3.89	-1	2	0
							N*	N*	N*
	Bottom Elements	Max +ve	24.79	31.70	16.72	26.42	7	-8	2
							N*	N*	N*
		Max -ve	-27.19	-35.22	-72.83	-50.29	-8	-46	-23
							N*	168%	N*
14E	Top Elements	Max +ve	159.91	203.23	238.61	250.01	43	79	90
							27%	49%	56%
		Max -ve	-193.11	-175.34	-220.18	-208.36	18	-27	-15
							N*	14%	N*
	Bottom Elements	Max +ve	165.46	145.34	146.02	152.38	-20	-19	-13
							N*	N*	N*
		Max -ve	-160.45	-207.46	-233.88	-249.00	-47	-73	-89
							29%	46%	55%
13E	Top Elements	Max +ve	60.05	79.64	96.72	91.34	20	37	31
							N*	61%	52%
		Max -ve	-2.34	-3.00	-3.63	-3.45	-0.7	-1	-1
							N*	N*	N*
	Bottom Elements	Max +ve	26.53	34.43	41.52	39.49	8	15	13
							N*	N*	N*
		Max -ve	-26.39	-34.68	-41.96	-39.75	-8	-16	-13
							N*	N*	N*
12E	Top Elements	Max +ve	0.416	0.553	0.668	0.633	0.1	0.3	0.2
							N*	N*	N*
		Max -ve	-0.035	-0.046	-0.056	-0.053	0.0	0.0	0.0
							N*	N*	N*
	Bottom Elements	Max +ve	0.078	0.104	0.126	0.119	0.0	0.0	0.0
							N*	N*	N*
		Max -ve	-0.461	-0.597	-0.712	-0.683	-0.1	-0.3	-0.2
							N*	N*	N*

N*(Negligible): The difference is less than 25 psi.

Table 47
Case IV - Effects of truck configurations on flexural stresses - Girder F

Span	Location	Stress	HS20-44 (psi)	3S3 (psi)	GVW148 Opt-1 (psi)	GVW148 Opt-2 (psi)	Change in Stresses		
							3S3 vs. HS20-44	Opt-1 vs. HS20-44	Opt-2 vs. HS20-44
15E	Top Elements	Max +ve	38.85	45.14	49.31	51.76	6	10	13
							N*	N*	N*
		Max –ve	-2.68	-3.20	-3.20	-3.65	-1	-1	-1
							N*	N*	N*
	Bottom Elements	Max +ve	16.94	20.20	19.48	22.44	3	3	6
							N*	N*	N*
		Max -ve	-14.27	-16.56	-20.46	-20.13	-2	-6	-6
							N*	N*	N*
14E	Top Elements	Max +ve	121.87	140.32	156.55	159.32	18	35	37
							N*	28%	31%
		Max -ve	-105.09	-118.66	-131.14	-135.90	-14	-26	-31
							N*	25%	29%
	Bottom Elements	Max +ve	88.28	98.19	108.53	112.37	10	20	24
							N*	N*	N*
		Max -ve	-109.77	-126.61	-140.87	-143.70	-17	-31	-34
							N*	28%	31%
13E	Top Elements	Max +ve	42.50	47.42	51.81	53.69	5	9	11
							N*	N*	N*
		Max -ve	-5.33	-6.92	-8.38	-7.95	-2	-3	-3
							N*	N*	N*
	Bottom Elements	Max +ve	29.20	35.86	41.79	40.95	7	13	12
							N*	N*	N*
		Max -ve	-19.21	-21.58	-23.40	-24.31	-2	-4	-5
							N*	N*	N*
12E	Top Elements	Max +ve	0.049	0.067	0.085	0.078	0.0	0.0	0.0
							N*	N*	N*
		Max -ve	-0.820	-1.142	-1.445	-1.323	-0.3	-0.6	-0.5
							N*	N*	N*
	Bottom Elements	Max +ve	0.753	1.044	1.319	1.210	0.3	0.6	0.5
							N*	N*	N*
		Max -ve	-0.302	-0.420	-0.531	-0.486	-0.1	-0.2	-0.2
							N*	N*	N*

N*(Negligible): The difference is less than 25 psi.

Table 48
Effects of truck configurations on deflections - Girder A

Span	Case	Maximum Deflections			
		HS20-44 (in)	3S3 (in)	GVW148 Opt-1 (in)	GVW148 Opt-2 (in)
15E	I	-9.7E-03	-9.8E-03	-13E-03	-14E-03
	II	-10E-03	-13E-03	-5.7E-03	-7.7E-03
	III	-2.4E-03	-2.7E-03	-3.1E-03	-3.4E-03
	IV	-2.3E-03	-2.7E-03	-3.1E-03	-3.1E-03
14E	I	0.12	0.14	0.16	0.17
	II	0.11	0.13	0.14	0.14
	III	0.01	0.01	0.01	0.02
	IV	0.01	0.01	0.01	0.01
13E	I	-7.4E-03	-11E-03	-12E-03	-13E-03
	II	-6.1E-03	-8.7E-03	-9.6E-03	-9.0E-03
	III	-1.2E-03	-1.6E-03	-1.4E-03	-1.9E-03
	IV	-0.92E-03	-1.2E-03	-1.4E-03	-1.3E-03
12E	I	3.8E-06	4.3E-06	4.7E-06	5.1E-06
	II	3.5E-06	4.6E-06	5.2E-06	5.1E-06
	III	3.7E-06	6.3E-06	4.3E-06	7.2E-06
	IV	2.2E-06	3.2E-06	4.3E-06	3.7E-06

Note: Downward deflections of the girder are assumed positive.

Table 49
Effects of truck configurations on deflections - Girder B

Span	Case	Maximum Deflections			
		HS20-44 (in)	3S3 (in)	GVW148 Opt-1 (in)	GVW148 Opt-2 (in)
15E	I	-6.3E-03	-6.2E-03	-8.6E-03	-9.3E-03
	II	-7.1E-03	-8.7E-03	-2.0E-03	-4.0E-03
	III	-3.8E-03	-4.1E-03	-5.2E-03	-5.6E-03
	IV	-4.1E-03	-5.0E-03	-3.6E-03	-4.2E-03
14E	I	0.13	0.14	0.16	0.17
	II	0.12	0.14	0.15	0.15
	III	0.04	0.05	0.06	0.06
	IV	0.04	0.05	0.05	0.05
13E	I	-7.2E-03	-11E-03	-12E-03	-13E-03
	II	-5.9E-03	-8.5E-03	-9.4E-03	-8.9E-03
	III	-2.4E-03	-3.4E-03	-3.8E-03	-4.0E-03
	IV	-1.8E-03	-2.4E-03	-2.9E-03	-2.7E-03
12E	I	-3.8E-06	-12E-06	-12E-06	-13E-06
	II	-2.6E-06	-5.6E-06	-6.8E-06	-5.7E-06
	III	-9.8E-06	-14E-06	-16E-06	-17E-06
	IV	-6.9E-06	-9.5E-06	-12E-06	-11E-06

Note: Downward deflections of the girder are assumed positive.

Table 50
Effects of truck configurations on deflections - Girder C

Span	Case	Maximum Deflections			
		HS20-44 (in)	3S3 (in)	GVW148 Opt-1 (in)	GVW148 Opt-2 (in)
15E	I	-3.5E-03	-3.3E-03	-4.9E-03	-5.2E-03
	II	-4.0E-03	-4.9E-03	-1.5E-03	-3.6E-03
	III	-4.6E-03	-4.9E-03	-6.5E-03	-7.1E-03
	IV	-5.5E-03	-6.9E-03	-3.0E-03	-3.8E-03
14E	I	0.10	0.10	0.12	0.13
	II	0.09	0.11	0.12	0.12
	III	0.09	0.10	0.11	0.12
	IV	0.08	0.09	0.10	0.10
13E	I	-7.0E-03	-10E-03	-11E-03	-12E-03
	II	-5.8E-03	-8.2E-03	-9.1E-03	-8.6E-03
	III	-4.2E-03	-6.0E-03	-6.7E-03	-7.1E-03
	IV	-3.1E-03	-4.1E-03	-5.1E-03	-4.7E-03
12E	I	9.8E-06	21E-06	26E-06	27E-06
	II	6.4E-06	11E-06	12E-06	10E-06
	III	-34E-06	-54E-06	-61E-06	-63E-06
	IV	-23E-06	-32E-06	-41E-06	-37E-06

Note: Downward deflections of the girder are assumed positive.

Table 51
Effects of truck configurations on deflections - Girder E

Span	Case	Maximum Deflections			
		HS20-44 (in.)	3S3 (in.)	GVW148 Opt.1 (in.)	GVW148 Opt.2 (in.)
15E	I	-0.5E-03	-0.5E-03	-0.6E-03	-0.7E-03
	II	-0.5E-03	-0.6E-03	-0.6E-03	-0.7E-03
	III	-2.5E-03	-2.6E-03	-1.3E-03	-4.1E-03
	IV	3.1E-03	4.0E-03	1.3E-03	2.9E-03
14E	I	0.02	0.02	0.02	0.03
	II	0.02	0.02	0.03	0.03
	III	0.10	0.10	0.12	0.13
	IV	-0.10	-0.11	-0.12	-0.12
13E	I	-3.6E-03	-4.5E-03	-5.1E-03	-5.5E-03
	II	-3.2E-03	-4.2E-03	-4.6E-03	-4.5E-03
	III	-7.7E-03	-10E-03	-9.5E-03	-13E-03
	IV	6.1E-03	7.9E-03	9.5E-03	9.0E-03
12E	I	1.0E-04	1.6E-04	1.8E-04	1.8E-04
	II	0.8E-04	1.2E-04	1.3E-04	1.2E-04
	III	2.1E-05	3.0E-05	2.4E-05	3.8E-05
	IV	-1.5E-05	-2.0E-05	-2.4E-05	-2.3E-05

Note: Downward deflections of the girder are assumed positive.

Table 52
Effects of truck configurations on deflections - Girder F

Span	Case	Maximum Deflections			
		HS20-44 (in)	3S3 (in)	GVW148 Opt-1 (in)	GVW148 Opt-2 (in)
15E	I	3.4E-05	3.6E-05	5.8E-05	5.9E-05
	II	4.7E-05	6.9E-05	3.8E-06	2.5E-05
	III	-1.5E-03	-1.5E-03	-2.1E-03	-2.2E-03
	IV	-1.7E-03	-2.1E-03	-2.1E-03	-2.3E-03
14E	I	-2.4E-03	-2.7E-03	-3.3E-03	-3.4E-03
	II	-2.3E-03	-3.1E-03	-3.3E-03	-3.4E-03
	III	5.8E-02	6.1E-02	7.7E-02	8.0E-02
	IV	6.0E-02	6.9E-02	7.7E-02	7.9E-02
13E	I	-1.3E-03	-1.3E-03	-1.5E-03	-1.7E-03
	II	-1.3E-03	-1.5E-03	-1.7E-03	-1.7E-03
	III	-0.86E-02	-1.1E-02	-1.1E-02	-1.3E-02
	IV	-7.3E-03	-9.0E-03	-11E-03	-10E-03
12E	I	1.3E-04	1.7E-04	1.9E-04	2.1E-04
	II	1.2E-04	1.6E-04	1.7E-04	1.7E-04
	III	1.5E-04	2.3E-04	1.8E-04	2.8E-04
	IV	1.1E-04	1.5E-04	1.8E-04	1.7E-04

Note: Downward deflections of the girder are assumed positive.

APPENDIX C

Effects of Truck Configurations on Deck Stresses

Table 53
Case II- Effects of truck configurations on deck stresses

Direction	Location	Stress	HS20-44 (psi)	3S3 (psi)	GVW148 Opt-1 (psi)	GVW148 Opt-2 (psi)
Longitudinal	Top	Max +ve	52	63	75	73
		Max -ve	-221	-106	-112	-110
	Bottom	Max +ve	222	104	112	110
		Max -ve	-58	-70	-83	-81
Transverse	Top	Max +ve	150	121	173	167
		Max -ve	-435	-294	-306	-312
	Bottom	Max +ve	435	294	306	312
		Max -ve	-150	-121	-173	-166
Shear	Top	Max +ve	27	35	50	45
		Max -ve	-41	-35	-34	-33
	Bottom	Max +ve	42	36	35	34
		Max -ve	-27	-34	-50	-45

Table 54
Case III- Effects of truck configurations on deck stresses

Direction	Location	Stress	HS20-44 (psi)	3S3 (psi)	GVW148 Opt-1 (psi)	GVW148 Opt-2 (psi)
Longitudinal	Top	Max +ve	43	64	64	68
		Max -ve	-223	-109	-116	-123
	Bottom	Max +ve	223	108	112	119
		Max -ve	-47	-59	-64	-64
Transverse	Top	Max +ve	152	137	152	155
		Max -ve	-450	-301	-322	-332
	Bottom	Max +ve	450	301	322	332
		Max -ve	-152	-137	-152	-155
Shear	Top	Max +ve	32	35	37	44
		Max -ve	-47	-39	-33	-37
	Bottom	Max +ve	48	40	34	39
		Max -ve	-31	-33	-37	-45

Table 55
Case IV- Effects of truck configurations on deck stresses

Direction	Location	Stress	HS20-44 (psi)	3S3 (psi)	GVW148 Opt-1 (psi)	GVW148 Opt-2 (psi)
Longitudinal	Top	Max +ve	44	52	61	63
		Max -ve	-224	-102	-114	-111
	Bottom	Max +ve	224	101	113	111
		Max -ve	-46	-130	-66	-69
Transverse	Top	Max +ve	151	130	159	159
		Max -ve	-447	-295	-322	-323
	Bottom	Max +ve	447	295	322	323
		Max -ve	-151	-56	-158	-159
Shear	Top	Max +ve	36	36	50	47
		Max -ve	-40	-31	-32	-33
	Bottom	Max +ve	42	32	32	30
		Max -ve	-36	-37	-66	-47

APPENDIX D

Bridge Instrumentation Drawings

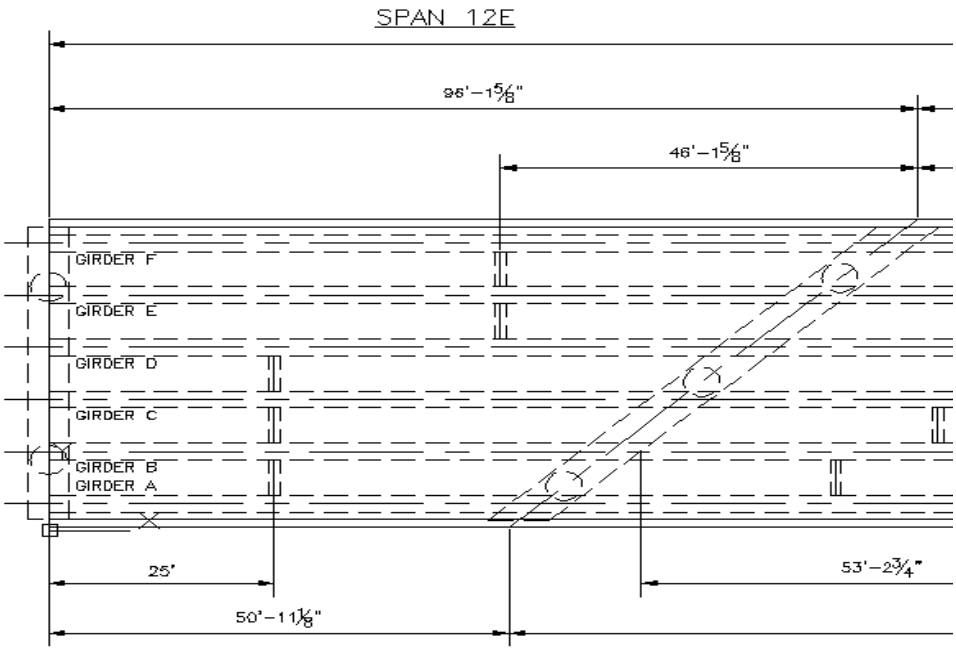

Figure 112
Plan view of bridge instrumentation- Span 12E

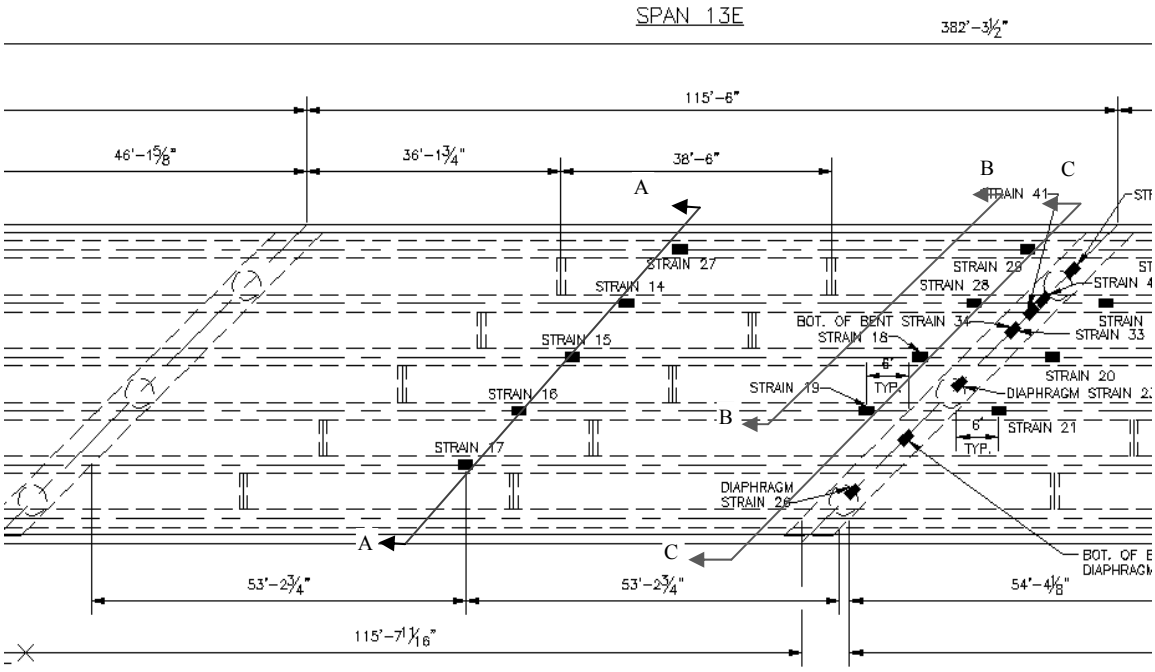

Figure 113
Plan view of bridge instrumentation- Span 13E. [Saber, A., 2010]

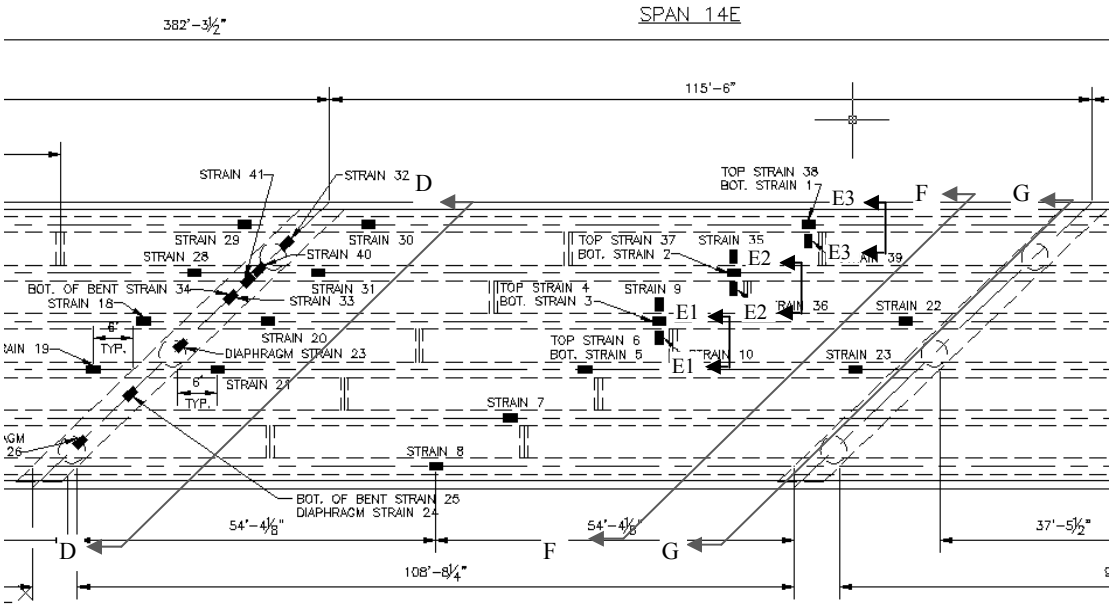

Figure 114
Plan view of bridge instrumentation- Span 14E. [Saber, A., 2010]

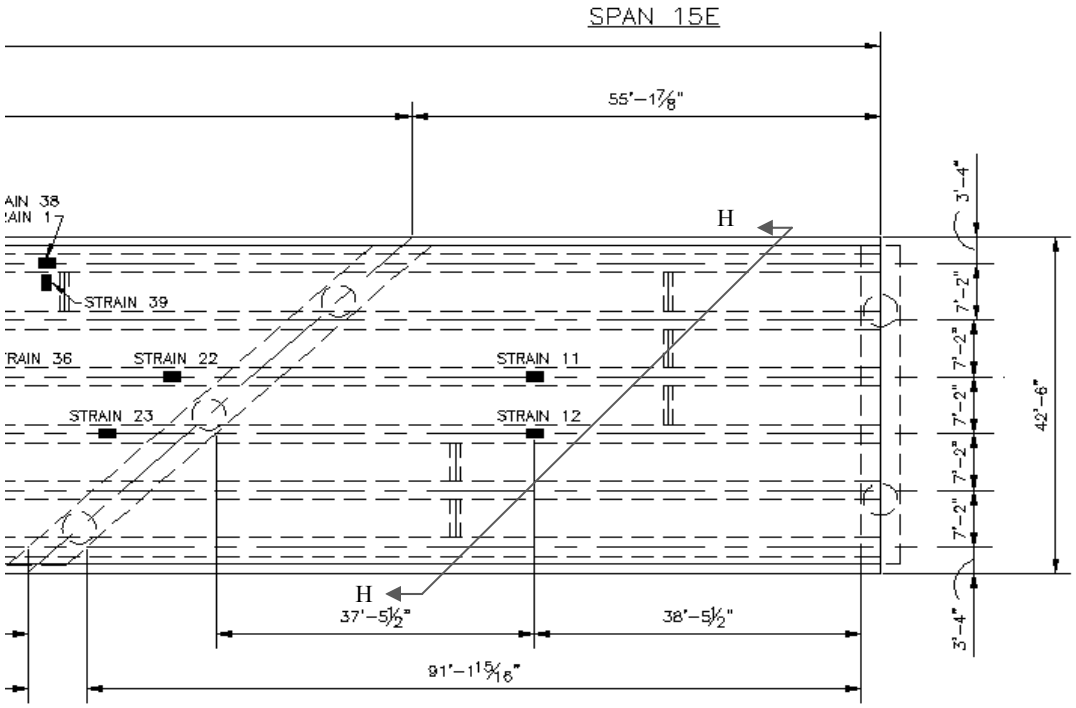

Figure 115
Plan view of bridge instrumentation- Span 15 E. [Saber, A., 2010]

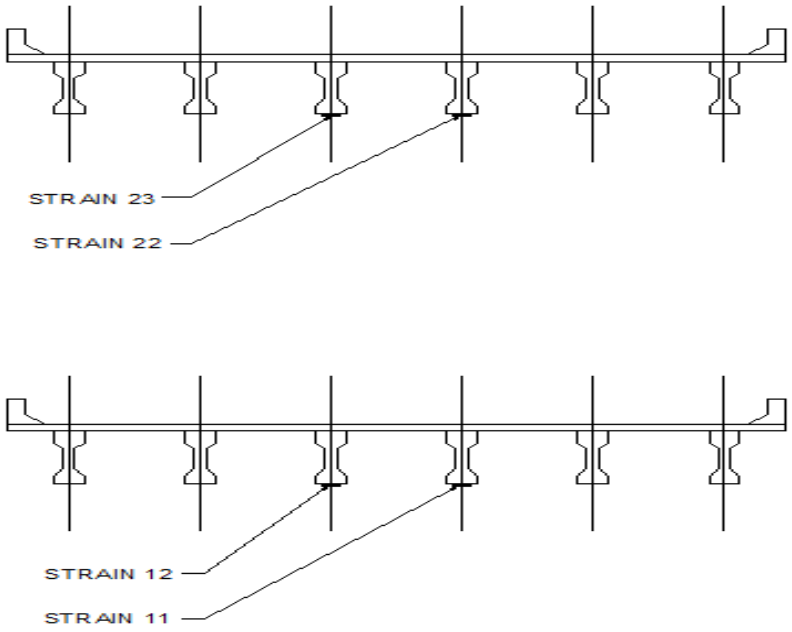

Figure 116
Strain gauges in section G-G and section H-H. [Saber, A., 2010]

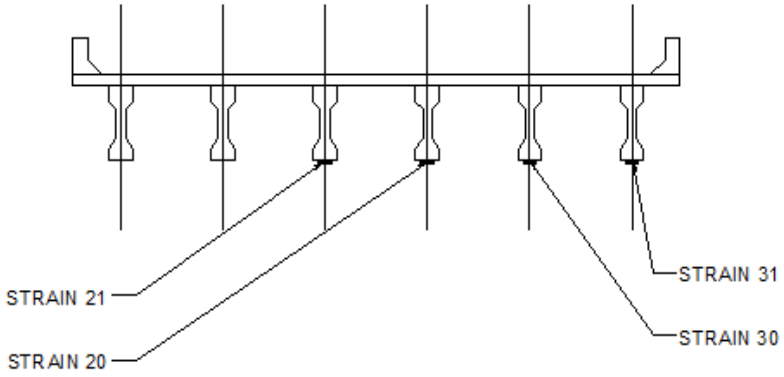

Figure 117
Strain gauges in section D-D. [Saber, A., 2010]

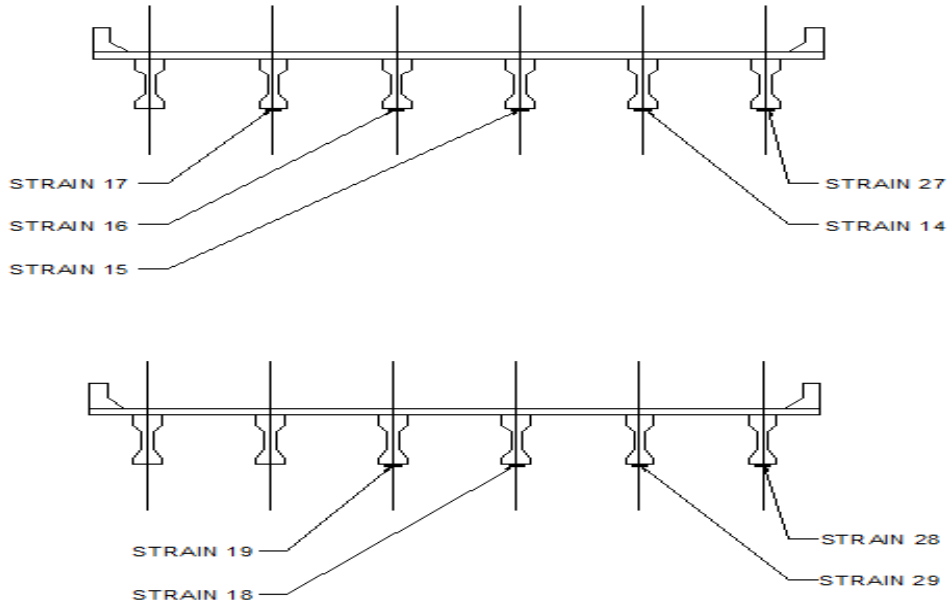

Figure 118
Strain gauges in section A-A and section B-B. [Saber, A., 2010]

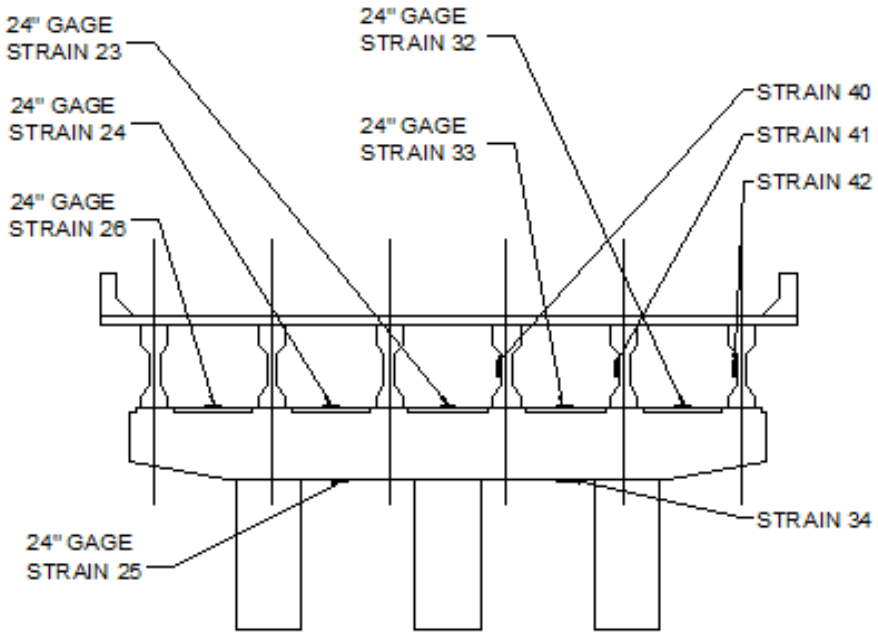

Figure 119
Strain gauges in section C-C. [Saber, A., 2010]

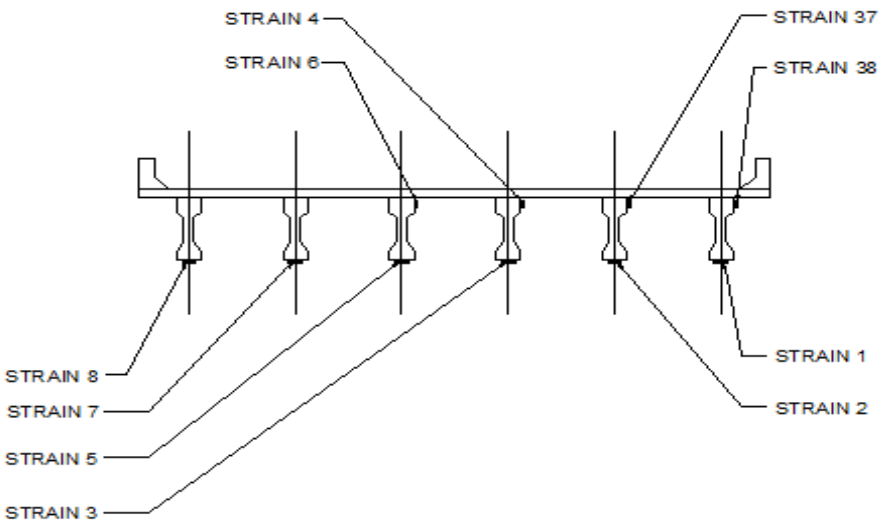

Figure 120
Strain gauges in section F-F. [Saber, A., 2010]

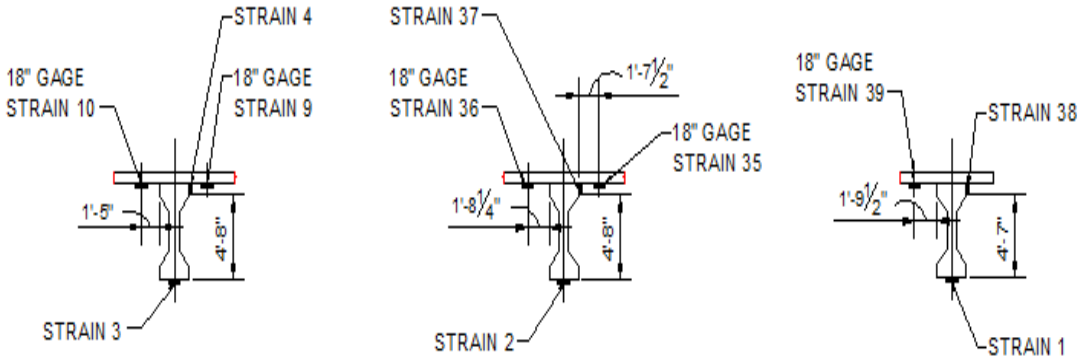

Figure 121
Strain gauges in sections E1-E1, E2-E2 and E3. [Saber, A., 2010]

APPENDIX E

Plot of Strains of the Auto Triggered Test

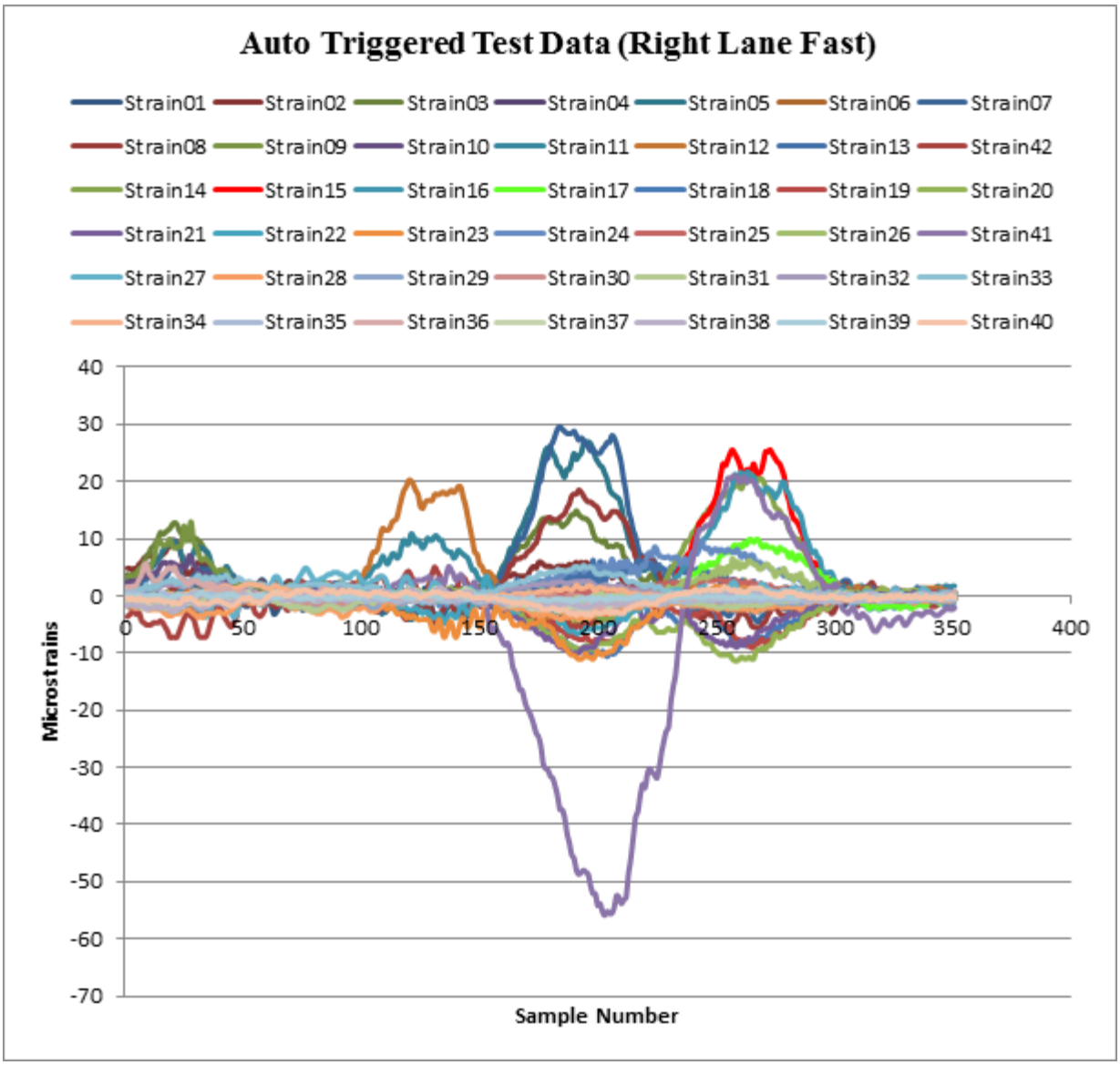

Figure 122
Plot of strains of the auto triggered test (truck on right lane)

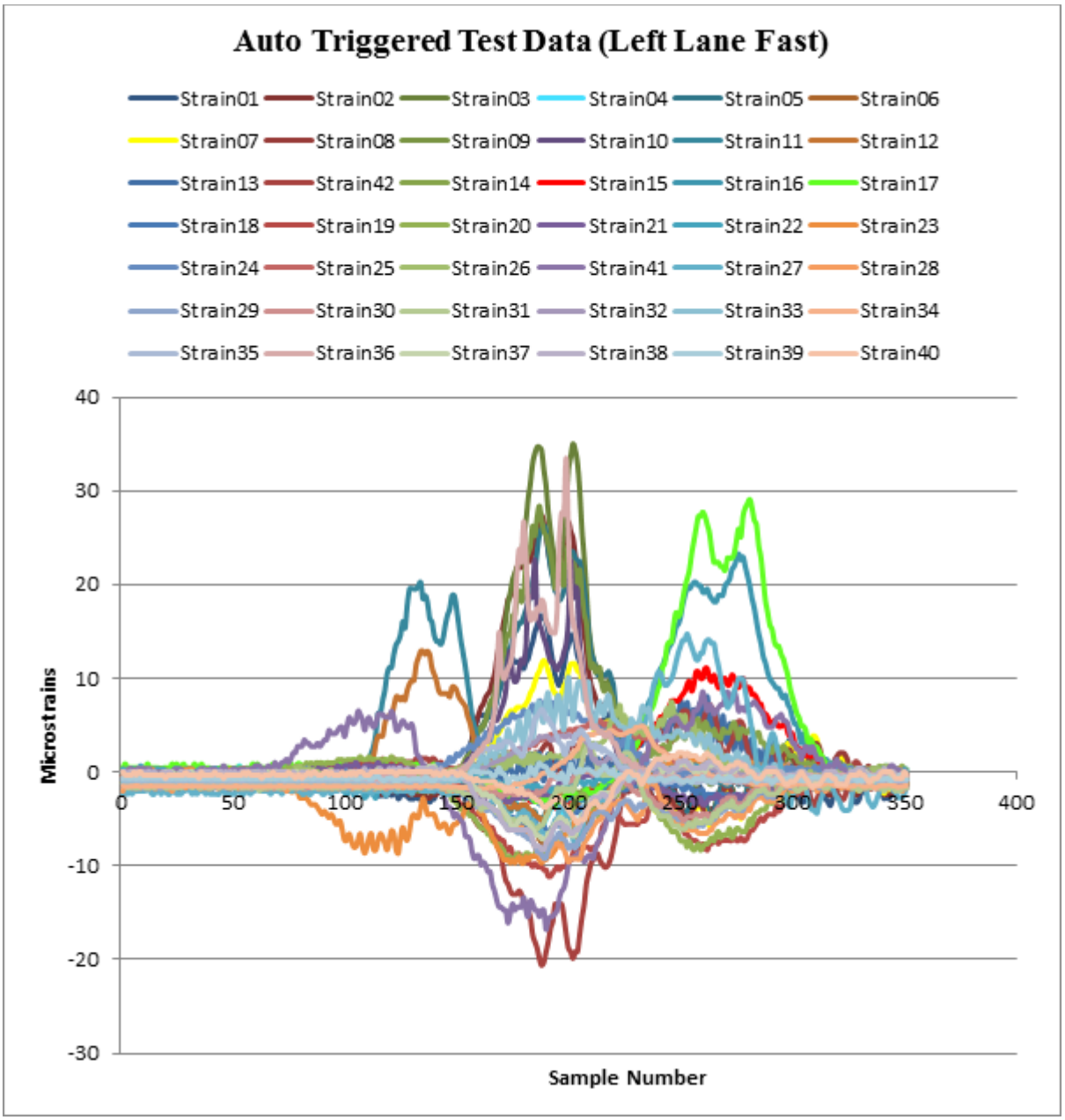

Figure 123
Plot of strains of the auto triggered test (truck on left lane)

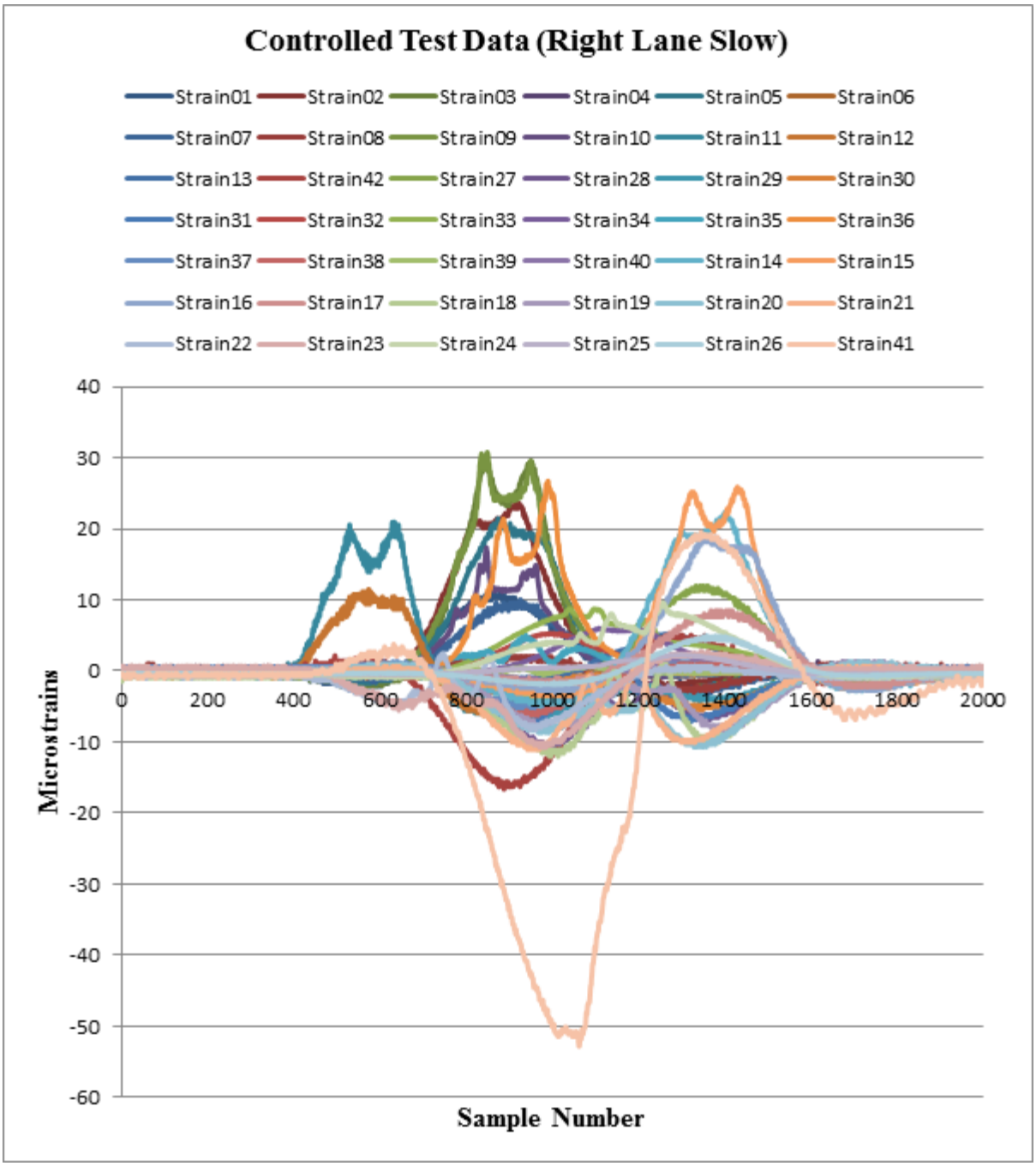

Figure 124
Plot of strains of the controlled test (out lane slow)

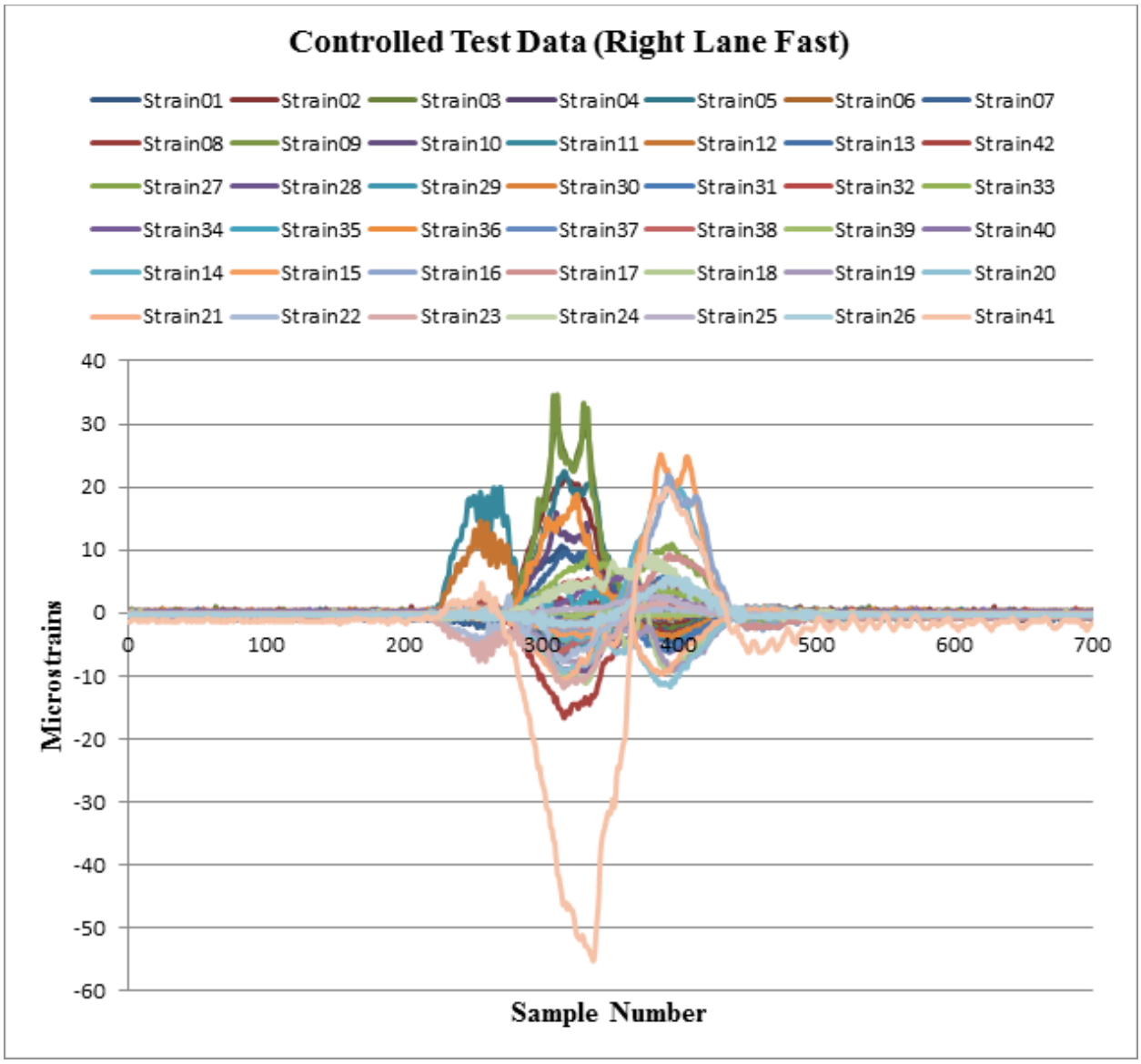

Figure 125
Plot of strains of the controlled test (out lane fast)

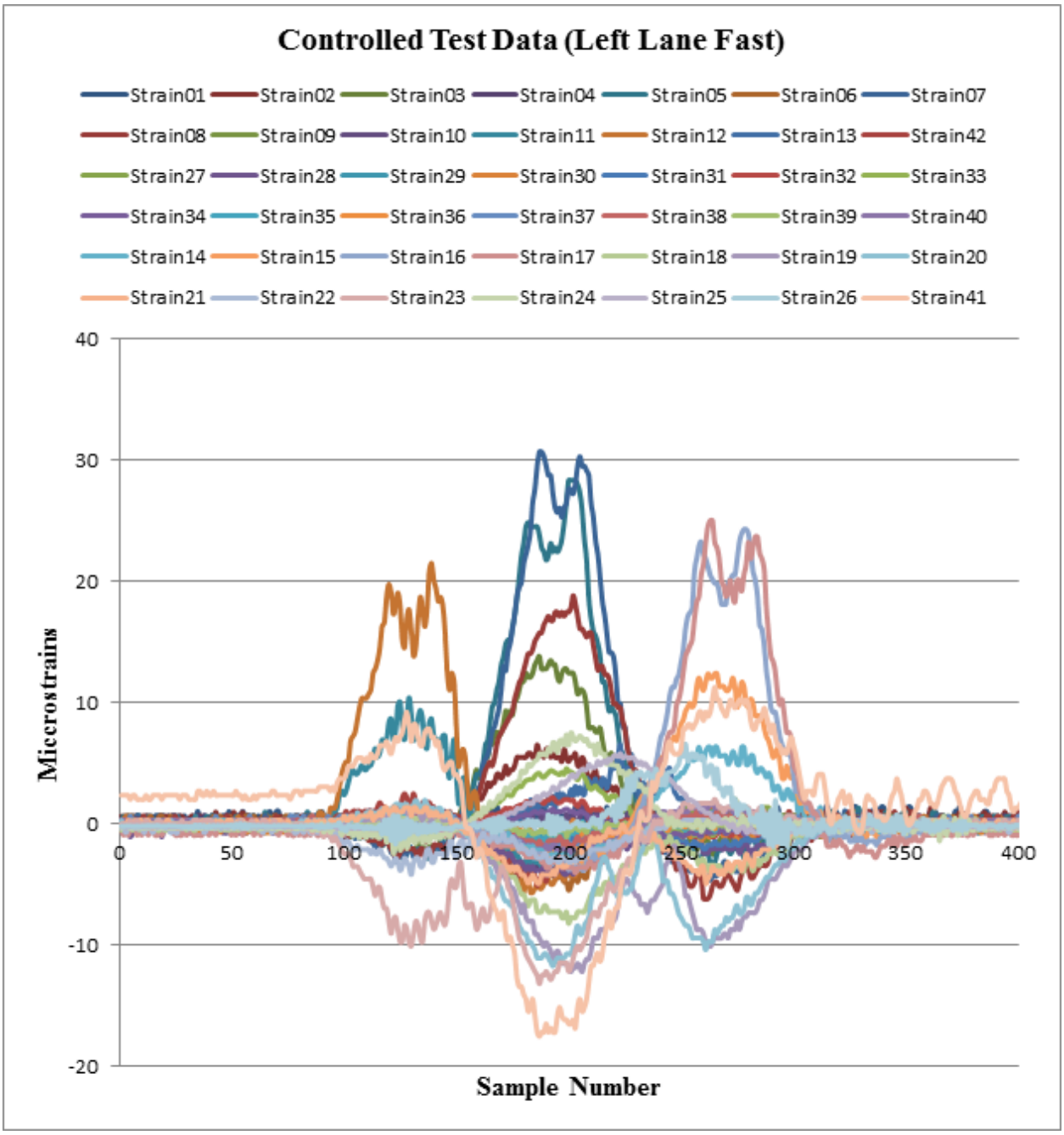

Figure 126
Plot of strains of the controlled test (in lane fast)

APPENDIX F

Truck Types

Figure 127
Truck type 3S2

Figure 128
Truck type 3S2 sugarcane

Figure 129
Truck type 3S3

Figure 130
Truck type 3S3 sugarcane

Figure 131
Truck type FHWA Class 6

Figure 132
Truck type FHWA Class 7

APPENDIX G

November Live Load Test Data

Table 56
November live load test data

					Girder D	Girder E	Girder E	Girder F
TIME STAMP	**RECORD**	**Stamp #**	**TRUCK TYPE**	**WEIGHT (FULLY LOADED LEGAL LOAD)(lb.)**	**Strain 40**	**Strain 14**	**Strain 41**	**Strain 42**
20:52.8	3525	258	3S3 (Type 8)	100,000	1.38	6.374	0.367	9.26
20:52.9	3529	262	3S3 (Type 8)	100,000	1.38	6.374	0.367	8.91
20:52.9	3530	263	3S3 (Type 8)	100,000	1.722	6.374	1.09	9.26
20:53.0	3532	265	3S3 (Type 8)	100,000	1.38	6.374	0.728	11.31
20:53.0	3533	266	3S3 (Type 8)	100,000	1.38	6.374	1.09	10.28
20:53.2	3544	277	3S3 (Type 8)	100,000	1.38	6.374	0.728	10.28
20:53.2	3545	278	3S3 (Type 8)	100,000	1.38	6.374	1.451	9.94

					Girder D	Girder E	Girder E	Girder F
					Strain 40	**Strain 14**	**Strain 41**	**Strain 42**
11/3/2010 10:39	10171	1400	3S3 (Type 8)	100,000	1.713	22.31	17.82	3.252
39:56.0	10173	1402	3S3 (Type 8)	100,000	1.713	22.31	17.82	2.89
39:56.1	10176	1405	3S3 (Type 8)	100,000	1.713	22.31	17.48	2.89

					Girder D	Girder E	Girder E	Girder F
					Strain 40	**Strain 14**	**Strain 41**	**Strain 42**
58:51.8	16089	399	3S3 (Type 8)	100,000	2.051	20.55	16.79	3.976

					Girder D Strain 40	Girder E Strain 14	Girder E Strain 41	Girder F Strain 42
19:20.2	24282	1992	3S3 (Type 8)	100,000	1.383	6.731	0.354	7.196
19:20.2	24283	1993	3S3 (Type 8)	100,000	1.383	6.731	0.354	6.853
19:20.2	24286	1996	3S3 (Type 8)	100,000	1.383	6.731	-0.007	6.167

					Girder D Strain 40	Girder E Strain 14	Girder E Strain 41	Girder F Strain 42
18:18.3	2777222	266	3S3 (Type 8)	100,000	1.373	21.25	19.88	0.362
18:18.3	2777223	267	3S3 (Type 8)	100,000	1.373	21.25	19.19	1.447

					Girder D Strain 40	Girder E Strain 14	Girder E Strain 41	Girder F Strain 42
07:13.8	2777916	258	3S3 (Type 8)	100,000	1.393	5.657	6.863	4.335

APPENDIX H

Live Load Test Data for Different Truck Types

Table 57
Live load data for 3S3 truck type

TIME STAMP	RECORD	Stamp #	TRUCK TYPE	WEIGHT (fully loaded legal load) (lb.)	GIRDER E	GIRDER D	GIRDER E	GIRDER F
					Strain14	Strain40	Strain41	Strain42
9/1/2010 9:48	677542	1970	3S3 (Type 8)	88,000	28.33	1.709	18.17	5.423
9/1/2010 13:19	681064	1980	3S3 (Type 8)	88,000	28.69	1.022	10.96	4.699
9/1/2010 13:20	681410	1981	3S3 (Type 8)	88,000	29.75	0.681	13.02	2.892
9/1/2010 14:27	682109	1983	3S3 (Type 8)	88,000	25.86	3.413	6.847	4.34
9/1/2010 18:59	685269	1992	3S3 (Type 8)	88,000	33.29	2.047	22.28	4.701
9/1/2010 19:24	685974	1994	3S3 (Type 8)	88,000	38.24	2.04	32.57	5.061
9/1/2010 19:33	686313	1995	3S3 (Type 8)	88,000	31.86	1.681	26.74	4.7
9/2/2010 10:24	702490	2044	3S3 (Type 8)	88,000	25.85	1.022	17.14	4.338
9/2/2010 12:35	704216	2049	3S3 (Type 8)	88,000	24.09	1.367	8.22	2.168
9/2/2010 18:04	710540	2067	3S3 (Type 8)	88,000	24.09	1.367	8.22	2.168
9/2/2010 18:19	710884	2068	3S3 (Type 8)	88,000	32.56	2.041	20.23	5.061
9/2/2010 18:31	711602	2070	3S3 (Type 8)	88,000	32.58	1.705	24.68	4.7
9/2/2010 18:34	712295	2072	3S3 (Type 8)	88,000	33.64	1.703	21.6	5.784
9/2/2010 18:43	712987	2074	3S3 (Type 8)	88,000	40.01	2.047	22.63	6.146
9/2/2010 18:50	714067	2077	3S3 (Type 8)	88,000	33.65	2.035	27.42	5.786
9/2/2010 18:58	714418	2078	3S3 (Type 8)	88,000	34.7	2.384	28.79	5.06
9/2/2010 19:01	714738	2079	3S3 (Type 8)	88,000	40.02	2.036	31.19	6.148
9/3/2010 18:16	764447	2225	3S3 (Type 8)	88,000	33.65	3.387	19.87	3.254
9/3/2010 18:21	764808	2226	3S3 (Type 8)	88,000	35.08	2.73	15.41	3.978
9/3/2010 18:33	765836	2229	3S3 (Type 8)	88,000	43.19	2.385	22.29	3.616

Table 58
Live load test data for 3S3 sugarcane truck type

TIME STAMP	RECORD	Stamp #	TRUCK TYPE	WEIGHT (fully loaded legal load)(lb.)	GIRDER E	GIRDER D	GIRDER E	GIRDER F
					Strain14	Strain40	Strain41	Strain42
10/1/2010 12:00	1152708	3349	3S3 (Type 8)	100,000	28.68	1.044	27.08	9.04
10/1/2010 12:47	1158789	3367	3S3 (Type 8)	100,000	28.68	0.686	26.73	7.227
10/1/2010 12:54	1160293	3371	3S3 (Type 8)	100,000	29.74	1.034	22.62	5.062
10/1/2010 13:06	1161948	3376	3S3 (Type 8)	100,000	28.33	1.011	22.62	6.146
10/1/2010 14:17	1171726	3404	3S3 (Type 8)	100,000	22.63	1.031	14.42	2.169
10/2/2010 13:02	1198885	3482	3S3 (Type 8)	100,000	26.91	0.683	21.6	5.422
10/2/2010 17:00	1213635	3525	3S3 (Type 8)	100,000	30.45	1.024	18.51	2.529
10/3/2010 13:32	1229430	3570	3S3 (Type 8)	100,000	27.27	1.018	20.56	5.785
10/4/2010 15:19	1272175	3694	3S3 (Type 8)	100,000	29.4	0.69	19.87	3.617
10/4/2010 16:22	1280457	3718	3S3 (Type 8)	100,000	26.91	4.782	16.46	5.06
10/4/2010 18:29	1292768	3755	3S3 (Type 8)	100,000	34.37	0.695	21.58	0.363
10/5/2010 14:11	1312452	3812	3S3 (Type 8)	100,000	29.74	1.371	19.2	5.421
10/5/2010 14:21	1313505	3815	3S3 (Type 8)	100,000	25.48	1.367	15.78	3.617
10/5/2010 14:46	1317015	3825	3S3 (Type 8)	100,000	23.02	0.675	14.74	4.701
10/5/2010 17:46	1333490	3873	3S3 (Type 8)	100,000	30.1	1.024	17.48	0.361
10/5/2010 18:25	1335596	3879	3S3 (Type 8)	100,000	29.4	1.032	29.47	0
10/6/2010 12:46	1348583	3916	3S3 (Type 8)	100,000	24.8	0.691	21.58	6.869
10/6/2010 14:47	1358911	3946	3S3 (Type 8)	100,000	25.5	0.697	13.36	3.612
10/7/2010 13:14	1388652	4031	3S3 (Type 8)	100,000	28.68	1.025	13.03	3.252
10/7/2010 14:40	1399587	4063	3S3 (Type 8)	100,000	28.32	0.702	15.77	3.254

Table 59
Live load test data for 3S2 truck type

TIME STAMP	RECORD	Stamp #	TRUCK TYPE	WEIGHT (fully loaded legal load) (lbs.)	GIRDER E	GIRDER D	GIRDER E	GIRDER F
					Strain14	Strain40	Strain41	Strain42
8/9/2010 17:40	341900	986	3S2 (Type 6)	80,000	20.89	2.003	10.97	2.169
8/19/2010 11:59	474460	1367	3S2 (Type 6)	80,000	26.2	1.716	17.49	3.249
8/21/2010 14:42	498005	1437	3S2 (Type 6)	80,000	19.14	2.009	4.105	2.17
8/24/2010 18:36	526317	1522	3S2 (Type 6)	80,000	27.27	1.363	15.41	3.254
8/27/2010 18:01	637537	1853	3S2 (Type 6)	80,000	29.75	1.022	15.43	2.892
8/31/2010 19:09	660929	1920	3S2 (Type 6)	80,000	25.13	2.388	21.26	4.338
9/2/2010 14:06	705650	2053	3S2 (Type 6)	80,000	27.99	2.064	14.73	2.893
9/3/2010 12:41	750001	2183	3S2 (Type 6)	80,000	26.2	1.364	7.888	2.893
9/7/2010 14:32	793937	2311	3S2 (Type 6)	80,000	31.52	2.725	8.91	3.977
9/7/2010 14:49	794302	2312	3S2 (Type 6)	80,000	26.56	2.378	7.881	2.892
9/8/2010 9:06	809549	2356	3S2 (Type 6)	80,000	22.32	1.718	18.5	4.7
9/9/2010 11:10	865855	2520	3S2 (Type 6)	80,000	23.37	1.025	17.48	4.701
9/9/2010 12:53	875817	2549	3S2 (Type 6)	80,000	23.02	1.023	7.194	2.168
10/2/2010 14:09	1204251	3498	3S2 (Type 6)	80,000	21.25	0.694	14.39	3.615
10/2/2010 16:59	1213284	3524	3S2 (Type 6)	80,000	28.68	0.347	22.28	2.889
10/4/2010 9:14	1249947	3629	3S2 (Type 6)	80,000	25.15	1.718	3.428	3.614
10/4/2010 12:53	1255118	3644	3S2 (Type 6)	80,000	24.8	1.038	19.53	5.419
10/4/2010 12:59	1255820	3646	3S2 (Type 6)	80,000	28.34	0.685	20.56	5.421
10/4/2010 13:06	1256623	3649	3S2 (Type 6)	80,000	4.244	0.684	5.832	0.723
10/20/2010 8:12	2023183	5864	3S2 (Type 6)	80,000	25.14	1.042	4.456	6.508

Table 60
Live load test data for 3S2 sugarcane truck type

TIME STAMP	RECORD	Stamp #	TRUCK TYPE	WEIGHT (fully loaded legal load)(lbs.)	GIRDER E	GIRDER D	GIRDER E	GIRDER F
					Strain14	Strain40	Strain41	Strain42
10/6/2010 12:35	1347179	3912	3S2 (Type 6)	100,000	27.27	1.034	20.91	6.509
10/6/2010 13:10	1349636	3919	3S2 (Type 6)	100,000	28.33	1.048	17.48	6.144
10/6/2010 13:23	1351040	3923	3S2 (Type 6)	100,000	27.97	0.693	18.85	4.334
10/6/2010 13:37	1352444	3927	3S2 (Type 6)	100,000	34	0.683	14.39	4.702
10/6/2010 14:05	1354199	3932	3S2 (Type 6)	100,000	24.43	0.352	9.94	2.53
10/6/2010 14:09	1354550	3933	3S2 (Type 6)	100,000	31.17	1.37	19.53	5.058
10/6/2010 14:18	1355401	3936	3S2 (Type 6)	100,000	25.49	0.683	12.34	7.953
10/6/2010 14:54	1359613	3948	3S2 (Type 6)	100,000	24.06	1.017	12.01	3.253
10/6/2010 15:00	1360315	3950	3S2 (Type 6)	100,000	25.15	0.684	12.68	1.806
10/6/2010 15:01	1360828	3952	3S2 (Type 6)	100,000	27.62	0.689	14.74	2.531
10/6/2010 15:12	1361625	3954	3S2 (Type 6)	100,000	26.57	1.022	20.56	2.891
10/6/2010 15:26	1363029	3958	3S2 (Type 6)	100,000	24.79	0.688	12.34	2.893
10/6/2010 16:01	1366539	3968	3S2 (Type 6)	100,000	29.04	0.01	11.31	1.444
10/6/2010 16:26	1368645	3974	3S2 (Type 6)	100,000	32.94	0.34	15.08	2.53
10/6/2010 17:18	1371804	3983	3S2 (Type 6)	100,000	27.99	1.027	13.7	0.721
10/7/2010 11:37	1383387	4016	3S2 (Type 6)	100,000	24.08	0.692	20.22	8.67
10/7/2010 12:59	1386546	4025	3S2 (Type 6)	100,000	27.61	0.688	15.43	5.063
10/7/2010 13:32	1390056	4035	3S2 (Type 6)	100,000	26.56	1.384	13.37	4.341
10/7/2010 13:43	1391109	4038	3S2 (Type 6)	100,000	28.69	0.352	22.62	3.253
10/7/2010 14:08	1394461	4048	3S2 (Type 6)	100,000	29.03	1.374	17.14	3.253

Table 61
Live load data for FHWA Class 6 truck type

TIME STAMP	RECORD	Stamp #	TRUCK TYPE	WEIGHT (fully loaded legal load) (lbs.)	GIRDER E	GIRDER D	GIRDER E	GIRDER F
					Strain14	Strain40	Strain41	Strain42
8/9/2010 12:45	318021	918	FHWA Class 6 (Type 2)	53,000	34.35	1.702	11.66	4.338
8/11/2010 14:02	417179	1203	FHWA Class 6 (Type 2)	53,000	26.92	1.022	10.28	2.892
8/11/2010 15:15	419968	1211	FHWA Class 6 (Type 2)	53,000	24.08	1.043	1.029	1.446
8/12/2010 11:06	434608	1253	FHWA Class 6 (Type 2)	53,000	26.91	1.363	22.28	4.339
8/12/2010 12:25	436693	1259	FHWA Class 6 (Type 2)	53,000	26.21	2.043	22.28	5.422
8/12/2010 13:40	439135	1266	FHWA Class 6 (Type 2)	53,000	26.56	1.71	25.02	4.7
9/1/2010 14:09	681793	1982	FHWA Class 6 (Type 2)	53,000	21.95	1.364	3.773	1.445
9/1/2010 15:21	682808	1985	FHWA Class 6 (Type 2)	53,000	26.91	2.386	5.827	2.893
9/3/2010 9:19	735380	2140	FHWA Class 6 (Type 2)	53,000	24.09	1.045	15.42	3.976
9/3/2010 11:09	741685	2158	FHWA Class 6 (Type 2)	53,000	26.2	1.368	19.88	5.784
9/3/2010 12:20	747335	2175	FHWA Class 6 (Type 2)	53,000	30.45	0.694	10.29	5.062
9/3/2010 13:01	751323	2187	FHWA Class 6 (Type 2)	53,000	22.32	0.69	6.161	2.53
9/3/2010 13:19	752691	2191	FHWA Class 6 (Type 2)	53,000	26.56	1.03	7.882	2.531
9/3/2010 14:34	758447	2208	FHWA Class 6 (Type 2)	53,000	22.33	2.401	6.155	1.446
9/8/2010 11:33	822640	2394	FHWA Class 6 (Type 2)	53,000	31.52	1.371	20.91	5.784
9/9/2010 8:47	856883	2494	FHWA Class 6 (Type 2)	53,000	21.96	1.372	22.27	5.422
9/9/2010 10:50	864245	2515	FHWA Class 6 (Type 2)	53,000	29.03	2.051	25.03	7.955
9/11/2010 9:59	926365	2695	FHWA Class 6 (Type 2)	53,000	23.73	1.036	21.25	4.7
9/15/2010 13:14	949128	2761	FHWA Class 6 (Type 2)	53,000	21.59	1.025	55.88	2.892
9/16/2010 9:06	958630	2788	FHWA Class 6 (Type 2)	53,000	22.31	0.7	16.45	4.698

Table 62
Live load data for FHWA Class 7 truck type

TIME STAMP	RECORD	Stamp #	TRUCK TYPE	WEIGHT (fully loaded legal load) (lbs.)	GIRDER E	GIRDER D	GIRDER E	GIRDER F
					Strain14	Strain40	Strain41	Strain42
9/3/2010 8:08	732856	2132	FHWA Class 7 (Type 18)	61,000	19.83	1.024	6.17	3.615
9/3/2010 9:09	735042	2139	FHWA Class 7 (Type 18)	61,000	21.96	1.397	17.48	6.145
9/3/2010 9:29	735764	2141	FHWA Class 7 (Type 18)	61,000	22.29	1.024	17.5	3.975
9/3/2010 9:50	737166	2145	FHWA Class 7 (Type 18)	61,000	19.84	0.35	8.22	-2.529
9/3/2010 10:17	738196	2148	FHWA Class 7 (Type 18)	61,000	20.54	2.049	18.51	3.252
9/3/2010 10:21	738550	2149	FHWA Class 7 (Type 18)	61,000	25.15	1.72	21.59	3.976
9/3/2010 10:32	739249	2151	FHWA Class 7 (Type 18)	61,000	32.23	2.077	22.96	6.145
9/3/2010 10:42	739637	2152	FHWA Class 7 (Type 18)	61,000	26.57	1.729	20.56	5.784
9/3/2010 11:04	740978	2156	FHWA Class 7 (Type 18)	61,000	27.63	1.715	19.19	3.615
9/3/2010 11:05	741296	2157	FHWA Class 7 (Type 18)	61,000	34	2.056	27.76	6.867
9/3/2010 11:29	743061	2162	FHWA Class 7 (Type 18)	61,000	19.14	1.37	16.09	6.145
9/3/2010 11:38	743879	2165	FHWA Class 7 (Type 18)	61,000	31.15	1.031	11.32	3.615
9/3/2010 11:57	745324	2169	FHWA Class 7 (Type 18)	61,000	28.33	1.708	15.77	4.339
9/3/2010 12:04	746377	2172	FHWA Class 7 (Type 18)	61,000	32.58	1.723	13.36	3.977
9/3/2010 12:16	746687	2173	FHWA Class 7 (Type 18)	61,000	28.68	1.024	15.43	4.699
9/3/2010 12:28	748047	2177	FHWA Class 7 (Type 18)	61,000	25.85	1.36	6.173	1.085
9/3/2010 12:34	748418	2178	FHWA Class 7 (Type 18)	61,000	34	1.72	13.71	4.701
9/3/2010 12:40	749336	2181	FHWA Class 7 (Type 18)	61,000	27.26	0.691	5.487	2.17
9/3/2010 13:13	752337	2190	FHWA Class 7 (Type 18)	61,000	26.54	1.709	7.553	3.977
9/3/2010 13:21	753060	2192	FHWA Class 7 (Type 18)	61,000	25.48	1.036	9.61	3.976

Table 63
Live load test data for Type 2 truck

TIME STAMP	RECORD	Stamp #	Truck Type	WEIGHT (fully loaded legal load) (lbs.)	GIRDER B	GIRDER D	GIRDER E	GIRDER F
					Strain17	Strain40	Strain41	Strain42
8/9/2010 16:13	336920	972	Type 2	53000	31.78	0.674	-0.687	0.723
8/11/2010 15:23	420265	1212	Type 2	53000	27.75	1.03	2.744	2.169
8/12/2010 9:33	432055	1246	Type 2	53000	29.09	0.341	8.23	0.363
8/25/2010 11:50	554682	1608	Type 2	53000	30.88	2.387	8.56	0.001
9/3/2010 10:48	740230	2154	Type 2	53000	29.54	1.017	-15.76	-6.145
9/3/2010 13:59	754657	2197	Type 2	53000	34.01	2.048	-5.491	1.084
9/8/2010 8:30	807022	2349	Type 2	53000	30.88	1.024	1.375	-1.086
9/10/2010 13:24	903844	2630	Type 2	53000	37.59	1.367	3.77	1.809
10/6/2010 11:58	1346017	3909	Type 2	53000	27.3	0.69	7.204	0.721

Table 64
Live load test data for Type 18 truck

TIME STAMP	RECORD	Stamp #	Truck Type	WEIGHT (fully loaded legal load) (lbs.)	GIRDER B	GIRDER D	GIRDER E	GIRDER F
					Strain17	Strain40	Strain41	Strain42
8/9/2010 15:40	334462	965	Type 18	61000	30.44	0.682	1.035	0.723
8/10/2010 9:09	348854	1006	Type 18	61000	33.57	1.025	5.143	-3.616
8/10/2010 9:13	349204	1007	Type 18	61000	30.88	1.05	25.37	1.447
8/10/2010 9:56	352367	1016	Type 18	61000	8.5	0.682	13.03	2.892
8/10/2010 12:23	365908	1055	Type 18	61000	42.51	0.367	-2.753	-1.085
8/10/2010 12:55	368714	1063	Type 18	61000	37.15	1.029	2.054	1.446
8/10/2010 13:14	371519	1071	Type 18	61000	29.09	1.376	0.006	-1.444
8/10/2010 13:27	372225	1073	Type 18	61000	31.33	1.052	-16.79	-3.617
8/10/2010 13:40	373275	1076	Type 18	61000	36.25	0.347	-3.097	0.36
8/10/2010 14:25	377841	1089	Type 18	61000	35.36	1.366	12.34	-0.723
8/10/2010 15:06	381153	1099	Type 18	61000	11.2	1.017	12.36	2.17
8/12/2010 8:49	430302	1241	Type 18	61000	36.26	0.691	10.97	1.447
8/24/2010 14:51	521350	1506	Type 18	61000	34.02	1.717	-3.083	0.721
9/3/2010 10:26	738877	2150	Type 18	61000	32.67	1.038	7.204	0.724
9/3/2010 11:12	741988	2159	Type 18	61000	37.59	0.347	8.9	-1.083
9/8/2010 12:14	825376	2402	Type 18	61000	37.15	1.362	11.31	0.361
9/8/2010 12:47	827484	2408	Type 18	61000	37.14	1.037	2.387	2.17
9/8/2010 13:40	832290	2422	Type 18	61000	34.91	0.697	4.463	0.724
9/8/2010 14:22	835530	2432	Type 18	61000	38.04	1.36	12	5.784
9/8/2010 16:09	842302	2452	Type 18	61000	38.04	1.372	0.688	-0.723
9/8/2010 16:19	843708	2456	Type 18	61000	43.41	1.015	5.828	-0.36
9/9/2010 12:36	873665	2543	Type 18	61000	34.91	0.377	0.003	-0.001
9/10/2010 11:11	896822	2610	Type 18	61000	32.22	1.017	2.738	-0.361

Table 65
Live load test data for 3S2 truck type

TIME STAMP	RECORD	Stamp #	Truck Type	WEIGHT (fully loaded legal load) (lbs.)	GIRDER B	GIRDER D	GIRDER E	GIRDER F
					Strain17	Strain40	Strain41	Strain42
8/9/2010 17:32	341482	985	3S2	80000	28.2	2.316	-9.93	0
8/10/2010 9:49	351659	1014	3S2	80000	27.75	0.34	9.25	1.807
8/10/2010 13:55	374725	1080	3S2	80000	28.65	0.346	9.95	1.086
8/10/2010 19:49	391830	1130	3S2	80000	32.23	1.014	12.69	2.17
8/11/2010 14:40	418876	1208	3S2	80000	36.25	1.036	3.769	-0.362
8/12/2010 13:26	438373	1264	3S2	80000	29.09	1.354	16.46	3.255
8/19/2010 11:49	473306	1364	3S2	80000	29.09	0.701	9.25	3.254
8/21/2010 13:58	497551	1436	3S2	80000	27.75	1.022	17.14	2.892
8/22/2010 16:21	501413	1447	3S2	80000	29.54	-0.006	5.488	-1.808
10/9/2010 17:56	1500054	4354	3S2	80000	34.01	0.669	16.45	-1.446
9/8/2010 18:52	847212	2466	3S2	80000	28.2	-0.001	4.465	-2.169
9/13/2010 13:23	935156	2721	3S2	80000	28.19	0.68	-1.034	-0.722
9/14/2010 18:46	943229	2744	3S2	80000	27.75	2.727	6.508	-1.084
10/5/2010 14:57	1317963	3828	3S2	80000	30.44	0.342	0.689	1.085

Table 66
Live load test data for 3S3 truck type

TIME STAMP	RECORD	Stamp #	Truck Type	WEIGHT (fully loaded legal load) (lbs.)	GIRDER B	GIRDER D	GIRDER E	GIRDER F
					Strain17	Strain40	Strain41	Strain42
8/10/2010 16:03	386212	1114	3S3	88000	29.54	0.681	-6.171	-1.085
8/18/2010 19:29	468911	1351	3S3	88000	32.23	1.355	9.94	0.36
8/19/2010 13:39	477882	1377	3S3	88000	33.57	1.363	12.34	2.171
8/19/2010 15:23	479285	1381	3S3	88000	34.92	2.057	7.895	1.083
8/24/2010 19:30	529693	1533	3S3	88000	36.7	0.663	-5.145	-1.085
9/1/2010 19:08	685618	1993	3S3	88000	34.91	1.013	13.71	1.085
9/1/2010 19:38	687130	1998	3S3	88000	34.91	1	3.084	1.447
9/2/2010 17:14	710170	2066	3S3	88000	31.33	1.035	3.773	0.358
9/2/2010 18:22	711232	2069	3S3	88000	35.36	0.68	10.96	0.362
9/2/2010 6:41	712635	2073	3S3	88000	33.57	0.659	3.435	1.809
9/2/2010 19:35	715095	2080	3S3	88000	34.01	1.023	14.05	0.36
9/3/2010 18:06	763344	2222	3S3	88000	34.92	2.711	-8.21	0.362
9/3/2010 18:39	766152	2230	3S3	88000	33.57	1.017	-2.054	-0.363
9/3/2010 19:19	769210	2239	3S3	88000	32.23	0.662	-7.875	-1.446
9/3/2010 19:32	770273	2242	3S3	88000	33.57	1.015	2.403	0.362
9/7/2010 15:37	796701	2319	3S3	88000	28.64	1.364	1.363	1.447
9/8/2010 11:06	820108	2387	3S3	88000	27.75	1.038	6.862	0.725
9/8/2010 17:55	846162	2463	3S3	88000	31.78	1.364	3.775	1.085
10/1/2010 18:11	1184260	3440	3S3	88000	34.46	1.356	6.177	0
10/7/2010 17:43	1416140	4111	3S3	88000	33.57	1.018	4.124	0.361

Table 67
Live load test data for 3S2 sugarcane truck type

TIME STAMP	RECORD	Stamp #	Truck Type	WEIGHT (fully loaded legal load) (lbs.)	GIRDER B	GIRDER D	GIRDER E	GIRDER F
					Strain17	Strain40	Strain41	Strain42
10/10/2010 14:24	1523571	4421	3S2 SC	100000	34.9	-2.385	-23.3	-12.29
10/12/2010 14:13	1607289	4662	3S2 SC	100000	30.88	-1.014	-45.22	-8.86
10/14/2010 14:32	1724775	5003	3S2 SC	100000	33.11	0.002	17.48	-2.528
10/5/2010 15:39	1322745	3842	3S2 SC	100000	28.2	0.343	6.171	-1.444
10/9/2010 7:14	1467587	4260	3S2 SC	100000	28.64	0.692	2.735	0.724
10/9/2010 11:59	1472853	4275	3S2 SC	100000	28.19	0.01	8.22	-3.255

Table 68
Live load test data for 3S3 sugarcane truck type

TIME STAMP	RECORD	Stamp #	Truck Type	WEIGHT (fully loaded legal load) (lbs.)	GIRDER B	GIRDER D	GIRDER E	GIRDER F
					Strain17	Strain40	Strain41	Strain42
59:53.0	1443205	4189	3S3 SC	100000	35.35	35.35	1.021	-1.087
35:52.6	1627210	4720	3S3 SC	100000	30.43	30.43	4.807	-0.362
36:10.5	1654382	4799	3S3 SC	100000	28.63	28.63	5.462	0.724

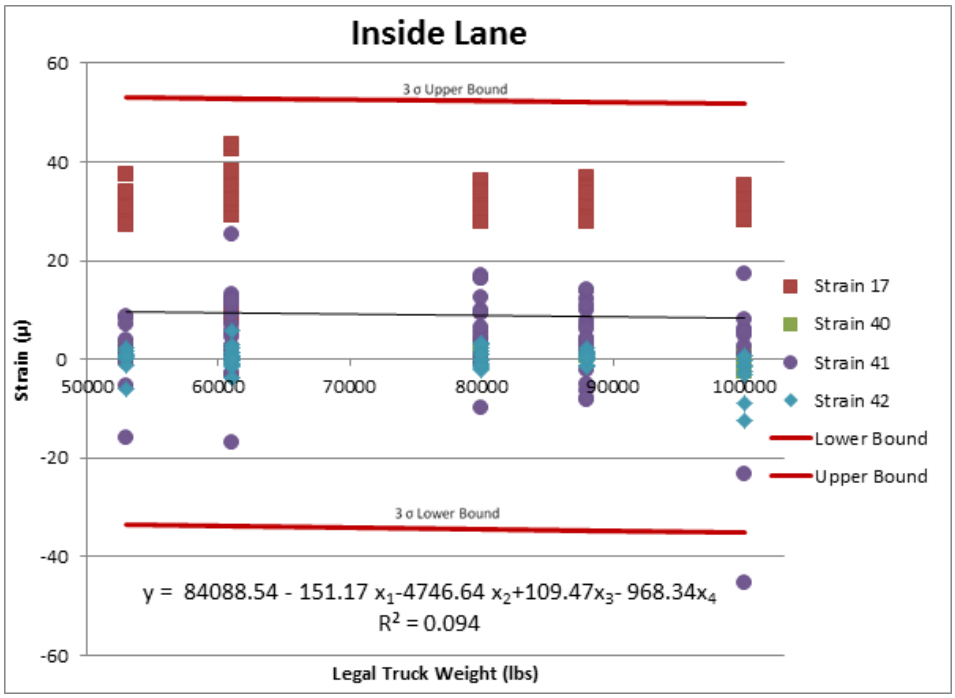

Figure 133
Live field data strain values vs. legal truck weight (inside lane)

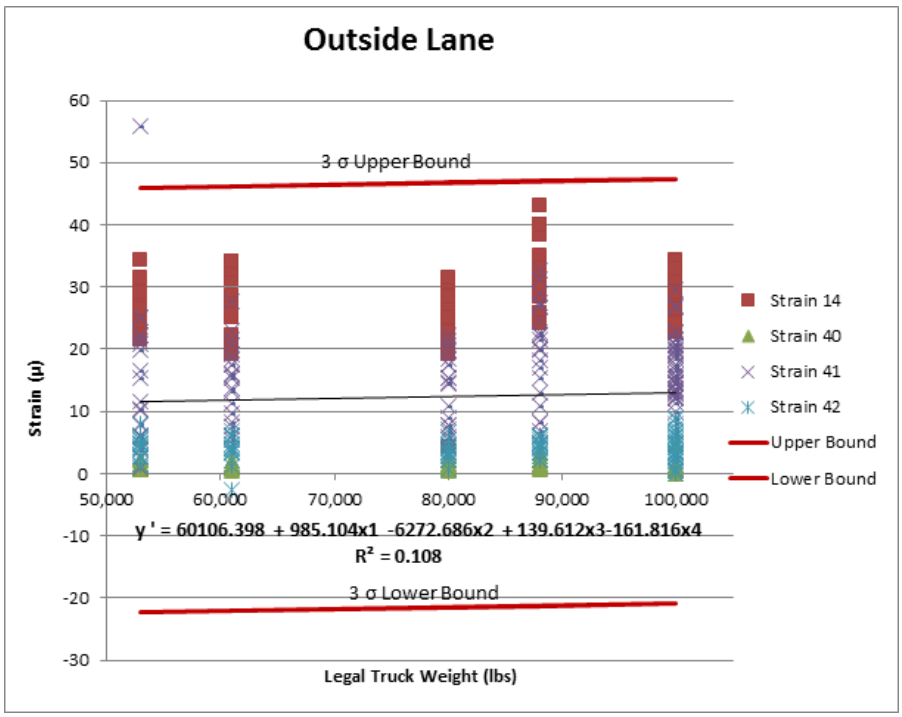

Figure 134
Live field data strain values vs. legal truck weight (outside lane)